UNIVERSITY OF KWAZULU-NATAL

COMBUSTION STUDIES OF BIODIESEL FUEL FROM MORINGA, JATROPHA AND RESTAURANT OIL

ONUH, Emmanuel Idoko, *B.Eng, M.Eng*

212561710

Supervisor: Prof. Freddie L. Inambao

Thesis submitted in fulfilment of the requirement for the degree of DOCTOR OF PHILOSOPHY IN ENGINEERING (PhD)

(MECHANICAL ENGINEERING)

School of Engineering, University of KwaZulu-Natal, Durban, South Africa

November, 2016

"As the candidate's supervisor, I agree/do not agree to the submission of this thesis". The supervisor must sign all copies after deleting which is not applicable.

………………………………………………   ………………………………….

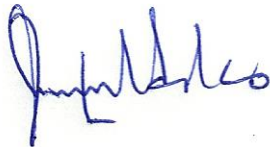NAME OF SUPERVISOR   SIGNATURE

Declaration 1 -Plagiarism

I, **Onuh, Emmanuel Idoko** declare that:

1. The research reported in this thesis, except where otherwise indicated is my original research.

2. This thesis has not been submitted for any degree or examination at any other university.

3. This thesis does not contain other persons' data, pictures, graphs or other information, unless specifically acknowledged as being sourced from other persons.

4. This thesis does not contain other persons' writing, unless specifically acknowledged as being sourced from other researchers. Where other written sources have been quoted, then:

   a) Their words have been re-written but the general information attributed to them has been referenced

   b) Where their exact words have been used, then their writing has been placed in italics and inside quotation marks, and referenced.

5. This thesis does not contain text, graphics or tables copied and pasted from the internet, unless specifically acknowledged, and the source being detailed in the thesis and in the References sections.

Signed……………………

Declaration 2 -Publications

This section presents the articles that form part and/or include the research presented in this thesis. The following papers have been published or are under review:

ISI/DoHET Accredited Journals

(1) **Onuh, E. I.** and Inambao F. L. (2015). An evaluation of neat biodiesel/diesel performance, emission pattern of NO_X and CO in compression ignition engine. *International Journal of Global Warming.* Inderscience Publisher. (Accepted and in press. Abstract listed in forthcoming articles at: http://www.inderscience.com/info/ingeneral/forthcoming.php?jcode=ijgw)

(2) **Onuh, E. I.** and Inambao F. L. (2015). Performance and emission evaluation of pure biodiesel from non-edible feedstock and waste oil in a diesel engine. *African Journal of Science, Technology, Innovation and Development.* Thomson Reuters Publisher (Accepted and in press. Will be available at: http://dx.doi.org/10.1080/20421338.2016.1219483)

(3) **Onuh, E. I.** and Inambao, F. L. (2014). A study of the properties and performance of biodiesel/diesel blends in a diesel engine. *Journal of Energy in Southern Africa.* (Submitted)

International and DoHET Accredited Conferences

(1) **Onuh, E. I.** and Inambao, F. L. (2013). A study of extraction yield and properties of some oils for biodiesel application. Proceedings of the 13th biennial Botswana Institution of Engineers Conference, Gaborone, Botswana: 15-18th October, 2013: pp 233-241. ISBN 978-99912-0-910-4.

(2) **Onuh, E. I.** and Inambao, F. L. (2014). An evaluation of the extraction yield, properties and performance of some biodiesel in a diesel engine with emission pattens. 13th International Conference on Sustainable Energy technologies (SET2014) 25-28th August, 2014. Geneva, Switzerland. Paper ID: SET2014-E10043.

(3) **Onuh, E. I.** and Inambao, F. L. (2015). An experimental investigation of performance, emission patterns of NO_X and CO in ignition compression engine running on pure biodiesels and diesel. International Conference on clean energy for sustainable growth in developing countries. September 16-18th, 2015. Palapye, Botswana.

(4) **Onuh, E.** I. and Inambao, F. L. (2015). A review of computational fluid dynamics (CFD) schemes in biodiesel studies. International Conference on clean energy for sustainable growth in developing countries. September 16-18th, 2015. Palapye, Botswana.

(5) **Onuh, E. I.** and Inambao, F. L. (2015). A proposal to perform computational and experimental evaluation of biodiesel in HCCI using combined modula kinetic and premixed/DI strategies. Proceedings of the 14th biennial Botswana Institution of Engineers Conference, Gaborone, Botswana. 6th -8th October, 2015.

(6) **Onuh, E.** I. and Inambao, F. L. (2016). A property prediction scheme for biodiesel derived from non-edible feedstock. 24th Domestic Use of Energy Conference. Cape Peninsular University, Cape Town. 29th -31st March, 2016. (http://dx.doi.org/10.1109/DUE.2016.7466718)

For all the publications the candidate is the main and corresponding author while Dr Freddie L. Inambao is the supervisor

Dedication

This work is dedicated to the entity with the most influence in my life, the Man from Galilee who is the oracle of the infinite and only sovereign.

Acknowledgements

This thesis had been my most exciting and exerting endeavour yet. I have had to call forth every reserve of physical, mental and emotional strength for this undertaking. Fortunately, I am surrounded with family, friends and colleagues, not to mention those who play oversight role in my career development, who have been most supportive. Acknowledging their contribution therefore is the least I could do.

Atinuke, my spouse and our two boys Enpe and Ekofu were just the perfect team with me on this journey. Their tugging and loving constantly reminds me of what this was all about, they are my irreplaceable team. Mary, my elder sibling, has always held out a hand to me since I knew how to call her name, I salute her steadfastness. To my sister Edugwu, whose passing was the most distressing period during this research, I can never forget you my noble comrade and how we dug our way out of the hood. I acknowledge your humanity, valour and courage; you will never be dead to me. To the rest of my siblings, you are all reminders of the great values inherent in a united family. To my most pivotal support unit, the church of God in Kwazulu Natal, I have nothing but gratitude for your sheltering ramp which evidently takes us all closer to the ultimate destination.

Prof. Inambao has been more than a supervisor to me. With a calm and steady nerve, he has stirred this research on a productive path. His humane disposition has been most reassuring. His depth of vision and clear perspective is hereby acknowledged. Prof. Glen Bright and the research team at the discipline of mechanical engineering has been a wonderful host; the fecundity of the faculty has been most inspiring and is hereby acknowledged. To my boss, Dr. Musa Shuaibu who made it possible for me to study at Howard College, your administrative skills are above par. Beyond that, I value most deeply your graciousness and kind heartedness. To my senior friend and colleague Surv. Suleiman, I owe you a chapter of acknowledgment and I promise to write it at the opportune time.

To my friends: Dr. Ejilah Robinson, your camaraderie and facilitations deserve mention, Dr. Andrew Eloka, the multi-talented, multi-tasking mastermind, it's been a real pleasure gaining your acquaintance. Dr. Samuel Ilupeju, your kind words and encouragement are acknowledged. And to Dr. Mike Olusanya, my brother from another mother, thank you. Space will not permit the mentioned of all others who are not any less important; I will always celebrate you all.

Table of Contents

List of Tables

List of Figures

List of Plates

List of Appendixes

Nomenclature

ROMAN

$\bar{R}$	Universal gas constant
$\bar{S}_p$	Piston mean speed
S_p	Instantaneous piston speed
0_3	Ozone
0D	Zero Dimensions
3D	Three Dimension
4D	Fully Resolved Spatial and Temporal Dimension
C_P	Specific heat capacity at constant pressure
C_V	Specific heat capacity at constant volume
F/A	Fuel air ratio
G	Gibbs free energy
h	Specific enthalpy
H	Enthalpy
H_P	Heat of product
H_R	Heat of reaction
Q_{HHV}	High heating value
Q_{LHV}	Low heating value
R	Ratio of connecting rod/length of crank
R_{bs}	Ratio of cylinder bore
r_c	Compression ration
S	Entropy
S	Stroke
N	Number of mole
S_{fc}	Specific fuel consumption (kg/s)
SOC	Start of combustion
SOI	Start of ignition
T	Engine torque (Nm)
TC	Top centre
TVC	Total cylinder volume (m^3)
u	Specific internal energy (kJ/kg)
V	Volumetric flow rate (m^3/s)
V_C	Clearance volume (m^3)
V_d	Displaced volume (m^3)
A	Combustion chamber surface area (m^2)
N	Engine speed (rpm)

GREEK

ɥ	Chemical potential
P	Cylinder pressure (N/m^2)
P	Engine power (W)
W_i	Indicated work per cycle
ρ	Density
θ	Crank angle

DIMENSIONLESS

η_f	Fuel conversion efficiency
λ	Stoichiometric Air/Fuel Ratio
ϕ	Equivalent ratio
A/F	Air fuel ratio
F/A	Fuel air ratio

Acronyms and Abbreviations

ASTM	American Society for Testing and Materials
ATDC	After Top Dead Centre
B	Bore
BC	Bottom centre
BSFC	Brake specific fuel consumption
BTDC	Before Top Dead Centre
CA50	50% Accumulated Heat Release
CAI	Control Auto Ignition
CCM	Chemistry Coupled Tabulation Method
CFD	Computational Fluid Dynamics
CH_4	Methane
CI	Compression ignition
CN	Cetane Number
CO	Carbon Monoxide
CO_2	Carbon Dioxide
CPU	Central Processing Unit
CSP	Computational Singular perturbation
DAC	Dynamic Adaptive Chemistry
DI	Direct Injection
DME	Di-methyl Ether
DNS	Direct Numerical Simulation
DRG	Direct Relation Graph
DRGEP	Direct Relation Graph Aided sensitivity Analysis
EGR	Exhaust Gas Recirculation
EP	Error Propagation
EPA	Environmental Protecting Agency
EPC	Exhaust port closing
EPO	Exhaust port opening
EVO	Exhaust valve opening
FAME	Fatty acid methyl ester
FFA	Free fatty acid
GDP	Gross Domestic Product
HCCI	Homogenous Charge Compression Ignition
HRR	Heat Release Rate
HTHR	High Temperature Heat Release
HTR	High temperature reaction
ICCD	Intensified Charge Coupled Device
ICE	Internal Combustion Engine
ID	Ignition Delay
ILDM	Intrinsic Low Dimensional Manifold
IMEP	Indicated Mean Effective Pressure

IPC	Inlet port closing
IPO	Inlet port opening
ISAT	In-situ Adaptive Tabulation
ISFC	Indicated Specific Fuel Consumption
ISO	International standard organisation
IVC	Inlet valve closing
JAME	Jatropher oil methyl ester
JSR	Jet Stirred Reactor
KMC	Kinetic Monte Carlo
LES	Large Eddy Simulation
LHR	Low heat rejection
LIF	laser Induced Fluorescence
LII	Laser Induced Incandescence
LLNL	Lawrence Livermore National Laboratory
LTC	Low Temperature Combustion
LTHR	Low Temperature Heat Release
LTK	Low Temperature Kinetics
LTR	Low temperature reaction
M	Molecular weight
MB	Methyl Butanoate
MD	Methyl Decanoate
MolD	Molecular Dynamics
MK	Modulated Kinetics
MOME	Moringa oil methyl ester
NA	Natural aspirated
NO_x	Oxides of Nitrogen
NVO	Negative Valve overlap
ON	Octane Number
OPPDIF	Opposed – Flow Diffusion Flame
PCCI	Premixed Charge Compression Ignition
PFA	Path Flux Analysis
PLTF	Planner Laser Induced Fluorescence
PM	Particulate matter
PSR	Perfectly Stirred Reactor
RANS	Reynolds Averaged Navier – Stokes
RES	Renewable Energy Sources
RGF	Residual Gas Fraction
ROHR	Rate of Heat Release
SA	Sensitivity Analysis
SCCI	Stratified Charge Compression Ignition
SI	Spark Ignition
SO_2	Sulphur Dioxide
SOI	Start of Ignition
ST	Shock Tube
TDAC	Tabulation of Dynamic Adaptive Chemistry

TDC	Top Dead Centre
TU	Turbo unit
UHC	Unburnt Hydrocarbon
VOME	Vegetable oil methyl ester
VVT	Variable Valve Timing
WOME	Waste oil methyl ester

Abstract

Biodiesel is a renewable alternative to finite diesel and, has the capacity to reduce emission and broaden energy access particularly in sub-Saharan Africa where economic growth has been, to some extent, constrained by global warming and a lack of universal access to sustainable source of energy. In the transport sector, a niche exist for biodiesel derived from non-edible feedstock such as waste oil, jatropha and moringa in sub-Saharan Africa. Extraction of oil from jatopha and moringa were achieved via manual as well as soxhlet method using normal hexane, petroleum ether and distilled gasoline. A numerical property prediction scheme was implemented (and validated with experimental data) to obtain the thermo-physical as well as the transport properties of the resulting fuel for the various samples. This prediction scheme reduced the number of experimentation for property determination from nine to one per sample. The pure fuel samples were evaluated in a 3.5kw diesel engine to determine their performance and emissions. The Brake Specific (BS in g/kWh) emissions across the full load spectrum were benchmarked against the United State Environmental Protection Agency (US, EPA) and the European Union (EU) emission caps. This study is a follow-up to an earlier work by Eloka Eboka which focused on the determination of optimal production process for biodiesel using different technique and catalyst. In that work, the engine test was a qualitative evaluation of different mixture ratio forming new hybrids and the engine test protocol did not follow the ISO 8178-4:2006 test cycle categorization nor was the emission benchmarked against the EPA/EU emission caps (both of which were implemented in this study).

The extraction results not only confirmed normal hexane solvent and soxhlet method as the optimal means of extraction (with a 37.1% and 51.8% yield for moringa and jatropha respectively) but, gave hint of the potential of distilled Gasoline as a viable solvent (with a 40.2% and 34.1% yield for moringa and jatropha respectively). The validated numerical prediction scheme reduce research cost and time without compromising accuracy. The performance and emission revealed that the Brake specific fuel consumption (BSFC) and brake thermal efficiencies for both diesel and the biodiesels only differ marginally ($\pm 4\%$ and ± 5 respectively at peak load). Carbon monoxide (CO), unburnt hydrocarbon (UHC) and particulate matter (PM) emissions (in part per million-ppm) showed decreasing trend with load increase and were lower than those of diesel. Oxides of nitrogen (NO_X) emission for the biodiesel were lower than those of diesel. The Brake Specific (BS) emission results in comparison to the EU and EPA regulation showed various level of compliance and non-compliance to the emission limits. The result also showed that samples with higher proportion of unsaturated FAME have poorer engine performance and results in higher unwanted emission than saturated FAME. In broad terms, engine retrofitting and novel design could effectively bridge the performance and emission gaps observed between diesel and biodiesel. A multi-blend (saturated and unsaturated FAME) and multi-strategy (Modular kinetic and premix/DI) was recommended as a remediation strategy. For numerical prediction purpose, a 3D CFD with multi zone and detailed chemistry using KIVA-3V code was proposed.

CHAPTER 1: INTRODUCTION

1.1 Introduction

Emerging trends in the transportation sector at the global level over several decades have forced the convergence of opinion on the need to diversify supply source, improve efficiency, curb emission and reduce the consumption of non-renewable fuel. Currently, in the United States for example, 85% of energy is sourced from hydrocarbons. These sources include gas, petroleum and coal. Transportation accounts for a large portion of that consumption. This pattern reflects global trends. Indeed global oil consumption is projected to increase from 162 Quads in 2003 to 239 Quads in 2030 with 60% of that increase being used for transportation [1]. This increasing demand for conventional oil is coming against the backdrop of dwindling global reserves. At current consumption rates of about 18 billion barrels of crude oil per annum, these reserves would last for approximately 70 years. Added to this is the negative impact of emissions on the environment. Recent studies have shown strong correlations between atmospheric temperature and the level of greenhouse emissions [2]. Clearly, there is a need to explore the potential of bio-fuel in meeting these challenges. Biodiesel presents an opportunity to switch dependency from finite to renewable supply sources, reduced or eliminate the negative impact on the environment, and build new supply architecture that could stimulate accelerated economic growth and improve living conditions in sub-Saharan Africa.

The current global energy architecture and technology is designed to run on conventional fuel. Despite their positive impact on the pace of development over a century, these technologies are still in need of improvement to increase efficiency and reduce emission. For instance, while the pre-mix, spark ignition (SI) engine burns fuel more efficiently at near stoichiometric air, its high combustion temperature leads to a higher production of nitrogen oxide gases. The compression ignition (CI) engine has its challenges as well. Liquid fuel spray atomization, evaporation, mixing and combustion all takes place spontaneously in the CI engine cylinder leaving insufficient time for optimal mixing and thus producing a mix of soot and nitrogen oxides. These are the trends observed with conventional fuels (namely, gasoline for SI engine and diesel for CI engine). A lot still needs to be learnt about biodiesel combustion and the most effective combustion strategy that will produce optimal engine performance. Biodiesel has a diverse supply source with a unique chemical finger print that requires careful evaluation and categorization. Given Africa's rapid urbanization and land resources, moringa, jatropha and waste vegetable oil provide a unique niche

for biodiesel production on a large scale. A comparative evaluation of pure biodiesel derived from these sources may provide useful insights about these new supply options and alter the energy equation in sub-Saharan Africa.

Traditionally, biodiesel had been sourced from edible vegetable oil; about 93% of global biodiesel is produced from edible oil and supply sources have been mostly secured from agricultural industries [3]. However, it is becoming increasingly clear to most stakeholders that this trend is unsustainable in the longer term because of the food versus fuel dispute it has triggered [4]. Biodiesel production uses around 4.4 million hectares of arable land in the European Union [10]. Replacing 10% of EU diesel with biodiesel would account for around 19% of world edible oil production in 2020 which means more land will be planted with crops and more land somewhere in the world will be converted into farmland, thereby releasing greenhouse gas emissions. The alternative to these are non-edible oils, hence the focus on moringa, jatropha and waste restaurant oil.

Moringa and jatropha trees are tropical and sub-tropical trees growing easily on marginal land and having an oil yield of 40% to 60%. They can be propagated easily in drought prone areas and are highly adaptable [5]. Both plants have found multiple uses and this is particularly so for moringa whose leaves and other extracts serve as remedies for a diverse range of ailments in sub-Saharan Africa. Large scale cultivation of these plants for biodiesel production will offer additional incentives to farmers.

Waste restaurant oil is set to play an important role in biodiesel fuel source in the coming decades on the continent. The demographic shift on the continent toward a younger more urbanised and educated population has become a dominant trend in the last few decades. By 2030 Africa's population is projected to reach 1.5 billion, with 748 million (53.5%) of this population living in urban centres [6, 7]. This trend is set to accelerate and accompanying this will be an increase in restaurant waste oil generation. The only economically beneficial and sustainable ways of disposing off this waste is its use it in the production of biodiesel oil.

1.2 Statement of Problem

Primarily, the world relies on five main sources of energy, namely: petroleum, natural gas, nuclear, solid fuels (coal etc) and renewable energy source (RES). The share of petroleum and natural gas usage along with nuclear energy has remained fairly constant at approximately 61% and 13 - 14% respectively within

the period of 1999 - 2009 [8]. Renewable energy source (RES) has increased from 5% to 9% within the same period as a result of marginal decrease in the use of coal. According to British Petroleum, global energy consumption for the year 2003 was estimated at 9.7 Gtoe with North America and Europe accounting for most of the consumption [9]. The likelihood of these numbers accelerating is quite strong as the rest of the world's economy is increasing at a fast pace. Given the convergence of technology and the free movement of capital, this has become the default trend.

Fossil energy sources (petroleum, natural gas and coal) account for about 80% of global energy sources. Fossil sources are finite, environmentally unsustainable, and reserves are unevenly distributed hence, are subject to geopolitical risk and price fluctuation. The Middle East, for example, accounts for about 63% of global oil reserves [9]. Given their finite nature, oil is projected to peak at around 2015 - 2030. The issue of environmental degradation poses significant challenge to the use of fossil fuel. Thus, historically, fossil fuels have been associated with insecurity, price volatility and negative environmental impacts. Nuclear energy sources have their challenges as well. Nuclear technology has always been viewed with suspicion since Hiroshima and Nagasaki [1,25]. This suspicion heightened when the Chernobyl meltdown occurred in Russia and, since the Fukushima incidence, public resistance to nuclear energy source has crystallized into a phase-out policy in Japan and Germany [25]. This inevitably indicates that the only scope for growth in the energy spectrum to meet growing demand is through renewable energy source (RES).

Beside the finite nature of fossil fuel, its potential for political instability, and the risk associated with the use of nuclear energy, the most significant challenge, going forward, is concern for the environment. Significant bodies of evidence exist which suggest that continuous use of the current energy mix is environmentally unsustainable. The use of petroleum derivatives as fuel is associated with the emissions of particulate matter (PM), oxides of sulphur (SO_2) and poly-aromatic hydrocarbon [9]. The extraction process of petroleum, to some degree, involves harmful practices such as echo-sounding (causing sub-surface geological deformation that could potentially destroy ground water supply), gas flaring, oil spills, well blowout (e.g horizon deep spill, Niger-delta spills [26]) use of radioactive material for well logging. Mid-stream refining activities pose risks such as harmful discharges of effluent and other toxins. Griffin Shay [10] stated that increased use of petroleum fuel will intensify global warming caused by carbon dioxide (CO_2) emission. Besides CO_2, Methane (CH_4) and oxides of Nitrogen (NO_X) are some of the other emissions associated with activities related to petroleum usage that will also intensify global warming.

In addition to climate change concerns, the health impacts of these emission are significant. During combustion of petroleum derivatives in internal combustion engines, the following are emitted into the atmosphere through the exhaust: oxides of Nitrogen (NO_X), soot, carbon monoxide (CO), unburnt hydrocarbon (UHC), aldehyde (with their carcinogenic derivatives), sulphur oxide (SO_2) and lead compounds amongst others. NO_2 can react with some hydrocarbon to concentrate Ozone (O_3). NO_2 is linked with increase susceptibility to respiratory infection, influenza, lung irritation, increase of air way resistance in asthma, bronchitis and pneumonia, decreased pulmonary function, increased sensitivity to allergies [11]. Ozone (O_3) irritates mucous membranes of the respiratory system causing coughing and clogging. Damage to lung tissue can aggravate chronic heart disease, asthma, bronchitis and emphysema [12]. SO_2 is also a respiratory irritant. It can impair lung function, damage lung tissue, aggravate asthma, emphysema and lead to suffocation and throat irritation. It is clear that from a public health point of view, mitigation strategies for these emissions are a global imperative. Therefore, as the world races toward a sustainable solution to the energy challenge, sub-Saharan Africa must find and secure a renewable source that is fully domesticated, universally accessible and provides a competitive edge that guarantees healthy economic growth.

1.3   Research Motivation

Transportation is one of the key components of modern society; without efficient and convenient public and private transport, the living standards attained today would have been impossible. In the U.S.A for example (one of the countries with the most advanced economy and highest standard of living), transportation accounted for 28% of the total energy consumption in 2005, with 97% of that energy derived from petroleum [1]. At the domestic level, South African production of petrol and diesel has decreased marginally from 20.2 billion litres in 2002 to 19.7 billion litres in 2013 due to capacity constrains but, consumption has grown at 3% annually during the same period (see figure 1.1) [28]. There are fears that the widerning gap between production and consumption could potentially inhibit economic growth if local solutions are not found.
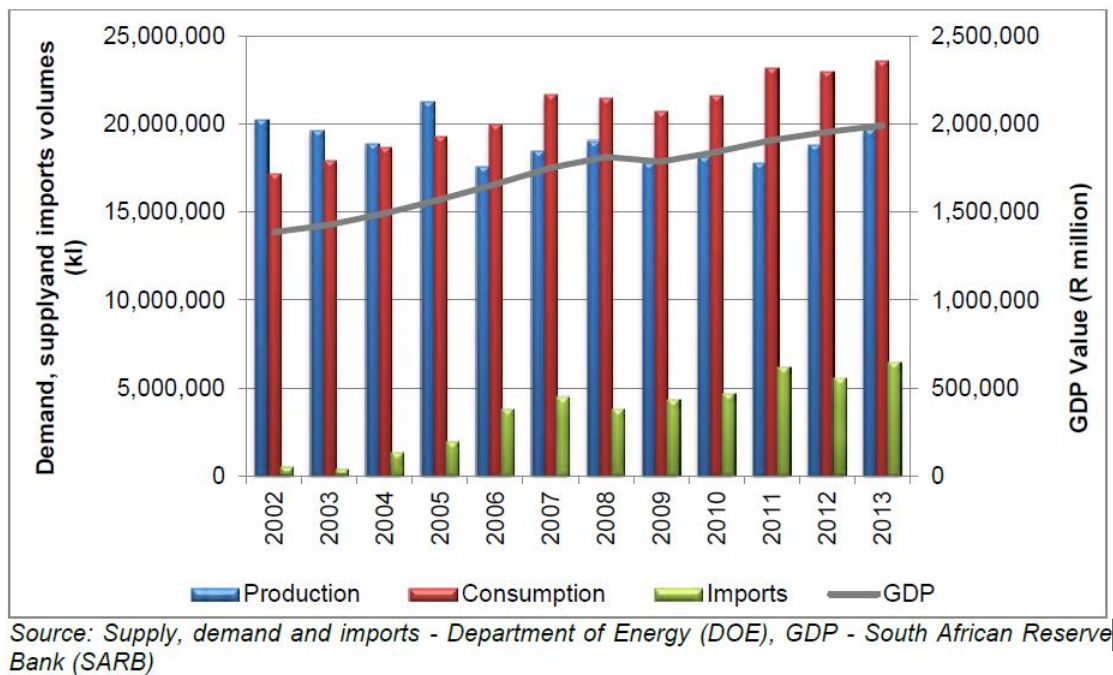
Figure 1 1: South Africa supply and demand data of petrol and diesel

Considering that the most important prime movers for this sector is the internal combustion engine. Substituting petroleum sourced fuel for renewable fuel in this sector will therefore have a direct impact in mitigating some of the challenges identified with the use of petroleum based fuel. Biodiesel has been identified as one suitable alternative in compression ignition (CI) engines. This fuel source is considered carbon neutral [8]. It is more universally accessible. Biodiesel is produced from transesterification of vegetable oil or animal fats using alcohol in the presence of an alkaline catalyst. Comparatively, its use in the internal combustion engine (ICE) is considered less harmful to the environment because it leads to reduction in carbon monoxide (CO) [13, 14], particulate matter (PM) [15, 16] and soot precursors [17]. However, contradictory findings were reported about oxides of Nitrogen (NO_X) emissions [13, 18-20] and reduction in engine power has been reported in the literature [21, 22]. Hence, continued research has been recommended to provide further insight and find better ways of employing its inherent advantages.

On the supply side, significant mileage has been covered although a lot still needs to be achieved. Biofuels sources such as barley, wheat corn, sugar, soybeans, castor, rapeseed and palm have been extensively cultivated and used for biofuel production but resistance against their use has built over time because these edible oil sources were in direct competition with human food requirements. It stood therefore to reason

that, going forward, these first generation sources will not be viable. For example, as at 2010, 12.5% of the world's population were malnourished [23]. It was also clear that the supply gap between petroleum and vegetable oil sources could not be bridged through a perilous and controversial source because global petroleum and vegetable oil production were at 4.018 and 0.107 billion tonne respectively [9]. This supply dilemma is further observed by looking at the major suppliers and importers of vegetable oil. The major exporters of vegetable oil are Malaysia, Argentina, Indonesia, Philippines and Brazil (countries with inelastic production infrastructure because of their expanding population and limited land resources) and the major importers were China, Pakistan, Italy and the United Kingdom (most of whom are straining with insatiable demand or are desperately poor).

As a result, a second generation of biodiesel source has been identified and is currently being aggressively researched and, includes non-edible biodiesel source such as waste restaurant oil, jatropha, algae, lignocellulose biomass etc. These possess the advantage (particularly the algae) of high growth rate, tolerance to adverse environmental condition, high CO_2 trapping and fixation abilities, high oil content (sometime exceeding 80% of their dry weight), and high yield per hectare. The most significant drawbacks are that production is not yet cost effective and there are many technical barriers that still need to be overcome [24]. Despite these, the use of RES in transportation is on the increase particularly in the EU and North America [8].

Table 1.1: Top world oil producers, exporters, consumers, and importers
(millions of barrels per day)

Producers[1]	Total oil production	Exporters[2]	Net oil exports	Consumers[3]	Total oil consumption	Importers[4]	Net oil imports
1. *Saudi Arabia*	10.72	1. *Saudi Arabia*	8.65	1. United States	20.59	1. United States	12.22
2. Russia	9.67	2. Russia	6.57	2. China	7.27	2. Japan	5.10
3. United States	8.37	3. Norway	2.54	3. Japan	5.22	3. China	3.44
4. *Iran*	4.12	4. *Iran*	2.52	4. Russia	3.10	4. Germany	2.48
5. Mexico	3.71	5. *United Arab Emirates*	2.52	5. Germany	2.63	5. South Korea	2.15
6. China	3.84	6. *Venezuela*	2.20	6. India	2.53	6. France	1.89
7. Canada	3.23	7. *Kuwait*	2.15	7. Canada	2.22	7. India	1.69
8. United Arab Emirates	2.94	8. *Nigeria*	2.15	8. Brazil	2.12	8. Italy	1.56
9. *Venezuela*	2.81	9. Algeria	1.85	9. South Korea	2.12	9. Spain	1.56
10. *Norway*	2.79	10. *Mexico*	1.68	10. Saudi Arabia	2.07	10. Taiwan	0.94
11. *Kuwait*	2.67	11. Libya	1.52	11. Mexico	2.03		
12. *Nigeria*	2.44	12. *Iraq*	1.43	12. France	1.97		
13. Brazil	2.16	13. Angola	1.36	13. United Kingdom	1.82		
14. *Iraq*	2.01	14. Kazakhstan	1.11	14. Italy	1.71		

NOTE: OPEC members in italics.
Source: Energy Information Administration (EIA) [27].

Currently the flagships of the internal combustion engine are the spark ignition (SI) engine and the compression ignition (CI) engine. The SI engine is characterized by premixed charge at near stoichiometric air-fuel ratio (Ø~ 1), flame propagation is spark assisted with a spark plug and load control is achieved by varying the pumping of charge into the cylinder via the throttle effect which leads to low thermal efficiency at partial load. These, coupled with high temperature at peak load, causes significant

N0$_X$ production constituting the major challenge faced with the use of the SI engine. The compression ignition (CI) engine on the other hand is characterized by a compression ratio of between 12 - 24, diffuse flame, turbulent flow and auto-ignition via elevated pressure and temperature around top deal centre (TDC). The compression ignition has a higher thermal efficiency comparatively than the SI engine. A critical part of its operation is the ignition delay (defined as the time difference between the start of injection and the start self-ignition). The ignition delay mechanism is governed by physical as well as chemical kinetic processes. The physical process proceeds sequentially through droplet formation, collision, break-ups, evaporation and vapour diffusion. The chemical kinetic process involves species and radical formation proceeding through low temperature reaction (LTR), negative temperature co-efficient (NTC) and high temperature reaction (HTR). The challenge is that the time scales for the physical processes are often larger than those of the chemical processes hence, ignition often commence before the physical processes are completed. This inevitably leads to a complex system of charge, flame and thermal stratification that produces both high NO$_X$ in some regions and high soot precursors and UHC in others. Research focus therefore, has been to develop engines that synergizes the performance of SI and CI by increasing thermal efficiencies (as is the case with the CI engine) and mitigating NO$_X$ UHC and soot formation (as is the case with the SI engine). From the foregoing it is clear that there are many challenges facing the efforts to utilize biodiesel as fuel in transportation. These challenges are encountered as knowledge gaps in performance of biodiesel from non-edible sources, supply constraints and lack of technology platforms that can combust biodiesel from diverse backgrounds to give acceptable performance.

1.4   Research Question

Given the rationale for this study, the relevant question that if answered, could address some of the problems identified with the extraction, production and use of biodiesel derived from jatropha, moringa and waste restaurant oil, include to the following:

1. To what extent are extraction and production method/data for biodiesel derived from non-edible sources identified in this work aligned with historical data and in line with set standards for biodiesel application?

2. Can biodiesel extraction and production technique be further simplified and associate cost reduced?

3. Is a numerical approach to property determination of biodiesel applicable and are the data consistent with biodiesel standards?

4. Are the case study sample performance and emission data from compression ignition engines comparable to conventional diesel fuel and international benchmarks? Where gaps exist, what are the likely remediation strategies?

5. Can a generic combustion strategy be proposed to achieve relative convergence in performance and emission for the test samples and conventional diesel?

1.5   Aims and Objectives

The aim of this research is to evaluate the viability of using pure biodiesel derived from non-edible food sources such as jatropha, moringa and waste restaurant oil in compression ignition (CI) engines and in doing so, identify the difficulties associated with the application. At the end of the study, it is hoped that observed discrepancies in performance and emission data existing between the test samples and industry benchmarks can be properly contextualized and likely remediation strategies proposed where unacceptable gaps exist. The objectives of the research include the following:

1. To extract and produce biodiesel from jatropha, moringa and waste restaurant oil that meet ASTM standards for fuel use in compression ignition engines.

2. To develop a numerical scheme that can consistently predict the transport and thermodynamic properties of the fuel samples, and to experimentally validate the scheme.

3. To evaluate the performance and emission of a compression ignition (CI) engine running on the fuel samples under investigation in comparison to diesel fuel with the purpose of benchmarking the performance and emissions against industry standards and emission regulations.

4. To investigate the extent and reasons for the gaps (if any) observed in (3) and suggest remediation consistent with established scientific knowledge in the field.

5. To propose a generic combustion strategy for compression ignition engines that will accommodate biodiesel derived from the test samples in a manner that achieves performance convergence with diesel while producing better emission results. This will also require the identification of a numerical pathway for the research.

1.6   Research Significance

Across the globe, significant resources have been mobilized to find alternative sources of energy for the reasons stated earlier. Different regions and countries have focused attention at source of supply and technical processes that give them comparative advantages. In sub-Saharan Africa, renewable energy alternatives for transportation have huge potential sources, one of which is biodiesel derived from jatropha, moringa and waste restaurant oil. Considerable research has been ongoing in this area but some gaps have not been addressed.

There is a clear need to conduct evaluations that enable precise technical classification of the performance and emission of pure biodiesel derived from niche sub-Sahara Africa sources and to filter the data through global standards and regulations. Through this, challenges can be identified and plans of action mapped out to tackle them. It is necessary to identify and assemble the right set of tools and technique needed to conduct studies on these biodiesel sources in a manner that optimises available resources.

The stated goal of this work is to extract, produce and test biodiesel from moringa, jatropha and waste restaurant oil using a traditional as well as a 'wild card' approach (through the use of distilled gasoline as a solvent), to compare performance data with international standards and regulations while also identifying numerical pathways for further studies that could potentially lead to developing an optimal combustion strategy. If these goal are realised, they could secure a viable renewable energy source for sub-Saharan Africa.

1.7   Thesis Overview

The thesis chapters are structured in a manner to sequentially tackle the questions posed in this study. The thesis is a compilation of research outcomes of publications and conference papers as stipulated by the University of KwaZulu-Natal for the awarding of the postgraduate degree. It consists of eight chapters.

Chapter 1 introduced the study, identified the challenge, highlighted the motivation, raised the question, and pointed out the aims and objectives of the study. The significance of the study was also stated.

Chapter 2 reviews the extraction, production and testing of biodiesel. Highlights of experimental methods of determining biodiesel properties were reviewed.   Performance and emission work on biodiesel/biodiesel blend and normal diesel using experiment were also reviewed.

Chapter 3 presents the first paper contribution which reviewed numerical approaches to combustion studies of biodiesels.

Chapter 4 provides detailed information on the material and experimental method adopted in the work.

Chapter 5 presents the second paper contribution which provides details of the extraction, production and experimental property data. The numerical scheme for determining the sample fuel properties with the experimental validation data are presented.

Chapter 6 presents the third paper contribution to the research. It describes the detailed approach adopted in obtaining the performance and emission data for the test samples and presents a comparative evaluation of the results with internationally accepted benchmarks for performance and emissions of compression ignition (CI) engines.

Chapter 7 is the fourth paper contribution to the thesis. This paper, besides presenting a brief interpretation of the performance data, gives an in-depth evaluation of emission patterns particularly for oxide of nitrogen (NO_x) and carbon (ii) oxides (CO) and suggested possible remediation.

Chapter 8 summarizes the results and draws a conclusion from the findings.

1.8   Research Scope and Delineation

This thesis covers research materials gleaned from theoretical and experimental work on, or related to, the sourcing, extraction, production and testing of biodiesel derived from moringa, jatropha and waste restaurant oil. On the fuel samples properties, a numerical prediction tool is presented along with primary and secondary experimental data used for its validation. Remediation strategies proposed for observed gaps in fuel sample performance and emissions (obtained from test runs on an engine test rig) are provided as action plans for future studies in the form of a full CFD (computational fluid dynamics) numerical studies with prescribed validation tools. The thesis scope did not cover the execution of the CFD proposal owing to the absence of the relevant equipment and software to facilitate the work scheme.

References

[1]   A. McIlroy. et al. "Basic research needs for clean and efficient combustion of 21st century transportation fuels,", Report of the Basic Energy Sciences *Workshop on Clean and Efficient Combustion of 21st Century Transportation Fuels, Office of Science, U.S. Department of Energy.*2006. Available at: http://science.energy.gov/~/media/bes/pdf/reports/files/ctf_rpt.pdf.

[2]   Health Effects Institute. "Airborne particles and health: HEI epidemiologic evidence," Cambrige, MA: Health Effects Institute, Available*:* www.healtheffects.org. 2001, date accessed 15/11/2015

[3]   M. M. Gui, K. T. Lee, and S. Bhatia, "Feasibility of edible oil vs. non-edible oil vs. waste edible oil as biodiesel feedstock," *Energy* vol. 33 pp. 1646-1653, 2008.

[4]   A. A. Refaat, "Different techniques for the production of biodiesel from waste vegetable oil," *International Journal of Environmental Science and Technology,* vol. 7, pp. 183-213, 2010.

[5]   B. N. Divakara, H. D. Upadhyaya, S. P. Wani, and C. L. L. Gowda, "Biology and genetic improvement of Jatropha curcas L.: A review," *Applied Energy,* vol. 87, pp. 732-742., 2010.

[6]   M. Mubila, "Briefing notes for AfDB long term strategy," *African Development Bank Group,* pp. 2-3, 2012.

[7]   B. Cohen, "Urbanization in developing countries: current trends, future projections, and key challenges for sustainability, committee on population " Washington DC: National Research Council, Committee on Population, 2005.

[8]   N. P. Komninos and C. D. Rakopoulos, "Modeling HCCI combustion of biofuels: A review," *Renewable and Sustainable Energy Reviews* vol. 16 pp. 1588-1610, 2012.

[9]   R. K. Pandey, A. Rehman, and R. M. Sarviya, "Impact of alternative fuel properties on fuel spray behavior and atomization " *Renewable and Sustainable Energy Reviews* vol. 16 (2012), pp. 1762-1778, 2011.

[10]   M. Balat, "Potential alternative to edible oils for biodiesel production- A review work," *Energy conversion   and management,* vol. 52(2011), p. 12, 2010.

[11]   U. N. D. Programme, "World energy assessment," *Energy and the Challenge of Sustainability,* New York: United Nations, 2016.

[12]   E. Alptekin and M. Canakci, "Determination of the density and the viscosities of biodiesel-diesel fuel blend," *Renewable Energy,* vol. 33, pp. 2623-30, 2008.

[13]   H. K. Ng and S. Gan, "Combustion performance and exhaust emissions from the non-pressurised combustion of palm oil biodiesel blends," *Applied Thermal Engineering,* vol. 30, no. 16, pp. 2476-2484, 2010.

[14]   A. Ghorbani, B. Bazooyar, A. Shariati, S. Mohammad Jokar, and H. Ajami, and A. Naderi, "A comparative study of combustion performance and emission of biodiesel blends and diesel in an experimental boiler," *Applied Energy* vol. 88, no. 12, pp. 4725-4732, 2011, .

[15]   M. Balat and H. Balat, "Progress in biodiesel processing," *Appied. Energy,* vol. 87, 6, pp. 1815-1835, 2010.

[16]   P. Rounce, A. Tsolakis, and A. P. E. York, "Speciation of particulate matter and hydrocarbon emissions from biodiesel combustion and its reduction by after treatment," *Fuel,* vol. 96, pp. 90-99, 2012.

[17]   C. K. Westbrook, W. J. Pitz, and H. J. Curran, "Chemical kinetic modeling study of the effects of oxygenated hydrocarbons on soot emissions from diesel engines," *Journal of Physical Chemistry* vol. 110, pp. 6912-6922, 2006.

[18]   J.-H. Ng, H. K. Ng, and S. Gan, "Engine-out characterisation using speed-load mapping and reduced test cycle for a light-duty diesel engine fuelled with biodiesel blends," *Fuel,* vol. 9, pp. 27002709, 2011. .

[19]   M. Lapuerta, O. Armas, and J. Rodriguez-Fernandez, "Effect of biodiesel fuels on diesel engine emissions," *Progress in Energy and Combustion Science,* vol. 34, p. 198-223, 2008.

[20]   G. Fontaras, *et al.*, "Effects of biodiesel on passenger car fuel consumption, regulated and nonregulated pollutant emissions over legislated and real-world driving cycles," *Fuel,* vol. 88, p. 1608-1617, 2009.

[21]   S. Murrilo, J. L. Miguez, J. Porteiro, E. Granada, and J. C. Moran, "Performance and emission study in the use of biodiesel in outboard diesel engines," *Fuel,* vol. 86, p. 1765-1771, 2007.

[22]   X. L. Zheng, T. F. Lu, and C. K. Law, "Experimental counterflow ignition temperatures and reaction mechanisms of 1,3-butadiene,"*Proceedings of the Combustion Institute,* vol. 31, pp. 367-375, 2007.

[23]   FAO of UN, (2010), Global hunger declining, but still unacceptably high [Online]. Available: http://www.fao.org/docrep/012/al390e/al390e00.pdf,.date accessed: 14/10/2015.

[24]   S. N. Naik, V. V. Goud, P. K. Rout, and A. K. Dalai, "Production of first and second generation biofuels: a comprehensive review," *Renewable and Sustainable Energy Reviews,* vol. 14, pp. 578–97, 2010.

[25]   Z. Csereklyei "Measuring the Impacts of Nuclear Accidents on Energy Policy" *Department of Economics Working Paper No. 151*, 2013 Available at http://epub.wu.ac.at/3826/1/wp151.pdf

[26]   A. A. Kadafa "Oil Exploration and Spillage in the Niger Delta of Nigeria" *Civil and Environmental Research* Vol 2, No 3 pp 38-49, 2012.

[27]   http://www.infoplease.com/ipa/A0922041.html, date accessed: 16/10/2016

[28]   http://www.energy.gov.za/files/media/explained/Overview-of-Petrol-and-Diesel-Market-in-SA-between-2002-and-2013.pdf. Date accessed: 29/10/2016.

CHAPTER 2: FUNDAMENTALS OF BIODIESEL TECHNOLOGY

2.1 Background

Over a century ago, Rudolf Diesel used vegetable oil as fuel for the compression ignition (CI) engine [1]. The introduction of cheap petroleum fuel subsequently led to the evolution of the diesel derivative of petroleum being used as the main fuel source for diesel engines. However, in the 1930s and 1940s, vegetable oil resurfaced and was used intermittently as a fuel in the CI engine, albeit in emergency cases. The growing concern for the environment, finite reserves of crude oil and increasing demand for automotive fuel has intensified the need to explore the potential of biodiesel.

As an alternative to diesel, biodiesel has the advantage of being a renewable source as well as being biodegradable and non-toxic. Biodiesel emissions are low comparatively [2]. Biodiesel produced from vegetable oil can be used directly or as blends with petroleum diesel; it can be produced through micro emulsions, thermal cracking (pyrolysis) or trans-esterification. The use of biodiesel is associated with a reduced pollutant emission and therefore reduced exposure to probable carcinogens [3].

Fat and oil are generally water insoluble substances found in plant and animals. They contain one mole of glycerol and three moles of fatty acids which is why they are called triglycerides [4]. The fatty acids have varying carbon chain lengths and double bond numbers. Normally the transesterification process converts the triglycerides into fatty acid methyl esters (FAME) using alcohol in the presence of a catalyst. The transesterification process is affected by the free fatty acid (FFA) content and water when an alkaline or acid catalyst is used [2].

High levels of unsaturation in some natural glycerides results in their being found as liquid at room temperature, but their high viscosity makes their use as biodiesel impracticable. Fats, on the other hand, because of their high level of saturation, are commonly found in solid state at room temperature [2].

2.2 Biodiesel Production and Standards

2.2.1 Biodiesel Oil Extraction

Across the globe, 350 oil bearing crops have been identified as potential feedstocks for biodiesel extraction [5-7]. The factors that govern the best choice of feedstock are the cost and the possible scale of production,

regional climatic condition as well as soil condition and agricultural practices. Edible oils were the feedstocks for producing the first generation biodiesel accounting for 95% of production currently [8]. But concerns have been raised about the possibility of fuel need crowding-out food supply sources. As a result, attention has been redirected to non-edible feedstock. Non-edible feedstock also has the advantage of being readily available, utilizing waste land and reducing deforestation.

Oil extraction from seed can be achieved via: (i) mechanical extraction; (ii) solvent extraction; and (iii) enzymatic extraction. Mechanical extraction can be achieved through a manual ram press. A yield of between 60% - 65% and 68% - 80% respectively can be obtained from the processes. Oil extracted by mechanical means requires a further process of filtering and degumming. A further drawback to mechanical extraction is that each seed requires a different extraction design for optimal yield [9, 10].

Solvent extraction otherwise known as leaching is the means by which oil constituents are removed from solids using liquid solvents. The rate of extraction is determined by particle size, the type of liquid chosen, temperature and the degree of agitation. Often, the solvent chosen has low viscosity which allows for deep penetration of the seed fibre matrix. Solvent extraction is only economically viable if production scale exceeds 50 ton of biodiesel per day [9]. The three common methods here are: (i) Hot water extraction; (ii) Soxhlet extraction; and (iii) Ultrasonic technique [8].

Oil extraction via the use of enzymes is one of the most promising extraction methods available. The process involves the use of enzymes to extract oil from pulverized seeds. Its key advantage is that it is environmentally friendly and no volatile organic material is produced. Long residence time has been identified as the only major drawback for this process.

2.2.2 Direct use of Vegetable Oil or its Blends

Bartholomew [11] suggested that vegetable oil, which is a renewable fuel source, should be the primary energy and that petroleum (or any finite source) should be the 'alternative' to ensure the security of supply and guarantee sustainability. This idea began to gain traction in the 1980s. A blend of 10% sunflower oil was used by Caterpillar in a pre-combustion engine to achieve 100% engine load without any engine retrofitting in South Africa during the oil embargo [2]. A 100% vegetable oil substitution was not practicable but a 20% vegetable oil to 80% diesel was successful. A 50/50 ratio for short term runs was found to be technically feasible.

A blend of 95% used cooking oil to 5% diesel was also employed to power a fleet of diesel engines with satisfactory results [12]. The oil was preheated to compensate for lower ambient temperature. Coking and carbon build-up was not observed. The only challenge observed was lubricating oil contamination caused by the increase in viscosity owing to the polymerization of poly-unsaturated vegetable oils. A 4000 mile to 4500 mile lubricating oil change-over was employed to remedy the problem.

Direct use of vegetable oil as fuel in place of diesel has the following advantages: (i) ready availability; (ii) it is renewable; (iii) it's heat content is 80% of the heat content of diesel; (iv) it is portable because of higher density. The disadvantages are: (i) high viscosity leading to cold flow challenges; (ii) reduced volatility; (iii) reduced reactivity of the unsaturated component [13]. Problems only manifest after vegetable oil has been used for an extended period of time and take the form of: (1) coking which make fuel atomization difficult; (2) deposition of carbon; (3) sticking of oil rings; (4) gelling of the lube oil.

Degummed soybean oil and diesel fuel blends in the ratio of 1:2 and 1:1 have been tested in a John Deere 6-cylinder engine with a 6.6L displacement. The engine was direct injection, turbo-charged running on a 600h test protocol [14]; a ratio of 1:2 was found to give an acceptable performance. This implies that this blend can be used on a temporary basis for agricultural equipment for short runs in times of fuel shortages.

The two most severe problems associated with the direct use of vegetable oil are incomplete combustion and lube oil deterioration [15]. The unsaturated component of the fatty acid methyl esters (FAME) are susceptible to polymerization and gum formation caused by oxidation. During combustion, the gums' combustion are incomplete leading to carbon deposits. To tackle this problem, blending is often employed [15]. A 25% sunflower oil blended with 75% diesel has a viscosity of 4.88 cSt at 40°C but the recommended American Society of Testing and Material (ASTM) value is 4.0 cSt at 40 ^{o}C [16]. As result, this blend was not recommended for long term use.

2.2.3   Micro Emulsions

One of the methods adopted to solve the problem of high viscosity of vegetable oil was the use of micro emulsions. Butanol, ethanol or methanol has been tested as a micro emulsion solvent in vegetable oil [17]. This process works via the colloidal dispersion of isotropic fluid at the micro structural level. This has the effect of improving spray characteristics through explosive vaporization of the solvent with the lower boiling point of the two immiscible fluids. This method of producing fuel from vegetable oil can

give results that are as good as diesel on a short term basis regardless of the lower energy content and cetane number [18].

Shipp non-ionic (SNI) diesel produced from 50% diesel, 25% alkaline refined and degummed soybean oil, 5% ethanol, and the remaining portion being 1-butanol, when subjected to 200h EMA test, passed fairly well except with some deposits on the injector tip, in-take valves and some cylinder parts [19]. A ternary phase equilibrium diagram was used to determine the best formulations [17]. Butanol, hexanol and octanol all met ASTM standards for viscosity.

2.2.4   Pyrolysis

The thermal cracking of oil in the presence of a catalyst can yield two or more smaller molecules with the right property for use in a CI engine [20]. This process involves heating vegetable oil in the absence of oxygen. The process is difficult to characterize owing to multiple reaction pathways that are possible and the diverse nature of the end product. Animal fat, vegetable oil and natural fatty acids can be thermally cracked. Vegetable oil pyrolysis on a large scale has been ongoing since the First World War. Chang and Wan [21] reported large scale pyrolysis of Tung oil. After saponification in line, Tung oil was thermally cracked to yield a crude oil which was further refined to obtain diesel.

Using ASTM standard distillation apparatus, soybean oil was thermally cracked and distilled in air [22, 23]. The main components resulting from the cracking process were alkanes and alkenes.

2.2.5   Transesterification

The reaction of fat or oil with alcohol to form esters and glycerol is known as transesterification. It is the most widely used means of producing biodiesel. The yield and reaction rate can be improved by using a catalyst. Methanol, ethanol, propanol and butanol are the most common alcohols used for the transesterification process. Methanol and ethanol are often preferred because of their cost and the ease with which NaOH (Sodium hydroxide) dissolves in them. The catalyst could be alkaline such as sodium hydroxide (NaOH), potassium hydroxide (KOH), carbonates or acid such as sulphuric acid and hydrochloric acid [2]. Catalysts are needed for transesterification because alcohol is barely soluble in oil. The catalyst enhances the solubility of alcohol in oil. Alkaline catalysts have been found by most researchers to be much faster than acid catalysts [8]. They are 4000 times faster than other compounds in

the same amount [24]. Alkaline catalyst can produce high quality biodiesel within a short time (30 minutes – 60 minutes) but there is a caveat to its use, that is, FFA levels should be between the range of 0.5% to 3% as anything above this level produces soap instead of ester [25]. Other disadvantages associated with the use of alkaline catalysts are: an energy intensive process; the recovery of glycerol is problematic; the catalyst has to be removed from the product.

Some researchers have observed that acid catalysts are more tolerant than alkaline catalysts particularly for oil having high FFA and water contents but the reaction is too slow (3 hrs. - 48 hrs) [8]. As a compromise method, acid catalysts are sometimes used to reduce the FFA levels before alkaline catalysts are then used for the actual transesterification process. But again, this process produce salt through the neutralization reaction and requires large amounts of water for post processing washing to remove the salt from the product [24].

2.2.6 Biodiesel Standard and Properties

With increasing interest being shown in the use of biodiesel as an alternative source of liquid fuel, it became necessary to set standards for its properties [26, 27]. Various jurisdictions established or are in the process of developing a property benchmark for biodiesel. These include, the United States (ASTM D6751), Europe (EN 14214), South Africa and Brazil. The first two are the most widely accepted standards and their details are provided in Table 2.1 and 2.2.

Table 2. 1: ASTM Biodiesel Standard D 6751 [28]

Property	Test method	Limits	Units
Flash point (closed cup)	D 93	130.0 min	°C
Water and sediment	D 2709	0.050 max	% volume
Kinematic viscosity, 40°C	D 445	1.9–6.0	mm²/s
Sulfated ash	D 874	0.020 max	% mass
Sulfur	D 5453	0.0015 max (S15)	
		0.05 max (S500)	% mass
(ppm)			
Copper strip corrosion	D 130	No. 3 max	
Cetane number	D 613	47 min	
Cloud point	D 2500	Report	°C
Carbon residue	D 4530	0.050 max	% mass
Acid number	D 664	0.50 max	mg KOH/g
Free glycerin	D 6584	0.020	% mass
Total glycerin	D 6584	0.240	% mass
Phosphorus content	D 4951	0.001 max	% mass
Sodium/potassium	UOP 391	5 max. combined	ppm
Distillation temperature, atmospheric equivalent temperature, 90% recovered	D 1160	360 max	°C

[a]The limits are for Grade S15 and Grade S500 biodiesel, with S15 and S500 referring to maximum sulfur specifications (in ppm).

Table 2. 2: European Biodiesel Standards EN 14214 for Vehicle Use and EN 14213 for Heating Oil Use [28]

Property	Test method	Limits EN 14214	Limits EN 14213	Unit
Ester content	EN 14103	96.5 min	96.5 min	% (mol/mol)
Density; 15°C	EN ISO 3675, EN ISO 12185	860–900	860–900	kg/m³
Viscosity; 40°C	EN ISO 3104, ISO 3105	3.5–5.0	3.5–5.0	mm²/s
Flash point	EN ISO 3679	120 min	120 min	°C
Sulfur content	EN ISO 20846; EN ISO 20884	10.0 max	10.0 max	mg/kg
Carbon residue (10% distillation residue)	EN ISO 10370	0.30 max	0.30 max	% (mol/mol)
Cetane number	EN ISO 5165	51 min	—	
Sulfated ash	ISO 3987	0.02 max	0.02 max	% (mol/mol)
Water content	EN ISO 12937	500 max	500 max	mg/kg
Total contamination	EN 12662	24 max	24 max	mg/kg
Copper strip corrosion (3h, 50°C)	EN ISO 2160	1	—	degree of corrosion
Oxidative stability, 110°C	EN 14112	6.0 min	4.0 h	h
Acid value	EN 14104	0.50 max	0.50 max	mg KOH/g
Iodine value	EN 14111	120 max	130 max	g I₂/100 g
Linolenic acid content	EN 14103	12.0 max	—	% (mol/mol)
Content of FAME with ≥4 double bonds		1 max	1 max	% (mol/mol)
Methanol content	EN 14110	0.20 max	—	% (mol/mol)
MAG content	EN 14105	0.80 max	0.80 max	% (mol/mol)
DAG content	EN 14105	0.20 max	0.20 max	% (mol/mol)
TAG content	EN 14105	0.20 max	0.20 max	% (mol/mol)
Free glycerine	EN 14105, EN 14106	0.020 max	0.02 max	% (mol/mol)
Total glycerine	EN 14105	0.25 max	—	% (mol/mol)
Group I metals (Na + K)	EN 14108, EN 14109	5.0 max	—	mg/kg
Group II (Ca + Mg)	prEN 14538	5.0 max	—	mg/kg
Phosphorus content	EN 14107	10.0 max	—	mg/kg
Cold filter plugging point	EN 116	—		°C
Pour point	ISO 3016	—	0 max	°C
Heating value	DIN 51900-1			
	DIN 51900-2			
	DIN 51900-2	—	35 min	MJ/kg

2.3 Engine Test Protocol, Performance and Emission Regulation

Beyond the basic engine data logging template which requires the measurement of power/torque, engine speed, air flow rate and fuel flow rate alongside the emission, increasingly sophisticated approaches are being recommended to enhance standardization and benchmarking of performance and emissions. An array of measuring equipment is being deployed and stringent test protocols have been recommended to ensure test result reliability and validation. One of the notable test protocols which has been internationally adopted is 1SO 8178-1:2006 with test cycle categorization range between C1, C2, E1, E2, F, G, G3 and H which covers the broad range of engine application types currently in use [29]. This test protocol gives specific detail about loading profile, speed range, test cycle duration etc. The protocol sets rule on the format for obtaining specific performance and specific emission measures which eases the comparative evaluation of those measures with emission regulations in different jurisdictions. Nettles-Anderson et al. [30] used it in their performance evaluation of biodiesel from multiple feedstocks making it possible for them to conduct a qualitative as well as a quantitative evaluation of performance and emissions in absolute terms. Most studies on biodiesel, in failing to adopt this protocol, have only been able to provide a relative measure of emission. This makes it difficult to calibrate accurately and develop remediation strategies given the increasingly stringent regulations on emission.

Rafts of emission regulations have been legislated in numerous countries around the world, including Canada, USA, EU, UK, China, India, Japan, Israel and South Africa. Momentum is clearly in the direction of a common global emission cap that could effectively reduce climate change caused by emissions [31]. The most prominent of these are the United State of America's Environmental Protecting Agency (EPA) standard [32] and the European Union emission cap [33] that spell out in specific terms the limits and enforcement measures. The limits are set to curtail emissions from all internal combustion engines regardless of the fuel types and the application modes. Few attempts have been made to use this test protocol and the emission regulations to evaluate the performance and emission of pure biodiesel from non-edible sources. As a result, only a general review of performance and emissions of biodiesel in CI have been under taken.

2.3.1 Performance of CI Engines Running on Biodiesel

The majority of literature on performance of engines running on biodiesel agree that engine power will drop when biodiesel substitutes diesel in CI engine; most attribute this loss of power to the reduced heating

value of biodiesel [34-36]. The degree of losses varied in all the studies. Some of the studies showed a lower than expected reduction [37-39]. A study conducted by Utlu and Kocak [40] on WFOME (waste frying oil methyl ester) showed a 4.3% and 4.5% drop in torque and power respectively. This reduction, in their opinions, was as a result of high viscosity, density and lower heating value. A 9.1% brake torque loss was observed by Hansen et al. [37] for pure biodiesel at 1900 rpm relative to diesel where the heating value variation was 13.3%. Murillo et al. [35] observed a 14% drop in power for pure biodiesel in a 3-cylinder, naturally aspirated (NA) diesel engine used to power a marine vehicle. The difference in heating value in this case was 13.5% compared to diesel. A 3% − 6% torque and power reduction was observed in a study comparing biodiesel derived from cotton seed oil and diesel where the heating value difference was stated to be 5% [36]. This drop was attributed to difficulties associated with fuel atomization rather than heating value.

Some work showed no significant difference in engine power when pure biodiesel and diesel were comparatively evaluated [41, 42]. A study on diesel and pure biodiesel derived from eight different types of VOME (Vegetable oil methyl ester) established differences of 1.49% and -0.64%, 1.39% and -1.25% between maximum and minimum torque and power respectively.[43]. The results were attributed to higher viscosity, higher BSFC (brake specific fuel consumption), higher oxygen content and higher combustion efficiency for the biodiesel.

2.3.2   Emission Pattern of CI Engine Running on Biodiesel

i.   Particular Matter (PM)

An overwhelming majority of work surveyed showed that when biodiesel substitutes diesel in a CI engine, PM emissions reduce [40, 44 - 46]. In a study conducted by Wu et al. [47] with five pure biodiesels on a turbo-charge Cummins ISBe6 engine with intercoolers, a 53% - 69% reduction of PM was achieved when biodiesel was used in place of diesel. Lin et al. [43] recorded similar reduction patterns of PM for eight types of VOME fuel when it was compared with diesel. Not less than a 50% reduction in PM was common in most of the studies [45, 48, 49].

Some of the work surveyed showed a slightly different outcome where an insignificant level of reduction in PM emission was observed [50]. In all of these works, the reason provided for the result was high viscosity which impeded fuel atomization and considerably reduced the combustion efficiency of the

engine [34, 50]. Among the reasons advanced for PM emission pattern are low heat rejection (LHR) device and load profile. It was also established that the higher the speed, the lower the PM emission [38]. This was because of improved combustion efficiency caused by heightened turbulence in the combustion chamber which reduces thermal as well as charge stratification.

Exhaust gas recirculation (EGR) has been known to increase PM emission. Tsolakisa [51] and Agarwal et al. [52] showed in their work that PM increases by as much as 20% when EGR is used in the engine although the increase was found not as much as that observed in EGR use in the diesel test. In low temperature tests the advantage of low PM in biodiesel driven engines tends to significantly reduce PM emission from a Turbo-unit and direct injection (DI) engine in cold and hot start as investigated by Fontaras et al. [53]. The researchers observed that all emanations tend to increase during cold starts and PM emission increased by 148% during cold starts mainly because of higher viscosity and lower boiling point.

ii.   Oxide of Nitrogen Emission

Close to two-thirds of literature surveyed recorded an increase in NO_X with the use of pure biodiesel. A 15% increase in NOx was observed for a 12% increase in oxygen content of pure biodiesel at high load [54]. Lin et al. [43] conducted a comparative study of eight different kinds of VOME in a diesel engine. Findings showed that higher NO_X emission was associated with the use of the biodiesels. The increases ranged from 5.58% to 25.97% when compared with emission from diesel test runs. But there have also been instances where no significant differences in NO_X emission were established between biodiesel and diesel [55, 56]. In some rare cases, NO_X emission actually reduced with the use of biodiesel [40, 57].

Factors that determine the NO_X emission trend in biodiesel according to the literature surveyed include: (a) the oxygenated content of the biodiesel [44, 57]. Most literature surveyed agreed that oxygen content of biodiesel increases the likelihood of high NO_X emissions. However, some literature also pointed out that this trend was not always consistent [58]; (b) Properties of the feedstock such as cetane number which leads to early burn and a less rapid thermal gradient leading to lower NO_X formation [47, 59]. (c) Engine operating condition. Karabekta [60] conducted a comparative study of NO_X emission from NA and TU and observed that the emissions were higher by as much as 21% for TU compared to NA due to the increase in excess air and the elevated temperature; however, NO_X was also found to increase as load increased [35, 55]. Engine speed also had an effect on NO_X formation. It was observed that NO_X emission

reduced with increased speed and this was attributed to the shorter residence time that proved insufficient for NO formation.

iii.   Carbon (II) oxide (CO)

When biodiesel replaces diesel, a reduction of CO emission is observed [34, 40, 44, 45, 60]. In a work conducted on rapeseed methyl ester by Krahl et al. [61], a 50% reduction in CO was observed when biodiesel replaces diesel. A higher reduction of 73% - 94% was measured by Raheman and Phadatere [62] when karanga methyl ester replaced diesel in their study. Lower reductions have been observed by some authors, for example, Puhan et al. [63], who noted a 30% reduction.

Some work surprisingly showed increases in CO emission [53, 64]. Sahoo et al. [65] observed an increase in CO mission from Jatropha oil. Fontaras et al. [53] also reported a 95% increase of CO emission. The reasons given by the authors for these surprising results were the high viscosity and poor spray characteristics of the biodiesel which led to charge stratification and, subsequently, poor combustion.

In the literature the general trend of reduced CO emissions was attributed to: (i) Oxygen content of fuel [34, 35]. Munillo et al. [35] observed that at full loading, CO emission of diesel gave the highest value at 15.2 g/kWh compared to pure biodiesel value of 11.4 g/kWh. (ii) Properties of biodiesel. Knothe et al. [66] found that CO emission reduction is much higher with increasing chain length of the methyl ester. Wu et al. [47] suggested that the combustion of oxygenated molecules and the high cetane number leads to higher combustion efficiency which reduces CO emission.   (iii) Engine operating conditions. Karabektas's [60] study on a DI engine under TU and NA regimes observed that CO was higher for both diesel and biodiesel in the NA combustion regime. This was because the TU regime delivers more air into the cylinder than the NA regime. Hence, the combustion is more complete. CO emission was also found to increase with increasing load in biodiesel combustion [67]. The reverse is the case for increasing speed. Increasing engine speed leads to reduction in CO emission for biodiesel [57].

iv.   Unburnt Hydrocarbon (HC)

It has been well established that substituting diesel for biodiesel in CI engine leads to a reduction in unburnt hydrocarbons [45, 46]. Wu et al. [47], after conducting studies on five different biodiesels concluded that HC emission reductions were in the range of 45% - 67% on average. Puhan et al. [63] reported a 63% average reduction of HC emission when biodiesel replaces diesel. Sahoo et al. [65]

compared pure biodiesel from Jatropha, Karanga and Polanga with diesel on a 3-cylinder tractor engine using a test mode of 8 cycles and reported a 20.73%, 20.64% and 6.75% reduction of HC respectively. Some studies showed only marginal differences [50, 58].

References

[1] E. Griffin Shay, "Diesel fuel from vegetable oils: status and opportunities," *Biomass and Bioenergy,* vol. 4, pp. 227-242, 1993.

[2] F. Ma, L. D. Clements, and M. A. Hanna, "The effect of mixing on transesterification of beef tallow," *Bioresource Technology,* vol. 69, pp. 289-293, 1999.

[3] T. Krawczyk, "Biodiesel - Alternative fuel makes inroads but hurdles remain," *INFORM* vol. 7, pp. 801-829, 1996. .

[4] N. O. V. Sonntag, "Structure and composition of fats and oils," in *Bailey's Industrial Oil and Fat Products,* vol. 1, D. Swern, Ed. 4th ed.New York: John Wiley and Sons, 1979, p. 1.

[5] E. M. Shahid and J. Jamal, "Production of biodiesel: a technical review," *Renewable and Sustainable Energy Reviews,* vol. 15, pp. 4732-45, 2011.

[6] J. Janaun and N. Ellis, "Perspectives on biodiesel as a sustainable fuel," *Renewable and Sustainable Energy Reviews,* vol. 14, pp. 1312-1320, 2010.

[7] I. M. Atadashi, M. K. Aroua, and A. Abdul Aziz, "High quality biodiesel and its diesel engine application: a review," *Renewable and Sustainable Energy Reviews,* vol. 14, pp. 1999-2008, 2010.

[8] A. E. Atabania, A. S. Silitonga, Irfan Anjum Badruddina, T. M. I. Mahliaa, H. H. Masjukia, and S. Mekhilefd, "A comprehensive review on biodiesel as an alternative energy resource and its characteristics," *Renewable and Sustainable Energy Reviews* vol. 16 pp. 2070-2093, 2012.

[9] W. M. J. Achten, L. Verchit, Y. J. Mathijs Franken, E. Singh, V. P. Aerts, and R. B. Muys, "Jatropha bio-diesel production and use," *Biomass and Bioenergy,* vol. 32, pp. 1063-1084, 2008.

[10] P. Mahanta and A. Shrivastava. (2011). Technology development of bio-diesel as an energy alternative [Online]. Available : http://www.newagepublishers.com/samplechapter/001305.pdf; 2011. Date accessed:25/01/2016

[11] D. Bartholomew, "Vegetable oil fuel," *Journal of the American Oil Chemists' Society,* vol. 58, pp. 286A-288A, 1981.

[12] Anon, "Filtered used frying fat powers diesel fleet," *Journal of the American Oil Chemists' Society,* vol. 59, pp. 780A-781A, 1982.

[13] E. H. Pryde, "Vegetable oil as diesel fuel: Overview," *Journal of the American Oil Chemists' Society,* vol. 60, pp. 1557-1558, 1983.

[14] C. Adams, J. F. Peters, M. C. Rand, B. J. Schroer, and M. C. Ziemke, "Investigation of soybean oil as a diesel fuel extender: Endurance tests," *Journal of the American Oil Chemists' Society,* vol. 60, pp. 1574-1579, 1983.

[15] C. L. Peterson, D. L. Auld, and R. A. Korus, "Winter rape oil fuel for diesel engines: Recovery and utilization," *Journal of the American Oil Chemists' Society,* vol. 60, pp. 1579-15, 1983. .

[16] M. Ziejewski, H. Goettler, and G. L. Pratt, Comparative Analysis of the Long-Term Performance of a Diesel Engine on Vegetable Oil Based Alternate Fuels. Paper no. 860301. International Congress and Exposition, Detroit, MI, 24±28 February, 1986.

[17] A. W. Schwab, M. O. Bagby, and B. Freedman, "Preparation and properties of diesel fuels from vegetable oils," *Fuel,* vol. 66, pp. 1372-1378, 1987.

[18] C. E. Goering, R. N. Camppion, A. W. Schwab, and E. H. Pryde, "Evaluation of soybean oil-aqueous ethonol microemulsion s for diesel engines," In *Proceedings of the International Conference on Plant and VegetableOoils as Fuels*, Fargo, North Dakota, American Society of Agricultural Engineers, St Joseph, MI 4*,* pp. 279-286, 1982.

[19] C. E. Goering and B. Fry, "Engine durability screening test of a diesel oil/soy oil/alcohol microemulsion fuel," *Journal of the American Oil Chemists' Society,* vol. 61, pp. 1627-1632., 1984.

[20] P. B. Weisz, W. O. Haag, and P. G. Rodeweld, "Catalytic production of high-grade fuel (gasoline) from biomass compounds by shapedelective catalysis," *Science,* vol. 206, pp. 57-58, 1979.

[21] C. C. Chang and S. W. Wan, "China's motor fuels from tung oil," *Industrial and Engineering Chemistry ,* vol. 39, pp. 1543-1548, 1947

[22] R. A. Niehaus, C. E. Goering, L. D. Savage, Jr. , and S. C. Sorenson, "Cracked soybean oil as a fuel for a diesel engine," *Transactions of theAmerican Society of Agricultural Engineers,* vol. 29, pp. 683-689, 1986.

[23] A. W. Schwab, G. J. Dykstra, E. Selke, S. C. Sorenson, and E. H. Pryde, "Diesel fuel from thermal decomposition of soybean oil," *Journal of the American Oil Chemists' Society,* vol. 65, pp. 1781-1786, 1988.

[24] M. Balat and H. Balat, "Progress in biodiesel processing," *Applied Energy,* vol. 87, pp. 1815-35, 2010.

[25] Y. Chisti, "Biodiesel from microalgae," *Biotechnology Advances,* vol. 25, pp. 294-306, 2007.

[26] G. Knothe, J. Van Gerpen, and J. Krahl (eds.), *The Biodiesel Handbook*. Champagne, Ill: AOCS Press*,* 2005.

[27] M. Mittelbach and C. Remschmidt, *Biodiesel: the Comprehensive Handbook.* Published by M. Mittelbach, Universität Graz, Graz, Austria, 2004.

[28] G. Knothe, "Analyzing biodiesel: standards and other methods," *Journal of the American Oil Chemists' Society,* vol. 83, pp. 823-833, 2006.

[29] International Standards Organisation, "Reciprocating Internal combustion engines – Exhaust emission measurement," vol. ICS 13.040.50.27.020, 2011.

[30] S. Nettles-Anderson, D. B. Olsen, J. J. Jonson, and J. N. Enjalbert, "Performance of a direct injection IC Engine on SVO and biodiesel from multiple feed stocks," *Journal of Power and Engineering,* vol. 2, pp. 1-13, 2014.

[31] Wikipedia, "Emission_standard," 11/01/2016.

[32] U. S. EPA, (2004). Emission standards for non-road diesel engines [Online]. Available: https://www.dieselnet.com/standards/us/nonroad.php. Date accessed: 14/06/2015.

[33] E. Commission, "Directive 2003/44/ of the European Parliament and of the council of 16th June 2003 amending directive 94/25/EC on the approximation of the laws, regulations and administration provisions of the member stated relating to recreational craft," *Official Journal L214,* pp. 18-35, 2003.

[34] H. Aydin and H. Bayindir, "Performance and emission analysis of cottonseed oil methyl ester in a diesel engine," *Renewable Energy,* vol. 35, pp. 588-592, 2010.

[35] S. Murillo, J. L. Mıguez, J. Porteiro, E. Granada, and J. C. Moran, "Performance and exhaust emissions in the use of biodiesel in outboard diesel engines," *Fuel,* vol. 86, pp. 1765-71, 2007.

[36] H. S. Yücesu and I. Cumali, "Effect of cotton seed oilmethyl ester on the performance and exhaust emission of a diesel engine," *Energy Sources Part A* vol. 28, pp. 389-398, 2006.

[37]	A. C. Hansen, M. R. Gratton, and W. Yuan, "Diesel engine performance and NOx emissions from oxygenated biofuels and blends with diesel fuel," *Transactions of the American Society of Agricultural and Biological Engineers,* vol. 49, pp. 589-595, 2006.

[38]	C. Kaplan, R. Arslan, and A. Sürmen, "Performance characteristics of sunflower methyl esters as biodiesel," *Energy Sources Part A* vol. 28, pp. 751-755, 2006.

[39]	S.-H. Choi and Y. Oh, "The emission effects by the use of biodiesel fuel," *International Journal of Modern Physics B* vol. 20, pp. 4481-4486, 2006.

[40]	Z. Utlu and M. S. Kocak, "The effect of biodiesel fuel obtained from waste frying oil on direct injection diesel engine performance and exhaust emissions," *Renewable Energy,* vol. 33, pp. 1936-1941, 2008.

[41]	B. Ghobadian, H. Rahimi, A. M. Nikbakht, G. Najafi, and T. F. Yusaf, "Diesel engine performance and exhaust emission analysis using waste cooking biodiesel fuel with an artificial neural network," *Renewable Energy,* vol. 34, pp. 976-982, 2009.

[42]	H. Oˇguz, H. Oˇgüt, and T. Eryilmaz, "Investigation of biodiesel production, quality and performance in Turkey.," *Energ Source Part A* vol. 29, pp. 1529–35, 2007.

[43]	B. F. Lin, J. Huang, H. , and D. Y. Huang, "Experimental study of the effects of vegetable oil methyl ester on DI diesel engine performance characteristics and pollutant emissions," *Fuel* vol. 88, pp. 1779–85, 2009.

[44]	H. Hazar, "Effects of biodiesel on a low heat loss diesel engine," *Renew Energ,* vol. 34, pp. 1533–7, 2009.

[45]	A. N. Ozsezen, M. Canakci, A. Turkcan, and C. Sayin, " Performance and combustion characteristics of a DI diesel engine fueled with waste palm oil and canola oil methyl esters. ," *Fuel* vol. 88, pp. 629–36, 2009.

[46]	H. Özgünay, S. Colak, G. Zengin, Ö. Sari, H. Sarikahya, and L. Yüceer, "Performance and emission study of biodiesel from leather industry pre-fleshings," *Waste Manage* vol. 27, pp. 1897–901, 2007.

[47]	F. Wu, J. Wang, W. Chen, and S. S., "A study on emission performance of a diesel engine fueled with five typical methyl ester biodiesels," *Atmos Environ,* vol. 43, pp. 1481–5, 2009.

[48]	Y. Ulusoy, Y. Tekin, M. Cetinkaya, and F. Kapaosmanoglu, "The engine tests of biodiesel from used frying oil. ," *Energy Source Part A* vol. 26, pp. 927–32, 2004.

[49]	E. Buyukkaya, "Effects of biodiesel on a DI diesel engine performance, emission and combustion characteristics. ," *Fuel* vol. 89, pp. 3099–105, 2010.

[50]	L. Turrio-Baldassarri, C. L. Battistelli, L. Conti, Crebelli R, B. De Berardis, and A. L. Iamiceli, "Emission comparison of urban bus engine fuelled with diesel oil and biodiesel blend. ," *Sci Total Environ* vol. 327, pp. 147–62, 2004;.

[51]	A. Tsolakisa, A. Megaritis, M. L. Wyszynski, and K. Theinnoi, "Engine performance and emissions of a diesel engine operating on diesel-RME (rapeseed methyl ester) blends with EGR (exhaust gas recirculation)," *Energy,* vol. 32, pp. 2072–80, 2007.

[52]	D. Agarwala, S. Sinhab, and A. K. Agarwal, "Experimental investigation of control of NOx emissions in biodiesel-fueled compression ignition engine," *Renew Energ,* vol. 31, pp. 2356–69, 2006.

[53]	G. Fontaras et al., "Effects of biodiesel on passenger car fuel consumption, regulated and non-regulated pollutant emissions over legislated and real-world driving cycles," *Fuel* vol. 88, pp. 1608-17, 2009.

[54] M. N. Nabi, S. M. Najmul-Hoque, and M. S. Akhter, "Karanja (Pongamia Pinnata) biodiesel production in Bangladesh, characterization of karanja biodiesel and its effect on diesel emissions. ," *Fuel Process Technol* vol. 90, pp. 1080–6, 2009.

[55] M. Lapuerta, J. M. Herreros, L. L. Lyons, R. García-Contreras, and Y. Brice, "Effect of the alcohol type used in the production of waste cooking oil biodiesel on diesel performance and emissions," *Fuel* vol. 87, pp. 3161–9, 2008.

[56] W. G. Wang, D. W. Lyons, N. N. Clark, M. Gautam, and P. M. Norton, "Emissions from nine heavy trucks fuelled by diesel and biodiesel blend without engine modification," *Environ Sci Technol* vol. 34, pp. 933–9, 2000;.

[57] D. H. Qi, L. M. Geng, H. Chen, Y. Z. H. Bian, J. Liu, and X. C. H. Ren, "Combustion and performance evaluation of a diesel engine fueled with biodiesel produced from soybean crude oil," *Renew Energ* vol. 34, pp. 2706–13, 2009;.

[58] G. Labeckas and S. Slavinskas, "The effect of rapeseed oil methyl ester on direct injection diesel engine performance and exhaust emissions," *Energ Convers Manage* vol. 47, pp. 1954–67, 2006.

[59] M. I. Al-Widyan, G. Tashtoush, and M. Abu-Qudais, "Utilization of ethyl ester of waste vegetable oils as fuel in diesel engines. ," *Fuel Process Technol* vol. 76, pp. 91–103, 2002;.

[60] M. Karabektas, "The effects of turbocharger on the performance and exhaust emissions of a diesel engine fuelled with biodiesel," *Renewable Energy,* vol. 34, pp. 989-993, 2009.

[61] J. Krahl, A. Munack, O. Schröder, H. Stein, and J. Bünger, "Influence of biodiesel and different designed diesel fuels on the exhaust gas emissions and health effects," *SAE paper* vol. 2003-01-3199, 2003.

[62] H. Raheman and A. G. Phadatare, "Diesel engine emissions and performance from blends of karanja methyl ester and diesel," *Biomass and Bioenergy* vol. 27, pp. 393–7, 2004.

[63] S. Puhan, N. Vedaraman, B. V. B. Ram, G. Sankarnarayanan, and K. Jeychandran, "Mahua oil (Madhuca Indica seed oil) methyl ester as biodiesel-preparation and emission characterstics," *Biomass Bioenerg* vol. 28, pp. 87–93, 2005.

[64] J. M. Luján, V. Bermúdez, B. Tormos, and B. Pla, "Comparative analysis of a DI diesel engine fuelled with biodiesel blends during the European MVEG-A cycle: Performance and emissions (II)," *Biomass and Bioenergy* vol. 33, pp. 948–56, 2009.

[65] P. K. Sahoo, L. M. Das, M. K. G. Babu, P. Arora, V. P. Singh, and N. R. Kumar, "Comparative evaluation of performance and emission characteristics of jatropha, karanja and polanga based biodiesel as fuel in a tractor engine," *Fuel,* vol. 88, pp. 1698–707, 2009.

[66] G. Knothe, C. A. Sharp, and T. W. Ryan, "Exhaust emissions of biodiesel, petrodiesel, neat methyl esters, and alkanes in a new technology engine," *Energ Fuel,* vol. 20, pp. 403–8, 2006.

[67] N. Usta, "An experimental study on performance and exhaust emissions of a diesel engine fuelled with tobacco seed oil methyl ester," *Energ Convers Manage* vol. 46, pp. 2373–86, 2005.

CHAPTER 3

Paper 1: A REVIEW OF COMPUTATIONAL FLUID DYNAMIC (CFD) SCHEME IN BIODIESEL STUDIES.

E. I. Onuh[*] and Freddie Inambao.

Mechanical Discipline, School of Engineering, University of Kwazulu-Natal, Durban, South Africa.
[*]*Corresponding email:212561710@stu.ukzn.ac.za*
inambaof@ukzn.ac.za

Abstract

Biodiesel fuel represents a unique opportunity in the context of the current global energy challenge owing to its sustainability, renewability and potential capacity to be universally accessible. Experimental and analytical works have established a mismatch between fuel chemistry and current diesel engine design. This, to some extent, accounts for observed challenges in performance and emission from engines running on biodiesel. Computational schemes have increasingly played an important role in defining the scope of these challenges. The models' fidelity have improved over time in predicting engine performance and emissions. This review broadly defines the scope of this research and identifies the high points and gaps.

Keywords: biodiesel, fuel chemistry, performance, emission, model, novel engine.

Nomenclatures/Symbols

O_3	:	Ozone
0D	:	Zero Dimensions
3D	:	Three Dimensional
4D	:	Fully Resolved Spatial and Temporal Dimension

ATDC	:	After Top Dead Centre
BTDC	:	Before Top Dead Centre
CO	:	Carbon Monoxide
CA50	:	50% Accumulated Heat Release
CAI	:	Control Auto Ignition
CCM	:	Chemistry Coupled Tabulation Method
CFD	:	Computational Fluid Dynamics
CH_4	:	Methane
CI	:	Compression Ignition
CN	:	Cetane Number
CO_2	:	Carbon Dioxide
CPU	:	Central Processing Unit
CSP	:	Computational Singular perturbation
DAC	:	Dynamic Adaptive Chemistry
DI	:	Direct Injection
DME	:	Di-methyl Ether
DNS	:	Direct Numerical Simulation
DRG	:	Direct Relation Graph
DRGEP	:	Direct Relation Graph Aided Sensitivity Analysis
EGR	:	Exhaust Gas Recirculation
EP	:	Error Propagation
EVO	:	Exhaust Valve Opening
FAME	:	Fatty Acid Methyl Ester
GDP	:	Gross Domestic Product
HCC	:	Homogenous Charge Compression Ignition
HRR	:	Heat Release Rate
HTHR	:	High Temperature Heat Release
HTR	:	High temperature reaction

ICCD : Intensified Charge Coupled
Device
ICE : Internal Combustion Engine
ID : Ignition Delay
ILDM : Intrinsic Low Dimensional
Manifold
IMEP : Indicated Mean Effective
Pressure
ISAT : In-situ Adaptive Tabulation
ISFC : Indicated Specific Fuel
Consumption
IVC : Inlet Valve Closing
JSR : Jet Stirred Reactor
KMC : Kinetic Monte Carlo
LES : Large Eddy Simulation
LIF : laser Induced Fluorescence
LII : Laser Induced Incandescence
LLNL : Lawrence Livermore National
Laboratory
LTC : Low Temperature Combustion
LTHR : Low Temperature Heat Release
LTK : Low Temperature Kinetics
LTR : Low temperature reaction
MB : Methyl Butanoate
MD : Molecular Dynamics
MD : Methyl Decanoate
MK : Modulated Kinetics
NO_x : Oxides of Nitrogen
NVO : Negative Valve overlap
ϕ : Fuel/Air Ratio
ON : Octane Number
OPPDIF: Opposed-Flow Diffusion Flame
PCCI : Premixed Charge Compression
Ignition
PFA : Path Flux Analysis
PLTF : Planner Laser Induced
Fluorescence
PM : Particulate matter
PSR : Perfectly Stirred Reactor
RANS : Reynolds Averaged Navier-
Stokes
RES : Renewable Energy Sources
RGF : Residual Gas Fraction
ROHR : Rate of Heat Release
SA : Sensitivity Analysis
SCCI : Stratified Charge Compression
Ignition
SI : Spark Ignition

SO_2 : Sulphur Dioxide
SOI : Start of Ignition
ST : Shock Tube
TDAC : Tabulation of Dynamic Adaptive
Chemistry
TDC : Top Dead Centre
UHC : Unburnt Hydrocarbon
VVT : Variable Valve Timing
λ : Stoichioetric Fuel/Air Ratio

3.1.1 Introduction

One of the difficult question demanding urgent attention in the 21st century is how to guarantee access to renewable, cheap and environmentally sustainable source of energy. An ever increasing demand for energy in the face of obviously depleting reserves, coupled with the unacceptable after-effect of fossil sourced production, processing and usage, has brought this question to the front burner of global discuss. This is more so because of the pivotal role energy plays in economic development. A direct correlation has been established between energy consumption and economic development. The Asia pacific region, for example, has been growing at a much faster pace than the average global GDP growth rate. Between 2002 and 2030, it has been projected that global energy demand growth will be 1.7% to peak at 16487 Mtoe but the growth in the Asian pacific region is projected to be 3.9% [1]. Hence, to ensure long term economic development, energy sources need to be affordable, accessible and environmentally friendly.

3.1.1.1　Global Energy Mix

Primarily, the world relies on five main source of energy, namely: petroleum, natural gas, nuclear, solid fuels (coal etc.) and renewable energy source (RES). The share of petroleum and natural gas usage along with nuclear energy has remained fairly constant at approximately 61% and 13 % - 14% respectively within the period of 1999 - 2009 [2]. Renewable energy sources (RES) has increased from 5% to 9% within the same period as a result of marginal decrease in the use of coal. According to British Petroleum, global energy consumption for the year 2003 was estimated at 9.7 Gtoe with North America and Europe accounting for most of it [1]. The likelihood of this number increasing is quite strong as the rest of the world plays catch-up in terms of economic development.

Fossil sources (petroleum, natural gas and coal) account for about 80% of global energy sources (see Figure 3.1). Fossil sources are finite, environmentally unsustainable, and reserves are unevenly distributed, hence, are subject to geopolitical risk and price fluctuation. The Middle East, for example, accounts for about 63% of global oil reserves [1]. Given their finite nature, oil is projected to peak in the period 2015 – 2030. The issue of environmental degradation occasioned by the production, processing and use of fossil fuels is another factor that poses significant challenges. These are historically

why, in large part, insecurity, price volatility and negative environmental impact have been associated with the use of fossil fuels. Nuclear energy source has not had a smooth run either. Nuclear technology has always been viewed with benign suspicion since Hiroshima and Nagasaki. This suspicion heightened when the Chernobyl meltdown occurred in Russia and, since the Fukushima incident, public resistance to nuclear energy source has crystallized into a phase-out policy in Japan and Germany. This inevitably indicates that the only scope for growth in the energy spectrum to meet growing demand is through renewable energy sources (RES).

3.1.1.2　Need for Renewable Alternatives

Beside the finite nature of fossil fuel, its potential for political instability, and the risk associated with the use of nuclear energy, the most significant challenge going forward, if the status-quo is retained, is the environment. Significant bodies of evidence exist which suggest that continuous use of the current energy mix is environmentally unsustainable. The use of petroleum derivatives as fuel is associated with the emission of particulate matter (PM), oxides of sulphur (SO_2) and poly-aromatic hydrocarbons [1]. The extraction process of petroleum, to some degree, involves harmful practices such as echo-sounding (causing sub-surface geological deformation that could potentially destroy ground water supply),

radioactive material used for well logging, gas flaring, oil spills, well blowout (e.g. horizon deep spill, Niger delta spills). Mid-stream refining activities also pose risks such as harmful discharges of effluents and other toxins. Griffin Shay [3] stated that increasing use of petroleum fuel will intensify global warming caused by carbon dioxide (CO_2) emission. Besides CO_2, methane (CH_4) and oxides of nitrogen (NO_X) are some of the emissions associated with activities related to petroleum usage that also intensify global warming.

In addition to climate change concerns, the health impact of these emissions are substantial. During combustion of petroleum derivative in internal combustion engines, the following are emitted into the atmosphere through the exhaust; oxides of nitrogen (NO_X), soot, carbon monoxide (CO), unburnt hydrocarbons (UHC), aldehydes (with their carcinogenic derivatives), sulphur oxide (SO_2) and lead compounds amongst others. NO_2 can react with some hydrocarbons to concentrate Ozone (O_3). NO_2 is linked with increased susceptibility to respiratory infection, influenza, lung irritation, increased air ways resistance in asthma, bronchitis and pneumonia, decreased pulmonary function, increased sensitivity to allergies [4]. Ozone (O_3) irritates mucous membranes of the respiratory system causing coughing and clogging. Damage to lung tissue can aggravate chronic heart disease, asthma,

bronchitis and emphysema [5]. SO_2 is also a respiratory irritant. It can impair lung function, damage lung tissue, aggravate asthma, emphysema and lead to suffocation and throat irritation. It is clear therefore, from a public health point of view, mitigation strategies for these emissions are a global imperative.

3.1.1.3 Renewable Energy Resource and Transportation

Transportation is one of the key components of modern society; without efficient and convenient public and private transport, the living standard attained today would have been impossible. In the U.S.A for example (one of the countries with the most advanced economy and enhanced standard of living), transportation accounted for 28% of total energy consumption in 2005, with 97% of that energy derived from petroleum [6]. One of the most important prime movers for this sector is the internal combustion engine. Substituting petroleum sourced fuel for renewable fuel in this sector will therefore have a direct impact in mitigating some of the challenges already identified with the use of petroleum based fuel. Biodiesel has been identified as one of the suitable alternatives in compression ignition (CI) engines. This fuel source is considered carbon neutral [2]. It is more universally accessible. Biodiesel is produced from transesterification of vegetable oil or animal fats using alcohol in the presence of an

alkaline catalyst. Comparatively, its use in the internal combustion engine (ICE) is considered less harmful to the environment because it leads to reduction in carbon monoxide (CO), [7, 8], unburnt hydrocarbons [9, 10], particulate matter (PM) [11, 12] and soot precursors [13]. However, contradictory findings have been reported regarding oxides of nitrogen (NO_X) emissions [9, 10, 14, 15] and reduction in engine power has been reported in the literature [16, 17]. Hence, continued research has been advocated to provide further insight and to find better ways of employing its inherent advantages.

On the supply side, significant millage has been covered although a lot still needs to be achieved. Biofuels sources such as barley, wheat, corn, sugar, soybeans, castor, rapeseed, jatropha and palm have been extensively cultivated and used for biofuel production but resistance against their use has built overtime because these edible oil sources were in direct competition with human food requirements. It stands to reason, therefore, that, going forward, these first generation sources (edible oils) will not be viable. The reality is that, in 2010, for instance, 12.5% of the world's population was malnourished [18, 19]. It was also clear that the supply gap between petroleum and vegetable oil sources could not be bridged anyway, because global petroleum and vegetable oil production was at 4.018 and 0.107 billion tonne respectively [1]. This supply dilemma is

further observed by looking at the major suppliers and importers of vegetable oils. The major exporters of vegetable oil are Malaysia, Argentina, Indonesia, Philippines and Brazil (countries with inelastic production infrastructure because of their expanding population and limited land resources) and the major importers are China, Pakistan, Italy and the United Kingdom (most of whom are straining with insatiable demand or are desperately poor).

As a result, a second generation of biodiesel sources has been identified and is currently being aggressively researched. Non-edible biodiesel sources such as waste restaurant oil, jatropha, algae, lignocellulosic biomass etc. These poses the advantages (particularly the algae) of high growth rate, tolerance to adverse environmental conditions, high CO_2 trapping and fixation abilities, high oil content (sometimes exceeding 80% of their dry weight), and high yield per hectare. The most significant drawbacks are that their production is not yet cost effective and there are many technical barriers that still need to be overcome [20]. Despite these, the use of RES in transportation is on the increase particularly in the EU and North America [2].

3.1.1.4 Engine Development and Challenges

Currently the flagships of the internal combustion engine are the spark ignition (SI) engine and the compression ignition (CI) engine.

The SI engine is characterized by premixed charge at near stoichiometric fuel-air mixtures ($\emptyset \sim 1$), flame propagation is spark assisted with a spark plug and load control is achieved by varying the pumping of charge into the cylinder via the throttle effect which leads to low thermal efficiency at partial load. These coupled with high temperature at peak load causes significant $N0_X$ production constituting the major challenge faced with the use of the SI engine. The compression ignition (CI) engine on the hand is characterized by: a compression ratio of between $12 - 24$, diffuse flame, turbulent flow and auto-ignition via elevated pressure and temperature around top deal centre (TDC). It has a comparatively higher thermal efficiency. A critical part of its operation is the ignition delay (defined as the time difference between the start of injection and the start of self-ignition). The ignition delay mechanism is governed by physical as well as chemical kinetic processes. The physical process proceeds sequentially through droplet formation, collision, break-ups, evaporation and vapour diffusion. The chemical kinetic process involves species and radical formation proceeding through low temperature reaction (LTR), negative temperature co-efficient (NTC) and high temperature reaction (HTR). The challenge is that the time scales for the physical processes are often larger than those of the chemical processes, hence, ignition often commence before the physical processes are completed. This inevitably leads to a complex system of charge, flame and thermal stratification that produces both high NO_X in some regions and high soot precursors and UHC in others. Research focus therefore, has been to develop engines that synergize the performance of SI and CI by increasing thermal efficiencies (as in the CI engine) and mitigating NO_X UHC and soot formation (as in the SI engine). A clue on how this can be achieved has been proposed with the concept of low temperature combustion. (See Figure 3.2).

Low temperature combustion (LTC) via homogenous charge compression ignition (HCCI) has been identified as the most viable to accomplish this low UHC and NO_X emission regime. When the advantages of HCCI are coupled to those of biodiesel successfully, it could potentially present a significant breakthrough in novel engine development and renewable energy fuel sources.

3.1.1.5 Numerical and Experimental Approach to Engine Research.

Combustion activities in internal combustion engines occur at multi-scale (time and space), multi-phase and depend on a diverse range of thermo-physical properties which involve intense levels of interaction between multiple properties. Chemical kinetic behaviours of fuel for instance affect mixture auto-ignition, combustion rate and

emission formation. Fuel transport properties such as viscosity, density and surface tension affect fuel breakup, vaporization, mixing and fuel jet impingement on combustion walls. Other general transport properties also affect heat and mass transfer, thermal stratification and charge stratification. It is practically impossible to study all these engine phenomena experimentally at a reasonable cost and within reasonable time frames. Numerical studies supported with well scaled experiments (for the purpose validation) have increasingly become the most effective way to conduct research in this area at a reasonable cost and within an acceptable time limit. Numerical studies also makes it easy to isolate specific properties and study their effects independently to measure the exact effects on the different processes within the engine. Numerical studies with high technology engine diagnostics have increasingly been deployed to shorten time for engine development. Numerical studies involve the use of either a detailed or reduced chemical kinetic mechanism for the real fuel or its surrogate in a zero dimensional, single zone or a full computational fluid dynamics (CFD) analysis in three dimensional multi zones with cell mesh size in hundreds of thousands. Figure 3.3 presents the different stages in CFD studies of biodiesel combustion studies. CFD modeling is a powerful computational approach used to simulate biodiesel combustion with high fidelity at a much lower operating cost compared to

experiment. Its accuracy lies in choosing the right model to optimize the complex calculation which provides useful insight into the combustion process in ICE [21]. Combustion kinetics are often coupled to CFD in a bid to understand in-cylinder processes. Pang et al. [22], for instance, studied the growth of soot precursors in diesel reaction kinetic using this approach. The use of surrogates in place of actual fuel became necessary because it was difficult to use the exact composition of biodiesel comprising complex, long chained fatty acid methyl esters (FAME) in 3D engine simulation. Hence, the use of simple, well characterized chemical kinetic mechanisms are applied as a surrogate to emulate the kinetic behaviour of actual biodiesel chains. The most common biodiesel surrogates in use are methyl butanoate (MB, $C_5H_{10}O_2$) [23]and methyl decanoate (MD, $C_{11}H_{22}O_2$) [24]. The need for more accuracy has spurred the development of detailed mechanisms. A shift from small to large and complex mechanisms in order to study the combustion kinetic accurately has been observed [25]. This shift, although important, has come with some disappointments. For instance, these large mechanisms lack accuracy in predicting negative temperature co-efficient (NTC) [26, 27] and low temperature reactions (LTR) [28]. Also, in these detailed mechanisms, modeling difficulties were experienced even for zero dimensional (0D) kinetic modeling [28]. Large sizes of detailed

mechanisms are not practicable in 3D CFD combustion because they are extremely time consuming, not to mention other challenges [29].Lu and Law [25] stated that detail mechanisms are highly sensitive to changes in operating conditions and reaction rates. Hence, their reduction to smaller and more efficient mechanisms to facilitate their use in 3D CFD in a bid to reduce cost and runtime.

On the other hand, there is a risk associated with oversimplifying mechanism. These include the inability to emulate the kinetics of the detailed mechanism as well as generating erroneous modeling results. As a fallback measure, some methods have been proposed as a useful means by which runtime can be reduced when using large detailed mechanisms. These include: in-situ adaptive tabulation [30], tabulation of dynamic adaptive chemistry (TDAC) [31], and chemistry coupled tabulation methods (CCM) [32, 33]. CCM has been known to save up to 90% central processing unit (CPU) runtime [32, 33]. Because reduced mechanisms are associated with reduced CPU runtime and simulation cost, complex combustion chemistry and associate computation stiffness are often avoided where possible. Computational stiffness occurs when computational stability cannot be reached as a result of complex combustion chemistry. This phenomenon particularly occurs in 0D kinetic modeling for which combustion chemistry is

dominant [25]. Computational shiftiness is primarily dependent on the sizes of a mechanism, where an increase in mechanism size leads to an overall increased in the number of iterations to reach computational stability.

Mechanism reduction processes involve the elimination of unimportant species and reactions from the chemical kinetics which lowers the subsequent number of iterations required for convergence thus avoiding computational stiffness. This results in reduction in CPU runtime and simulation cost. Mechanism reduction types include: direct relation graph (DRG) [34-36], dynamic adaptive chemistry (DAC) [37, 38] error propagation (EP) [39], sensitively analysis (SA) [39], computation perturbation (ESP) [40], intrinsic low dimensional manifold (ILDM) [41].

CFD have been extensively used to evaluate combustion processes that are based on the thermo-physical properties of biodiesel. For example, in spray development and combustion phasing, Ra et al. [42] suggested that thermo-physical properties of fuel influence combustion development of soybean diesel, based on his numerical analysis. Also, optical study of spray behaviour of diesel and biodiesel [43] showed that continuous liquid-phase penetration was closely related to thermo-physical properties (i.e. liquid surface tension, liquid viscosity and

density of the biodiesel). In another numerical work, injection pressure of biodiesel was found to be affected by fuel viscosity and density [44].

3.1.1.6 HCCI Strategies

Homogenous charge compression ignition (HCCI) is a combustion strategy that adopts premix charge and achieve auto-ignition as a result of high temperature and pressure during the compression stroke. HCCI is similar to SI because it is premixed. It is also similar to CI because the charge is auto-ignited but it is different from both in the sense that while SI is spark assisted, HCCI auto-ignites. Its spontaneous combustion with multiple flame fronts differs from CI's diffused flame propagation. As a result, HCCI is able to achieve a higher efficiency than SI and also has a greater ability to curb NO_X and UHC emissions when compared to CI. HCCI displays two stages of heat release, namely: low temperature heat release (LTHR) and high temperature heat release (HTHR). The dwell between the two is described as the Negative Temperature co-efficient. During NTC, overall heat release decreases but temperature increases [45, 46]. Essentially, low temperature kinetic (LTK) is responsible for knocks in SI engines [47, 48]. The higher the cetane number the more likely LTK (or early auto-ignition) takes place (knock). High octane (anti-knock) is used to curb LTK.

Pioneering work on HCCI reported that radicals associated with LTHR are formaldehyde (CH_2O), hydroxide radical (HO_2) and O [49, 50]. This trend was observed in a two stroke gasoline engine. It was also observed via optical spectroscopic analysis that the radicals associated with HTHR were CH, H and OH [50]. Nay and Foster [51] using a four stroke engine with gasoline concluded that HCCI auto-ignition is controlled by low temperature chemistry (< 1000 k) while the bulk energy heat release rate is controlled by high temperature chemistry dominated by carbon monoxide (CO) oxidation (> 1000 k). These, combined with the work of Onishi [49] and Noguchi [50], led to the conclusion that unlike SI which relies strongly on flame propagation, and CI which relies on fuel/air mixing, HCCI relies more on chemical kinetics (controlled by temperature, pressure and charge composition). As a result, its limitation includes: a lack of auto-ignition control and limited operating range. HCCI has sometimes been called controlled auto-ignition (CAI) and aggressive work on it started in the 1990s spurred by the need to reduce emissions. Port fuel injection is the most straight forward way to obtain premix charge and has been deployed extensively [52, 53]. All HCCI results have consistently reported strong potential to increase thermal efficiency, reduce NO_X and soot emissions. But HCCI has faced some challenges which include: difficulties in combustion

phasing, high noise levels, UHC and CO emissions, limited operating range, problems with cold start and homogenous mixture preparation.

An earlier review by Cheng et al. [54] focused on advances in CFD with respect to surrogate chemical kinetics, mechanism reduction and thermo-physical characteristics. Lai et al.'s [55] review focused on 0D kinetic modeling and its combustion feature, especially reactivity and early formation of CO and CO_2, using biodiesel. Westbrook, et al. [56] focused on the development of very large mechanisms. Yao et al. [4] broadly discussed trends in HCCI strategy without specific details on biodiesel applications. Komminos and Rakopoulos [2] highlighted work on HCCI combustion of biofuel in a concise manner but did not discuss the new strategies in HCCI and the likely impact they could have on biodiesel research. Panday et al. [1] provided a comprehensive review of the thermochemical properties of biodiesel and their effect on the physical as well as chemical process involve in combustion and its emission. The current review's aim is to highlight the important work conducted on chemical kinetics, 3D CFD biodiesel studies, new strategies in HCCI and how important facts regarding biodiesel properties can be deployed in these new schemes to remove obstacles hampering the technical viability of biodiesel as an alternative to diesel.

3.1.2 Chemical Kinetic and Reaction Pathways

Basically all simulation models used in biodiesel combustion studies and simulation that involves changes of chemical composition include chemical kinetics. This is an indication that chemical kinetics plays an important role in the combustion process, particularly for strategies that include auto-ignition such as CI and HCCI. This is because since no external means is deployed to initiate combustion, CI and HCCI rely exclusively on the reaction kinetic of the fuel for the commencement of ignition. Normally ignitions will only commence when the correct thermodynamic condition of pressure, temperature and species concentration are favourable. Chemical kinetics also determine the reaction pathways and intermediate species formation of pollutants. These clearly highlights the importance of chemical kinetics in combustion studies and why great attention is given to building reaction pathways which correctly describe the level of detailed oxidation characteristics of combustion charges under various operating conditions. The difficulties associated with the task of determining appropriate chemical kinetics reaction pathways come about as a result of the complexity involved in identifying primary and secondary reaction pathways as well as the subsequent reduction of the mechanism. The reduction of the resulting mechanism is essential if the chemical kinetic is

to be used in simulation. This is because simulation time increases non-linearly with an increase in the number of species and reactions [2]. The need for the mechanism to be reduced is further emphasised by constraints placed on models because of computational time cost which has already been made exorbitant by the solving of the Navier-Stokes equations.

In selecting chemical mechanism for any combustion strategy, great care is taken to avoid wrong fit since existing mechanisms do not always provide similar result. As a result, caution is exercised when interpreting ignition timing, global combustion rate and emission especially when differences between fuels are assessed [57]. In selecting the mechanism, it is important to determine the condition under which the mechanism was developed and the experiments used in validating it (shock tube, flow reactor, jet-stirred reactor, rapid compression machine, laminar flame, HCCI engine etc.) [2]. It should be noted also that fuel chemical kinetics of surrogate (for actual fuel) cannot be describe in exhaustive detail. It is obvious that even detailed mechanisms have limits and their validation can never be comprehensive enough given the diverse operating condition of the various combustion strategies [2].

3.1.2.1 Biodiesel Surrogates

In CFD modeling, it is not practicable to adopt the exact chemical composition of the actual biodiesel fuel consisting of complex, long chained FAMEs [58]. As a result, simple and well-characterised chemical kinetic mechanism are used as surrogates to mimic the behaviour of the actual fuel [59]. Biodiesel surrogate could be small (short carbon chain, < 5) or large (long carbon chain < 5) [54]. Given the increasing demand for more accurate simulation, progressive development of very large chemical kinetics has taken place but they have not received sufficient enthusiasm because of large errors in the determination of negative temperature co-efficients (NTC) and low reactivity, modeling difficulties even for zero-dimension (0D) modeling and because its unwieldiness restricts its use in 3D CFD [25, 27, 28].

The advantages of using small mechanisms include: simple structure, short CPU runtime and the availability of wide range of in-cylinder engine validation data. Its disadvantages include: lack of low-temperature reactivity, unclear NTC region, and different auto-ignition characteristic from actual biodiesel. The advantages of large mechanisms include: similar ester structure to actual biodiesel fuel, clear low-temperature reactivity, obvious NTC region and similar auto-ignition characteristic to actual

biodiesel fuel. The disadvantages include: complex structure, it rely on smaller sub-mechanism, longer CPU runtime and limited in-cylinder engine validation data [54].

3.1.3 Biodiesel Properties and Implication for ICE Application

Precise thermo-physical properties are important inputs in numerical studies of FAME. These properties could be experimentally determined or numerically/analytically computed using well validated correlations. The properties could either be thermodynamic or transport in nature. And they have a profound effect on biodiesel behaviour in internal combustion engines (ICE). For example, it has been traditional that saturated FAME (low iodine numbers) will have higher cetane number and low temperature properties will be poor [60]. By the same token, high unsaturated FAME (high iodine number) will have low cetane number and low temperature properties are better. Knothe and Sterdley [61] in their study to investigate the relationship between FAME structure and kinematic viscosity observed that carbon chain length; position, number and nature of the double bond, and nature of oxygenated moieties are related to the kinematic viscosity. Gaboski and McCormich [62] in their study of chemical composition and FAME structures found out that the cetane number (CN) increases as the carbon chain length increases, and the CN decreases as the

number of carbon double bonds ($C = C$) move toward the centre of the carbon chain. Table 3.1 gives the names and structures of common FAME compositions.

Yamane et al. [63] investigated FAME content in terms of peroxide value and acid value of biodiesel. The result showed that: poly-unsaturated FAME linolenic acid (18:3) oxidizes easier than linoleic (18:2) and oleic (18:1), saturated FAMEs have much higher CN than unsaturated FAMEs, and FAME composition affects fuel properties such as viscosity, pour point, cetane number (CN) and oxidation stability. Fuel atomization, for example, is governed by properties such as viscosity, surface tension, density, latent heat of vaporization, thermal conductivity, specific heat capacity, boiling point and heat of combustion.

3.1.3.1 Biodiesel Properties and FAME Structure

Given that fatty acid methyl esters (FAME) are made from vegetable oil and fat, their structure will generally depend on the feedstock structure. These properties are both physical and chemical. The properties that have immediate and direct impact on fuel behaviours are: cetane number, viscosity, density, bulk modulus and pour point. Combustion characteristics properties determine process activities such as fuel injection, ignition delay and ignition timing. These properties could

also affect engine emission pattern such as unburnt hydrocarbon (UHC), carbon monoxide (CO), oxide of nitrogen (NO_X) and particulate matter (PM). The relationship between some of the properties and FAME structures are highlighted below.

3.1.3.1.1 Density

Density is normally expressed as specific gravity and is directly proportional to the bulk modulus. Density, bulk modulus and speed of sound have the greatest effect on injection timing. Normally, higher density and bulk modulus requires earlier injection timing. It should be noted also that in conventional CI and SI engines, earlier injection timing produces high peak temperature, pressure and consequently higher NO_X [64]. Typically, density, bulk modulus and speed of sound increases as the carbon chain length increases and is higher for more unsaturated esters [65]. Saturated FAMEs with the same carbon length have lower density than unsaturated FAME types. Correspondingly, the bulk modulus for saturated FAMEs is lower than those of unsaturated FAMEs [62].

3.1.3.1.2 Kinematic Viscosity

Kinematic viscosity is the measure of fluid resistance to flow. High viscosity means a reduced readiness to flow. In CI engines, high viscosity of fuel leads to: poorer atomization of fuel spray, less accurate operation of fuel injector, more deposit formation in fuel injector and combustion chamber [66]. High viscosity also leads to a decrease in cone angle of the fuel spray, giving rise to an increase in diameter of fuel droplet ensuring a deeper penetration of fuel spray into the combustion chamber. This results in wall and piston wetting causing heavy carbon deposit on walls, pistons and piston ring sticking/breaking post flame. This could also lead to the dilution of the lubricating oil [67]. In FAMEs, when chain length increases, viscosity increases. Viscosity decreases with increase in the degree of unsaturation [61].

3.1.3.1.3 Distillation Temperature

Distillation temperature is the measure of fuel volatility. A lower distillation temperature (or boiling temperature) means high or good volatility. High or good volatility means an enhanced fuel/air mixing which subsequently leads to better combustion. The boiling point (distillation temperature) of FAME increases with an increase in carbon chains. This means longer chain FAMEs have low volatility and the shorter the carbon chain, the better the volatility. Distillation temperature decreases when the level of unsaturation increases [61]. This implies that good volatility is associated with a higher degree of unsaturation.

3.1.3.1.4 Pour Point

This is the measure of the cold flow property of a fuel. At a temperature equal to or below pour point, fuel no longer flows. Cold flow properties are immensely important in cold regions where near zero or sub-zero temperatures are common. Pour point increases as chain length in saturated FAME increases and it becomes lower for more unsaturated FAMEs [1, 68]. Vegetable oil methyl esters which do not have sufficient cold flow properties are difficult to use in cold regions. Cold flow properties can be improved by using additives [1].

3.1.3.2 Theoretical and Experimental Determination of Biodiesel Properties for CFD Application

Thermo-physical properties which include thermodynamic as well as transport properties are useful in the determination of combustion characteristics of FAMEs as stated earlier. Emission patterns are also greatly dependent on these properties [69]. These properties include: critical properties, liquid density, liquid viscosity, liquid surface tension, liquid heat capacity liquid conductivity, vapour pressure, latent heat of vaporization, vapour viscosity, vapour thermal conductivity vapour diffusivity and second viral coefficients [54]. These properties can be determined numerically (with the iterative formulation couple to a CFD solver) as well as experimentally. The numerical

correlations were developed from extensive experimental data measured for a variety of hydrocarbon based fuels. These correlations can also be used to determine the thermo-physical properties of biodiesel provided the assumption used for their derivation and the range fits. Two handbooks are useful in the estimation of FAME properties. They include the work of Reid et al. [70, 71] and Poling et al. [72] which provide useful references for the comprehensive compilation of group contribution and experimentally determined correlations. Software has also been developed for use in the estimation of hydrocarbon thermo-physical properties. These include Knovel critical tables [73], DIPPR [74] and BDProp [75, 76]. Mixing rules [77, 78] are also considered when computing the thermo-physical properties of biodiesel fuels, which depends on the thermo-physical properties of the constituent FAME components.

Properties software is often a useful alternative to conventional correlation because of the ease associated with its use [73-76]. However, their major drawback is the sometimes limited scope of coverage and the fact that access to their use is through paid subscription. As a result, the conventional correlations are still preferred because of unrestricted access, low cost and availability of a wider range of correlations.

3.1.4 Numerical Techniques and Engine Diagnostics

The application of numerical techniques range from simple general processes with approximation using zero dimensions (0D) to fully resolved 3D or 4D (space and time) CFD simulations. The former are more cost effective in terms of CPU runtime and hardware, although significant errors are associated with the former in comparative terms. Length and time scale in ICE plays an important role in model fidelity. Length scale in ICE ranges from angstroms (10^{-10} m, atomic/molecular process), to several nanometres (10^{-9} m, soot precursor) to micrometers (10^{-6} m, spray droplets), to fractions of a millimetre (10^{-3} m, smallest aerodynamic flow scales), to centimetres (10^{-2} m, cylinder diameter). Time scale also ranges from pico-second (10^{-12} s), to nanosecond (10^{-9} s), to micro second (10^{-6} s), to millisecond (10^{-3} s) through to seconds (s) [6].

As shown in Figure 3.3 the range of simulation approaches applicable to combustion system include: quantum mechanics (QM) which describes intra-atomic processes for a small number of atoms; molecular dynamics (MolD); the kinetic Monte Carlo (KMC) method which describes intermolecular activities for a population of molecules; and continuum mechanics which describes chemical and physical activities at the macro-scales.

Continuum mechanics currently has three identifiable categories based on their range for resolved spatial and temporal scale. They consist of: direct numerical simulation (DNS) where the continuum mechanics governing equations are solved directly and all relevant continuum scales are resolved; Large Eddy Simulation (LES), where spatially filtered forms of the governing equations are solved and the dynamics of the large scales are captured explicitly while the effects of small scales must be modeled; and finally Reynolds averaged Navier-Stokes (RANS) where the probabilistic averaged forms of the governing equations are solved and the effects of any fluctuation about the averaged must be modeled. Figure 3.3 shows the time and length scale for the various simulation approaches.

An example of a typical DNS fully resolved simulation of a turbulent, premixed, methane-air, slot Bunsen flame with chemical model consisting of just 12 reactive species had a computational domain decomposed into 200 million cells. The simulation itself was performed by on 7000 processors on a CrayXT3 machine [6]. This underscores the challenge associated with the use of high resolution technique such as QM, MD and KMC. Currently, only RANS and to some extent, LES, are practicable for ICE studies, given the current

computing resources available. And these computations are done in zero dimension (0D), one dimension (1D) and 3D.

3.1.4.1 Application of Numerical Simulation

Proceeding from advances in computing power, numerical simulation has assumed an important position in theoretical studies of combustion processes in internal combustion engines particularly for biodiesel powered engines (see figure 3.4). Five categories of application are currently in use and are discussed below.

3.1.4.1.1 Single Zone with Detailed Chemistry in Zero Dimensions

Zero dimensions, single zone with detailed chemistry is the simplest model in engine simulation. In this approach, the engine is modeled using the first law of thermodynamics by resolving the work absorbed/produced by the piston; heat exchange between charge (not in all cases) and the mass blow-by is usually neglected. In this model, the thermodynamic (pressure, temperature, composition) and transport (viscosity and conductivity) properties are considered homogenous. Since temperature and charge stratification are neglected, this model tends to overestimate the heat release rate, pressure rise and maximum combustion pressure. The model also experiences difficulties in describing the formation of UHC and CO [79] because of the assumed charge homogeneity,

particularly in HCCI engines. Apart from these limitations, this model can be used to effectively estimate ignition timing and the formation of NO_X emission. This is because both events are linked to the highest temperature region which is also to the mean gas temperature. A single zone model in zero dimensions can be used as an effective tool in comparing the closeness or accuracy of a reduced chemical kinetic to that of the detailed chemical kinetic [1]. The ability of a zero dimension, single zone model to assess the relative importance of chemical reactions in reduced chemical kinetics to the detailed chemical kinetics is an important advantage because it helps to fast-track the process of developing new reduced mechanisms for use especially in Biodiesel studies [2]. In addition, this model strategy can be adopted to study the combustion chemistry of not only neat biodiesel but also various blends of biodiesel/diesel, biodiesel alcohol/diesel, etc. and their effect on ignition timing, fuel emissions of NO_X and behaviours in HCCI control strategy (since this represents the future of combustion research of biodiesel) [80].

Brakora and Reitz [81] conducted a zero dimension, single zone model study using the SENKIN code of the CHEMKIN package where the zone was considered adiabatic for study purposes to investigate the formation of NO_X from biodiesel and diesel fired HCCI engines.

The diesel surrogate was n-heptene and a mixture of 2/3 n-heptane and 1/2 methyl butanoate was used as the biodiesel surrogate. This proportion was found to yield a better C:H:O approximation of the biodiesel ratio for real biodiesel than either neat methyl butanoate or methyl decanoate. For the biodiesel, the chemical reaction mechanism consisted of 56 species and 169 reaction [82]. The NO_X formation mechanism was included via 7 species and 19 reactions developed by Yoshikawa and Reitz [83].

It was observed that ignition timing played an important role in the formation of NO_X. With similar energy release and same ignition timing, the two surrogates produced approximately same (separated by only 20k) peak combustion temperatures and yielded similar NO_X emissions at exhaust valve opening (EVO). It was difficult to establish a connection between the oxygen content of the fuel to the produced NO_X emissions. NO_X in the biodiesel was 26% higher than in the diesel surrogate. However, the peak temperature was about 13 k lower for the biodiesel. This indicates that fuel bound oxygen could play a role in NO_X formation under limited O_2 concentrations. In the same study, it was observed that under same energy content ignition timing and total N:O ratio for the two fuels, diesel yielded higher NO_X emissions. This implies that having the same amount of oxygen in the air as oppose to fuel-bound oxygen increases NO_X emission because of the alteration of the heat capacity of the mixture which gives rise to higher flame temperatures for the diesel surrogate.

3.1.4.1.2 Multi–Zone with Detailed Chemistry: Quasi-dimensional

One way to arrest the problem associated with the use of the single zone is to deploy multi-zone models. The combustion chamber is divided into several regions or zones with each zone possessing uniform thermodynamic properties. The acceptable number of zones is determined by a sensitivity analysis where the minimum number is defined as the number beyond which the simulation result tends to converge. Each zone is initialized by different initial parameters. Mass and heat transfer between the zones can be assumed. Normally, crevices and boundary layers (low temperature zones) are included to obtain good resolution of UHC and CO production for HCCI combustion. A number of works on multi-zone have been published with differences between them being based on any of the following: the numbers of zones, the type of zone (e.g adiabatic core zones, boundary layers, crevices and mass exchange zones) and the types of interaction between the zones (pressure-volume work, heat transfer, mass exchange). They are described as quasi-dimensional because they represent crevices, core zones and boundary layers.

Fiveland and Assanis [80] developed a comprehensive quasi-dimensional model to predict performance and emissions especially under turbo-charge conditions. This is a full cycle simulation code with adiabatic core, a predictive boundary layer model and crevice region. The unburned thermal boundary layer is driven by compressible energy considerations and hence is of varying thickness and is resolved at multiple geometries along the piston line interface. Given the thermal gradient between the adiabatic core and the boundary layer, there is an enthalpy flux and turbulent interaction between them. The adiabatic core is a perfectly stirred reactor with turbulent mixing and interacts with the piston via work transfer. The model produced a good result for UHC but the CO results were not satisfactory due to lack of detailed thermal resolution at the near wall regime (See Figure 3.5)

3.1.4.1.3 Detail Chemistry with One-Dimensional Engine Cycle

The limitation of the zero dimensions and the quasi-dimensional model described above is that these models only capture engine processes at the start of intake valve closure (IVC) and the end of exhaust valve opening (EVO). This means that initial parameters have to be specified at IVC. This is often riddled with difficulties because average mixture temperature, equivalent ratio and residual gas fraction (RGF) are difficult to determine. To overcome these challenges, the aforementioned models are combined with engine cycle stimulation codes which can compute the parameters at IVC. These one-dimensional codes which predict engine parameters from air intake to exhaust pipe. Given that the computation includes a complete engine cycle, the gas exchange processes are modelled.

Ogink [84] produced a BOOST-SENKIN single-zone model which predicted auto-ignition timing and heat release rate for a HCCI gasoline engine. Variable valve timing (VVT) impact on gas exchange processes in an HCCI engine was studied by Milovanovic et al. [85]. Gasoline was used in both the experimental and simulation studies. The simulation was executed with the Aurora detailed chemical kinetic code from CHEMKIN III with the ID fluid dynamic Lotus engine simulation (LES) code. This model was extended to BOOST-SENKIN multi-zone detailed chemical kinetic [86] to accurately predict fuel consumption, emissions and indicated mean effective pressures (IMEP) for various ranges of experimental conditions.

3.1.4.1.4 3D CFD with Detailed Chemistry

Multi-dimensional fluid dynamics with detailed chemistry possesses the best potential to predict more accurately engine activities when the complete geometry of the combustion chamber is

fully resolved and detailed kinetic chemistry is employed to evaluate chemical events. The computational resources for such procedures are significant and depend on CFD mesh resolution and the size of the chemical kinetic mechanism.

Agarwal and Assanis [87] performed a simulation of natural gas ignition consisting of detailed chemical kinetic mechanism of 22 species and 104 reactions using the multi-dimensional CFD reacting flow code KIVA-3V. The purpose was to explore auto-ignition of natural gas injected into a quiescent chamber in CI-like condition. The complete kinetic was executed up to the ignition point. Kong et al. [88] used a similar approach up to ignition point but post-ignition, a reaction rate with chemical kinetic and turbulent mixing was incorporated. The turbulent time scale was the time for eddy break up while the kinetic time scale was the time needed for a species to reach the equilibrium state under perfect mixing conditions. Kong et al.'s [59] numerical scheme also studied the effect of turbulence on a premixed iso-octane HCCI engine. The model used the KIVA code modified to use CHEMKIN as the chemistry solver. HCCI was found to be impacted by turbulence with it main effect being wall heat transfer. The result provided hints that it is better to incorporate detailed chemistry in CFD codes for HCCI evaluation to better understand the effect of turbulence on wall heat transfer. In addition, it was observed that ID onset of ignition was highly sensitive to initial condition, hence a higher level of accuracy at initial state was essential for good prediction, further underscoring the importance of detailed chemistry and complete resolution of flow conditions. Tominaga et al. [89] evaluated the effect of inhomogeneous distribution of EGR within the combustion chamber using multi-dimensional CFD with detailed chemistry for natural gas. The results showed that when EGR is densely located in low temperature zones (near walls and crevices), their effect on combustion was reduced compared to when its distribution is homogenous. But when EGR were density packed in high temperature zones (near the cylinder centre) their effects were more pronounced and they tended to moderate combustion as opposed to when it is uniformly distributed.

3.1.4.2 Engine Diagnostics

Optical diagnostics has evolved as an effective means by which in-cylinder processes can be effectively observed since its discovery in 1979 [90, 91]. It possesses the capability to deliver comprehensive as well as detailed information on flow pattern, species and temperature distribution with high spatial and temporal resolution in a combustion chamber. Its non-intrusive in-situ technique which enables non-interference in flow or combustion processes are valuable features

that makes it an essential tool in validation of combustion modeling results [91].

3.1.4.2.1 Diagnostic for In-Cylinder Charge/Air Mixing

Optical diagnostics is frequently used to evaluate the inhomogeneity in fuel distribution and temperature in the pre-mixture in HCCI and their effects on auto-ignition and combustion process.

Richter et al. [92] used planner laser induced fluorescence (PLIF) in HCCI to evaluate distribution of fuel and OH in the combustion chamber. The researchers achieved homogeneity of mixture by using two different premixing procedures. The first was the standard port injection and the second was the use of a 20 L preheated mixing tank. The PLIF confirmed that fuel preparation affects the fuel/air homogeneity and inhomogeneity had a modest effect on spatial variation of the combustion process. Lida et al. [93, 94] used a framing camera with an optically accessible engine to build 2D images of the chemiluminescence of the engine charge. Di-methyl ether (DME) was the test fuel. Various optical diagnostics have been deployed to observe in-cylinder mixture formation and many have suggested (as a result of these observation) practical ways such as stratified charge compression ignition (SCCI), premixed charge compression ignition (PCCI), and low

temperature combustion (LTC) as a means of increasing the high load limits for HCCI.

3.1.4.2.2 Optical Diagnostics for Combustion Process

(i) Chemiluminescence and Spectral Analysis
Glassman [95] stated that chemiluminiscence normally starts at low temperature because of the relaxation of excited combustion radicals in their base. This normally indicates the start of exothermic reactions (fuel oxidation and heat release) for diesel fuel, and involves two aspects: chemiluminiscence and soot luminosity. Chemiluminiscence in diesel originates from the visible and near ultraviolet band due to OH, CH, CH_2O and C_2 radicals [96]. Even though this occurs after the start of ignition (SOI), it often comes with weak signals. An intensified charge coupled device (ICCD) camera is normally deployed to observe these early non-luminous flames. It has been observed that although chemiluminiscence exists for the entire length of the combustion process, it is effectively drawn-out by the much stronger radiation from the soot luminosity. It has been further stated that soot signal is not a good marker for tracking the flame front because it only represents rich-burn ($\emptyset > 1$) areas. The same problem is encountered when spectral analysis is adopted. But these two methods can be used for low soot regime combustion strategies such as the SI and HCCI As well as, very significantly, biodiesel

combustion diagnostics where soot precursors are minimal.

Kawahara et al. [97] evaluated the combustion of DME in a HCCI regime with a single cylinder using chemiluminiscence spectral analysis. It was observed that light emission from HCHO appeared at LTR as predicted by Emel$e$ons cool flame band. The CO-O recombination spectrum was strong in the course of the main heat release. This signifies a strong correlation between rate of heat release (ROHR) and CO-O recombination. Mancaruso et al. [98] studied the auto-ignition and combustion of HCCI in CI engines. Using the common rail system, the fuel injection was staggered in five split intervals. The ultra-violet-visible imaging and spectra indicated the presence of HCO and OH evenly distributed within the chamber. The process appears to be dominated by OH radicals and it was observed that the radical significantly reduced PM in the Chamber. Another observation was that OH radicals are a good indicator of the start of high temperature combustion.

Person et al. [99] studied the early development of flame in spark assisted HCCI by employing high speed chemiluminescence imaging. It was observed that even for large negative valve overlap (NVO) resulting from early closure of the exhaust value and late opening of the inlet valve to achieve EGR strategy, it is the growing SI flame that controls the next HCCI combustion. It was concluded that spark timing could be deployed to phase the combustion timing despite the HCCI being responsible for the major heat release.

(ii) Planar Laser Induced Fluorescence (PLIF) Diagnostic

When an atom or a molecule has laser beamed on it, the beam causes excitation which leads to emission of light (fluorescence) from the atom or molecules. Laser induced fluorescence (LIF) in its early stage was driven by single point measurements but subsequent application of LIF in ICE has led to multi-point planar imaging. Planar laser induced fluorescence (PLIF) is one of the modern means by which flow can be visualized. PLIF is useful in qualitative as well as semi-quantitative characterization of flows. It provides spatial resolution of flows in-plane rather than integrating over line of sight. The PLIF has more fluorescence strength than Rayleigh and Raman [100] scattering and hence are more widely applied than the latter. Furthermore, PLIF can reveal the presence of intermediate species such as formaldehyde (HCHO) making it possible to determine spatial as well as temporal detection of auto-ignition precursors prior to the observation of chemiluminescence early in the cool flame.

It has been determined from chemical kinetic mechanisms that in HCCI combustion formaldehyde (HCHO) and OH radicals constitute important intermediate and active radicals prior to auto-ignition. This implies that ignition and the subsequent combustion process can be mapped by tracing the distribution of HCHO and OH.

Collin et al. [101] used a blend of iso-octane and n-heptane in an HCCI engine to simultaneously measure OH and formaldehyde (HCHO) using LIF. At the beginning of LTC, dense formation of HCHO was detected which continued to grow as LTC progressed. At the end of LTC, HCHO filled the entire measured region. OH signal was only picked up with PLIF when HCHO was absent. Peak OH was only observed when most fuel had been consumed (which occurred close to peak temperature). This and the work of Sarner et al. [102] shows that HCHO is more feasible as a fuel tracer for studying fuel visuals in HCCI at the LTR region.

3.1.5 HCCI Model Strategies for Biodiesel and Validation

An important concern for biodiesel application as a transport fuel, on the performance and emission side, has been a reduced efficiency due to marginal differences between its heating value and that of diesel, and a tendency to emit higher NO_X in comparative terms to diesel because of

the oxygenated nature of the fuel which makes it susceptible to high NO_X production at elevated temperature. These challenges put HCCI in the spot light as the most viable combustion strategy to deploy in biodiesel application, going forward. The reason for this is fairly obvious as the advantages of HCCI include a significant reduction of NO_X emission (because HCCI is an LTC concept), the absence of soot in the exhaust, and, because it is an un-throttled operation, it produces a higher indicated thermal efficiency. Even the challenge of high UHC and CO emission in HCCI because of bulk quenching at low loads, wall quenching and crevice flow at high load can be addressed using the EGR strategy of NVO. The warm/hot EGR at steady state operation will effectively improve reactivity and the fear of oxygen starvation will not materialize because of the oxygenated nature of biodiesel. Numerical as well as experimental research in this direction is beginning to bring these points to light. HCCI does have some draws back, which have been highlighted earlier, but overall, its potentials are significant. HCCI, through intense research, has evolved to include strategies such as: early direct injection, late direct injection and premixed/direct-injected HCCI combustion.

At the early stage of HCCI development, when diesel was used for HCCI combustion, difficulties were encountered in the preparation

of homogenous mixtures because of low volatility, high viscosity and lower resistance to auto-ignition. All these challenges exist with the use of biodiesel for HCCI but with far greater impact. As a result, conditions necessary to achieve diesel HCCI combustion must be given greater attention in biodiesel HCCI. These conditions include: mixture control (both charge component and temperature) and high pre-ignition mixing rate. Ryan et al. and Grey et al. [52, 53] used port injection in their study to achieve this. They, along with Christensen et al. [103], found that port injection in HCCI for diesel reduced NO_X emission but the smoke emission was significant and this was attributed to poor vaporization of the fuel leading to an inhomogeneous mixture. It was also observed that to reduce the likelihood of knock, the compression ratio had to be reduced. These early challenges were what informed the development of other injection strategies.

3.1.5.1 Early Direct Injection in HCCI

The early direct injection strategy was proposed in anticipation of its ability to mitigate some of the challenges associated with port injection in HCCI. The strategy, in comparison to the port injection, has three key advantages, including: (1) injecting fuel during the compression stroke implies that the high pressure and temperature effectively vaporizes the fuel and promotes good mixing. This permits cooler intake temperature

and reduces the risk of early ignition; (2) with a carefully design injector, fuel wall wetting is avoided which also reduces combustion inefficiency; (3) in theory, only one fuelling system is used for both HCCI and conventional CI operation. Again, early DI in HCCI increases the possibility of wetting, which constitute the main disadvantage of this strategy. Several versions of this approach have been developed and are discussed below.

3.1.5.1.1 Premixed Lean Diesel Combustion (PREDIC)

Takeda et al. [104] and Nakagome et al. [105] described DI HCCI strategy conducted by the New ACE institute in Japan. Early results from this study showed very low NO_X and smoke emission but the UHC emission and fuel consumption increased beyond levels observed in conventional CI engine. This was attributed to poor combustion efficiency and advanced combustion phasing. In a bid to reduce fuel spray over-penetrating and wall wetting which produces UHC and combustion inefficiencies when injection is executed well ahead of TDC, when air density and temperature in the combustion chamber are low, three injectors were employed in this strategy (one at the centre and two on the sides). The injectors on the sides were positioned such that their flows were designed to collide at the centre to prevent wall wetting. The nozzle at the centre had its diameter

reduced from 0.17mm to 0.08mm and hole numbers were increased from 6 to 16. To overcome early ignition, special fuel blends with cetane numbers between 19 and 40 were developed. Employing these changes, the engine could be operated with PREDIC. A subsequent work on the strategy reported the development of swirling flow achieved with pintle-nozzle injector [106] which produced a more uniform mixture and improved efficiency.

A follow-up work to scale-up power density was initiated with a second injection near TDC [107]. This was achieved with dual side-mounted impinging-spray injectors to obtain a lean premix charge while a centre mounted injector was deployed to execute the second injection near TDC. The NO and PM in this approach were much higher than in the normal HCCI but lower when compared to conventional CI strategy. Smoke emission was decreased but UHC was higher. Akagawa et al. [108] used this approach to study the effect of EGR rate and oxygenated fuels on fuel consumption, UHC and CO emission. Much higher load was achieved at low NO_X emission but at the cost of higher fuel consumption.

3.1.5.1.2 UNIBUS

Yanagihara et al. [109] used HCCI combustion with diesel fuel (Toyota UNIBUS). The UNIBUS approach adopted here was operated up to half load and half speed. Mixture preparation was key in this strategy. Piezo-actuators with Pintle size nozzles to reduce spray penetration were used. The strategy involved early injection (around 50° BTDC) and late injection (about 13° ATDC). Most of the data were obtained at a compression ratio of 12:1 to avoid early combustion of premixed charge. The parameters under investigation were: impact of injection timing, level of fuelling, EGR rate and double injections on emissions, torque, instantaneous heat release and load. The result generally showed negligible PM emission. An EGR rate of 60% was shown to delay HCCI combustion by about 7° crank angles.

It was clearly established that a dual-injection strategy can be developed. At the second injection, 50% of the fuel was introduced which significantly improved combustion efficiency of the first injection, reduced UHC emission by about 60% and CO emission by about 75%. The second injection can thus be considered as the trigger. Although the NO_X increased from a near zero levels, the increase was still less than what is obtainable with conventional CI diesel strategies. However, fuel consumption penalties are still a challenge.

3.1.5.1.3 MULINBUMP

Su et al. [110] proposed a diesel HCCI strategy called MULINBUMP (so named because it is a

flash mixing technology which evolved from the so called BUMP combustion chamber designed with a special bump ring). These strategies combine premixed combustion with "lean diffusion combustion". The premix was achieved using multi-pulse fuel injection. The start of pulse injection, pulse number, pulse injection period for each pulse, and the dwell between pulses were controlled. The main objective for the control was to prevent wall impingement of fuel and to enhance mixing rate of each pulse parcel. The last pulse was set at TDC. The bump ring enhances the flash mixing and enables a fuel/air mixing rate higher than conventional DI diesel engine. The auto-ignition and heat release rate for this strategy were investigated. By advancing the start of multi-pulse injection, noisy auto-ignition was avoided (reduced knock) but over advancing of start timing led to over-mixing resulting in higher THC emission. It was observed that small amounts of fuel in multi-pulse injections did not lead to a reduction in NO_X emission, hence, an increase was advocated

This strategy has the potential to widen the operating conditions of the HCCI engine. The basic idea behind this strategy is that (1) at low load HCCI control is established via multi-pulse fuel injection which enables very low NO_X and PM emission (< 10 ppm); (2) at medium to high load the advantage of premixed combustion with

"lean diffusion combustion" is improved further by super high injection pressure which ensures clean and high efficiency that can be achieved at the full load range. An IMEP (indicated mean effective pressure) of 0.93 MPa has been achieved with this [90].

3.1.5.1.4 Small Angle Injection

It has been well established that small angle (narrowing of angle) for the fuel spray cone reduces wall wetting and piston head wetting at early injection timing while maintaining high efficiency for HCCI combustion [111-114].

Kim and Lee [115] examined this phenomenon using two different injection nozzles with spray cone angle of 156º and 60º in a HCCI combustion. In this study, the compression ratio was reduced from 17.8:1 to 15:1 in a bid to prevent early ignition of the early premix. Results obtained revealed that for conventional CI engines the IMEP decreased rapidly as injection timing was advanced beyond 20ºBTDC indicating that specific fuel consumption (ISFC) data became unacceptably high. Early injection helped create HCCI but led to poor fuel evaporation and piston bowl spray impingement leading to high UHC and CO emission.

It was further observed that a modest decrease was observed for ISFC for the IMEP although the injection timing was advanced to 50º- 60º for the

smaller cone angle injector. This shows that a small angle cone was effective for early injection in HCCI.

3.1.5.2 Late Direct Injection in HCCI

A modulated kinetic (MK) combustion system developed by Nissan motor company was the most successful late injection HCCI strategy. This strategy was discussed by Kawashima et al. [116, 117] and Kimura et al. [117]. To achieve the diluted homogenous mixture needed for HCCI, a long ignition delay and rapid mixing was required. The ignition delay was achieved by retarding injection timing from 7^0 BTDC to 3^0 ATDC and using a higher EGR to lower oxygen concentration to 15% - 16%. Rapid mixing was accomplished by using high swirl with toroidal combustion-bowl geometry. The operating range for the first generation MK was limited to 1/3 peak torque and ½ speed. This MK mode substantially reduced NO_X to about 50 ppm without any increase in PM. Combustion noise was also reduced. In this strategy, combustion phasing is controlled by injection timing.

The second generation MK expanded the range of operation through several modifications [118]. Higher injection pressure (through a high pressure common-rail fuel system) was executed to reduce fuel injection time at all speeds. The ignition delay was increased by reducing the compression ratio and adding EGR cooling to reduce the intake temperature. To reduce fuel spray wall impingement, the piston bowl was increased from 47 mm to 56 mm. This significantly reduced UHC emission during cold starting. It was observed that the second generation MK strategy could be used for the entire range of engine operations. This strategy also met the targets of about ½ load and ¾ speed. NO_X emission was reduced by 98% compared with conventional EGR, and PM emissions were similar to conventional CI engines.

Recent work on MK by Kawamoto et al. [119] recommended higher CN fuel to reduce UHC in cold start conditions. The most strategic advantage of MK is that it does not require additional hardware and its operation with existing hardware did not negatively impact the engine's specific power output. However, the injection timing retardation reduced engine cycle efficiency and gave rise to higher UHC emission [90].

3.1.5.3 Premixed/DI HCCI

In this strategy, port injection was adopted as the primary fuel supply source to create a homogenous charge and the DI fuel injection subsequently was used to change the concentration and special position of the rich regions with the aim of controlling HCCI combustion.

Odaka et al. [120-123] proposed a homogenous charge compression ignition diesel combustion (HCDC) which used the premixed/direct-injected HCCI system. In this system, most of the fuel was injected into the intake manifold to form a homogenous pre-mixture in the cylinder and a small amount of fuel was directly injected into the homogenous premix in the cylinder. This strategy reduced both NO_X and smoke emission better than the conventional CI engine. It was also observed that smoke was reduced uniformly as the premixed fuel ratio increased.

Midlam-Mahler et al. [124-126] also built a premixed/direct-injected HCCI system. A low pressure atomizer system was employed to achieve port/manifold fuel injection and a high pressure injection system was employed for the direct injection of fuel into the combustion chamber. In low load mode, the main torque comes from the premixed lean homogenous fuel and the DI fuel only serves to initiate ignition at high loads, the maximum homogenous charge is employed and DI fuel proportion is increased to full load. Atomization to droplet size of less than $1\mu m$ mean diameter allows fast evaporation during the compression stroke, making the heating of intake unnecessary. Results obtained showed that by varying intake conditions, an IMEP of up to 4.7 bar can be achieved at a speed range of between 1600 rom - 3200 rom. In

addition, this strategy achieved vary low NO_X of less than 4 ppm and smoke emission of 0.02 FSN.

Foster et al. [51] and Berntsson and Danbratt [127] also proposed various strategies incorporating the key component of the premix/direct-injected HCCI combustion with varying degree of success. The most interesting was the use of different fuels for the different stages of the injection process in a bid to use fuel properties to greatest advantage. This was developed by Inagaki et al. [128]. In this strategy gasoline (high octane, low cetane number) was used at the intake air-port for the homogenous premixed fuel, and diesel fuel (low octane, high cetane number) was injected directly into the combustion chamber at the DI stage to initiate ignition at timing BTDC. It was observed that ignition phasing of the combustion can be controlled via the changing of fuel ratios for the two stages to the extent that combustion proceeds mildly. The operating load range where NO_X and smoke emission were 10 ppm and 0.1 FSN respectively was extended to an IMEP of 12 bar when an intake air boost system was employed.

3.1.5.4 LTC (Low Temperature Combustion)

Low temperature combustion is achieved in a CI engine with the use of EGR. It uses high levels of dilution to reduce combustion temperature and increase ignition delay. The increased ignition

delay gives ample time for fuel evaporation and increases fuel homogeneity in the reactant mixture, thus reducing NO_X formation as a result of spikes in local temperature [90, 129]. This also inevitably reduce soot formation because of the absence of fuel rich zone. Alrikson and Dentbratt [129] calculated the Q-T map for soot and NO concentration with the help of the SENKIN code using n-heptane and toluene mixtures as diesel surrogates and concluded that to completely avoid NO_X and soot formation regardless of equivalent ratio, local temperature must be kept below 1650 k. This is what is referred to as low temperature combustion [90]. However, research in HCCI combustion has warned that if local temperature falls below 1400k, the oxidation rate from CO to CO_2 becomes too low [130]. The ideal temperature (1400 k $< T_2 <$ 1650 k) become fairly obvious. The challenge had been how to control this strategy and a significant volume of research has been conducted with this objective in mind.

Natti [131] investigated soot and PM characteristics in a single cylinder HSDI diesel engine under CI and LTC regimes. The outcome observed was that soot nucleation requires higher temperature whilst surface growth proceeds at a lower temperature in the presence of the right hydrocarbon environment. Increased EGR was observed to kinetically slow down the reaction and give more scope for heat transfer. In conventional CI this reduced temperature sufficiently decreases oxidation but not accumulation. In LTC other reactions are also hindered and as a result the accumulation mode begins to slow down and thus reduces the soot as EGR increases.

Henein et al. [132] and Choi et al. [133] studied the effect of injection pressure and swirl on engine emission under LTC. The injection pressure, swirls ratios and injection timing ranges investigated were broad in scope. Henein et al. [132] used EGR ranges that covered engine operating ranges that encapsulated conventional CI engine and LTC regimes. They observed that combustion is sensitive to small variations in EGR particularly around the misfiring EGR limits in the LTC regime. Choi et al. [133] conducted their study at 15% O_2 concentration and found that increased injection pressure enhanced mixing, resulting in increases in the peak of heat release and decreased soot. The trade-off between soot and NO_X at different injection pressures, swirl ratios and EGR rates along with the misfiring thresholds were also identified. Other works on LTC are listed in the references [134-136].

3.1.5.5 HCCI Control Strategy

Given the heavy dependence on charge composition, it is clear that for effective HCCI combustion, mixture and temperature control are

essential tasks that demand a reasonable amount of attention. Control measures for improving mixing rate of fuel includes: (1) high pressure / ultra-high pressure injection and small nozzle holes investigated by Dodge et al. [137] (2) high boost pressure evaluated by Alfuso et al. [138] (3) design and reconfiguration of chamber geometry studied by Su and Zhang [139] (4) multi-pulse fuel injection using modulating injection studied by Su et al. [110].

Aside from using mixing to control HCCI, ignition delay could also be deployed to control HCCI and this could be achieve by: (1) EGR using the MK system (2) varying of compression ratio and variable valve actuation investigated by Reitz et al. [140] (3) fuel modification studied by caterpillar Inc. in 2004 [141].

3.1.6 Conclusion

Employing numerical evaluation along with experimental investigation in biodiesel combustion studies has fast-tracked research in this area and reduced costs significantly. It has also provided deeper insight into biodiesel combustion phenomena and their interrelations. From the trend observed in these studies, it has become obvious that biodiesel fuel sources can be competitively deployed with acceptable performance and emission levels. The concept of an ideal renewable fuel source with an ideal combustion strategy in CI having acceptable

performance and emissions is no longer far-fetched. And as the technical feasibility converges, the cost (which still poses significant challenges to biodiesel application) will exponentially decrease to economically acceptable levels.

In the meantime observed research gaps in numerical studies of biodiesel combustion requiring bridging exist at almost every level of the research effort. These gaps are highlighted below.

(1) The weakness of Methyl Butanoate (MB) as a suitable chemical kinetic mechanism surrogate in numerical studies has been highlighted in this review. Added to this is the fact that MB2D lacks extensive work on unsaturated alkyl mechanisms. More retooling is needed at this level to improve computational accuracies since most biodiesel sources consist of various mixtures of saturated and unsaturated fatty acid methyl ester (FAME) and given that the unsaturated components are the weak link in the formation of polycyclic aromatic hydrocarbons (PAH).

(2) Significantly large chemical kinetic mechanisms for studying saturated and unsaturated FAME have been proposed with the most prominent been MDBio. But these large, often detailed mechanisms, are tailored either for

low or high temperature reactions and are therefore unsuitable for 3D CFD application. A single reduced MDBio that can model both low and high temperature activities is needed to aid studies in low and high temperature reactions of biodiesel in 3D CFD numerical studies.

(3) HCCI multi-blend strategy, at the computational level, has not been sufficiently explored in biodiesel combustion. Even at the experimental level, research studies are scant. But the potential to effectively solve the NO_X and UHC (at low temperature) in biodiesel applications is substantial. Very importantly, the reconfiguration of engines to allow biodiesel premixed and DI as a control strategies could potentially lead to a break through and open the doors for wider application of biodiesel with an algae foot print.

(4) A potentially promising HCCI strategy that has not been vigorously pursued both at the computational as well as experimental level is the use of Modula kinetic (MK) for multi-blend biodiesel. MK deployed in an HCCI environment with a higher unsaturated FAME blend for an homogenous premix (to delay ignition) and the use of a higher saturated FAME blend as DI near TDC or ATDC to trigger ignition is being proposed here. NVO can be used to achieve a mild EGR (to avoid expensive engine retrofitting) and consequently LTC. It is possible

to achieve high IMEP across the full load spectrum and near zero NO_X and soot emission with this strategy. A good swirl number and sufficient thermal homogeneity will result in low UHC and CO (more so because of the oxygenated nature of the fuel).

This thesis commenced the preliminary work on the attempt to bridge the gap identified in serial number 4. The first approach was to build a thermo-physical property prediction scheme for the samples used in this study. This was accomplished in chapter 5 (the paper has been published in IEEE explore). The next stage was to use a CFD software to set-up different scenario of the problem through the replica of the engine test rig (having full spatial and temporal resolution with in-cylinder monitoring device) configuration and to use the data obtained from the actual test rig for validation. But access to funding for these key component were not forthcoming hence, progress was stalled. The ANSYS forte built into ANSYS CFD (appropriate for full engine combustion simulation) available in the institution came with severe restrictions. The partly licence student version did not permit access to the software library or the professional customer portal where chemical kinetic mechanism, engine geometry, piston lift profile and valve lift profile files that could be used to set-up appropriate engine configuration and surrogate fuel of the sample

being studied to be downloaded, this is in addition to the absence of engine test rig that could be used for validation purpose. Funding for these key components is actively being pursued. As a result, a proposal for the next phase of the work has been outlined in this thesis for future study (see appendix IV).

References

1. Pandey, R.K., A. Rehman, and R.M. Sarviya, *Impact of alternative fuel properties on fuel spray behavior and atomization* Renewable and Sustainable Energy Reviews **2012 16**: pp. 1762-1778.

2. Komninos, N.P. and C.D. Rakopoulos, *Modeling HCCI combustion of biofuels: A review.* Renewable and Sustainable Energy Reviews 2012. **16** pp. 1588-1610.

3. Griffin Shay .E, *Diesel fuel from vegetable oils: status and opportunities. .* Biomass and Bioenergy 1993. **4**: pp. 227-242.

4. U.N.D. Programme,., *World energy assessment.* Energy and the Challenge of Sustainability, New York: United Nations, 2000.

5. Alptekin, E. and M. Canakci, *Determination of the density and the viscosities of biodiesel-diesel fuel blend.* Renewable Energy, 2008. **33**: pp. 2623-30.

6. McIlroy, A. et al. *Basic research needs for clean and efficient combustion of 21st century transportation fuels.* Report of the basic Energy Science Workshop on Clean and Efficient Combustion of 21st Century Transportation Fuels, Office of Science, U.S. Department of Energy, 2006.

7. Ng, H.K. and S. Gan, *Combustion performance and exhaust emissions from the non-pressurised combustion of palm oil biodiesel blends.* Applied Thermal Engineering, 2010. **30**(16): pp. 2476-2484.

8. Ghorbani, A., et al., *A comparative study of combustion performance and emission of biodiesel blends and diesel in an experimental boiler.* Applied Energy 2011, **88**(12): pp. 4725-4732.

9. Ng, J.-H., H.K. Ng, and S. Gan, *Engine-out characterisation using speed-load mapping and reduced test cycle for a light-duty diesel engine fuelled with biodiesel blends.* Fuel, 2011. **90**: p. 2700-2709.

10. Ng, J.-H., H.K. Ng, and S. Gan, *Characterisation of engine-out responses from a light-duty diesel engine fuelled with palm methyl ester (PME).* Applied Energy 2012, **90**: pp. 58-67.

11. Balat, M. and H. Balat, *Progress in biodiesel processing.* Applied Energy, 2010. **87**(6): pp. 1815-1835.

12. Rounce, P., A. Tsolakis, and A.P.E. York, *Speciation of particulate matter and hydrocarbon emissions from biodiesel combustion and its reduction by after treatment.* Fuel, 2012. **96**: pp. 90-99.

13. Westbrook, C.K., W.J. Pitz, and H.J. Curran, *Chemical kinetic modeling study of the effects of oxygenated hydrocarbons on soot emissions from diesel engines.* Journal of Physical Chemistry 2006. **110**: pp. 6912-6922.

14. Lapuerta, M., O. Armas, and J. Rodriguez-Fernandez, *Effect of biodiesel fuels on diesel engine emissions.* Progress in Energy and Combustion Science 34 (2008) 198–223

15. Fontaras, G., et al.., *Effects of biodiesel on passenger car fuel consumption, regulated and nonregulated pollutant emissions over legislated and real-world driving cycles.* Fuel, 2009. **88**: pp. 1608-1617.

16. Murrilo, S., et al., *Performance and emission study in the use of biodiesel in outboard diesel engines.* Fuel., 2007. **86**: pp. 1765-1771.

17. Zhang, S., et al.., *Comparison of biodiesel performance ased on HCCI engine simulation using detailed mechanism with on-the-fly reduction.* Energy Fuels 2012, **26**: pp. 976-983.

18. http://www.fao.org/docrep/012/al390e/al390e00.pdf. Accessed on 1.6.10.

19. http://esa.un.org/unpd/wpp/Excel-Data/population.htm, Accessed on 1.6.10.

20. Naik, S.N., et al., *Production of first and second generation biofuels: a comprehensive review. Renewable and Sustainable Energy Reviews* 2010. **14**: pp. 578-97.

21. Mohamed Ismail, H., H.K. Ng, and S. Gan, *Evaluation of nonpremixed combustion and fuel spray models for in-cylinder diesel engine simulation.* Applied Energy 2011. **90**(1): pp. 271-279.

22. Pang, K.M., H.K. Ng, and S. Gan, *Development of an integrated reduced fuel oxidation and soot precursor formation mechanism for CFD simulations of diesel combustion.* Fuel 2011. **90**: pp. 2902-2914.

23. Fisher, E.M., et al., *Detailed chemical kinetic mechanisms for combustion of oxygenated fuels.* Proceedures of the Combusttion Institute, 2000. **28**: pp. 1579−1586.

24. Seshadri, K., et al.., *Experimental and kinetic modelling study of extinction and ignition of methyl decanoate in laminar non-premixed flows.* Proceedures of the Combusttion Institute, 2009. **32**: pp. 1067-1074.

25. Lu, T. and C.K. Law, *Toward accommodating realistic fuel chemistry in large-scale computations.* Progress in Energy and Combustion Science, 2008. **35**: pp. 192-215.

26. Gail, S., et al., *A wide-range kinetic modeling study of methyl butanoate combustion.* Proceedures of the Combusttion Institute, 2007. **31**: pp. 305-311.

27. Dooley, S., H.J. Curran, and J.M. Simmie, *Autoignition measurements and a validated kinetic model for the biodiesel surrogate, methyl butanoate.* Combustion and Flame, 2008 **153**: pp. 2-32.

28. Gail, S., et al.., *Experimental and chemical kinetic modelling study of small methyl esters oxidation: Methyl(E)-2-butenoate and methyl butanoate.* Combustion and Flame, 2008. **155**: pp. 635-650.

29. He, K., I.P. Androulakis, and M.G. Ierapetritou, *On-the-fly reduction of kinetic mechanisms using element flux analysis.* Chemical Engineering Science, 2010. **65**: pp. 1173-1184.

30. Pope, S.B., *Computationally efficient implementation of combustion chemistry using in situ adaptive tabulation.* Combustion Theory and Modelling, 1997. **1**: pp. 41-63.

31. Contino, F., et al., *Coupling of in situ adaptive tabulation and dynamic adaptive chemistry: An effective method for solving combustion in engine simulations.* Proceedures of the Combustion Institute, 2011. **33**: pp. 3057-3064.

32. Jangi, M. and X.-S. Bai, *Multidimensional chemistry coordinate mapping approach for combustion modeling with finite-rate chemistry.* Combustion Theory and Modelling, 2012. **16**(6): pp. 1109-1132.

33. Jangi, M., et al., *Numerical simulation of the ECN spray A using multidimensional chemistry coordinate mapping: n-dodecane diesel combustion.* SAE paper, 2012-01-1660. 2012

34. Lu, T. and C.K. Law, *A directed relation graph method for mechanism reduction. .* Proceedures of the Combustion Institute, 2005. **30**: pp. 1333-1341.

35. Lu, T. and C.K. Law, *Linear time reduction of large kinetic mechanisms with directed relation graph: n-Heptane and iso-octane.* Combustion and Flame 2006. **144**: pp. 24-36.

36. Lu, T. and C.K. Law, *On the applicability of directed relation graphs to the reduction of reaction mechanisms.* Combustion and Flame, 2006. **146**: pp. 472-483.

37. Liang, L., J.G. Stevens, and J.T. Farrell, *A dynamic adaptive chemistry scheme for reactive flow computations.* Proceedings of the Combustion Inststitute, 2009. **32**: pp. 527-534.

38. Liang, L., et al., *The use of dynamic adaptive chemistry in combustion simulation of gasoline surrogate fuels.* Combustion and Flame, 2009. **156**: pp. 1493-1502.

39. Pepiot-Desjardins, P. and H. Pitsch, *An efficient error-propagationbased reduction method for large chemical kinetic mechanism.* Combustion and Flame, 2008. **154**: pp. 67-81.

40. Lam, S.H. and D. Goussis, *The CSP method for simplifying kinetics..* International Journal of Chemical Kinetics, 1994. **26**: pp. 461-486.

41. Mass, U. and S.B. Pope, *Simplifying chemical kinetics: Intrinsic lowdimensional manifolds in composition space.* Combustion and Flame, 1992. **88**: pp. 239-264.

42. Ra, Y., et al., *Effects of fuel physical properties on diesel engine combustion using diesel and biodiesel fuels.* SAE paper, 2008-01-1379, 2008

43. Ochoterena, R., et al., *Optical studies of spray development and combustion characterization of oxygenated and Fischer-Tropsch fuels.* SAE paper 2008-01-1393, 2008

44. He, C., et al., *Spray properties alternative fuels: A comparative analysis of biodiesel and diesel.* Internaitonal Journal of Energy Research, 2008. **32**: pp. 1329-1338.

45. Furutani, M., Y. Ohta, and K. Komatsu, *Onset behavior of low-temperature flames caused by piston compression.* JSAE Reviews, 1993. **14**(2): pp. 12-8.

46. Pucher, G.R., et al., *Alternative combustion systems for piston engines involving homogeneous charge compression ignition concepts – a review of studies using methanol, gasoline and diesel fuel.* SAE paper 962063, 1996.

47. Green, R.M., et al., *The role of low temperature chemistry in the auto-ignition on n-butane.* SAE paper 872108, 1987.

48. Addargarla, S., et al.., *Effect of fuel–air mixture stressing on pre-ignition heat release in a knock research engine.* SAE paper 892082, 1989.

49. Onishi, S., et al., *Active thermo-atmosphere combustion (ATAC) - a new combustion process for internal combustion engines.* SAE paper 7905011979.

50. Noguchi, M., T. Tanaka, and Y. Takeuchi, *A study on gasoline engine combustion by observation of intermediate reactive products during combustion.* SAE paper 790840, 1979.

51. Najt, P.M. and D.E. Foster, *Compression ignited homogeneous charge combustion.* SAE paper 830264, 1983.

52. Ryan III, T.W. and T.J. Callahan, *Homogeneous charge compression ignition of diesel fuel.* AE paper 961160, 1996.

53. Gray III, A.W. and T.W. Ryan III, *Homogeneous charge compression ignition (HCCI) of diesel fuel.* SAE paper 971676, 1997.

54. Cheng, X., et al., *Advances in Computational Fluid Dynamics (CFD) Modeling of In-Cylinder Biodiesel Combustion.* Energy Fuels, 2013. **27**: pp. 4489-4506.

55. Lai, J.Y.W., K.C. Lin, and A. Violi, *Biodiesel combustion: Advances in chemical kinetic modeling.* Progress in

Energy and Combustion Science, 2011. **37**: pp. 1-14.

56. Westbrook, C.K., et al., *Detailed chemical kinetic reaction mechanisms for soy and rapeseed biodiesel fuels.* . Combustion and Flame, 2011. **158**: pp. 742-755.

57. Komninos, N.P. and C.D. Rakopoulos, *Numerical investigation into the formation of co and oxygenated and nonoxygenated hydrocarbon emissions from isooctane- and ethanol-fueled HCCI engines.* Energy Fuels, 2010. **24**: pp. 1655-67.

58. Um, S. and S.W. Park, *Modeling effect of the biodiesel mixing ratio on combustion and emission characteristics using a reduced mechanism of methyl butanoate.* Fuel, 2010. **89**: pp. 1415-1142.

59. Dagaut, P., S. Gail, and M. Sahasrabudhe, *Rapeseed oil methyl ester oxidation over extended ranges of pressure, temperature, and equivalence ratio: Experimental and modeling kinetic study.* Proceedures of the Combustion Institute, 2007. **31**: pp. 2955-2961.

60. Knothe, G., A.C. Matheaus, and T.W. Ryan, *Cetane numbers of branched and straightchain fatty esters determined in an ignition quality tester.* Fuel, 2003. **82**: pp. 971-975.

61. Knothe, G. and K.R. Steidley, *Kinematic viscosity of biodiesel fuel components and related compound. influence of compound structure and comparison to petrol diesel fuel components.* Fuel, 2005. **84**: pp. 1059-1065.

62. Graboski, M.S. and R.L. McCormick, *Combustion of fat and vegetable oil derived fuels in diesel engines.* Progressin Energy nd Combustion Science, 1998. **24**: pp. 125-164.

63. Yamane, K., A. Ueta, and Y. Shimamoto, *Influence of physical and chemical properties of biodiesel fuels on injection, combustion and exhaust emission characteristics in a direct injection compression ignition engine.*

International Journal of Engine Research, 2001. **2**(No.4): pp. 1-13.

64. Holger, H., et al., *Combined NOx and PM exhaust gas after treatment approaches for HSDI diesel engines.* SAE Paper 872108, 2004.

65. Griffin Shay, E., *Diesel fuel from vegetable oils: status and opportunities.* Biomass and Bioenergy, 1993. **4**: pp. 227-42.

66. Kalam, M.A. and H. Masjuki, *Biodiesel from palm oil-an analysis of its properties and potential.* Biomass and Bioenergy, 2002. **23**: pp. 471-9.

67. Karaosmanoglu, F., G. Kurt, and T. Ozaktas, *Long term CI engine test of sunflower oil.* Renewable Energy, 2000. **19**: pp. 219-221.

68. Kusdiana, D. and S. Saka, *Effects of water on biodiesel fuel production by supercritical methanol treatment.* Bioresource Technology, 2004. **91**: pp. 289-295.

69. Chakravarthy, K., et al., *Physical properties of bio-diesel and implications for use of bio-diesel in diesel engines.* SAE paper, 2007-01-4030, 2007.

70. Reid, R.C., J.M. Prausnitz, and T.K. Sherwood, *The properties of gases and liquids.* 3rd ed. New York: McGraw-Hill, , 1977.

71. Reid, R.C., J.M. Prausnitz, and T.K. Sherwood, *The Properties of Gases and Liquids.* 4th ed. New York: McGraw-Hill, 1987.

72. Poling, B.E., J.M. Prausnitz, and J.P. O'Connel, *The Properties of Gases and Liquids.* 5th ed. New York: McGraw-Hill, 2001.

73. http://knovel.com/web/, *Knovel critical tables,* 2nd ed. Accessed July 26, 2012.

74. http://knovel.com/, *Design institute for physical property data.* Accessed July 26, 2012.

75. Stringer, V., et al., *Modeling biodiesel spray breakup with well-defined fuel properties;* Chicago, IL: ILASS-Americas, May 15-18, 2007.

76. Yuan, W., A.C. Hansen, and Q. Zhang, *Predicting the physical properties of biodiesel for combustion modeling.* Transaction ASAE 2003. **46**(6): pp. 1487-1493.

77. Lee, B.I. and M.G. Kesler, *A generalized thermodynamic correlation based on three-parameter corresponding states.* AIChE Journal, 1975. **21**: pp. 510-527.

78. Kay, W.B., *Density of hydrocarbon gases and vapors.* Industrial and Engineering Chemistry, 1936. **28**: pp. 1014-1019.

79. Rakopoulos, C.D. and C.N. Michos, *Generation of combustion irreversibilities in a spark ignition engine under biogas-hydrogen mixtures fueling.* International Journal of Hydrogen Energy, 2009. **34**: pp. 4422-4437.

80. Fiveland, S.B. and D.N. Assanis, *A four-stroke homogeneous charge compression ignition engine simulation for combustion and performance studies.* SAE paper 2000-01-0332, 2000

81. Brakora, J.L. and R.D. Reitz, *Investigation of NOx predictions from biodiesel-fueled HCCI engine simulations using a reduced kinetic mechanism.* SAE paper 2010-01-0577, 2010.

82. Brakora, J.L., Y. Ra, and R.D. Reitz, *Development and validation of a reduced reaction mechanism for biodiesel-fueled engine simulations.* SAE paper 2008-01-1378, 2008

83. Yoshikawa T, R.R., *Development of an improved NOx reaction mechanism for low temperature diesel combustion modeling,.* SAE paper 2008-01-2413, 2008.

84. Ogink, R., *Applications and results of a user-defined, detailed-chemistry HCCI combustion model in the AVL BOOST cycle simulation code.* International AVL User Meeting Austria, 2003: pp. 14-15.

85. Milovanovic, N., et al., *Influence of the variable valve timing strategy on the control of a homogeneous charge compression (HCCI) engine.* SAE paper 2004-01-1899, 2004.

86. Ogink, R. and V. Golovitchev, *Gasoline HCCI modeling: an engine cycle simulation code with a multi-zone combustion model.* SAE paper 2002-01-1745, 2002.

87. Agarwal, A. and D.N. Assanis, *Modeling the effect of natural gas composition on ignition delay under compression ignition conditions.* SAE paper 971711, 1997.

88. Kong, S.C., N. Ayoub, and R.D. Reitz, *Modeling combustion in compression ignition homogeneous charge engines.* SAE paper 920512, 1992.

89. Tominaga, R., et al., *Effects of heterogeneous EGR on the natural gas-fueled HCCI engine using experiments CFD and detailed kinetics.* SAE paper 2004-01-0945, 2004.

90. Yao, M., Z. Zheng, and H. Liu, *Progress and recent trends in homogeneous charge compression ignition (HCCI) engines.* Progress in Energy and Combustion Science 2009. **35**: pp. 398-437.

91. Ma, X, C. Jiang, H. Li, G. Tian, H. M. Xu, and M.L. Wyszynski., *Optical diagnostics of flow and combustion,* 2015.Available:www.birmingham.ac.uk, date accessed: 10/09/201592.

92. Richter, M., J. Engström, A. Franke, M. Aldén, A. Hultqvist, B. Johansson., *The influence of charge inhomogeneity on the HCCI combustion process.* SAE paper 2000-01-2868, 2000.

93. Kumano, K. and N. ida, *Analysis of the effect of charge inhomogeneity on HCCI combustion by chemiluminescence measurement.* SAE paper 2004-01-1902, 2004.

94. Ozaki, J. and N. Iida, *Effect of degree of unmixedness on HCCI combustion based on experiment and numerical analysis.* SAE paper 2006-32-0046, 2006.

95. Glassman, I., *Combustion.* 3rd ed. New York: Academic Press, 1996.

96. Dec, J.E. and C. Espey, *Chemiluminescence imaging of auto-ignition in a DI diesel engine.* SAE paper 982685, 1998.

97. Kawahara, N., E. Tomita, and H.H. Kagajyo, *Homogeneous charge compression ignition combustion with dimethyl ether spectrum analysis of chemiluminescence.* SAE paper 2003-01-1828, 2003.

98. Mancaruso, E., S.S. Merola, and B.M. Vaglieco, *Extinction and chemiluminescence measurements in CR DI diesel engine operating in HCCI mode.* SAE paper 2007-01-0192, 2007.

99. Persson, H., et al., *Investigation of the earlyn flame development in spark assisted HCCI combustion using high speed chemiluminescence imaging.* SAE paper 2007-01-0212, 2007.

100. Zhao, H. and N. Ladommatos, *Optical diagnostics for in-cylinder mixture formation measurements in IC engines.* Progress in Energy and Combustion Science, 1998. **24**(4): pp. 297-336.

101. Collin, R., et al., *Simultaneous OH- and formaldehyde-LIF measurements in an HCCI engine.* SAE paper 2003-01-3218, 2003.

102. Sa¨rner, G., et al., *Simultaneous PLIF measurements for visualization of formaldehydeand fuel-distributions in a DI HCCI engine.* SAE paper 2005-01-3869, 2005.

103. Christensen, M., A. Hultqvist, and B. Johansson, *Demonstrating the multi fuel capability of a homogeneous charge compression ignition engine with variable compression ratio.* SAE paper 1999-01-3679, 1999.

104. Takeda, Y., N. Keiichi, and N. Keiichi, *Emission characteristics of premixed lean diesel combustion with extremely early staged fuel injection.* SAE paper 961163, 1996.

105. Nakagome, K., et al., *Combustion and emissions characteristics of premixed lean diesel combustion engine.* SAE paper 970898, 1997.

106. Harada, A., et al., *The effects of mixture formation on premixed lean diesel combustion.* SAE paper 980533, 1998.

107. Hashizume, T., et al., *Combustion and emission characteristics of multiple stage diesel combustion.* SAE paper 980505, 1998.

108. Akagawa, H., et al., *Approaches to solve problems of the premixed lean diesel combustion.* SAE paper 1999-01-0183, 1999.

109. Yanagihara, H., *Ignition timing control at Toyota ''UNIBUS'' combustion system.* In: Proceedings of the IFP international congress, 2001: pp. 35-42.

110. Su, W.H., T.J. Lin, and Y.Q. Pei, *A compound technology for HCCI combustion in a DI diesel engine based on the multi-pulse injection and the BUMP combustion chamber.* SAE paper 2003-01-0741, 2003.

111. Walter, B. and B. Gatellier, *Near zero NOx emissions and high fuel efficiency diesel combustion: the NADITM concept using dual mode combustion.* Oil & Gas Science and Technology, 2003. **58**(1): pp. 101-111.

112. Shimazaki, N., T. Tsurushima, and T. Nishimura, *Dual mode combustion concept with premixed diesel combustion by direct injection near top dead center.* SAE paper 2003-01-0742, 2003.

113. Mueller, C.J., et al., *An experimental investigation of in-cylinder processes under dual-injection conditions in a DI diesel engine.* SAE paper 2004-01-1843, 2004.

114. Duret, P., et al., *Progress in diesel HCCI combustion within the european SPACE LIGHT project.* SAE paper 2004-01-1904, 2004.

115. Kim, M.Y. and C.S. Lee, *Effect of a narrow fuel spray angle and a dual injection configuration on the improvement of exhaust emissions in a*

HCCI diesel engine. Fuel, 2007. **86**(17-18): pp. 2871-80.

116. Kawashima, J.I., H. Ogawa, and Y. Tsuru, *Research on a variable swirl intake port for 4-valve high-speed DI Diesel engines.* SAE paper 982680, 1998.

117. Kimura, S., et al., *New combustion concept for ultra-clean and high-efficiency small DI diesel engines.* SAE paper 1999-01-3681, 1999.

118. Kimura, S., et al., *Ultra-clean combustion technology combining a low-temperature and premixed combustion concept for Meeting Future Emission Standards.* SAE paper 2000-01-0200, 2000.

119. Kawamoto, K., et al., *Combination of combustion concept and fuel property for ultra-clean DI diesel.* SAE paper 2004-01-1868, 2004.

120. Suzuki, H., N. Koike, and M. Odaka, *Exhaust purification of diesel engines by homogeneous charge with compression ignition. Part 1: experimental investigation of combustion and exhaust emission behavior under pre-mixed homogeneous charge compression ignition method.* SAE paper 970313, 1997.

121. Suzuki, H., N. Koike, and M. Odaka, *Exhaust purification of diesel engines by homogeneous charge with compression ignition. Part 2: analysis of combustion phenomena and NOx formation by numerical simulation with experiment.* SAE paper 970315, 1997.

122. Suzuki, H., N. Koike, and M. Odaka, *Combustion control method of homogeneous charge diesel engines.* SAE paper 980509, 1998.

123. Odaka, M., et al., *Search for optimizing method of homogeneous charge diesel combustion.* SAE paper 1999-01-0184, 1999.

124. Midlam-Mohler, S., Y. Guezennec, and G. Rizzoni, *Mixed-mode diesel HCCI with external mixture formation: preliminary results.* 9th Diesel engine emissions reduction (DDER) workshop, 2003.

125. Guezennec, Y., S. Midlam-Mohler, and G. Rizzoni, *A mixed mode HCCI/DI engine based on a novel heavy fuel atomizer.* 8th Diesel engine emissions reduction (DEER) workshop, 2002.

126. Midlam-Mohler, S., *Diesel HCCI with external mixture preparation.* 10th Diesel engine emissions reduction (DEER) workshop, 2004.

127. Berntsson, A.W. and I. Denbratt, *HCCI combustion using charge stratification for combustion control.* SAE paper 2007-01-0210, 2007.

128. Inagaki, K. and T. Fuyuto, *Combustion system with premixture-controlled compression ignition.* R&D Rev Toyota CRDL 2006. **41**(3): pp. 35-46.

129. Alriksson, M. and I. Denbratt, *Low temperature combustion in a heavy duty diesel engine using high levels of EGR.* SAE paper 2006-01-0075, 2006.

130. Potter, M., R. Durrett, and G. Motors, *Design for compression ignition high-efficiency clean combustion engines.* 12th Annual diesel engine emissions reduction (DEER) conference, 2006.

131. Natti, K.C., *PM characterization in an HSDI diesel engine under conventional and LTC regimes.* SAE paper 2008-01-1086, 2008.

132. Henein, N.A., et al., *Effect of injection pressure and swirl motion on diesel engine-out emissions in conventional and advanced combustion regimes.* SAE paper 2006-01-0076, 2006.

133. Choi, D., et al., *A parametric study of low-temperature, late-injection combustion in a HSDI diesel engine.* Spec Issue Adv Combust Technol Intern Combust Engines 2005. **48**(4): pp. 656-64.

134. Genzale, C.L., R.D. Reize, and M.P.B. Musculus, *Effects of piston bowl geometry on mixture development and late-injection low-temperature*

combustion in a heavy-duty diesel engine. SAE paper 2008-01-1330, 2008.

135. Opat, R., et al., *nvestigation of mixing and temperature effects on HC/CO emissions for highly dilute low temperature combustion in a light duty diesel engine.* SAE paper 2007-01-0193, 2007.

136. Kumar, R. and M. Zheng, *Fuel efficiency improvements of low temperature combustion diesel engines.* SAE paper 2008-01-0841, 2008.

137. Dodge, L.G., et al., *Effect of small holes and high injection pressures on diesel engine combustion.* SAE paper 2002-01-0494, 2002.

138. Alfuso, S., et al., *Analysis of a high pressure diesel spray at high pressure and temperature environment conditions.* SAE paper 2005-01-1239, 2005.

139. Zheng, X.L., T.F. Lu, and C.K. Law, *Experimental counterflow ignition temperatures and reaction mechanisms of 1,3-butadiene. Proceedings of the Combustion Institute*, 2007. **31**: pp. 367-375.

140. Reitz, R.D., et al., *PCCI investigation using variable intake valve closing in a heavy duty diesel engine.* SAE paper 2007-01-0903, 2007.

141. Caterpillar., *Heavy Truck Clean Diesel (HTCD) Program (Heavy Duty HCCI Development Activities).* 11th Diesel Engine-Efficiency and Emissions Research (DEER) Conference, Coronado, CA, 2004.

142. http://www.scania.com.
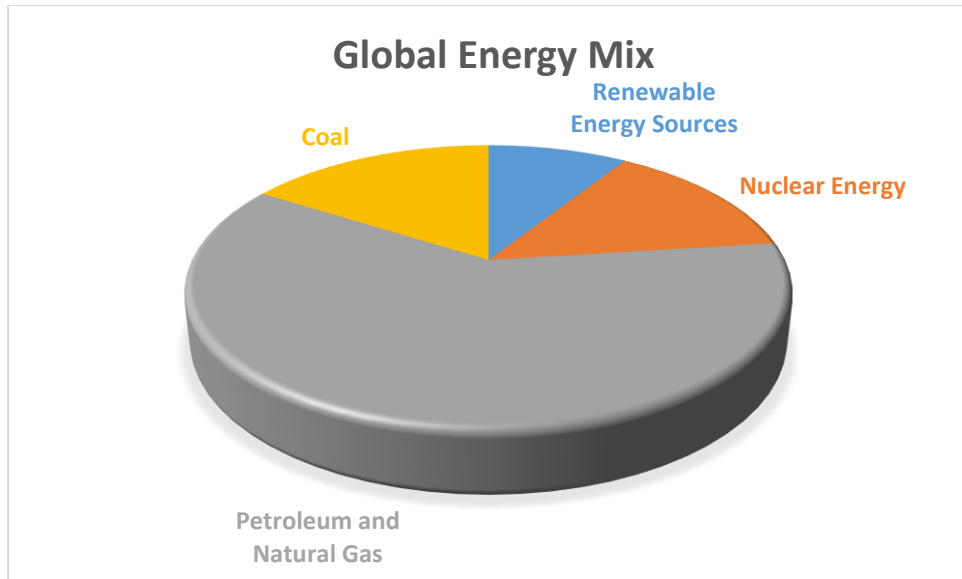
Figure 3 1: Global energy mix as at 2009 [1]
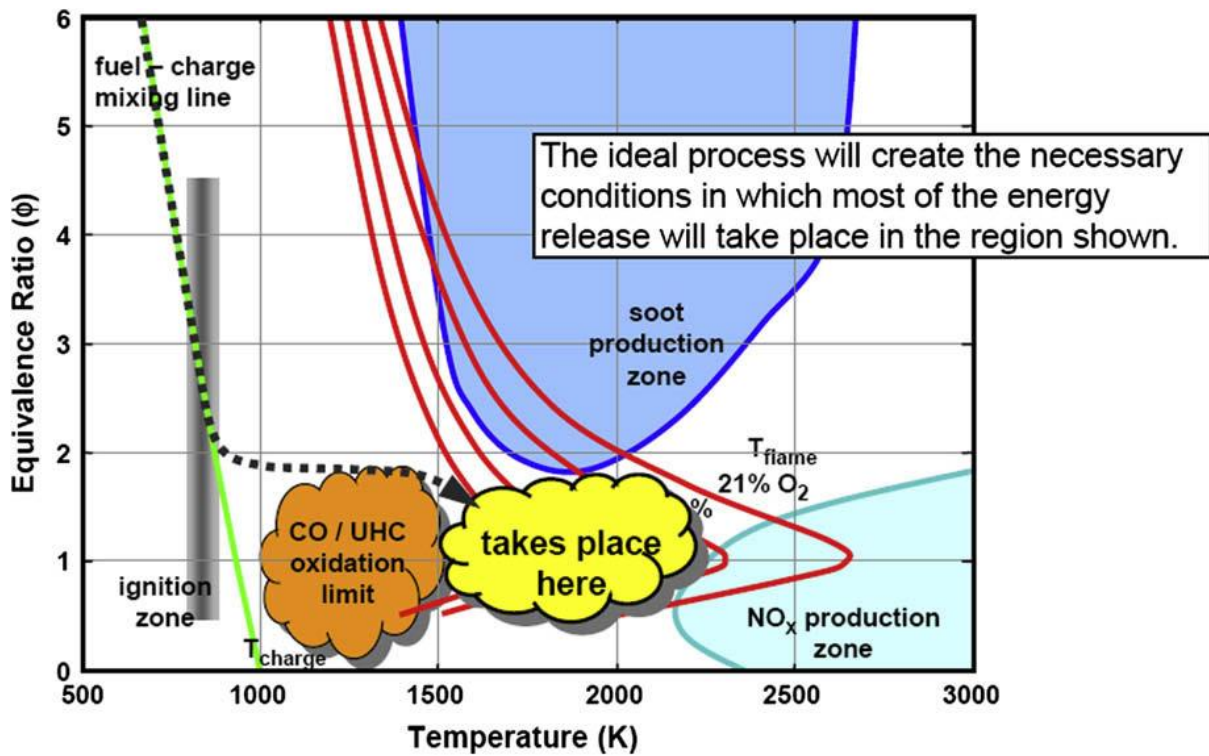
Figure 3 2: $\emptyset$-T map showing LTC concept [90]
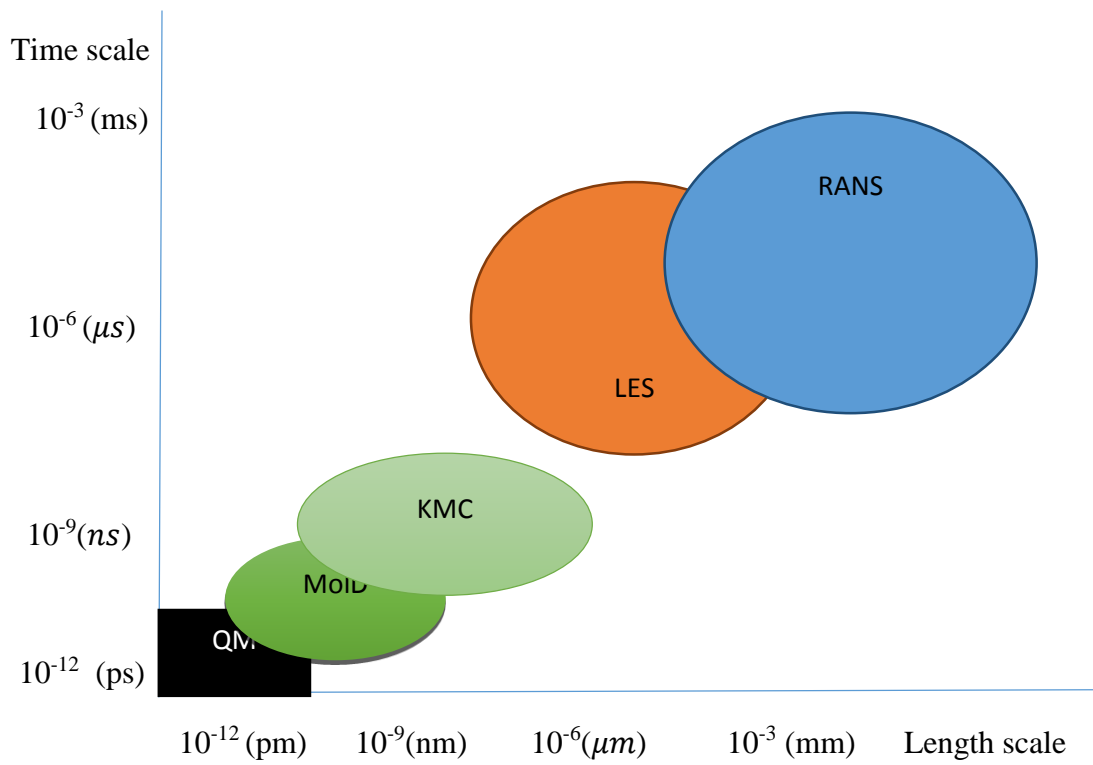
Figure 3 3: Spatial and temporal domain of common numerical simulation
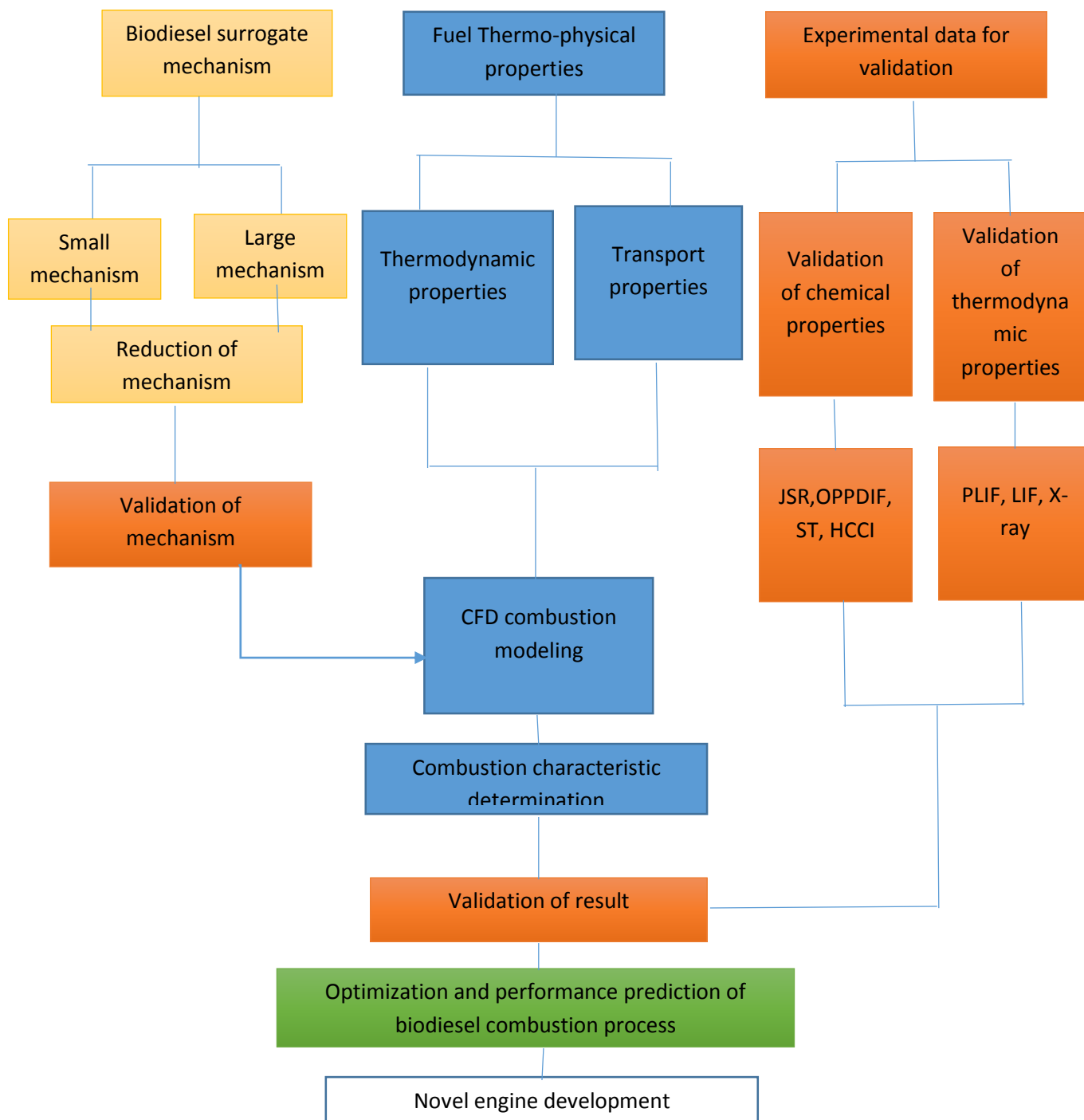
Figure 3 4: Interrelation between CFD and chemical kinetic in biodiesel study
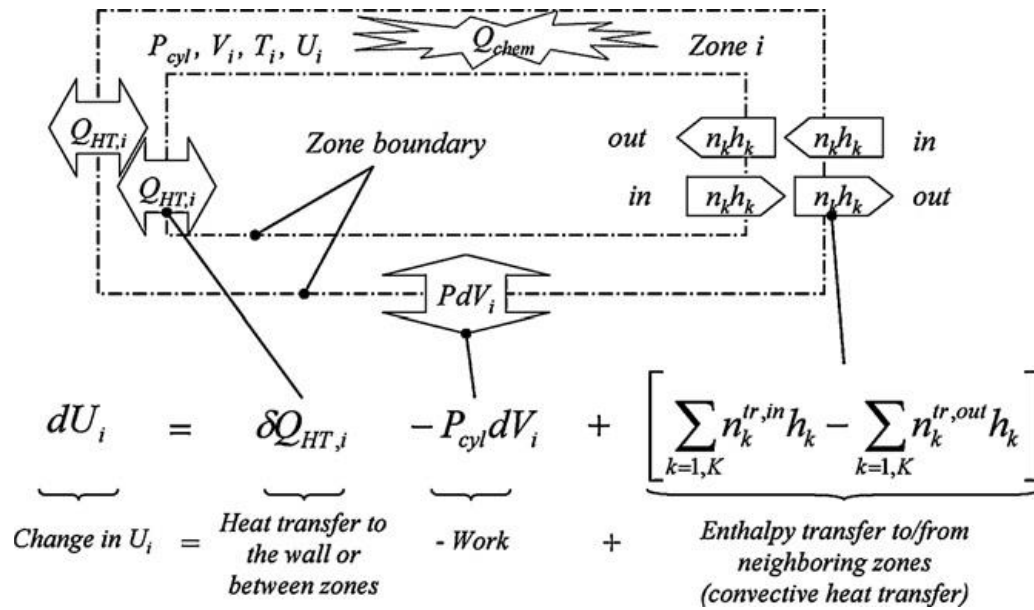
Figure 3 5: Multi-zone, Quasi-dimensional numerical study of biodiesel [85]

Table 3. 1: Common FAME constituents

Fatty Acid	Systematic name	Structure	Formula
Lauric	Dodecanoic	12:0	$C_{12}H_{24}O_2$
Myristic	Tetradecanoic	14:0	$C_{14}H_{28}O_2$
Palmitic	Hexadecanoic	16:0	$C_{16}H_{32}O_2$
Stearic	Octadecanoic	18:0	$C_{18}H_{36}O_2$
Arachidic	Eicosanoic	20:0	$C_{20}H_{40}O_2$
Behenic	Docosanoic	22:0	$C_{22}H_{44}O_2$
Lignoceric	Tetracosanoic	24:0	$C_{24}H_{48}O_2$
Oleic	Cis-9-Octadedeconoic	18:1	$C_{18}H_{34}O_2$
Linoleic	Cis-9,cis-12 Octadedeconoic	18:2	$C_{18}H_{32}O_2$
Linolenic	Cis-9,cis-12,cis15 ctadedeconoic	18:3	$C_{18}H_{30}O_2$
Erucic	Cis-13, Decosanoic	22:1	$C_{22}H_{42}O_2$

CHAPTER 4: BIODIESEL EXTRACTION AND ENGINE TURBULENCE THEORY

4.1 Introduction

This experimental work involves the sourcing, processing and extraction of oil from a seed source for production of biodiesel. The experimental determination of the property of the oil as well as the biodiesel was initiated to confirm their compliance with ASTM and European standards for diesel application in compression ignition engines. A numerical scheme was assembled to serve as a tool for the property prediction of the biodiesel with the aim of reducing research costs and time. The scheme was to be validated with the experimental data obtained in this work as well as data obtained from other studies with similar samples.

In the oil extraction stage, the manual as well as soxhlet extraction procedure were implemented using the traditional n-hexane and petroleum ether as solvent to determine the optimal extraction pathway. As part of efforts to test new solvents that are readily available and inexpensive, distilled gasoline was also introduced. Gasoline, because of the ubiquity of its supply, if confirmed as a viable solvent for seed oil extraction, could potentially facilitate the widespread production of biodiesel at a reduced cost with a flexible and adaptable technology. And since the gasoline can be recovered, this could serve as an additional incentive for the biodiesel processing value chain.

The theoretical framework for the numerical study of the remediation strategy for observed gaps is also outlined alongside proposals for the requisite validation tools for the study. The chapter presents the material and method employed to execute this work schedule.

4.2 Oil Seed Processing and Extraction.

Sufficient quantity of moringa and jatropha seeds were sourced from the wild and sun dried to facilitate easy processing. The process stage commenced with the manual removal of the seed husk. The seeds where then finely grinded using mechanical screw/crush plate grinder and, oven dried in batches. Plates 4.1, 4.2 and 4.3 show moringa, jatropha seeds and the oven drying process of the pulverized seed respectively.

Plate 4 1: Moringa seeds

Plate 4 2: Jatropha seed

Plate 4 3: Pulverized seed in oven

For the oil extraction, two methods, namely, manual and soxhlet extraction, were employed using three different solvents. The solvents were: normal hexane (n-hexane), petroleum ether and distilled gasoline. The first two are traditional solvents used for oil extraction, but distilled gasoline was introduced as a wild card for the reasons stated earlier. For every batch of 150 g of crushed seed sample, 400 mL of solvent was used to dissolve same for the manual soaking method of extraction, and 600 mL was used for the same purpose for soxhlet extraction. The extraction yield for the various methods and solvent types are presented in Chapter 5. Plate 4.4 and 4.5 show manual (filtration) extraction and soxhlet extraction of oil from crushed seed samples using the listed solvents respectively. After the solvent has been used, the distillation process is employed to separate the solvent from the oil using the distillation apparatus as shown in Plate 4.6. This process also effectively recovers a significant percentage of the solvent and ensures a clean sample of the oil in readiness for the transesterification process.

Plate 4 4: Pulverized seed sample soaked in solvent undergoing manual filtration extraction

Plate 4 5: Sample undergoing soxhlet extraction

Plate 4 6: Separation of oil from solvent using distillation

4.3 Biodiesel Production and Property Evaluation.

At the end of the oil extraction process, it was necessary to determine the properties of the oil since it is important to know the FFA composition of the oil before deciding on the best transesterification process to adopt. The FFA composition of the moringa oil was 9.96% while that of jatropha was 2.48%. Since moringa FFA composition was greater than 3%, a neutralization reaction using sulphuric acid prior to using the alkaline catalyst was initiated to avoid producing soap instead of biodiesel during the transesterificate process [1]. The neutralization reaction was aimed at reducing the FFA of moringa to a level that permitted the use of an alkaline catalyst since the use of alkaline is much faster and much more efficient.

Potassium hydroxide was chosen as the catalyst and methanol was used at the alcohol. The proportion of oil and methanol was $1:1/10^{th}$ to produce 1 part biodiesel. At the compression of the transeterification process, the glycerol produced being denser sinks to the bottom of the flask while the pure biodiesel is drained off. Plate 4.7 shows this displacement between the glycerol and biodiesel for

the moringa sample in this work. Product washing with water was executed to remove the salt produced during the neutralization reaction and the resulting fuel is dried in the oven to obtain clean biodiesel.

Plate 4 7: Moringa transesterification

4.4   Determination of Oil and Biodiesel Properties.

A broad range of properties for the oil as well as the biodiesel was determined. The Cannon Penske viscometer was employed to measure the viscosity of the samples [2]. For density, the specific gravity was estimated using a density bottle and the value was converted to density in Kg/m^3 at 40^oC. The Wijs solution method was deployed to determine the iodine value of the oil samples [3]. The refractive indexes of the oils were determined with the Abbe refractometer (Prolabo). Pensky-Martens cup flash tester was employed for flash point determination [4]. For free fatty acid (FFA), saponification values and peroxide values, the titrimetric method was employed using appropriate reagents. The pour and cloud points were determined using the Van Garpen et al. method. Details are outlined in Chapter 6.

4.5   Numerical Theory: Turbulence Model

Given substantial advancement in computing power over time along with the development of powerful numerical methods, it has now become routine to effectively predict details of flow field, heat transfer

and combustion process within the internal combustion engine with different types of engine geometry. Continuous progress is being recorded in chemical kinetic mechanisms, construction of high fidelity surrogates and advanced computation techniques along with state-of-the-art engine diagnostics.

In regards to computational fluid dynamics (CFD) based models, the most applicable to the open system CI are the turbulence model $(k - \varepsilon)$, spray model and combustion models. The coded numerical solution is typically running on KIVA or a coupled CHEMKIN-KIVA code. The chemistry solver best suited for this work is MDBio reduced mechanism. The basic structure of the turbulent model as presented by Amsden et al. [5] is given below.

The equation of motion for the fluid phase based on Navier-Stokes averaged solution is called Reynolds Averaged Navier-Stokes (RANS).

Given the unit vectors in the x, y and z direction denoted by i, j and k respectively, the position vector **x** is

$$x = xi + yj + zk \qquad\qquad 4.1$$

The vector operator ∇ is

$$\nabla = i\frac{\partial}{\partial x} + j\frac{\partial}{\partial y} + k\frac{\partial}{\partial z} \qquad\qquad 4.2$$

The fluid velocity vector u is given by

$$u = u(x, y, z, t)i + v(x, y, z, t)j + w(x, y, z, t)k \qquad\qquad 4.3$$

Where t is time.

In the fluid phase, both laminar and turbulent flows can be solved by KIVA but in CI engines the predominant flow is turbulent, hence the transport co-efficient are derived from a turbulent diffusivity that depends on the turbulent kinetic energy, k, and its dissipation rate, ε.

Assuming continuity of species m

$$\frac{\partial \rho}{\partial t} + \nabla(\rho_m u) = \nabla \left[\rho D \nabla \left(\frac{\rho_m}{\rho} \right) \right] + \dot{\rho}_m^c + \dot{\rho}^s \delta_{ml} \qquad\qquad 4.4$$

Where ρ_m density of species m, total mass density ρ, and u are density and fluid velocity respectively. D is diffusivity, $\dot{\rho}_m^c$ is source term due to chemistry and $\dot{\rho}^s$ for spray, species 1 is the species for which the spray droplets are composed and δ is the Dirac delta function. Summing equation (1) over all species gives the fluid total density equation

$$\frac{\partial \rho}{\partial t} + \nabla(\rho u) = \dot{\rho}^s \qquad\qquad 4.5$$

Because mass is conserved in a chemical reaction.

The momentum equation for the mixture is

$$\frac{\partial(\rho u)}{\partial t} + \nabla(\rho u \cdot u) = -\frac{1}{a^2}\nabla \rho - A_0 \nabla \left(\frac{2}{3} PK \right) + \nabla \sigma + F^s + Pg \qquad\qquad 4.5$$

Where p is the fluid pressure a is the dimensional quantity used in conjunction with the pressure gradient scaling (PGS) method Ramshaw et al. [6]. A_0 is unity when the turbulent model is used.

The viscous stress tensor is Newtonian in form

$$\sigma = \mu[\nabla u \cdot (\nabla u)^T] + \lambda \nabla \cdot uI \qquad\qquad 4.6$$

μ and λ are defined later. T is the transpose, I is the unit dyadic F^s is the rate of momentum gained per unit volume due to the spray and is defined later.

The internal energy equation is

$$\frac{\partial(\rho I)}{\partial t} + \nabla(\rho u I) = -\rho \nabla \cdot u + (1 + A_o)\sigma : \nabla u - \nabla J + A_o \rho \varepsilon + \dot{Q}^C + \dot{Q}^s \qquad\qquad 4.7$$

Where I is the specific internal energy exclusive of chemical energy. The heat flux vector J is the sum of contribution due to heat conduction and enthalpy diffusion

$$J = -K\nabla T - \rho D \sum_m h_m \nabla \left(\rho_m / \rho \right)$$
<div align="right">4.8</div>

Where T is the fluid temperature and hm the specific enthalpy of species m. The source term due to chemical heat release Q^c and spray interaction Q^s will be defined later.

When $A_o = I$ (Turbulent model), two additional transport equations are solved for the turbulent kinetic energy k and its dissipation rate, ε.

$$\frac{\partial \rho k}{\partial t} + \nabla (\rho u k) = -\frac{2}{3} \rho k \nabla \cdot u + \sigma : \nabla u + \nabla \left[\left(\frac{\mu}{P_{rk}} \right) \nabla k \right] - \rho \varepsilon + \dot{W}^s$$
<div align="right">4.9</div>

And

$$\frac{\partial \rho \varepsilon}{\partial t} + \nabla (\rho u \varepsilon) = -\left(\frac{2}{3} c_{\varepsilon 1} - c_{\varepsilon_2} \right) \rho \varepsilon \nabla \cdot u + \left[\left(\frac{\mu}{P_{r\varepsilon}} \right) \nabla \varepsilon \right] + \frac{\varepsilon}{k} \left[c_{\varepsilon 1} \sigma : \nabla u - c_{\varepsilon 2} \rho \varepsilon + c_s \dot{W}^s \right]$$ 3.116

Equation (4.8) and (4.9) are the standard $k - \varepsilon$ equations with some added terms $\left(c_{\varepsilon 3} - \frac{2}{3} c_{\varepsilon 1} \right) \nabla \cdot u$ in the ε-equation accounts for the length scale changes when there is velocity dilatation. Source terms involving the quantity arise due to interaction with the spray.

When SGS turbulent model is used, ε is constrained to satisfy

$$\varepsilon \geq \left[\frac{c_\mu}{P_{r\varepsilon} (c_{\varepsilon 2} - c_{\varepsilon 1})} \right]^{1/2} \cdot \frac{k^{3/2}}{L_{SGS}}$$
<div align="right">4.10</div>

LSGS is an input SGS length scale whose value is typically taken to be $4\delta x$, where δx is a representative computational cell dimension. The equation 10 is satisfied by integrating equations 4.8 and 4.9 in all special and temporal domains and then setting ε is equal to the right-hand side of equation 4.10 at points where the inequality is breached.

References

[1]   A. E. Atabania, A. S. Silitonga, Irfan Anjum Badruddina, T. M. I. Mahliaa, H. H. Masjukia, and S. Mekhilefd, "A comprehensive review on biodiesel as an alternative energy resource and its characteristics," *Renewable and Sustainable Energy Reviews* vol. 16 pp. 2070-2093, 2012.

[2]   H. J. Wilke, H. Kryk, J. Hartmann, and D. Wagner, "Theory and practice of capillary viscometry: an introduction " *Schott: glass made of idear,* vol. www.si-analytics.com/.../INT/Primer_VISCO, pp. 1-41, 2012.

[3]   M. Simurdiak, O. Olukoga, and K. Hedberg, "Obtaining the iodine value of various oils via bromination with pyridinium tribromide," *Journal of Chemical Educaton.,* vol. 93, pp. 322-325, 2016.

[4]   https://www.youtube.com/watch?v=bZ5TOecenyc, viewed on the 12th of June, 2013.

[5]   A. A. Amsden, P. J. O. Rourke, and T. D. Butler, *KIVA-II: A Computer Program for Chemically Reactive Flows with Sprays*, Los Alamos National Laboratory New Mexico, vol. 87545, 1989.

[6]   J. D. Ramshaw, P. J. Orourke, and L. R. Stein, "Pressure gradient scaling method for fluid flow with nearly uniform pressure," *Journal of Computational Physics,* vol. 58, pp. 361-376, 1985.

CHAPTER 5

Paper 2: A PROPERTY PREDICTION SCHEME FOR BIODIESEL DERIVED FROM NON-EDIBLE FEEDSTOCK

E. I. Onuh and Freddie L. Inambao.

Abstract

Biodiesel's renewability, universal accessibility and milder impact on the environment has positioned it as a potential fuel of choice for transport prime movers going forward. Biodiesel's unique fuel chemistry while conferring some advantage, has shown some mismatch between it and the current compression ignition (CI) combustion strategy. Computational as well as experimental research on biodiesel combustion are presently, in large part, geared toward resolving this mismatch. Numerical property prediction was implemented in this study to determine the thermo-physical and transport properties of biodiesel derived from moringa, jatropha and waste restaurant oil. Primary and secondary experimental data obtained in accordance with biodiesel standard ASTM D6751 were used to validate the scheme. The average relative deviation (ARD) for most key properties fell within acceptable limits ($\leq 5\%$). Obtaining higher computational fidelity was observed to correlate with improved accuracy in determining the free fatty acid (FFA) composition of the different components and group contribution of the biodiesel mixture.

Index Terms: Average relative deviation (ARD), biodiesel standard, compression ignition (CI), free fatty acid (FFA), group contribution and properties.

5.1 Introduction

The triple effect of depleting fossil fuel reserves, the polluting effect of combusting conventional fuel and the ever increasing demand for energy has led to the quest for sustainable sources of energy. In the transport sub-sector, biodiesel clearly possesses the requisite features to play that role [1]. Biodiesel use in the internal combustion engine (ICE) under the compression ignition (CI) combustion strategy has been known to reduce pollutants such as carbon monoxide (CO), unburned hydrocarbons (HC), particulate matter (PM and soot [2-6]. However, its use has been associated with a rise in oxide of nitrogen (NO_X) emission and a reduction in engine power [3, 6].

The challenges of increased NO_X emission in biodiesel combustion has been attributed to the oxygenated nature of the fuel, and loss of power to poor transport properties and a reduced specific heating value [7]. These challenges exist because the prevailing combustion strategies in the compression ignition (CI) regime do not adequately envisage the peculiarity of biodiesel's unique fuel chemistry. In the CI regime of diffused flame, turbulent flow and auto-ignition, the physical as well as chemical processes take place simultaneously, and even for diesel fuel with improved transport properties and higher heating value, the charge and thermal stratification in the turbulent environment does not permit orderly completion of the physical processes of injection, droplet formation,

atomization of fuel, evaporation and defuse spray before the chemical process of auto-ignition commences [1]. CI combustion strategy which depends heavily on high temperature and pressure for auto-ignition creates a rich nursery for thermal NO_X formation as predicted by the Zeldovich mechanism. It is, therefore, not surprising that oxygenated fuel such as biodiesel will perform poorly in terms of NO_X emission with such a combustion strategy.

Loss of power when biodiesel is used as fuel in a CI engine is another area where the mismatch between the fuel type and the combustion strategy is evident. In diesel powered CI combustion, better transport properties and sufficient explanation for advantage are observed. This is because biodiesel with a typically higher cetane number and oxygenated molecule has higher combustion efficiency than diesel and these should even-out the differences if the right combustion strategy is deployed. This is precisely why considerable efforts are being exerted to develop novel combustion strategies that can harness the unique features of emerging eclectic mixes of fuel [8-10].

Researching for best fit combustion strategies for specific fuel types or developing a generic engine that produces performance and emission outcomes acceptable to the automobile industry and meet emission regulations is an expensive, time consuming and intellectually exerting endeavour. It requires more than what any elaborate experimental engine diagnostic may provide, however detailed they may be. Detailed computational fluid dynamic (CFD) schemes along with a full range of engine diagnostic test rigs and an assortment of in-cylinder, non-intrusive diagnostic tools have emerged as the most efficient means by which novel engine combustion strategy can be developed [1]. CFDs require a multi-grid of fuel property data for computational purposes and, in most instances, the numerical scheme for computing property data are coupled to the main CFD code (that compute the physic of the flow) along with the chemical kinetic mechanism scheme (which compute the chemistry of the process) to provide step-wise, real time data in the full spatial and temporal domain [11]. Extensive work has been conducted on numerical correlation for compiling property data of biodiesel and these include; knovel critical tables, DIPPR and BDProp [12-14]. But the difficulties associated with resourcing these materials include their limited coverage of biodiesel sources and the restrictive barriers to accessing them (most are accessed via paid subscription). A common trend observed with biodiesel research is that most researchers focus on biodiesel sources in which their geographical regions have a competitive advantage.

This work is, therefore, an attempt to commence a preliminary compilation of a numerical scheme that can be employed to compute properties of biodiesel sources from moringa, jatropha and waste restaurant oil native to sub-Saharan Africa and progressively use same for CFD evaluation of these selected biodiesel source for novel combustion strategies evaluation that could potentially tackle known challenges.

5.2 Theories and Test Protocols

The thermo-physical and transport properties of fatty acid methyl esters (FAMEs) contribute significantly, to the combustion characteristics of biodiesel. The properties relationship with engine performance and emission are closely intertwined. Understanding that relationship is the key to determining the right composition of the FAME mix (biodiesel) and combustion regime that could give optional performance at an acceptable emission. Estimating these properties has always been an important objective. Gouw and Vlugter [15] in the mid-60s used the Smittenburg equation to compute the specific gravity of saturated FAME at 20°C and 40°C. A numerical correlation to estimate the viscosity of saturated and unsaturated methyl esters was proposed by Allen et al. [16], and was given as a quadratic expression of the molecular weight. Krisnangkura et al. [17] adopted a different approach in estimating viscosity of saturated and unsaturated FAME by making it a function of temperature and the number of carbons in the FAME chain. Allen et al. [18] and Ejim et al. [19] used Sugden's parachor method to compute the surface tension.

5.2.1 Theories of Properties Estimation

The theories selected for the various properties are discussed below.

5.2.1.1 Density (ρ_i)

In FAME density increases with increasing length of carbon chain. For FAME with the same number of carbon chain, saturated molecules have higher density when compared with unsaturated molecules. That is to say, the bulk modulus of saturated FAME is higher than that of unsaturated FAME with the same carbon chain length. The density of saturated and unsaturated FAME can be estimated by the expression [20] Biodiesel is a renewable alternative to finite diesel and, has the capacity to reduce emission and broaden energy access particularly in sub-Saharan Africa where economic growth has been, to some extent, constrained by global warming and a lack of universal access to sustainable source of energy. In the transport sector, a niche exist for biodiesel derived from non-edible food sources such as waste oil, Jatropha and Moringa in Sub- Saharan Africa. Extraction of oil from Jatopha and Moringa were achieved via manual as well as Soxhlet method using normal Hexane, Petroleum Ether and distilled Gasoline. A numerical property prediction scheme was implemented (and validated with experimental data) to obtain the thermo-physical as well as the transport properties of the resultant fuel for the various samples. The fuel samples were evaluated in a 3.5kw diesel engine to determine their performance and emissions. The Brake Specific (BS in g/kWh) emissions across the full load spectrum were benchmarked against the United State Environmental Protection Agency (US, EPA) and the European Union (EU) emission caps.

The extraction results not only confirmed normal Hexane solvent and Soxhlet method as the optimal means of extraction (with a 37.1% and 51.8% yield for Moringa and Jatropha respectively) but, gave hint of the potential of distilled Gasoline as a viable solvent (with a 40.2% and 34.1% yield for Moringa and Jatropha respectively). The validated numerical prediction scheme reduce research cost and time without compromising accuracy. The performance and emission results showed that the Brake specific fuel consumption (BSFC) and Brake thermal efficiencies gave marginal difference between diesel and the biodiesels ($\pm4\%$ and ±5 respectively at peak load). Carbon Monoxide (CO), Unburnt hydrocarbon (UHC) and Particulate Matter (PM) emissions (in part per million-ppm) showed decreasing trend with load increase and were lower than those of Diesel. Oxides of Nitrogen (NO_X) emission for the Biodiesel were lower than those of Diesel. The Brake Specific (BS) emission result in comparison to the EU and EPA regulation were mixed. In broad terms, engine retrofitting and novel design can effectively bridge the performance and emission gaps observed between Diesel and Biodiesel. A multi-blend (saturated and unsaturated FAME) and multi-strategy (Modular kinetic and premix/DI) was recommended as a remediation strategy. For numerical prediction purpose, a 3D CFD with multi zone and detailed chemistry using KIVA-3V code was proposed.

$$\rho_i = 0.8463 + \frac{4.9}{M_i} + 0.0118 N_{DB} \qquad (5.1)$$

Where ρ_i, M_i and N_{DB} are the density, molecular weight of ith FAME and the average weighted number of double bond respectively.

Given the mixing rule expression

$$f_b = \sum_{i=1}^{n} z_i f_i \qquad (5.2)$$

f_i represents the function of any given physical property and z_i is the mole or mass fraction of the ith FAME. The function could be replaced by any variable.

5.2.1.2 Higher Heating Value (δ_i)

According to Ramirez-Verduzco et al. [20], the higher heating value can be estimated with the expression

$$\delta_i = 49.19 - \frac{1794}{M_i} - 0.2N_{DB} \tag{5.3}$$

5.2.1.3 Average Relative Deviation (ARD)

The average relative deviation (ARD) which can be interchange with average absolute deviation (AAD) is computed with the expression.

$$ARD = \frac{1}{n}\left(\sum_{i=1}^{n}\left|\frac{(f_{iexp}-f_{ical})}{f_{iexp}}\times 100\right|\right) \tag{5.4}$$

n is the number of experimental or data points, and f_{iexp} and f_{ical} represents the function that determines the experimental and calculated properties of individual FAME or biodiesel properties.

5.2.1.4 Kinematic Viscosity (η)

Kinetic viscosity expresses the measure of fluid resistance to flow. In CI engines higher viscosity impact engine performance negatively. Higher viscosity reduces spray atomization and leads to charge stratification prior to auto-ignition and severe thermal stratification, post flame, which in turn produces the unwanted soot and NO_X region [21]. In FAME, increasing carbon chain length is associated with high viscosity but increasing level of unsaturation has an opposite effect [22]. The expression for estimating kinetic viscosity is [23]:

$$\eta = 0.235N_c - 0.468N_{DB} \tag{5.5}$$

Nc is the number of carbon chain length.

5.2.1.5 Cetane Number (CN)

Cetane number is the determining factor for ease with which auto-ignition commences and is governed by the low temperature heat release (LTHR) mechanism. Higher cetane numbers are associated with straight chain saturated hydrocarbons. The more straight and saturated the FAMEs are the higher the CN. High CN, although desirable for efficient combustion, could sometime cause early auto-ignition that creates other challenges in the engine. According to Su [23], the expression with acceptable accuracy is given by

$$CN = 3.930N_c - 15.936N_{DB} \tag{5.6}$$

5.2.1.6 Flash Point (T_f)

The flash point of any fuel is the temperature at which the fuel releases sufficient vapour to form a flammable mixture within an experimental environment. Flash point is an important consideration when fire explosion hazards are being evaluated. It is also related to flame velocity and ease of

combustion. Several methods have been proposed in the literature to predict flash point: group contribution was proposed by Albahri [24] and Stafanis et al. [25] as a viable method for predicting flash points, and Su [23] established that viscosity, cetane number and flash point increase with increasing length of carbon chain and their correlation was in agreement within 2%. This correlation is therefore, adopted here:

$$T_f = 23.362N_c + 4.854N_{DB} \qquad (5.7)$$

5.2.1.7 Cloud Point, Cp (C)

Cloud point is one of the low temperature characteristics of biodiesel that impedes its wider application. It is the temperature at which the cloudy appearance of dissolved wax crystals first forms in the liquid phase when the fuel is cooled in a controlled condition. This property has practical implications for fuel storage in vehicles used in a cold climate. Su [23] proposed an expression for predicting cloud point and it is given as:

$$C_p = 18.134N_c - 0.790(U_{FAME}) \qquad (5.8)$$

Where U_{FAME} is total unsaturated FAME in wt%

5.2.1.8 Pour Point, Pp (C)

Pour point is the temperature at which the fuel no longer flows as a result of gel formation [26]. Pour points are also a crucial consideration in operating environments with near zero or sub-zero temperatures. Pour point increases as chain length in saturated FAME increases but gets lower as the level of unsaturated FAME increase [7, 27]. Su's [23]expression for predicting pour point was adopted for this work. It is given as:

$$P_p = 18.880(N_c) - 1.00(U_{FAME}) \qquad (5.9)$$

5.2.1.9 Cold Flow Plugging Point (CFPP)

The cold flow plugging point is related to pour point and cloud point. It is the temperature at which the fuel blocks the filter device due to the formation of crystal agglomerates [28]. It is practically impossible to run engines on biodiesel when the ambient temperature equals or falls below the CFPP temperature. This is a natural barrier for biodiesel application in cold conditions. The expression adopted for its prediction is [23]:

$$CFPP = 18.019N_c - 0.804(U_{FAME}) \qquad (5.10)$$

5.2.2 Determination of FAME Composition

The biodiesel FAME composition data for the samples under investigation were obtained from secondary sources with similar weather conditions and seed variety. Typically, biodiesel FAME composition is analysed using gas chromatography (GC). Moringa biodiesel FAME composition was obtained from the work of Azad et al. [29], jatropha from Maina [30] and waste restaurant oil biodiesel from Chhetri et al. [31]. Details are provided in Table 5.1.

Table 5. 1: Sample FAME composition

S/No	FAME	WOME	MOME	JAME
1.	Myristic (C14:0)	0.9		
2.	Palmitic (C16:0)	20.4	6.5	15.3
3.	Palmitoleic (C16:1)	4.6	2.0	1.1
4.	Stearic (C16:0)	4.8	6.0	6.4
5.	Oleic (18:1)	52.9	72.2	40.1
6.	Linoleic (C18.2)	13.5	1.0	36.9
7.	Linolenic (18:3)	0.8		0.2
8.	Arachidic (C20:0)	0.12	4.0	
9.	Eicosenic (C20:1)	0.84	2.0	
10.	Behemic (C22:0)	0.03		
11.	Erucic (C22:1)	0.07		
12.	Tetracosanic (C24:0)	0.04		
13.	U$_{FAME}$	72.01%	77%	78.1%

Note: WOME, MOME and JAME are methyl esters of waste restaurant oil, moringa and jatropha respectively.

5.2.3 Biodiesel Properties and Standard

To produce biodiesel for the experimental determination of the properties in this work, seed samples were sourced, air dried and pulverized in clean, non-reactive vessels. The pulverized samples were then oven dried prior to oil extraction. Normal hexane, petroleum ether and distilled gasoline where used as solvents for the extraction process via the manual and soxhlet methods. Detail of the extraction yield are provided in previous work [32]. Subsequently, the properties of the resulting biodiesel were determined using experimental methods prescribed by the ASTM D6751 [33] as shown in Table 5.2.

Table 5. 2: ASTM Standard and test method

Fuel Properties	Biodiesel ASTM D6751	Test Methods ASTM	Diesel ASTM D175
Density @15°C (kg/m	880	D1298	850
Viscosity @ 40°C (CSt)	1.9-6.0	D − 445	2.6
Cetane number	Min 47	D − 613	40 − 55
Calorific value (MJ/kg)	-	-	42 − 46
Pour point ($^{\circ}$C)	-15 to -16	D − 97	-35
Flash point ($^{\circ}$C)	Min 100 − 170	D − 93	60 − 80
Cloud point ($^{\circ}$C)	-3 to -12	D − 2500	-20
Cold filter plugging point ($^{\circ}$C)	19	D − 6371	-25
Iodine number	Max 120	-	38.3

5.3   Algorithm of Prediction Scheme

The objective of the scheme is to predict seven properties of biodiesel derived from moringa, jatropha or waste restaurant oil using four independent variables. Biodiesel is a mixture of various components of fatty acid methyl esters (FAMEs). The samples under study may contain all or some of the FAME component as seen in Table 5.1. The FAME chemical structure is typically
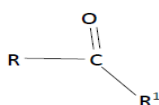
Where R and R^1 are alkyle radicals and R^1 corresponds to CH$_3$. The three elements that form the building blocks of all FAMEs are oxygen (O), hydrogen (H) and carbon (C) and their molecular weights are: C-12:011, H-1.008 and O-15.999. The generic chemical formula for the FAME structures are stated as follows:

i. Saturated FAME, Cn:0 ($C_{n+1}H_{2n+2}O_2$

Hence, the molecular weight of the ith FAME will be computed as

$$M_i = (n+1)M_c + (2n+2)M_H + 2M_o \tag{5.11}$$

Where: $M_i, M_c, M_H, \text{ and } M_o$ are molecular weight of ith FAME, carbon, hydrogen and oxygen respectively and, n is the number of carbons on the chain.

ii. Unsaturated FAME with one double bond (Cn:1)

$C_{m+1}H_{2n+1}O_2$
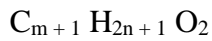
$$M_i = (n+1)M_c + (2n+1)M_H + 2M_o \tag{5.12}$$

iii. Unsaturated FAME with two double bonds (Cn:2) $C_{n+1}H_{2n}O_2$

$$M_i = (n+1)M_c + 2nM_H + 2M_o \tag{5.13}$$

iv. Unsaturated FAME with three double bond (Cn:3)

$C_{n+1}H_{2n-1}O_2$
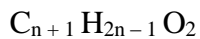
$$M_i = (n+1)M_c + (2n-1)M_H + 2M_o \tag{5.14}$$

Other correlations needed for computing the properties are provided in equation 5.1-5.10. The flow chart is shown in Figure 5.1.
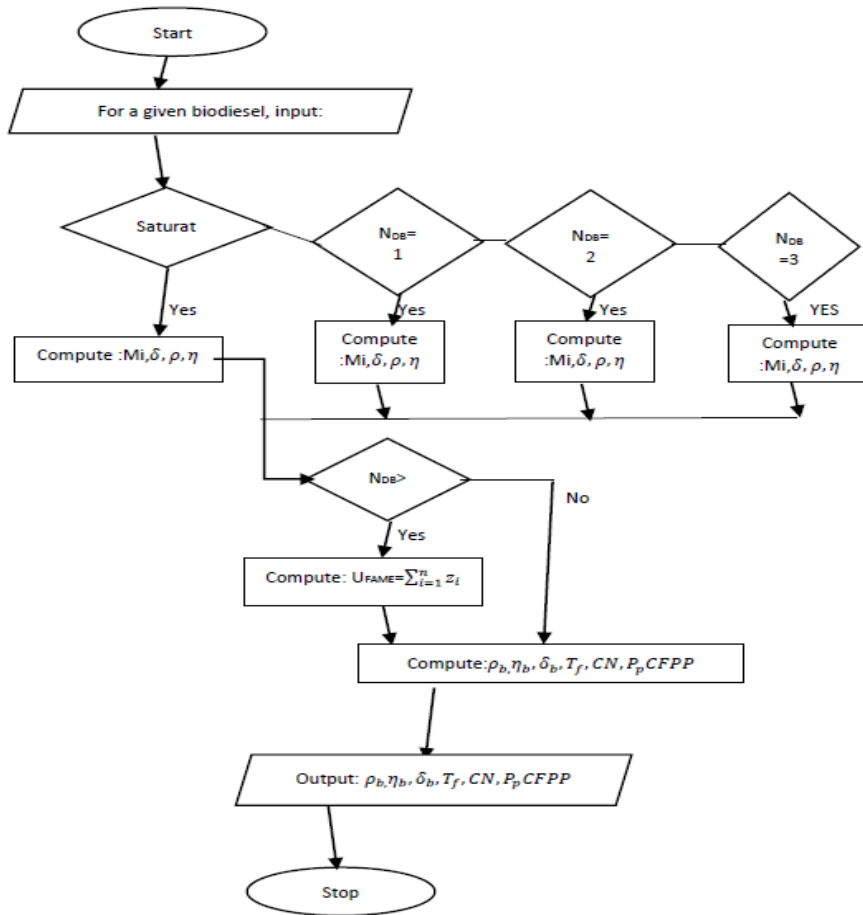
Figure 5 1: Flow of prediction scheme

5.4   Results and Discussion

Primary experimental data for this work was obtained via seed sourcing, oil extracting/testing and biodiesel production/testing. The extraction was achieved using two separate methods, namely: manual soaking and soxhlet extraction. Three different solvents, namely: petroleum either, normal hexane (n-hexane) and distilled gasoline were employed. For both jatropha and moringa, optimal oil yield of 51.8% and 37.1% were obtained respectively in soxhlet extraction using normal hexane. Yield with petroleum ether under soxhlet extraction were sub-optimal at 24.3% and 25.3% for jatropha and moringa respectively. Distilled gasoline, introduced as a 'wild card' solvent showed promise with a yield of 40.2% and 34.1% with soxhlet extraction for jatropha and moringa respectively. Manual soaking as an extraction method gave oil yield values that were below par for all the solvent types hence was considered economically non-viable. Table 4.3 shows the details of the extracted oil physico-chemical properties.

Table 5. 3; Oil sample properties

S/No	Properties	Moringa Oil	Jatopha Oil	ASTM D6751
1	Viscosity (mm²/s)@30°C	53.9±0.40	41.45±0.20	6(max)
2	Density (Kg/m³)	912.0±00.0	890.62±10.00	875-900
3	Iodine value	64.84±0.20	108.40±0.20	
4	Refractive Index	1.458±0.01	1.455±0.01	1.245-1.675
5	Flash point (°C)	215±0.05	195±0.05	90.00-130
6	Free Fatty Acid	9.96±0.1	2.48±0.1	3.00-5.00
7	SaponificationValue (mgKOH/gm)	185.15±0.1	196.44±0.1	
8	Peroxide Value	1.84±0.02	3.21±0.02	
9	Pour Point (°C)	8±0.05	5±0.04	-15- 10
10	Cloud Point (°C)	12±0.05	70.05	-15- 5

The trans esterification process involved the use of potassium oxide as a catalyst and methanol as the main reactant with the oil. Sulphuric acid was used with the moringa sample to lower the free fatty acid level prior to the trans esterification process to prevent the formation of soap. At the end of the trans esterification process the glycerol was separated from the fatty acid methyl ester mixture (Biodiesel) by means of a separating filter. The product was washed and heated to remove all traces of imputes prior to testing.

The prediction scheme coded in C+ was also executed simultaneously to estimate the properties of the biodiesel from moringa, jatropha and waste restaurant oil. In determining the average relative

deviation (ARD) for each estimate, as a tool for validation purpose, secondary data from five different sources along with primary data obtained in this work were used to compute the ARD. Table 5.4 shows the value of the estimates obtained from the code, the ARD computed from an Excel spreadsheet template and the primary data obtained experimentally in this work.

Table 5. 4: Computed properties and ARD

Property	Calculated values			ARD (%)			Experimental data		
	MOME	JAME	WOME	MOME	JAME	WOME	MOME	JAME	WOME
Density @40°C (Kg/m³)	832.6	875.9	864.09	4.07	1.16	1.49	892.98	880.0	874.20
Viscosity @40°C (cSt)	3.887	3.852	3.911	17.9	14.8	18.3	5.10	4.60	4.2
Calorific value (kJ/kg)	41.31	42.82	42.90	3.82	4.8	3.25	----	---	---
Cetane number	58.52	55.04	58.28	4.9	1.2	4.45	---	---	---
Flash point (°C)	146.78	158.11	152.40	9.3	5.3	7.0	215	195	219
Pour Point (°C)	-4.14	1.84	2.94	3.8	3.9	---	1	5	6
Cold flow plugging point (°C)	-5.34	1.05	1.009	---	---	---	---	---	---

MOME, JAME and WOME are methyl esters of moringa, jatropher and waste restaurant oil respectively.

The results are discussed in the following section.

5.4.1 Density

The scheme estimated the density of moringa, jatropha and waste restaurant oil biodiesel with an average relative deviation (ARD) of 4.07%, 1.16% and 1.49% respectively. These were all well within the tolerance limit of ARD < 5%. The experimental data from this work further confirms these estimates with values within ASTM D6731 regulation for biodiesel. As shown in the table, the estimate is well controlled for JAME and WOME but a wider swing was observed for MOME. The possible explanation for this is the additional processes required for moringa biodiesel production. The neutralization reaction undertaken to reduce free fatty acid composition before the trans esterification process increases the risk of higher levels of impurities such as salt deposits, glycerol remains that may not be completely removed from the fuel. Herein lies one of the advantage of predictive tools. A well validated predictive tool used alongside the ASTM regulation for biodiesel properties is an important safeguard for quality assurance in the commercial production of biodiesel.

In comparison, Ramirez-Verduzco et al. [20] used the same correlation to estimate biodiesel density and obtained an ARD of 0.11%. The key difference is that all the validation data were primarily sourced and laboratory protocols were more controlled with high accuracy measuring equipment.

5.4.2 Viscosity

The values of 3.887 cSt, 3.852 cSt and 3.911 cSt were computed for MOME, JAME and WOME. The ARD for all the samples were well above the tolerance limit of 5% and the experimental data from this study confirms these differences as shown in Table 5.4. In the work of Ramirez-Verduzco [20], the same correlation in a similar study gave an ARD estimate of 2.5%. The correlation also provided acceptable result in the works of Knothe [33]. This reduced accuracy of estimate can therefore only be explained by experimental test protocols and biodiesel processing procedures. Most of the work on biodiesel sourced from non-edibles in sub Saharan Africa were basically focused on meeting the ASTM regulation limit (which have a higher margin for error than the use of the correlation). Test protocols designed to produce biodiesel to meet ASTM standards as well as ARD tolerance limits of well

validated prediction tools have a good chance of providing more predictable performance and emission results in engine test rigs.

5.4.3   Calorific Value

The computed ARD using the correlation employed in the work are 3.8%, 4.8% and 3.2% for MOME, JAME and WOME respectively. These estimates are all within the tolerance limit of ± 5%. The consistency of prediction using this correlation was also confirmed in the works of Knothe [33] when calorific value were computed. Calorific value data are not as sensitive to experimental test protocol as the other two previous measures hence, their ARD did not experience swings observed in the computation of density and viscosity. But it can also be observed that high accuracy was impaired as the measure maintained a stable error of margin of values greater than ± 3.5%. Ramirez-Verduzco [20] obtained an ARD of 0.21% for the estimation of calorific value showing the high precision of this correlation in computing the calorific value of biodiesel.

5.4.4   Cetane number

In the compression ignition engine the cetane number is a measure of the ignition quality of the fuel. It enables the determination of the time available for physical processes such as spray formation, atomization and vapour build-up prior to the commencement of the chemical processes such as auto-ignition and combustion. The interrelationship between these two processes determines overall engine performance and emission.

Experimental determination of CN is often laborious and require large amounts of sample hence, are expensive. Added to that is the level of accuracy required in repeatability before data can be accepted as valid. Numerical prediction tools are therefore a huge advantage if their validity are assured. The ARD of 4.9%, 1.2% and 4.45% was obtained in this work for MOME, JAME and WOME respectively. These compared favourably with the estimates of Ramirez-Verduzco [20] for the same property and correlation which was 5.95%.

5.4.5   Flash Point

In computing the flash point of the fuel samples, the ARD of 9.3%, 5.3% and 7.0% were obtained for MOME, JAME and WOME respectively. Although the estimates all failed the accuracy tolerance limit, flash point data in this work as a gauge of fuel storage safety, met the ASTM regulation (100 - 170 minimum limit) as the estimated figures were 146.78^{o}C, 158.11^{o}C and 152.28^{o}C for MOME, JAME and WOME respectively. No reliable data were found in literature of similar estimates using the same correlation for comparative purposes. This is an indication of how much work has been left undone in this area and perhaps the neglect of researchers owing to the traditionally held view that since biodiesel flash point is largely higher than those of diesel, they are safer to handle and hence require no further research rigour. However, there are many reasons why this should not be the case.

5.4.6   Cold Flow Properties

Details of pour point and the cold flow plugging point of the fuel samples were also estimated and can be seen Table 5.4. Here again, reliable data on cold flow properties for ARD computation were hard to find and where they exist, the variations were too wide to be considered accurate. ARD of 3.8% and 3.9% were obtained for MOME and JAME in this study. But there were no reliable experimental data to compute the cold flow plugging point of the samples. The experimental data obtained for these properties in this work were insufficient to compute the ARD.

5.5 Conclusion

Predictive tools provide essential information on group contributions to overall material properties of biodiesel and they provide insight into how future biodiesel fuels can be engineered to obtained desirable properties for optimal performance in compression ignition engines. It can also be clearly seen that predictive tools are reliable safeguards for quality assurance.

i) Oil extraction yield with normal hexane as solvent gave the most optimal result, but distilled gasoline performance showed good potential that requires further exploration.

ii) The manual soaking extraction method is clearly not an extraction method worthy of any further studies as the yield was too poor when compared to the soxhlet method regardless of the solvent used.

iii) With the exception of density which gave low ARD indicating a low sensitivity to free glycerol and other impurities, all the other properties predicted showed high levels of sensitivity to biodiesel level of purity.

iv) All the low temperature properties such as pour point, flash point, CFPP and cloud point were extremely sensitive to free glycerol and other impurities. The advantages associated with this trend is that the prediction tool can be used as a feedback mechanism to ascertain the quality of any biodiesel produced regardless of the method used for its production or the source of the feedstock.

v) The prediction scheme significantly reduced the number of experiments needed to determine the properties of any given biodiesel while at the same time, providing information on the quality of the biodiesel at a much reduced cost and processing time

References

[1]   X. Cheng, H. K. Ng, S. Gan, and J. H. Ho, "Advances in Computational Fluid Dynamics (CFD) Modeling of In-Cylinder Biodiesel Combustion," *Energy Fuels,* vol. 27, pp. 4489-4506, 2013.

[2]   A. Ghorbani, B. Bazooyar, A. Shariati, S. Mohammad Jokar, H. Ajami, and A.Naderi, "A comparative study of combustion performance and emission of biodiesel blends and diesel in an experimental boiler," *Applied Energy* vol. 88, no. 12, pp. 4725-4732, 2011.

[3]   J.-H. Ng, H. K. Ng, and S. Gan, "Engine-out characterisation using speed-load mapping and reduced test cycle for a light-duty diesel engine fuelled with biodiesel blends," *Fuel,* vol. 90, pp. 2700-2709, 2011. .

[4]   M. Balat and H. Balat, "Progress in biodiesel processing," *Applied Energy,* vol. 87, no. 6, pp. 1815-1835, 2010.

[5]   C. K. Westbrook, W. J. Pitz, and H. J. Curran, "Chemical kinetic modeling study of the effects of oxygenated hydrocarbons on soot emissions from diesel engines," *Journal of Physical Chemistry,* vol. 110, pp. 6912-6922, 2006.

[6]   S. Murrilo, J. L. Miguez, J. Porteiro, E. Granada, and J. C. Moran, "Performance and emission study in the use of biodiesel in outboard diesel engines," *Fuel,* vol. 86, p. 1765-1771, 2007.

[7]   R. K. Pandey, A. Rehman, and R. M. Sarviya, "Impact of alternative fuel properties on fuel spray behavior and atomization," *Renewable and Sustainable Energy Reviews* vol. 16 (2012), pp. 1762-1778, 2011.

[8]   K. Nakagome, N. Shimazaki, K. Miimura, and S. Kobayashi, "Combustion and emissions characteristics of premixed lean diesel combustion engine," *SAE paper 970898,* 1997.

[9]   W. H. Su, T. J. Lin, and Y. Q. Pei, "A compound technology for HCCI combustion in a DI diesel engine based on the multi-pulse injection and the BUMP combustion chamber," *SAE paper 2003-01-0741,* 2003.

[10]   K. C. Natti, "PM characterization in an HSDI diesel engine under conventional and LTC regimes," *SAE paper 2008-01-1086,* 2008.

[11]   J. L. Brakora, Y. Ra, and R. D. Reitz, "Combustion model for biodieselfueled engine simulations using realistic chemistry and physical properties," *SAE paper 2011-01-0831*, 2011.

[12]   E. M. Fisher, W. J. Pitz, H. J. Curran, and C. K. Westbrook, "Detailed chemical kinetic mechanisms for combustion of oxygenated fuels," *Proceedings of the Combustion Institute,* vol. 28, pp. 1579-1586, 2000.

[13]   http://knovel.com/web/, *Knovel Critical Tables*, 2nd ed. Accessed July 26, 2012.

[14]   V. Stringer, J. McCrady, A. Hansen, and C. F. Lee, *Modeling Biodiesel Spray Breakup with Well-Defined Fuel Properties*, Chicago, IL: ILASS-Americas, May 15-18, 2007.

[15]   T. H. Gouw and J. C. Vlugter, "Physical properties of fatty acid methyl esters. I. Density and molar volume." *Journal of the American Oil Chemists' Society,* vol. 41, pp. 142-5, 1964.

[16]   C. A. W. Allen, K. C. Watts, R. G. Ackman, and M. J. Pegg, "Predicting the viscosity of biodiesel fuels from their fatty acid ester composition," *Fuel,* vol. 78, pp. 1319-1326, 1999.

[17]   K. Krisnangkura, T. Yimsuwan, and R. Pairintra, "An empirical approach in predicting biodiesel viscosity at various temperatures," *Fuel,* vol. 85, pp. 107-113, 2006.

[18]   C. A. W. Allen, K. C. Watts, and R. G. Ackmamn, "Predicting the surface tension of biodiesel fuels from their fatty acid composition," *Journal of the American Oil Chemists' Society,* vol. 76, pp. 317-323, 1999.

[19]   C. E. Ejim, B. A. Fleck, and A. Amirfazli, "Analytical study for atomization of biodiesels and their blends in a typical injector: surface tension and viscosity effects," *Fuel,* vol. 86, pp. 1534-1544, 2007.

[20]   L. F. Ramírez-Verduzco, J. E. Rodríguez-Rodríguez, and A. R. Jaramillo-Jacob, "Predicting cetane number, kinematic viscosity, density and higher heating value of biodiesel from its fatty acid methyl ester composition," *Fuel,* vol. 91, pp. 102-111, 2012.

[21]   M. A. Kalam and H. Masjuki, "Biodiesel from palm oil - an analysis of its properties and potential," *Biomass and Bioenergy,* vol. 23, pp. 471-479, 2002.

[22]   G. Knothe and K. R. Steidley, "Kinematic viscosity of biodiesel fuel components and related compound. influence of compound structure and comparison to petrol diesel fuel components," *Fuel* vol. 84, pp. 1059-1065, 2005.

[23]   Y. C. Su, "Selection of prediction methods for thermophysical properties for process modeling and product design of biodiesel manufacturing," Thesis submitted to the faculty of the Virginia Polytechnic Institute and State University in partial fulfillment of the requirements for the degree of Master of Science In Chemical Engineering, Blacksburg, VA, 2011.

[24]   T. A. Albahri, "Flammability Characteristics of Pure Hydrocarbons," *Chemical Engineering Science,* vol. 58, pp. 3629-3641, 2003.

[25]   E. Stefanis, L. Constantinou, and C. A. Panayiotou, "Group-Contribution Method for Predicting Pure Component Properties of Biochemical and Safety Interest," *Journal of Industrial and Engineering Chemistry,* vol. 43, pp. 6253-6261, 2004.

[26]   R. M. Johsi and M. J. Pegg, "Flow properties of biodiesel fuel blends at low temperatures," *Fuel,* vol. 86, pp. 143-151, 2007.

[27]   G. Dayma, S. Gail, and P. Dagaut, "Experimental and kinetic modeling study of the oxidation of methyl hexanoate," *Energy Fuels* vol. 22, pp. 1469-1479, 2008,

[28]   C. Boshui, S. Yuqiu, W. Jiu, and W. Jiang, "Cold flow properties and crystal morphologies of biodiesel blends," *Chemistry and Technology of Fuels and Oils,* vol. 46, pp. 52-57, 2010.

[29]   A. K. Azad, M. G. Rasul, Khan, M. M. K, , C. S. Sharma1, and R. Islam, "Prospect of Moringa seed oil as a sustainable biodiesel fuel in Australia: A review," *6th BSME International Conference on Thermal Engineering (ICTE 2014),* pp. 601-606, 2015.

[30]   P. Maina, "Investigation of fuel properties and engine analysis of Jatropha biodiesel of Kenyan origin," *Journal of Energy in Southern Africa,* vol. 25 pp. 107-116, 2014.

[31]   A. B. Chhetri, K. C. Watts, and M. R. Islam, "Waste Cooking Oil as an Alternate Feedstock for Biodiesel Production," *Energies* vol. 10.3390, pp. 3-18, 2008.

[32]   E. I. Onuh and F. L. Inambao, "A study of extraction yield and properties of some oil for biodiesel application," *BIE 13th Biennial Conference,* Gaborone, Botswana: 15-18th October, 2013: pp 233-241. ISBN 978-99912-0-910-4.

[33]   G. Knothe, "Analyzing biodiesel: standards and other methods," *Journal of the American Oil Chemists' Society,* vol. 83, pp. 823-833, 2006.

CHAPTER 6

Paper 3: PERFORMANCE AND EMISSION EVALUATION OF PURE BIODIESEL FROM NON-EDIBLE FEEDSTOCK AND WASTE OIL IN A DIESEL ENGINE

E. I. Onuh and Freddie L. Inambao.

Abstract

Biodiesels prepared from jatropha, moringa and restaurant waste oil were evaluated in a 3.5 kw diesel engine to determine their performance and pollutant emissions. The brake specific (BS) emissions across the full load spectrum were benchmarked against the United State Environmental Protection Agency (US, EPA) and the European Union (EU) emission caps. Results showed that the brake specific fuel consumption (BSFC) and brake thermal efficiencies gave marginal differences between ndiesel and the biodiesels ($\pm 4\%$ and ± 5 respectively at peak load). Carbon monoxide (CO), unburnt hydrocarbon (UHC) and particulate matter (PM) emissions (in parts per million) showed a decreasing trend with load increase and were lower than those of ndiesel. Oxides of nitrogen (NO_X) emission for the biodiesels were lower than those of ndiesel. This was because the 1650k peak temperature to activate thermal NO_X was sparingly breached for the biodiesels. BSHC (brake specific unburnt Hydrocarbon) for all fuel types failed the EPA as well as the EU emission caps at all loading conditions. All the fuel samples only met regulations at load conditions exceeding 65%. BSPM (brake specific Particulate Matter) for all fuel types failed the EPA and EU standards except those of waste oil and jatropha biodiesel for which the BSPM were well below the EU upper limit of 0.85g/Kwh.

Key Words: Pure biodiesel, Performance, Brake Specific Emission, EPA & EU standard, Zeldovich Mechanism.

6.1   Introduction

It is a well-documented fact that diesel engines running on biodiesel or its blends tend to reduce harmful emissions such as carbon monoxide (CO), particulate matter (PM) and total hydro-carbons accompanied with marginal drops in engine performance (Xue, Grift, and Hassen 2011; Nettles-Anderson et al. 2014). Further, biodiesel use in compression ignition (diesel) engines is associated

with increasing oxides of nitrogen emission and specific fuel consumption (Xue, Grift, and Hassen 2011; Roy, Alawi, and Wong 2013). This mixed picture along with other factors has created a feeling of cautious optimism in relation to the wider application of biodiesel as an alternative fuel source. However, the potential capacity of biodiesel to enhance sustainability, broaden energy access and reduce emissions remains clearly undisputed. Today's compression ignition (diesel) engine was conceived and designed for a specific type of fuel, but emerging scenarios of future fuel types are eclectic, and that ongoing research points to a determined effort to develop novel engines that can run on fuel types with a more diverse chemistry, suggesting that niches for biodiesel exist that should be fully explored (McIlroy, 2006). Exploring these niche will require an exhaustive investigation of all potential sources of biodiesel, a broader qualitative and quantitative evaluation of their performance and emissions in specific terms and benchmarking of these data with conventional fuels and prescribed emission standard proposed by regulating bodies. Only then will the extent of mitigation be determined and plans of action identified. These plans can take the form of adjustment to engines, retrofitting, and ongoing development of novel engines to accommodate biodiesel.

Pollutants exhaust emission limits have already been set by the United State Environmental protection Agency (EPA) (EPA 2004) and the European Commission (EC) (EC 1999). According to the EU document, the standards are harmonized in reference to International Standards Organization (ISO) ISO 8178-1:1996 (ISO 1996), all European Union states were required to apply directive 2003/44/EC (EC 2003) from 1st January, 2005. These measures came into effect in 1st January, 2006. The emission measurement for CO, NO_X, PM and THC were required to be in brake specific format (g/kWh). Rules on test cycle runs were also set to enable emission measurements to be made under steady state conditions. It is noteworthy that while some previous work on biodiesel mentioned these pollutant emission standards (Murillo et al. 2007), most did not benchmark their measurement against the limits set (Nettles-Anderson et al. 2014; Canakli and Van Gerpen 2003) and a few did not compute emissions based on the brake specific (g/kWh) format (Hifjur, Jena, and Jadav 2013 Santos, Capareda, and Capunitan 2013).

Against the backdrop of increasing rate of urbanisation and the consequent proliferation of a fast food culture, vast tracts of marginal land needing reforesting to stem the tide of desertification, and an acute need for safe drinking water and food beneficiation for the rural poor, sub-Sahara Africa has a clearly defined niche in producing biodiesel from non-edible sources such as waste restaurant oil, jatropha seed oil and moringa seed oil. By 2030, Africa's population is expected to peak at 1.5 billion with the percentage of those living in urban areas being 53.5% at 748 million (Mubila 2012; Cohen 2005). The promotion of these three sources of biodiesel, in sub-Saharan Africa, apart from limiting

greenhouse gas emissions and enhancing energy sustainability, will also improve universal access to energy sources and even out economic growth between resource rich and resource poor countries in the region.

This work involved sourcing, extracting and producing biodiesel from jatropha, moringa and waste restaurant oil. The physio-chemical properties of the oil/fuel where determined and benchmarked against ndiesel, subsequent to which their performance and emission trends were evaluated in a compression ignition (CI-diesel) engine. Comparative analyses were prepared to reinforce the accruing benefits of biodiesel and make recommendations to mitigate the challenges observed.

6.2   Experimental Methods

6.2.1   Oil Extractor/Biodiesel production

Seeds of moringa and jatropha sourced from the wild were processed appropriately (refer to Section 4.2 to 4.4). Oil extraction was achieved via two methods, namely: soaking and soxhlet. Three solvents were employed for this purpose and the focus was to determine the solvent with the best yield. The solvents were petroleum either, normal hexane (n-hexane) and distilled gasoline (which was introduced as a wild card solvent). For every 150 g of pulverized, oven dried sample, 400 ml of solvent was used for soaking extraction and 600 ml for soxhlet extraction. The waste oil (yellow grease) biodiesel was processed from used grand cereal oil originally extracted from soybeans.

A series of physio-chemical properties of the oil where determined, including: density, viscosity, pour and cloud point, iodine value, refractive index, flash point, free fatty acid (FFA) value, saponification and peroxide values. Details of the extraction yield and oil properties are provided in Tables 6.1 and 6.2. Trans-esterification was achieved with methanol using potassium oxide as an alkaline catalyst. The resulting biodiesel was processed and tested. The fuel properties are given in Table 6.3.

Table 6. 1: Oil extraction yield

Method	Oil Extraction Yield (w/w%)					
	Moringa			Jatropha		
	n-Hexane	Petroleum ether	Distilled gasoline	n- hexane	Petroleum ether	Distilled gasoline
Soxhlet	37.1	24.3	40.2	51.8	25.3	34.1
Manual soaking	13.7	14.1	20.8	26.7	17.7	23.13
Literature Comparison	43.17[1]	32.40[2]	---	47.2[3]	46[3]	---

Table 6. 2: Experimentally determined physio-chemical properties of extracted oil

S/No	Properties	Moringa Oil	Jatopha Oil	Waste Restaurant oil	ASTM D6751	Methods
1	Viscosity (mm^2/s)@30°C	53.9$\pm$0.40	41.45$\pm$0.20	34.64$\pm$0.40	6(max)	Cannon Fenske Viscometer
2	Density (Kg/m^3)	912.0$\pm$00.0	890.62$\pm$10.00	921.6$\pm$5.00	875-900	Density bottle
3	Iodine value	64.84$\pm$0.20	108.40$\pm$0.20	108.26$\pm$0.2		WUS method
4	Refractive Index	1.458$\pm$0.01	1.455$\pm$0.01	1.468$\pm$0.01	1.245-1.675	Abbe refractometer (prolabo)
5	Flash point (^{o}C)	215$\pm$0.05	195$\pm$0.05	164$\pm$0.05	90.00-130	Pensky-Martins Cup flash tester
6	Free Fatty Acid	9.96$\pm$0.1	2.48$\pm$0.1		3.00-5.00	Titrimetric method
7	SaponificationValue (mgKOH/gm)	185.15$\pm$0.1	196.44$\pm$0.1			Titrimetric method
8	Peroxide Value	1.84$\pm$0.02	3.21$\pm$0.02	9.52$\pm$0.2.23		Titrimetric method
9	Pour Point (^{o}C)	8$\pm$0.05	5$\pm$0.04	-16	-15- 10	Van Garpen et al. [4]
10	Cloud Point (^{o}C)	12$\pm$0.05	7. 05	-1$\pm$0.05	-15- 5	Van Garpen et al. [4]

Note: Raw oil properties improve significantly after Tran-esterification to meet ASTM D6751-2 fuel requirements.

Table 6. 3: Fuel properties of biodiesel

Properties	Moringa biodiesel	Jatropha biodiesel	Waste oil Biodiesel	ASTM D6751-2 [5]
Density (Kg/m^3) @ 30°C	892.9	880.52	897.4	875-900
Viscosity(mm^2/s) @ 30°C	4.65	4.56	4.27	1.9-6.0
Heating value (KJ/Kg)	40.05	39.45	39.4	(diesel-45.84)

6.2.2 Test Engine Set-Up

The test engine was a single cylinder, four-stroke and air cooled TD111 Techquipment direct injection diesel engine. The test rig set up is shown in Figure 6.1 and technical details are provided in Table 6.4. A hydraulic dynamometer TD 115 also from Techquipment with water flow pressure head of 6-12 m was used to measure the torque which is displayed on the instrument display panel TD114. The instrument panel also displays the engine speed, exhaust temperature, air flow and houses the fuel flow pipette which measures the fuel flow rate. Measurement input signals are received from the test bed via tachometer connector, thermocouple terminal, torque transducers and manometer tapping from the air bag. The engine speed is measured electronically by a pulse counting system. An optical head mounted on the dynamometer chassis contains an infrared transmitter and receiver. A rotating disc with radial slot is situated between the optical sources and the sensor. As the engine and slotted disc

rotates the beam is interrupted.   The pulse train is electronically processed to provide read-out of engine speed.
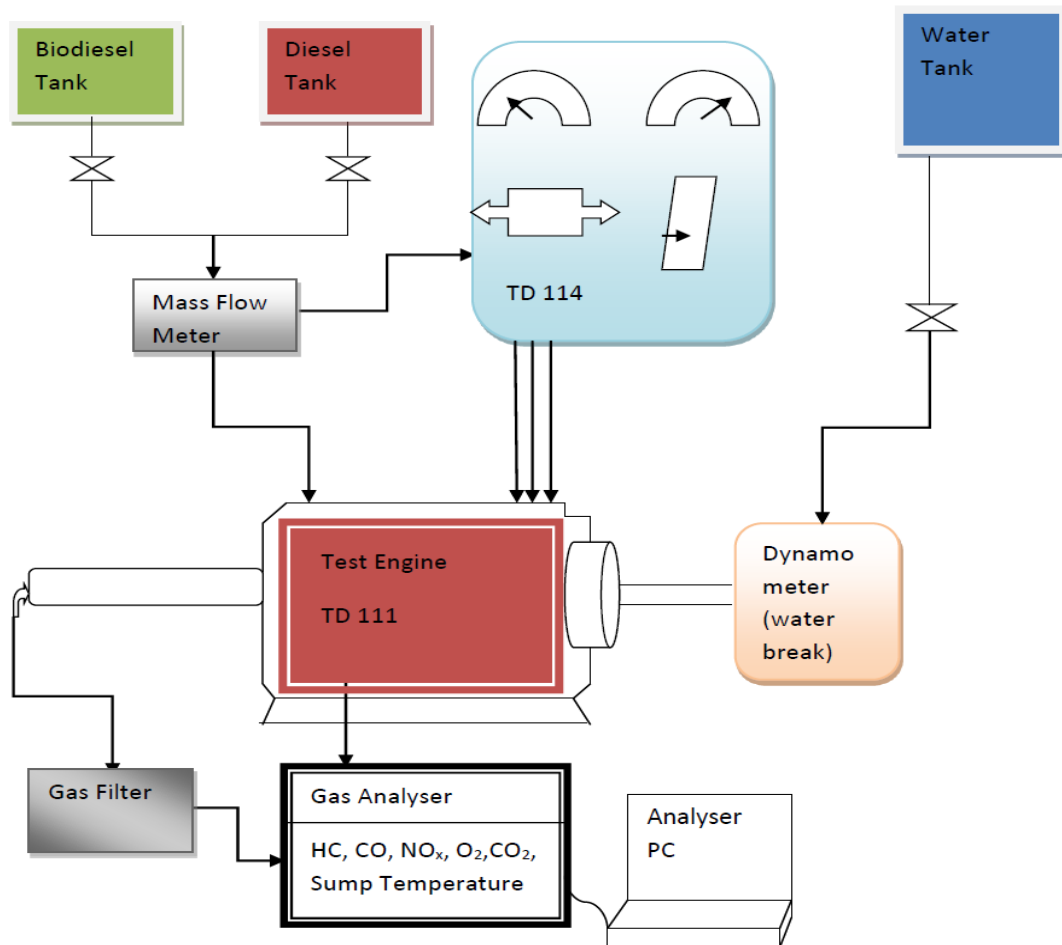
Figure 6 1: Test rig schematic

Table 6. 4: Technical specifications of test rig equipment

Device	Description	Detail
Engine	Model	TQ:TD 111
	Maximum power (Kw)	3.5
	Type	Naturally aspirated, four strokes
	Rated speed (rpm)	3900
	Number of cylinders	1
	Compression ratio	17.5:1
	Combustion	Direct injection
Hydraulic dynamometer	Model	TQ:TD115
	Type	Hydraulic
	Water pressure	6-12 m head of water (60 KPa)
	Range	0-14 Nm
	Water flow rate	4 lt/min
Exhaust gas analyzer	Model	SV-5Q
HC	Range	1-10000 10^{-6} (ppm) Vol.
	Resolution	1 ppm
CO	Range	1-1000 10^{-2} (%) Vol.
	Resolution	0.01%
CO_2	Range	0-20 10^{-2} (%) Vol.
	Resolution	0.01% Vol.
O_2	Range	0-25 10^{-2} (%) Vol.
	Resolution	0.01% Vol.
NO_x	Range	0-50000 10^{-6} (ppm) Vol.
	Resolution	1 ppm

Engine torque is measured by the TD115 Hydraulic Dynamometer and transmitted to a torque meter located on the TD114 instrument unit. A linear calibration of the torque meter is checked intermittently to confirm accuracy of the data set via an eight step process as per the equipment manual (Techquipment 2003). The exhaust gas temperature is measured with a chrome/Alumina thermocouple located in a 1/8"BSP union brazed into the exhaust port of the

engine. Color coded leads from the thermocouple are connected to terminals underneath theTD114 instrument unit.

6.2.2.1 Test Procedure

The test engine is a 3.5 kw rated, direct injection (DI), single cylinder diesel engine. Selected test speeds were 1800 rpm, 2500 rpm and 3600 rpm. Each test cycle at the selected torques consisted of running the engine for 1 minute at idle speed and 9 minutes at the selected load in accordance with test cycle G3 of ISO 8178-4 (EC 1999). The engine rated power was taken as 100% load. The test cycle was repeated for 20%, 40%, 60% and 80% load. This test cycle procedure was followed for diesel, jatropha, moringa and waste oil biodiesel.

6.2.2.2 Pollutant Emissions

The SV-5Q exhaust gas analyzer was in accordance with ND112 (non-dispersive infra-red) method utilized via micro computer analysis to measure the thickness of HC, CO and CO_2 in the exhaust gas and to inspect the density of NO_X and O_2 via electrochemical sensor. The excess air coefficient, λ, was also computed automatically by the analyzer and double checked manually to confirm accuracy. The analyzer is equipped with a microprocessor, an induction tachometer, temperature sensor, and an inner micro printer. The sampling probe is normally installed in the exhaust line where gas can be drawn through a filter into the analyzer.

A sampling tube is normally connected to the sampling probe on one end and a filter at the other end. A thermometer tube extends from the back of the filter to the sample gas vent of the analyzer. A leak check was conducted to ensure there were no leakages subsequent to which auto-zeroing procedures were initiated to prepare the analyzer for actual measurement. The analyzer as well as engine details are provided in Table 5.4.

HC and NO_X are measured in ppm while CO, CO_2 and O_2 are measured in percentages. Given the standard measure stipulated by ISO 8178-4, it was necessary to convert these measurements into g/kWh using the air and fuel flow method Cornell, 2015). Details of the correlation are provided below.

$$W_{NOx} = \left(G_{air} + G_{fuel}\right) \times \frac{M_{NO_2}}{M_{exh}} \times WNO_x \times K_H \times \frac{1}{10^6} \qquad (6.1)$$

$$W_{HC} = \left(G_{air} + G_{fuel}\right) \times \frac{M_{HCexh}}{M_{exh}} \times WHC \times \frac{1}{10^6} \qquad (6.2)$$

$$W_{CO} = \left(G_{air} + G_{fuel}\right) \times \frac{M_{CO}}{M_{exh}} \times WCO \times \frac{1}{10^6} \qquad (6.3)$$

Where

W_{NOx}, W_{HCexh}, W_{CO} mass flow-rate of NO_x, HC and CO in exhaust (g/hr)

G_{air} Intake of air mass flow-rate in dry basis (g/hr)

G_{fuel} Fuel mass flow-rate (g/hr)

M_{exh} Molecular weight of total exhaust given by

$$M_{exh} = \frac{M_{HCexh} \times WHC}{10^6} + \frac{28.01 \times WCO}{10^2} + \frac{44.1 \times WCO_2}{10^2} + \frac{46.01 \times WNO_x}{10^6} + \frac{2.016 \times WH_2}{10^2} +$$

$$18.01(1 - K) + \frac{28.01}{10^2}\left[100 - \frac{WHC}{10^4} - WCO - WCO_2 - \frac{WNO_x}{10^4} - WH_2 - 100(1 - K)\right]$$

$$(6.4)$$

$$M_{HCexh} = 12.01 + 1.008a \qquad (6.5)$$

A   Hydrocarbon/carbon atomic ratio of the fuel

WHC   HC volume concentration in exhaust ppm, wet

WCO   CO percent concentration in exhaust, wet

DCO   CO percentage concentration in exhaust, dry

WCO_2 CO_2 percent concentration in the exhaust, dry

WNO_X NO_X volume concentration in exhaust in ppm, wet

WH_2 H_2 percent concentration in exhaust, wet

K   Correction factor to be used when converting dry measurement to a wet basis

$$\therefore Wet\ concentration = dry\ concentration \times K \qquad (6.6)$$

$$K = \frac{1}{1 + 0.005 \times (DCO + DCO_2)a - 0.01 \times DH_2} \qquad (6.7)$$

$$DH_2 = \frac{0.5a \times DCO \times (DCO + DCO_2)}{DCO + 3DCO_2} \qquad (6.8)$$

W_{CO} mass rate of CO in exhaust (g/hr)

M_{CO} Molecular weight of CO (28.01)

WNO_x mass rate of NO_x in exhaust (g/hr)

M_{NO2} Molecules weight of NO_2 (46.01)

K_H Factor for correcting the effects of humidity in NO_2 formation for four stroke gasoline engines and it is given by;

$$K_H = \frac{1}{1 - 0.0329 \times (H - 10.71)} \qquad (6.9)$$

H   Specific humidity of intake air in grams of moisture per kilogram of dry air

For individual gas component, the reported emission in g/Kwhr is computed in brake specific terms (BSY_{wm}) as

$$BSY_{wm} = \frac{\sum(W_i + f_i)}{\sum(P_i + f_i)} \tag{6.10}$$

Y_{wm} Weighted mass emission level (HC, CO NO_x etc) for a test (g/Kwhr)

W_i Average mass flow rate of emission from the test engine during mode i (g/hr)

f_i Weighting factors for each mode according to test cycle recommendation.

P_i Average power measured during mode i (Kw) calculated according to test cycle recommendation.

6.2.2.3 Test Environment

The test was conducted in a North-Eastern Nigerian town located on latitude $10^{\circ}18'57"$ N and longitude $09^{\circ}50'39"$ E at an elevation of 2,021 ft (616 m). The prevailing ambient temperature at the time of the test ranges between $30^{\circ}C$ - $33^{\circ}C$ and the relative humidity between 71% - 75%. Recorded atmospheric pressure was 92 Kpa, air density 1.208 kg/m3 and absolute humidity, 0.022 kg/m3 from these data, the specific humidity as well as kH were computed.

6.2.2.4 Particulate Matter Emission

The exhaust gas sampling probe inserted in the exhaust line draws exhaust gas through a filter enroute to the gas analyzer. The pollutants NO_X, THC, CO and PM were measured in accordance with ISO 8178 with a constant speed test cycle prescribed in test cycle D1. This is the most appropriate given the rated power of the test engine. Most engines of this category operate at constant speed with loading profile in the range of 50% and above. The gas analyzer, SV – 5Q was used to measure NO_X, THC and CO in ppm and the result was converted to g/kWh. The PM was measured by trapping it with the analyzer's filter (which was replaced at the end of every test cycle) and weighing the filter to obtain a direct mass measurement on a weighting device with 1 micrograms resolution. This method was adopted because mass based PM is what is regulated by US EPA and the European Union.

6.3 Result and Discussion

6.3.1 Extraction Yield, Oil and Biodiesel Properties

Results obtained from the extraction yield (as shown in Table 6.1) indicated that the soxhlet method of extraction was found to be the optimal method of extraction as it showed a nearly 50% yield above the manual soaking method for all types of solvent with both samples. N-hexane was found to be a more efficient solvent in the extraction process followed by distilled

gasoline while petroleum either gave a sub-optimal yield of 24.3% for moringa and 25.3% for jatropha using the soxhlet method. All the solvents were recoverable post-extraction and it is worth noting that distilled gasoline, which was introduced as a wildcard gave satisfactory results. This is an important outcome given the ready availability of gasoline. The extraction yield result is broadly in agreement with previous work done under similar conditions (Abdulkareem et al. 2011; Belewu et al. 2010; Lalas and Tsaknis 2002). The superior yield observed for soxhlet in comparison to the soaking method underscores the importance of intense interaction between seed oil matrix with solvent. The differential yield for the various solvents shows the extent to which solubility plays a part in seed oil extraction.

For the physio-chemical properties of the extract, Table 6.2 shows the results obtained from various experiment conducted with the oil extracts. These results are within the range obtained for oil processed into biodiesel for diesel engine application. Table 6.3 also shows that the fuel properties of biodiesels produced from moringa (MO100), jathropha (JA100) and waste restaurant oil (WO100), when compared with the ASTM standard for diesel engine fuel, were within acceptable limits.

6.3.2 Engine Performance

In accessing the engine performance, the brake specific fuel consumption (BSFC), brake thermal efficiency (BTE) and exhaust gas temperature for ndiesel, W0100, M0100 and JA100 were studied. The results are presented and discussed in the following section.

6.3.2.1 Brake Power

At the engine speed of 1800 rpm, moringa biodiesel experienced a brake torque loss of 6.97% in comparison to diesel at the torque of 8.6 Nm. This loss increases to 7.69% as the torque reduces to 6.5 Nm. The trend is repeated in varying degrees as the engine is run with WO100 and JA100. The brake torque losses were generally within the range of 6% - 9%. These losses are attributed to the lower heating values and higher viscosities of the pure biodiesels where the heating value decreased in comparison to diesel. The decreases range between 5% to 7%. Figure 6.2 shows a plot of brake thermal efficiency (BTE) vs load. The BTE increases as the load increases for all fuel types and the results showed no significant difference between diesel and the biodiesels for loading < 40%, but as the load exceeds that value, diesel records an increasing range of between 2.5% to 8.9% above all the biodiesels. The highest range was recorded between diesel and MO100, the explanation for this being that with diesel's higher

heating value, it is bound to record higher BTE but this advantage is narrowed for lower rated engines particularly given the higher BSFC and fuel conversion efficiency of biodiesel (a characteristic that manifests as a result of biodiesel's extra oxygen in the fuel molecule). The difference in BTE between ndiesel and MO100 is wider because the latter has a higher composition of unsaturated fatty acid methyl esters (FAMEs) and thus a lower level of combustion efficiency (Pandey, Rehman, and Sarviya 2011). In the highly stratified thermal and charged environment of the CI engine, MO100 with high levels of oleic (72%) and low levels of palmitate (6.5%) was placed at a disadvantage in the context of combustion efficiency. In the rich zone of the combustion chamber, during high temperature reaction, post NTC (negative temperature co-efficient), post flame, bulk energy release is governed by the oxidation of CO to CO_2 but where double bond radicals dominate, recombination reactions prevail, leading to PAH (poly-aromatic hydrocarbon) formation, the precursors of soot which undercut energy release and produce higher levels of THC (this can be clearly seen in Figure 5.12 where, next to diesel, MO100 had the highest emission of THC). A higher level of unsaturation impedes fuel conversion efficiency and reduces heat release rate (Yao et al.)
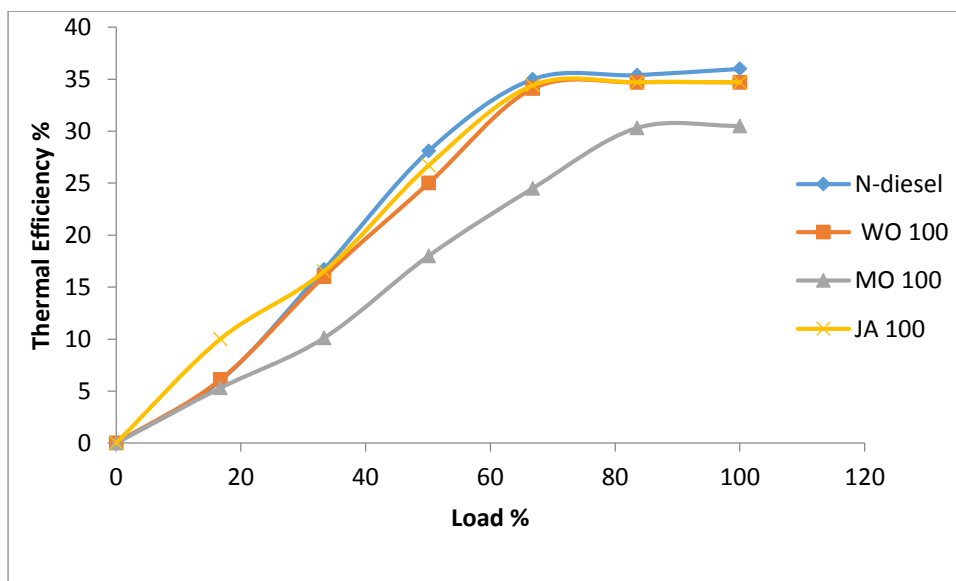
Figure 6 2: Brake thermal efficiency vs load

This result largely agrees with what was reported by Utlu and Kocak (2008) where average decreases in torque and power values of WFOME (waste frying oil methyl ester) was 4.3% and 4.5% respectively. Hansen, Gratton and Yuan (2006) also observed a brake torque loss of 9.1% for B100 (pure biodiesel) relative to diesel at 1900 rpm in a much larger engine. Murillo et al. (2007) reported a loss of 7.14% for biodiesel compared to diesel as observed on a 3 cylinder,

naturally aspirated submarine diesel engine at full load. This could be attributed to the variation in the heating value of the tested fuel samples.

6.3.2.2   Brake Specific Fuel Consumption (BSFC)

Figure 6.3 gives the relations between the BSFC and load in the test data obtained. The trend showed a general decrease in BSFC at increasing load profiles with most of the decrease taking place between 20% to 60% load (a decrease of between 400 g/kWh to 200 g/kWh) underscoring the technical and economic benefits to priming engines at higher rated power. M0100 showed a higher BSFC trend in comparison to diesel. The difference however, decreases from about 250 g/kWh to 20g/kWh at peak load. Interestingly, it was observed that W0100 and JA100 fuel samples (which recorded no significant difference between their BSFC) showed a trend lower than diesel starting from a difference of about 100 g/kWh at 20% to < 15% at peak load. This trend negates the result of findings published in related works by Nettles-Anderson et al. (2014) and Rahman, Jena, and Jadav (2013) respectively.

Figure 6 3: Brake specific fuel consumption vs load
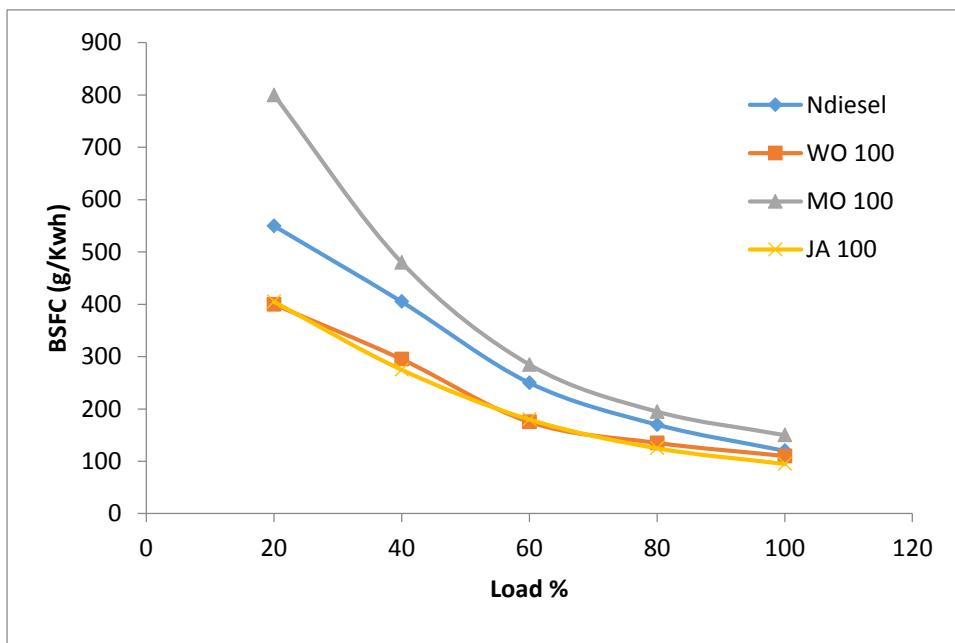
The comparative advantage observed for W0100 and JA100 in BSFC with respect to diesel could be attributed to the effect of engine scaling. That is, given that ignition commences at a low energy base, fuel types that have comparatively longer ignition delays such as diesel will be disadvantaged because the critical pressure and temperature is more difficult to achieve with

a small size engine. Conversely, fuel with short ignition delay because of a high cetane number resulting from straight chain carbon structure such as WO100 and JA100 achieve ignition fairly easily. At 3.5 kw rated power the single cylinder direct ignition diesel engine is slightly more challenging to crank during cold start hence initiating and sustaining combustion comes with some challenges. This gives an edge to oxygenated fuel with higher cetane numbers (WO100 and JA100. The reason this advantage does not extend to MO100 is because it has slightly higher levels of unsaturation, it is less oxygenated and has a lower reactivity in the context of start of ignition (auto-ignition). WO100 and JA100 with 20.4% and 15.3% palmitate (C16:0) compared to MO100 with 6.5% palmitate (C16:0) are more likely to auto-ignite easily because short chain saturated palmitate acts like spark plugs in a CI engine (Azad et al. 2015; Maina 2014; Chhetri, Watts, and Islam, 2008). This is precisely why WO100 and JA100 are more likely to initiate auto-ignition. Low temperature reactions (LTR) prior to negative temperature co-efficient (NTC) control auto-ignition in CI engines (Noguchi, Tanaka and Takeuchi 1979; Najt and Foster 1983; Yao, Zheng and Liu, 2009). But large composition of oleic in MO100 (72%) which is an unsaturated FAME attack the CH_2O, HO_2 and O radicals which drive this process and inhibit it because of the inherent recombination tendencies of unsaturated hydrocarbon at the lean phase to achieve saturation or form poly-aromatic hydrocarbons (PAH). This is the context in which 'less reactive' was used in the paper at the auto-ignition stage. There is a temptation to suggest that low temperature properties such as pour point, cloud point and cold flow plugging point could be the likely cause of the observed trend but if reference is made to section 2.2.3 in the paper, ambient temperature when the experiment was performed was $30^{o}C$ - $33^{o}C$, which is more than three times higher than the highest pour point of any of the sample oils used to produce the sample fuels (see Table 5.2 and note the comment on the table footnote clearly stating that even these property values improve significantly to meet ASTM D6751-2 fuel requirement after trans esterification).

The BSFC observed for M0100 in comparison follows the generally observed trend for higher rated engines. Qi et al. (2009) reported that engines deliver fuel on a volumetric basis and since biodiesel densities are higher than those of diesel, more biodiesel has to be supplied to compensate for the lower heating value.

6.3.2.3 Exhaust Gas Temperature

It has been shown earlier that a slightly higher viscosity and lower heating value combines to impede fuel flow, heat release and in effect power delivery when the engine is run on pure

biodiesel. These constraints become more obvious when the exhaust gas temperature of the various fuel types at 50%, 75% and 95% load are compared. Normal diesel, given its higher heating value and lower viscosity is clearly seen to be delivering higher power through higher heat release rate. The instantaneous exhaust gas temperature in Figure 6.4 is a clear gauge of this trend. Instantaneous reading was adopted for this data set with an error bar of ± 5% to compensate for intermittent fluctuation. At 95% load M0100 (which had the best EGT logged amongst the biodiesel) had its maximum temperature less than that of ndiesel by about 9%. Average exhaust gas temperature decreases of the three biodiesel at all load condition ranges were between 11% - 14%. This is well above the heating value decrease of between 5% - 7% indicating that viscosity plays a key role in combustion behavior of the oil. It could also be inferred that the advantage of lower viscosity for ndiesel is more significant than the advantage of a more efficient combustion for the biodiesel (arising from their oxygenated molecules) when heat release rate is being considered. Several numerical studies have highlighted these facts in considerable depth (Brakora, Ra, and Reitz 2011; Golovitchev and Yang 2009)
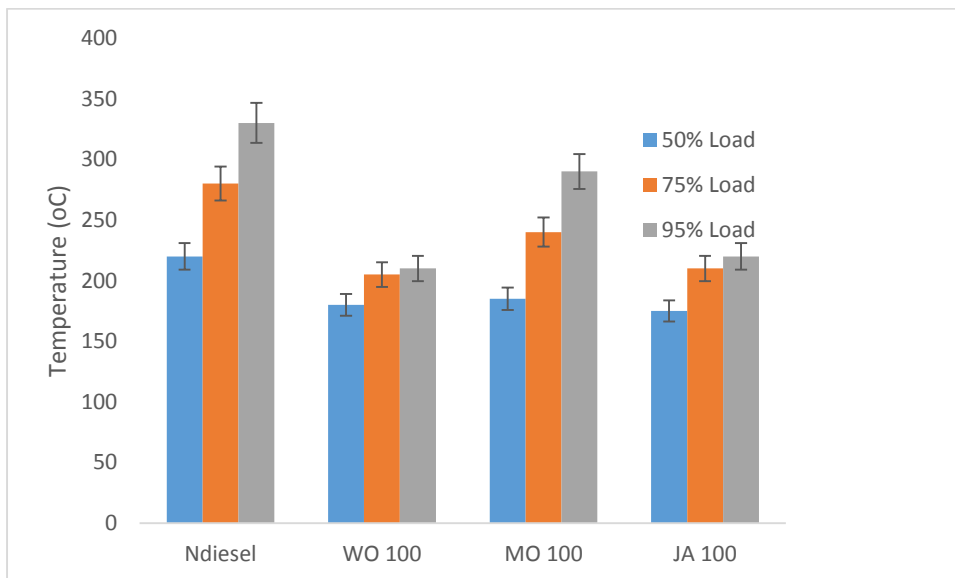
Figure 6 4: Exhaust gas temperature profile

6.3.3 Pollutant Emission

Table 6.5 gives the US EPA and EU emission standards against which the test data was compared.

Table 6. 5: EPA and EC emission standard for N0X, THC, C0 and PM

Standard	NO_X (g/kwh)	THC (g/kwh)	CO (g/kwh)	PM (g/kwh)
U.S.	$N0x + MNHC = 10.5$		8.0	0.4
EC	9.2	1.3	5.0 – 6.5	0.54 – 0.85

The trend observed for the emissions are presented and discussed in the following section.

6.3.3.1 Oxides of Nitrogen (NO_X) Emission
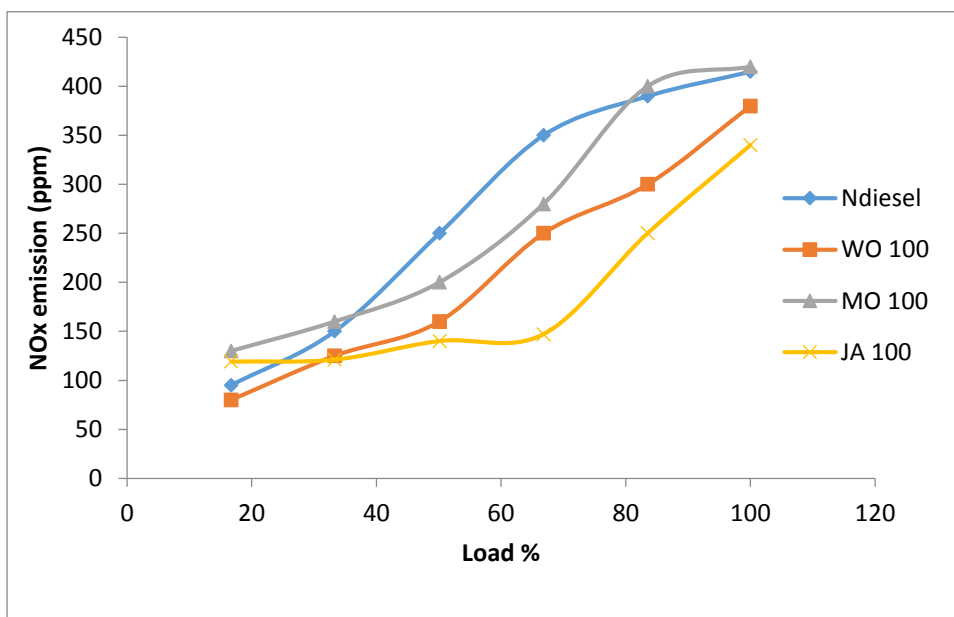
Figure 6 5: NOX emission (ppm) vs load

Figure 6.5 shows the NO_X emission trend for the normal diesel and the three biodiesel fuels under various loading conditions. Expectedly, the NO_X in ppm increases with increasing load. The results show a mixed trend with MO100 and JA100 having higher value at low loading condition when compared with ndiesel, but as the load increase, diesel NO_X increases well above the biodiesel fuel. Historically, NO_X emission has been observed in most works to trend higher for biodiesel than for ndiesel (Hazar 2009; Ozsezen et al. 2009; Karabektas 2009; Ozgtinay et al. 2007; Murillo et al. 2007). These results may appear to paint opposite pictures

when records of generalised experimental studies are evaluated but, a more intense investigation of both experimental as well as numerical studies have shown that NO_X production in the internal combustion engine is driven by the extended Zeldovich mechanism which describes the oxidation of atmospheric nitrogen into NO_X by a three step reaction which has a strong temperature (because of large activation energy) and O_2 concentration dependence (Heywood 1976). More importantly, elevated temperature was identified as the trigger with O_2 concentration serving the role of an enabler. In the Zeldovich mechanism, the primary reaction which triggers thermal NO_X is the breaking of Nitrogen's double bond (this requires high activation energy). Alrikson and Denbratt (2006) in their computation of the equivalent ratio-temperature ($\emptyset$-T) map for soot and NO_X concentration using the SENKIN code observed that NO_X and soot emission could be completely eliminated regardless of equivalent ratio if the combustion temperatures are kept below 1650 k. A comparative study of NQ_X emission for different fuel types can only be conducted quantitatively at similar temperature and excess air regime. Biodiesels typically have been observed to produce more NO_X because, given their oxygenated molecule, a higher O_2 concentration was prevalent in the reaction zone. Coincidentally in this test, when a comparative evaluation of $N0_X$ emissions for all the test cycle was conducted in relation to excess air and temperature, it was observed that maximum NO_X emissions were observed at the point of highest temperature and excess air regardless of the fuel type. This is shown in Figure 6.6. It is therefore safe to submit that biodiesel, given its oxygenated molecule, is more prone to higher NO_X emissions at the same exhaust gas temperature region but if the temperature is lower than the computed threshold, the emission will be subdued regardless of the presence of higher oxygen concentration.
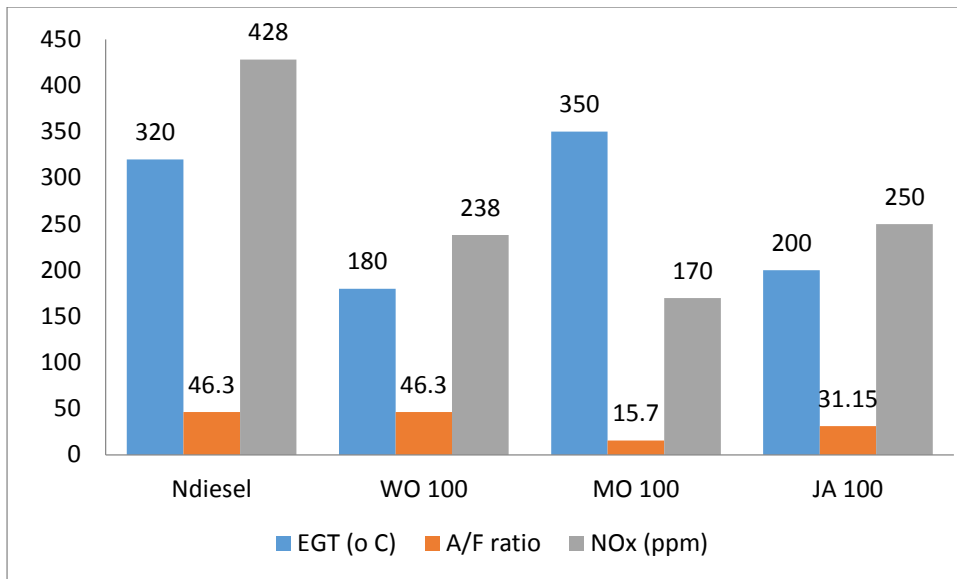
Figure 6 6: NOX emission in relation to A/F ratio and EGT

The BSNO$_X$ vs load trend shown in Figure 6.7 showed that in specific terms BSNO$_X$ decreases with increasing load for all the fuel types. All the biodiesel fuels showed BSNO$_X$ levels lower than ndiesel even though the decrease is more rapid for ndiesel. The BSNO$_X$ decrease rate appears to plateau between 65% load to maximum load. The value for all the fuel types for this particular engine also appear to have met the EPA maximum stipulated value of 9.5g/kWh and the EU value of 9.1g/kWh. This is typical of small engines that are naturally aspirated, single cylinder where low power rating speed limits tend to put a cap on maximum exhaust temperature and excess air. These values could change dramatically for higher rated engines.
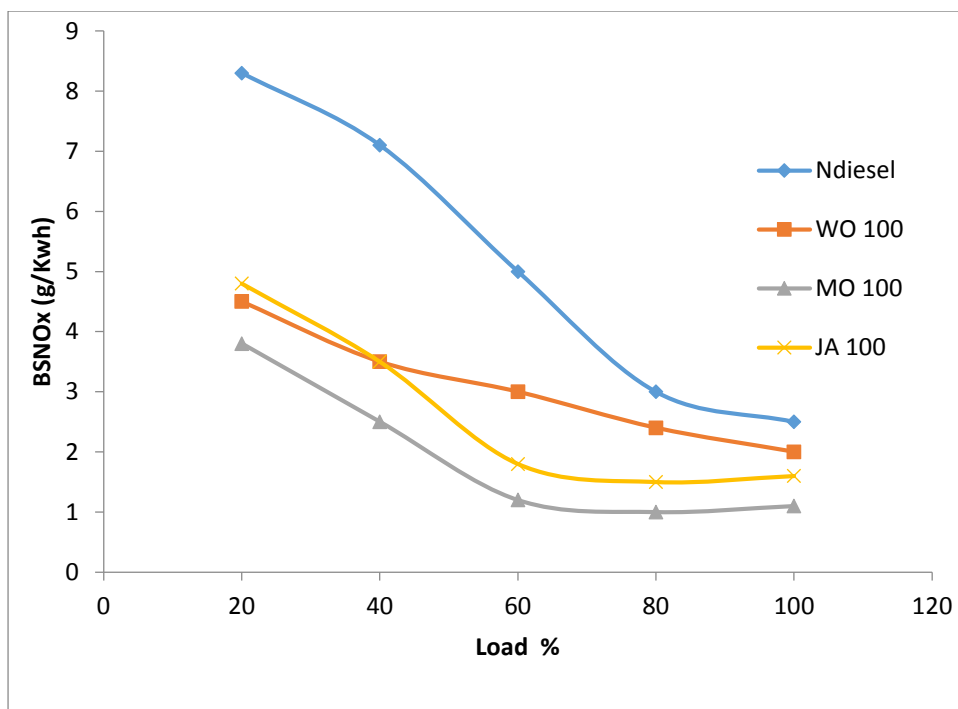
Figure 6 7: BSNOX vs Load

6.3.3.2 Carbon Monoxides (CO) Emission

Figure 6.8 describes the CO emission trend in ppm at varying loads for the four test samples. Expectedly, the CO emission decreases with increasing load, and ndiesel CO emission was highest at all loading conditions with the difference between it and the rest of the biodiesel varying from between 10% for WO100 and MO100 to 25% for JA100 at 20% loading to between 4% - 10% at peak load. Similar trends have been observed and reported extensively (Ulusoy et al. 2004; Buyukkaya 2010; Choi and Oh 2006; Ghobadian et al. 2009). The reason for the reduction in CO when a switch is made from ndiesel to pure biodiesel is primarily because of the extra oxygen in the biodiesel molecules. The observed decrease for all fuel types as the load increases could be attributed to the improved combustion efficiency and reaction dynamics as the engine revs up to higher load.
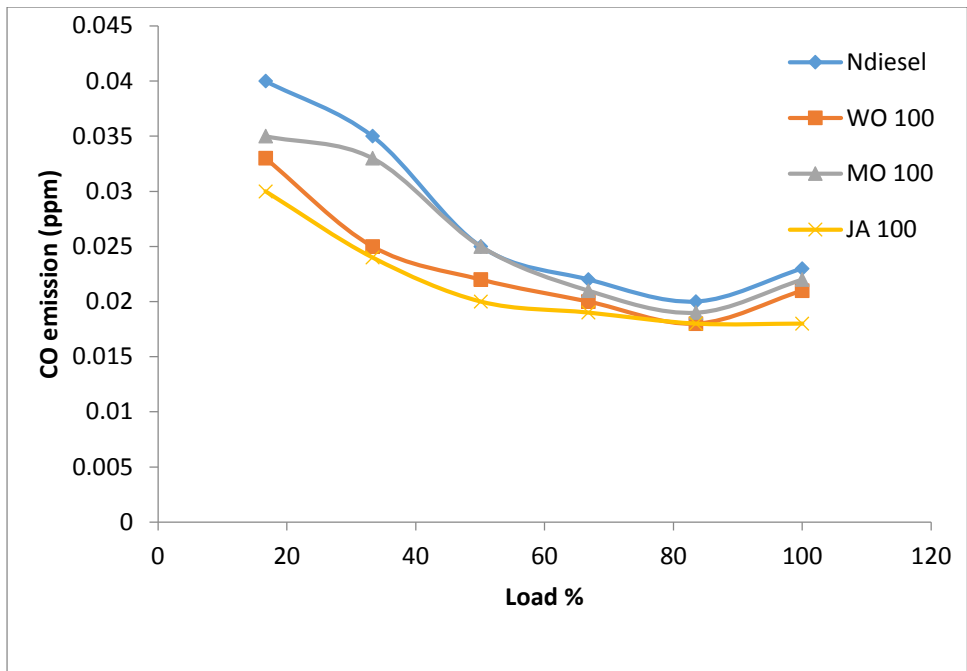
Figure 6 8: CO emission vs load

The CO emission, when measured in ppm for all fuel types appears insignificant at increasing load but when this is done in BSCO as stipulated by the EPA and EU, the emission tells a different story. Figure 6.9 shows a plot of BSCO vs load. Normal diesel still gave the most emission albeit at a much reduced margin except for JA100 within the loading profile of between 20% - 50%. Given the maximum emission limit of 8 g/kWh and 5 g/kWh - 6 g/kWh by the EPA and the EU respectively for CO emission (see Table 5.5), Figure 5.9 shows clearly that at between 20% - 65% loading for all the fuel types, the emission standard for CO was in breach. It could also be seen that ndiesel failed to meet the standard until it reached 80% loading. This demonstrates clearly the superiority of measuring emissions in g/kWh compared to in ppm, the former being more specific and highlighting problem areas requiring remediation. The results also suggest that for engines running at a constant high loading regime, the problem is more tolerable.
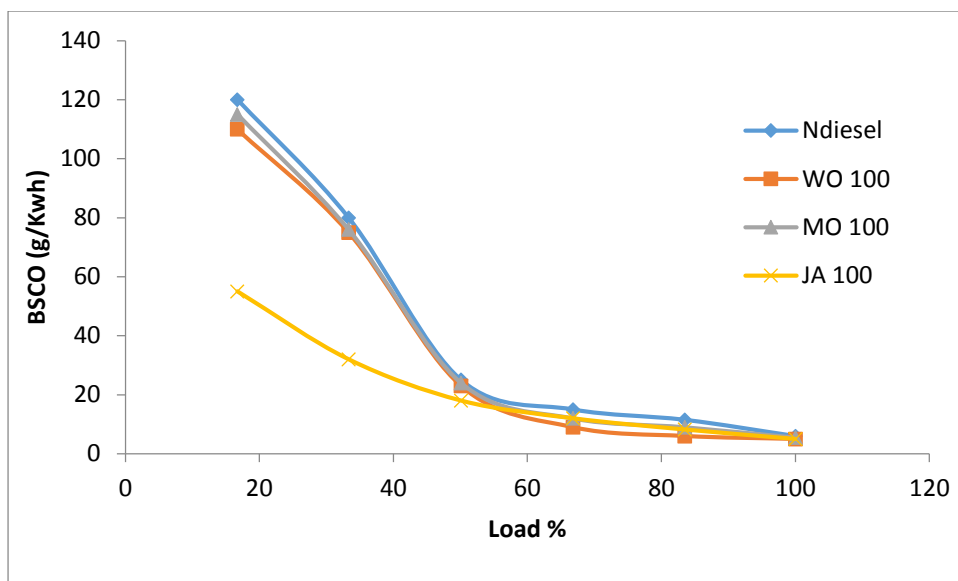
Figure 6 9: BSCO vs load

Another trend observed in the CO emission measure in ppm was that CO increases with increasing temperature for ndiesel by as much as 0.0064 ppm/^{o}C. This trend suggests that CO production, although a primarily equilibrium based reaction, could also be kinetically driven in certain types of engine. At higher combustion temperature, gas dissociation of CO_2 into CO does takes place and during the rapid expansion (common with a single cylinder's fast stroke action) stage, burnt gas assumes a frozen state thus preventing the oxidation of CO back to CO_2 in the exhaust (Heywood 1976). This, it is believed, is the likely cause of the trend observed here for ndiesel where CO increases with increasing temperature.

6.3.3.3 Unburnt/Total Hydrocarbon (HC) Emission

Figure 6.10 shows the HC emission verses load trend for the fuel samples used. The illustration (in ppm) shows clearly that HC emission reduces when pure biodiesel replaces ndiesel. The reduction on the average is 16.5% for WO100, 50% for MO100 and 67.5% for JA100. For all fuel types, between 20% to 40% load, HC emission reduces at between 2% - 5% then flattens out until 65% load and gradually peaks with a slightly tilted bath-curve. In general, the emissions are subdued given the likely mechanism of production for HC in a diesel engine. Primarily four mechanisms exist through which HC is produced in the engine (Heywood 1976). The first is flame quenching in the combustion chamber wall, the second is unburned mixture of crevice volume, and the third is absorption and de-absorption of fuel into/out of oil layers during intake and compression and finally, incomplete combustion of fuel during combustion. Of these four mechanisms, ndiesel and biodiesel have similar behaviour in the first three. Only

in the last mechanism does ndiesel differ from the pure biodiesels because of fuel chemistry. That is, given the oxygenated nature and high cetane number of pure biodiesel, combustion is more likely to be initiated earlier and proceeds in a more complete fashion than it will be for ndiesel. Al-Widyan, Tashtousir and Abu-Qudais (2002), Puhan et al. (2005) and Wu et al. (2009) in explaining a similar trend suggested that cetane number and extra oxygen in fuel molecules of biodiesel were the reason HC reduction was noticed in comparison to ndiesel.
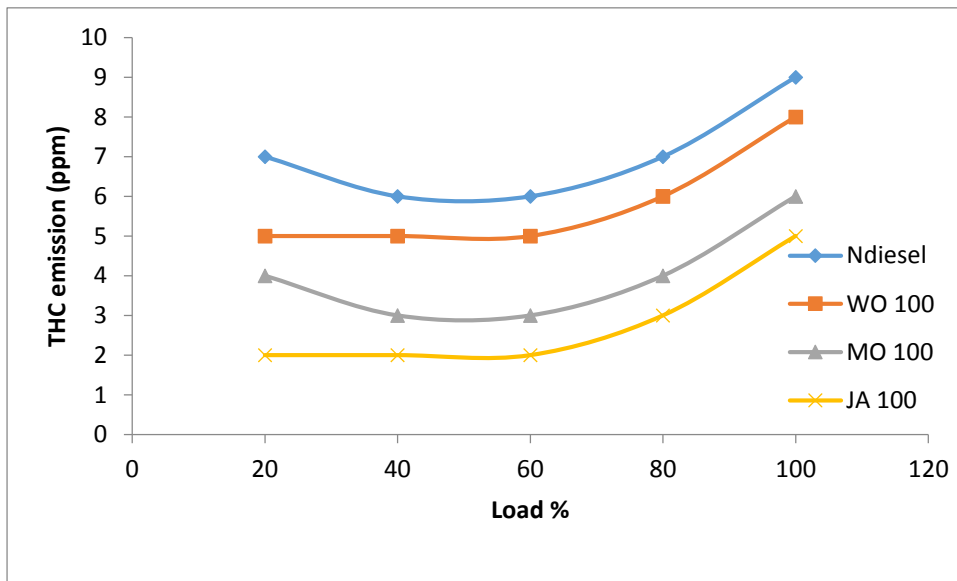
Figure 6 10: Total (unburnt) hydrocarbons vs load

Figure 6.11 shows the BSHC versus load. The trend showed that BSHC decreases rapidly with increasing load from 20% to 50% load. Beyond that level, the reduction became more gradual. The important thing to note is that the highest recorded BSHC for all the fuel types was less than the regulation limits set by the European Commission (1.3g/kWh) and the US EPA (1.2g/kWh). It could also be deduced from the data that ndiesel HC emission in BSHC is higher than all the biodiesel fuel types with the only exception being WO100 where BSHC was higher than ndiesel between 20% to 50% load. This could be as a result of wall and crevices quenching aggravated by inhomogeneous mixing of combustion charge on the part of the biodiesel because of poor transport properties (Pandey, Rehman and Sarviya 2011).
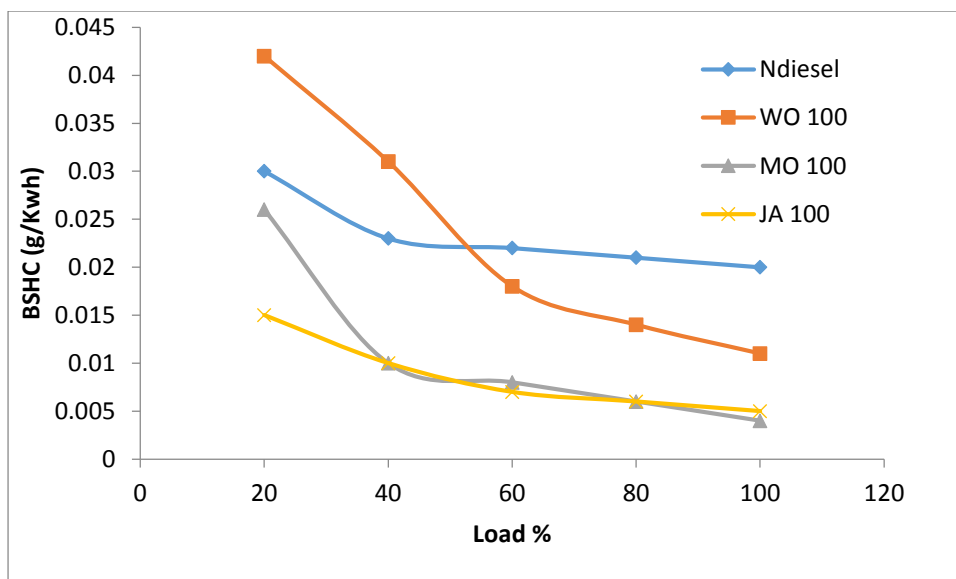
Figure 6 11: BSHC vs load

6.3.3.4 Particulate Matter (PM)

Particulate matter are primarily measured via two approach, namely, mass based PM measure and Bosch smoke number (Hermmerlein et al. 1991). The mass based measure was the approach adopted in this work because it is the measure regulated by the US EPA.

The Environmental Protection Agency and the EU (Nettles-Anderson et al. 2014). Figure 6.12 gives the weighted average PM emission for ndiesel, WO100, MO100 and JA100. Normal diesel showed the highest emission at 1.14 g/kWh. WO100, MO100 and JA100 showed 40.3%, 14.0% and 47.3% reduction in PM emission respectively when compared with ndiesel PM emission. The US EPA and EU standard regulations prescribe that PM should be less than 0.4g/kwh and 0.54 g/kwh - 0.85 g/kWh respectively so it is evident that ndiesel and MO100 PM emission in this work failed to meet both standards. It also showed that WO100 and JA100 passed the upper limit of the EU standard but failed the US EPA standard.
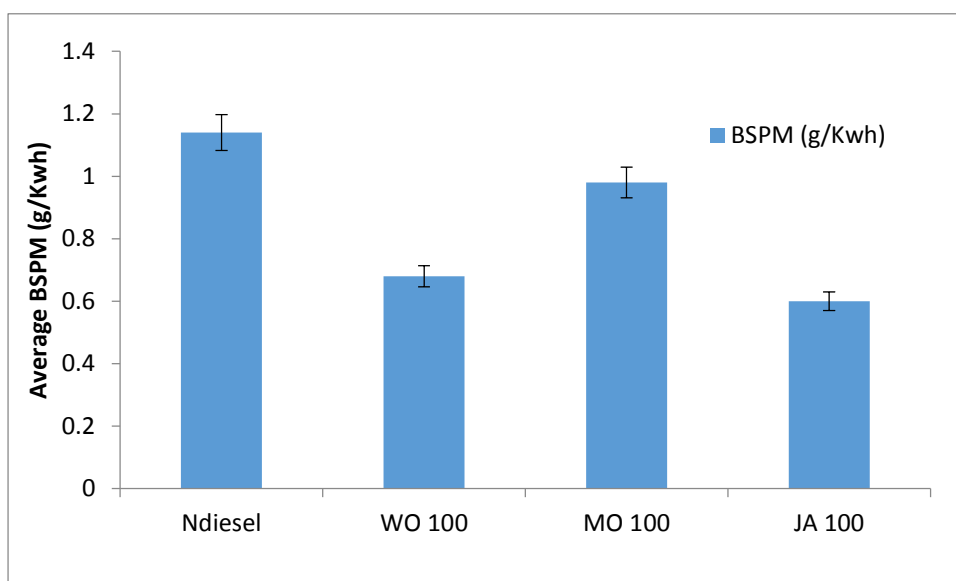
Figure 6 12: BSPM profile

The emission pattern observed here is consistent with results obtained from other work with diesel and biodiesel. Wu et al. (2009) in a study that investigated the emission of PM for five pure biodiesels on a Cummins ISBe6 D1 engine with turbocharger and inter cooler, observed a PM emission reduction of 53% - 69% average compared with diesel fuel. Lin, Huang and Huang (2009) also observed a reduction in PM that ranged between 50% - 72.73% when compared to diesel for eight kinds of VOME (vegetable oil methyl esters). The reasons for the observed decrease in PM emission for pure diesel are the fuel oxygen content and the lack of aromatics as well as sulphur in pure biodiesel. This position is supported by the findings of Frijters and Baert (2006).

6.3.3.5 Oxygen Concentration in Exhaust

Figure 6.13 shows the oxygen concentration in exhaust for the four different fuel types. The figure shows mean, maximum and the standard deviation of the measure for all the test cycles. Normal diesel has the least O_2 concentration in the exhaust at 11.5% while the biodiesel O_2 mean ranges between 13% - 14.5%. This result confirms the advantage bestowed on biodiesels in fuel combustion efficiencies on account of the oxygenated nature of their molecules, although on the performance side oxygen in biodiesel molecule and a higher density of biodiesel is a disadvantage. Also, the figure shows a higher fluctuation of O_2 for WO100 and MO100 when compared to JA100, indicating that the JA100 degree of saturation helped make combustion more stable and predictable. WO100's cooking history has significantly altered the

resulting fuel chemistry and made its combustion less predictable. MO100, because of its unsaturation, caused significant variation in O_2 concentrations.
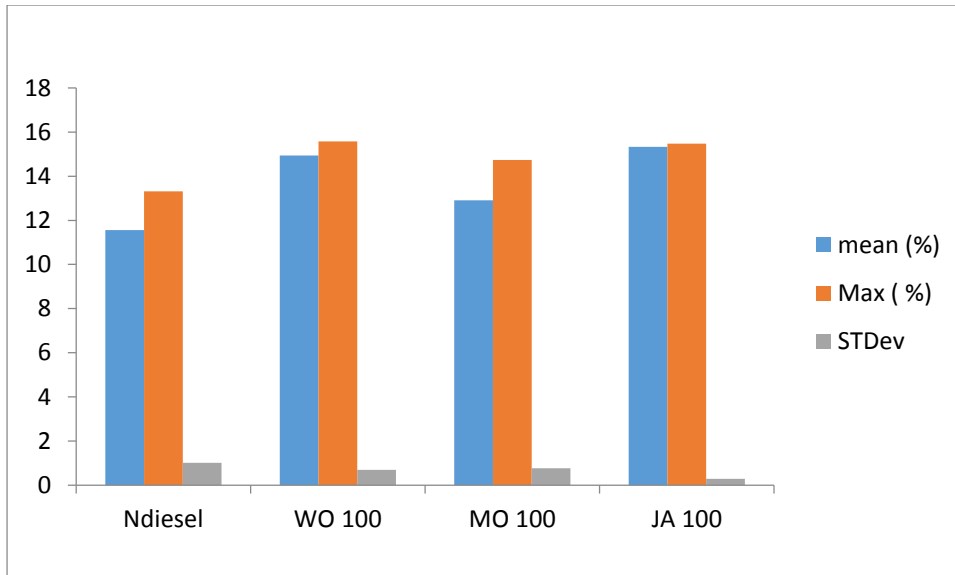
Figure 6 13: Percentage Oxygen Concentration

6.4 Conclusion

As a follow-up study of the work done earlier by Eloka-Eboka, there are areas of differences and some common features. The central focus of the thesis by Eloka-Eboka was the optimization of the production processes for biodiesel through the use of various technique and catalyst (As shown in paper 1: Eloka-Eboka, Igbum, and Inambao, 2014). That study also involved the determination of the right mix (blend) of biodiesel sample through a hybridization process (As shown in paper 3: Eloka-Eboka, and Inambao, 2014). The engine test and emission evaluation were qualitative hence, they did not follow the stringent international bench mark of the ISO 8178-4:2006 (for engine test) and the EPA/EU emission caps (As shown in paper 2 and 4: Igbum et al, 2014). Two samples were common to both studies, namely Moringa biodiesel and Jatropha but the objectives, method of evaluation, testing used and findings were different (but complementary). In addition, biodiesel derived from waste restaurant oil was evaluated in the current study.

As a follow-up work, the current study aimed to provide more clarity regarding the performance and emission of pure samples using standard engine test protocol and emission regulation. And to also suggest a research path that is less expensive in terms of experimentation and time. The numerical property prediction scheme implement in chapter 5 was developed to determine thermo-physical properties efficiently and accurately. This scheme reduced the number of experiment needed to determine sample properties from nine to one thus saving both time and money. Other experiments conducted for property determination were purely used for the purpose of validating the scheme. In addition the validated correlation in the scheme, which are all linear functions, could be coupled to a CFD solver to compute on demand any property during iterative process for these samples.

The engine test protocol in this study adopted the standard ISO 8178-4:2006 and the EPA/EU emission caps for a quantitative study of pure biodiesel samples. One of the benefits from this approach was that, it was easy to observe the difference in reactivity between FAME derived from Moringa (which has a higher proportion of unsaturation) and Jatropha (which has a lower proportion of unsaturation) in the engine test-rig. The lower reactivity for the former compared to the latter was linked to the unsaturated FAME chemistry. This had impact on both the engine performance and emission as stated in chapter 6 and 7. This led to a useful finding that oil (which are good for human consumption) perform poorly when converted into biodiesel, on the other hand, discarded waste restaurant oil (unfit for human consumption) with high proportion of saturated chains as shown in chapter 5, gives good performance and emission as biodiesel. This fact serves to assuage the fears in some quarters that biodiesel use is in direct competition with humans. The result here reflects a more symbiotic outcome.

Another useful outcome as a result of the approach adopted in this study is the observation that NO_X formation correlate strongly with combustion temperature. And, oxygenated molecule of the FAME chemistry in the samples used only help to further facilitate the thermal NO_X formation process. This observation is only possible when observed emissions are computed in the brake specific format of g/kWhr of the ISO regulation and pure sample data are compared.

In conclusion, given biodiesel renewable nature, sustainability, and varied source, biodiesel fuels are set to play an important role in the energy mix of the future. In this work, the technical viability of pure biodiesels have been highlighted and the findings from the foregoing are summarized below as follows:

i. In terms of oil extraction methods, the conventional solvent n-hexane was identified as the solvent with the best extraction yield in both the soxhlet and manual method. Distilled gasoline which was used as a wild card solvent showed potential and should be further explored. This fact is crucial in the biodiesel value chain given gasoline's supply ubiquity and affordability.

ii. Brake thermal efficiency (BTE) for the fuel samples, as a parameter to evaluate engine performance behaviour, showed marginal differences with ndiesel having a better performance (except for the marginally higher MO100 performance).

At loads exceeding 40%, the BTE difference between MO100 and the rest of the fuel samples exceeded 5%, indicating that MO100's unsaturation and the ensuing low reactivity caused by the recombination tendencies of the higher oleic component (72%) of MO100 have more significant effects on the BTE measure than the transport properties deficiencies of biodiesel in general.

iii. Strategies for meeting emission standards for all fuel samples may have little to do with fuel chemistry as the specific emissions, for the most part, indicated a similar trend in their failure to meet the maximum emission limits set by EPA (USA) and EU regulations. A generic approach to solving the emissions challenge via engine and combustion strategy development offers better means of reducing specific emissions to meet set limits.

References

Azad, A. K., M. G. Rasul, Khan, M. M. K, C S. Sharma1, and R Islam. 2015. "Prospect of Moringa seed oil as a sustainable biodiesel fuel in Australia: A review." 6th BSME International Conference on Thermal Engineering (ICTE 2014) (Procedia Engineering 105): 601-606.

Abdulkareem, A. S., H. Uthman, A. S. Afolabi, and O. L. Awenebi. 2011. "Extraction and optimization of oil from moringa oleifera seed as an alternative feedstock for the production of biodiesel." *Sustainable Growth and Applications in Renewable Energy*. Available at: http://www.intechopen.com.

Al-Widyan, M. I., G Tashtousir, and M. Abu-Qudais. 2002. "Utilization of ethyl ester of waste vegetable oils as fuel in diesel engines." *Fuel Processing Technology* 76: 91-103.

Alriksson, M., and I. Denbratt. 2006. "Low temperature combustion in a heavy duty dieselengine using high levels of EGR." *SAE paper 2006-01-0075*.

Belewu, M. A., F. A. Adekola, G. B. Adebayo, O. M. Ameen, N. O Muhammed, A. M. Olaniyan, O. F. Adekola, and A. K. Musa. 2010. "Physico-chemical characteristics of oil and biodiesel from Nigerian and Indian Jatropha curcas seeds." *International Journal of Biological and Chemical Science* 4(2): 524-529.

Benjumea, P., J. R. Agudelo, and A. F. Agudelo. 2011. "Effect of the degree of unsaturation of biodiesel fuels on engine performance, combustion characteristics, and emissions" *Energy Fuels* 25: 77-85.

Brakora, J. L., Y. Ra, and R. D. Reitz. 2011. "Combustion model for biodiesel fueled engine simulations using realistic chemistry and physical properties." *SAE paper No. 2011-01-0831*.

Buyukkaya, E. 2010. "Effects of biodiesel on a DI diesel engine performance, emission and combustion characteristics." *Fuel* 89: 3099-1105.

Canakci, M., and J. H. Van Gerpen. 2003. "Comparison of engine performance and emission for petroleum diesel fuel, yellow grease biodiesel, and soybean on biodiesel. Presented at the 2001 *American Society of Agricultural Engineers* Annual Meeting as Paper No. 016050.

Chhetri, A. B., K. C. Watts, and M. R. Islam. 2008. "Waste cooking oil as an alternate feedstock for biodiesel production." *Energies* 1(1): 3-18.

Choi, S. H., and Y. Oh. 2006. "The emission effects by the use of biodiesel fuel." *International Journal of Modern Physics B* 20: 4481-4486.

Cohen, B. 2005. "Urbanization in developing countries: current trends, future projections, and key challenges for sustainability, committee on population " Washington DC: National Research Council, Committee on Population.

Commission, European. 1999. "Emission testing of engines to be installed in non – road mobile machinery, environment nuclear safety, civil protection.".

Eloka-Eboka, A.C., Igbum, O.G. and Inambao, F.L., 2014. Optimization and effects of process variables on the production and properties of methyl ester biodiesel. *Journal of Energy in Southern Africa,* 25(2): 39-47.

Eloka-Eboka, A.C. and Inambao, F.L., 2014. Hybridisation of feedstocks – a new approach in biodiesel development: A case of Moringa and Jatropha seed oils. *Energy Sources Part A* (Taylor and Francis) (Accepted and in Press).

Eloka-Eboka, A.C. and Inambao, F.L., 2014. Engine Performance and Emission Characterization of biodiesel fuels from *Moringa oleifera* and *Jatropha curcas* seeds oils and hybrids. *Journal of Energy in Southern Africa* (submitted).

Environmental Protection Agency (EPA) U.S.A. 2004. "Emission standard for non – road diesel engine." *diesel net*.

European Commission. 1999. "Emission testing of engines to be installed in non-road mobile machinery, environment nuclear safety, civil protection." Available: https://www.dieselnet.com/standards/us/nonroad.ph.

European Commission. 2003. "Directive 2003/44/ of the European Parliament and of the council of 16th June 2003 amending directive 94/25/EC on the approximation of the laws, regulations and administration provisions of the member stated relating to recreational craft." *Official Journal L214*: 18-35.

Frijters, P. J.M., and R. S. G. Baert. 2006. "Oxygenated fuels for clean heavy-duty engines." *International Journal of Vehicle Design* 41: 242-55.

Ghobadian, B., H. Rahimi, A.M. Nikbakht, G. Najafi, and T.F. Yusaf. 2009. "Diesel engine performance and exhaust emission analysis using waste cooking biodiesel fuel with an artificial neural network." *Renewable Energy* 34: 976-982.

Golovitchev, V. I., and J. Yang. 2009. "Construction of combustion models for rapeseed methyl ester bio-diesel fuel for internal combustion engine applications. *Biotechnology Advances* 27(5): 641-655.

Hansen, A.C., M. R. Gratton, and W. Yuan. 2006. "Diesel engine performance and NOx emission from oxygenated biofuels and blends with diesel fuel." *Transactions of the American Society of Agricultural and Biological Engineers*, 49: 589-595.

Hazar, H. 2009. "Effects of biodiesel on low heat loss diesel engine." *Renewable Energy* 34: 533-537.

Hermmerlein, N., V. Korte, H. Richter, and G. Schroder. 1991. "Performance, exhaust emissions and durability of modern diesel engines running on rapeseed oil." *SAE paper no. 910848*.

Heywood, J. B. 1976. *Internal Combustion Engine*. New York: McGraw-Hill series in mechanical engineering, 572-575.

Igbum, O.G., Eloka-Eboka, A.C. Ubwa, S.T. and Inambao, F.L., 2014. Evaluation of environmental impact and gaseous emissions of biodiesel fuels and blends of selected feed-stocks. *International Journal of Global Warming*, 6(1): 99-112.

Cornell. 2015. http://www.Law.cornell.edu./cfr/text/40.91. 10 March, 2015.

International Standards Organization (ISO). 1996. "ISO 8178 Reciprocating internal combustion engines-exhaust emission measurement."

Karabektas, M. 2009. "The effects of turbocharger on the performance and exhaust emission of a diesel engine fuelled with biodiesel." *Renewable Energy* 34: 989-993.

Lalas, S., and J. Tsaknis. 2002. "charactarization of moringa oleifera seed oil variety." *journal of food composition and analysis* no. 15:65-77.

Lin, B. F., J. H. Huang, and D. Y. Huang. 2009. "Experimental study of the effects of vegetable oil methyl ester on DI diesel engine performance characteristics and pollutant emissions." *Fuel* no. 88:1779–85.

Maina, P. 2014. "Investigation of fuel properties and engine analysis of Jatropha biodiesel of Kenyan origin." Journal of Energy in Southern Africa no. 25 (2):107-116.

McIlroy, A. 2006. *Basic Research Needs for Clean and Efficient Combustion of 21st Century Transportation Fuels.* Report of the Basic Energy Science Workshop on Clean and Efficient Combustion of 21st Century Transportation Fuels, Office of Science, U.S. Department of Energy.

Mubila, M. 2012. "Briefing notes for AfDB long term strategy." *African Development Bank Group*: 2-3.

Murillo, S., J.L. Miguez, J. Porteiro, E. Granada, and J.C. Moran. 2007. "Performance and exhaust emissions in the use of biodiesel in outboard diesel engines." *Fuel*, 86: 1765-1771..

Nettles-Anderson, S., D. B. Olsen, J. J. Jonson, and J- N. Enablers. 2014. "Performance of a direct injection IC Engine on SVO and biodiesel from multiple feed stocks." *Journal of Power and Engineering* 2(8): 1-13

Najt, P. M., and D. E. Foster. 1983. "Compression ignited homogeneous charge combustion." SAE paper 830264.

Noguchi, M., T. Tanaka, and Y. Takeuchi. 1979. "A study on gasoline engine combustion by observation of intermediate reactive products during combustion." SAE paper 790840

Ozgtinay, H., S. Colak, G. Zengin, O. Sari, H. Sarikanya, and L. Yuceer. 2007. "Performance and emission study of biodiesel from leather industry pre-fleshings." *Waste manage* no. 27:1897-901.

Ozsezen, A.N., M. Canakci, A. Turkcan, and C. Sayin. 2009. "Performance and combustion characteristics of a DI diesel engine fuelled with waste palm oil and canola oil methyl esters." *fuel* no. 88:629 – 36.

Palafox, J.O., J.M., D. de la Fuente, E.A.F. Coronel, J.C. Sacramento-Rivero, C. Rubio-Atoche, P.A. Escoffie, and Jose Antonio Rocha-Uribe. "Extraction and characterization of oil from Moringa oleifera using supercritical CO_2 and traditional solvents" *Facultad de Ingeniería Química, Universidad Autónoma de Yucatán*.

Pandey, R. K., A. Rehman, and R. M. Sarviya. 2011. "Impact of alternative fuel properties on fuel spray behavior and atomization " *Renewable and Sustainable Energy Reviews* 16 : 1762-1778.

Puhan, S., N. Vedaraman, G. Sankaranarayanan, and Bharat Ram BV. 2005. "Performance and emission study of Mahua oil (Madhuca indica oil) ethyl ester in a 4-stroke natural aspirated direct injection diesel engine." *Renewable Energy* 30: 1269-1278.

Qi, D.H., L.M. Geng, H. Chen, Y. Z. H. Bian, and X. C. H. Ren. 2009. "Combustion and performance evaluation of a diesel engine fueled with biodiesel produced from soybean crude oil." *Renewable Energy* 34: 2106-2113.

Roy, M.M., Alawi, and W Wang. 2013. "Effects of canola biodiesel on a DI diesel engine performance and emission." *International Journal of Mechanical and Mechatronic Engineering* 13(2):46-53 (IJMME-IJENS).

Raheman, H., P. C. Jena, and S. S. Jadav. 2013. "Performance of a diesel engine with blends of biodiesel (from a mixture of oils) and high speed diesel." *International Journal of Energy and Environmental Engineering* 4(6):2-9.

Santos, B. S., S. C. Capareda, and J A. Capunitan. 2013. "Engine performance and exhaust emissions of peanut oil Biodiesel." *Journal of Sustainable Bioenergy Systems* (3): 272-286.

Sayyar, S., Z. Z. Abidin, R. Yunus, and A. Muhammad. 2009. "Extraction of oil from Jatropha seeds – optimization and kinetics." *American Journal of Applied Sciences* 6(7): 1390-1395.

Salamanca, M., F. Mondragon, J. R. Agudelo, P. Benjumea, and A. Santamaría. 2012. "Variations in the chemical composition and morphology of soot induced by the unsaturation degree of biodiesel and a biodiesel blend." *Combustion Flame*. 159: 1100-1108.

Singh, R. K., and S. K. Padhi. 2009. "Characterization of Jatropha oil for the preparation of biodiesel." *Natural Product Radiance,* 8(2): 127-132.

Schönborn, A., N. Ladommatos, J. Williams, R. Allan, and J. Rogerson. 2009. "The influence of molecular structure of fatty acid monoalkyl esters on diesel combustion." *Combustion Flame* 156: 1396-1412.

Techquipment. 2003. "TD110 – TD115 small engine test bed and instrumentation." *TQ Education and Training Ltd.*

Tesfa, B., Gu, F., Mishra, R., and Ball. A., 2014. "Emission characteristics of a C.I. engine running with a range of biodiesel feed stocks." *Energies* 7(1): 334-350.

Ulusoy, Y., Y. C. Tekin, M. Etinkaya, and F. Kapaosmanoˇglu. 2004. "The engine tests of biodiesel from used frying oil." *Energy Source Part A* 26: 927-932.

Utlu, Z. and M. S. Kocak. 2008. "The effect of biodiesel fuel obtained from waste frying oil on direct injection diesel engine performance and exhaust emission." *Renewable Energy* 33: 1936-1941.

Van Gerpen, J. H., B. Shanks, and R. Pruszko. 2004. "Biodiesel analytical method." *Iowa State University. National Renewable Energy Laboratory* 42(5): 3041-3393.

Wu, F., J. Wang, W. Chen, and S. Shuai. 2009. "A study on emission performance of a diesel engine fueled with five typical methyl ester biodiesels." *Atmospheric Environment* 43: 1481-1485.

Xue, Jinlin, Tony E. Grift, and Alan C. Hassen. 2011. "Effect of biodiesel on engine performance and emissions." *Renewable and Sustainable Energy Review* 15: 1098-1116.

Yao, M., Z. Zheng, and H. Liu. 2009. "Progress and recent trends in homogeneous charge compression ignition (HCCI) engines." *Progress in Energy and Combustion Science* 35: 398-437.

CHAPTER 7

Paper 4: AN EVALUATION OF NEAT BIODIESEL/DIESEL PERFORMANCE, EMISSION OF NOx AND CO IN COMPRESSION IGNITION ENGINE

E. I. Onuh* and, Freddie L. Inambao.

Mechanical Discipline, School of Engineering, University of KwaZulu-Natal, Durban, South Africa.
Corresponding email:eionuh@yahoo.com
inambaof@ukzn.ac.za

Authors Biography

Onuh, E. I. is a lecturer with the Federal Polytechnic, Bauchi, North-Eastern Nigeria on study leave at Howard College, University of KwaZulu-Natal, Durban, South Africa for his PhD.

Prof. Freddie L. Inambao holds a Master of Science (M.Sc) and Ph.D in Mechanical Engineering with specialization in Thermodynamics and Internal Combustion Engines from Volgograd Polytechnic Institute, Russia. He has lectured in several universities in Southern Africa including the University of Zambia, University of Botswana, University of Durban-Westville (before the merger with the University of Natal) and currently is an associate professor in the Discipline of Mechanical Engineering of the University of KwaZulu-Natal, Howard College, Durban, South Africa. He has supervised many undergraduate and post-graduate students including Masters and PhDs in the same universities. He is an expert in Thermodynamics, Internal Combustion Engines, Renewable and Alternative Energy and Energy Management.

Abstract

Oxides of Nitrogen (NO_x) and Carbon (II) oxide (CO) emissions from engines running on pure biodiesel constitutes a major challenge in terms of its application as a fuel. Verifying their sources and production patterns is an essential first step to tackling the challenge. 100% biodiesel derived from moringa, jatropha and waste oil along with petroleum diesel were evaluated in a single cylinder diesel engine. It was observed that oxygen concentration and combustion temperature are the primary drivers of a kinetically determined process. NO_x emission trended with Zeldovich mechanism prediction and thus increases with increasing O_2 concentration and temperature. CO_2 dissociation at elevated combustion temperature in a

suppressed O_2 concentration regime governs CO production for normal diesel running at high load, but low temperature and high viscosity account for some of this effect in biodiesel runs. CO therefore increases with increasing temperature and decreasing O_2 concentrations for petroleum diesel but for biodiesel, the reverse is the case. Novel EGR (exhaust gas recirculation) and LTC (low temperature combustion) engines therefore hold the key to unlocking biodiesel potential and remediating some of the difficulties observed with petroleum diesel.

7.1 Introduction

In the face of a dwindling petroleum reserve, increasing demand and stricter regulation against unmitigated emissions, biodiesel has emerged as an energy source in the transport subsector with the potential to provide some measure of respite. Biodiesel, an alternative to diesel, is a free fatty acid methyl ester, derived from vegetable oil or animal fats. It is renewable, biodegradable and oxygenated. It has the potential to be universally accessible and has the capacity to promote inclusive growth in sub-Saharan Africa. Extensive experimental work conducted on biodiesel performance and emission in diesel engines has revealed mixed results. It has been commonly reported that the use of 100% biodiesel or its blend with petroleum diesel generally leads to a drop in brake thermal efficiency, an increase in fuel consumption and a reduction in indicated mean effective pressure. The reasons given for these changes have been biodiesel's lower heating value, higher viscosity and density (Xue et al., 2011). In term of emissions, the use of biodiesel or its blends has resulted in varying degree of reduction in carbon monoxide (CO), particulate matter (PM), total hydrocarbons (THC), aromatics and sulphur oxides (SO_2). Increases in NO_X, acetaldehyde and propionaldehyde along with reduction in formaldehyde were also reported (Shi et al., 2006).

Increasing NO_X emissions when biodiesel or its blends are used as fuel in diesel engine and the increasing emissions of CO at idle to low load has been a source of concern (Ashrafur Rahman et al., 2014). The former because of emission regulation, and the later because it is an indication of inefficient combustion. In investigating these challenges, it has been observed that fuel chemistry, engine configuration and test environment/condition are some of the factors

that govern those emissions. Computational work has advanced this knowledge appreciably. But for a high fidelity model to be developed, more experimental data from a diverse range of biodiesel sources, with different engine types and test cycle regimes, needs to be investigated to enhance the coupling of the predominant kinetic mechanisms that fully describe the emission trend. This is important, in view of the increasingly stringent regulations governing emission in various jurisdiction e.g. Japan and the U.S. have finalized regulation for the next five to ten years which require that heavy duty engine NO_X emission be pegged at 0.7 g/kWh (2009 start year) and 0.20 g/kWh (2010 start year) respectively, for light duty vehicles (Johnson, 2008) The US EPA has pegged NO_X emission at 9.3 g/kWh and CO at 8 g/kWh while in the EU, it is 9.2 g/kWh and 5.0 g/kWh - 6.5 g/kWh respectively (Johnson, 2008; European Commission, 2003; EPA, 2004; European Commission, 1999). A critical first step to understanding, and subsequently mitigating this emission and aligning them to standards is the development of models that accurately predict and account for emission patterns for a wide variety of biodiesel sources. Experimental data assists in pointing the direction for this theoretical work and providing means of validation as well (McIlroy, 2006).

Between 2004 and 2007 an estimated increase in edible oils production of 6.6 million tons was observed globally, 34% of this increase was attributed to biodiesel use. Approximately 7.8 million hectares were used to provide biodiesel feedstock in four major producing regions, namely, Argentina, Brazil, USA and EU (Sigar et al., 2009). Any progress in dismantling obstacles to the widespread use of biodiesel creates opportunities for sub-Sahara Africa to leverage its niche in biodiesel production. Africa's landmass, population, and economic challenges suggest that biodiesel derived from non-edible sources could potentially open up new sources of energy. In addition, biodiesel production could strengthen food security and enhances the building of a sustainable urban ecosystem, invariably leading to energy self-sufficiency. By 2030 Africa's population is projected to reach 1.5 billion with 748 million (representing 53.5% of this population) will live in urban centers (Mubila, 2012; Cohen, 2006). A close look at the population data suggests a strong shift in favor of younger demographics indicating heighten energy demand with accruing opportunity for economic growth. Moringa, jatropha and waste oil are some of biodiesel sources that represent these opportunities. This work involved the evaluation of biodiesel performance and emission compared to diesel with specific focus on the emission pattern of NO_X and CO in the test cycle.

7.2   Experimental Methods

7.2.1 Oxides of Nitrogen (NOx)

Production mechanisms in diesel engine are varied and depend on a number of factors. The mechanism includes; thermal NO mechanisms, intermediate N_2O mechanisms, NNH mechanisms and NO_2 mechanisms. The thermal NO mechanism is described by the extended Zeldovich mechanism which consist of three reactions.

$$N_2 + O \leftrightarrow NO + N \qquad\qquad + 75.1 \text{ kcal/mole} \qquad\qquad (1)$$

$$O_2 + N \leftrightarrow NO + O \qquad\qquad - 32.1 \text{ kcal/mole} \qquad\qquad (2)$$

$$OH + N \leftrightarrow NO + H \qquad\qquad - 48.7 \text{kcal/mole}$$
$$(3)$$

This mechanism dominates at temperatures greater than 1800 K in a fuel lean environment (Seitzman, 2012). It takes longer residence time (mostly post flame gases) and higher oxygen normally correlates to higher NO production rate. The extended Zeldovich mechanism was used to describe the NOx production and data which correlated with the mechanism suggested that NO production in diesel engine takes place in the burnt gas stage, and the important parameters that govern the rate are the gas temperature and the equivalent ratio (Air/fuel ratio) (Brakora and Reitz, 2010). It was further stated that fuel composition plays little part in the process, hence to reduce NO emission, the engine should be run rich or peak temperature should be reduced. The latter could be achieved by low compression ratio, exhaust gas recirculation or water injection. Using the extended Zeldovich mechanism, a correlation was established between NO production rate, Oxygen concentration and temperature.

$$\frac{d[NO]}{dt} = \frac{6 \times 10^{16}}{T^{1/2}} exp\left(\frac{-69090}{T}\right) [O_2]_e^{1/2} [N_2]_e \qquad\qquad (4)$$

The correlations showed the strong dependence of NO production rate on temperature in the exponential terms. High temperature and high oxygen concentration results in high NO formation rate. The intermediate N_2O mechanism converts N_2 to N_2O then NO. It also consist of three reactions (Seitzman, 2012):

$$N_2 + O \leftrightarrow N_2O \qquad\qquad - 40 \text{ Kcal/mole} \qquad\qquad (5)$$

$$H + N_2O \leftrightarrow NO + NH \qquad\qquad + 35 \text{ Kcal/mole} \qquad\qquad (6)$$

$$O + N_2O \leftrightarrow NO + NO \quad \text{- 36kcal/mole}$$

7)
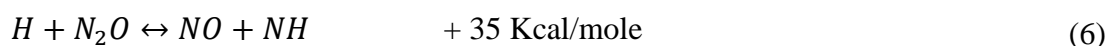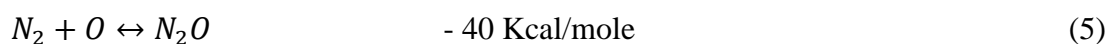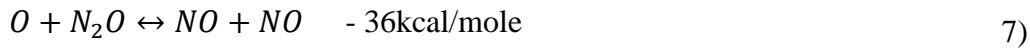
This mechanism requires a medium to high activation energy. It prevails at low temperature, fuel lean ($\emptyset<0.8$) system, high pressure. The NNH mechanism prevails in a Hydrogen rich environment and is most common with H_2 – air flames. It includes two reactions (Seitzman, 2012):

$$N_2 + H \leftrightarrow NNH \quad \text{- 6.5kcal/mole} \quad (8)$$
$$NH + O \leftrightarrow NO + NH \quad \text{- 11.3kcal/mole} \quad (9)$$
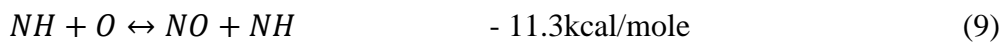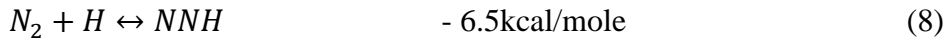
NH normally leads to NO. NNH mechanism is most common when the temperature exceeds 2200 K at stoichiometric to rich mix with low residence time system (mostly H_2 flame). The prompt mechanism can occur in any of the aforementioned mechanism from attack on N_2/O_2 via radicals containing only N, O, H nuclear. The mechanism sufficiently describes NO formation for wet air and hydrogen combustion. The general scheme is that CH_X (CH, CH_2 or CH_3) radical react with molecular nitrogen to form HCN (hydrogen cyanide) subsequent to which NO is formed through various intermediaries. The prompt mechanism thrives in a slightly fuel rich ($\emptyset < 1.2$), low pressure flame zone. The majority of work conducted on biodiesel has reported a substantial drop in carbon monoxide emission when biodiesel replaces diesel as a fuel in compression ignition engines (Karabektas, 2009; Utlu and Kocak, 2008; Ozgunay et al., 2007). This was attributed to the oxygenated nature and the higher cetane number of biodiesel. CO was also found to decrease with increasing load in biodiesel driven engines. The obvious explanation for this was that increasing combustion temperature led to a more complete combustion during the high load regime. Some works also reveal that CO emission was only lower in the intermediate load, but higher in idle load and peak load (Carraretto et al., 2004; Raheman, 2004).

It has been established that analysis based on chemical equilibrium alone does not explain most emission patterns observed with diesel engines. If that had been the case, CO emissions from biodiesel run engines would have been negligible at all loading conditions. It has been pointed out that had the assumption that the major energy producing reaction involving $C - O - H$ systems been in thermodynamic equilibrium near peak cylinder temperature, the level of CO emission would have been negligible (Keck, 1970). It was suggested that boundary

aerodynamic, gas dissociation and recombination all controlled by thermal gradient and cooling speed post flame plays significant parts in CO emission levels. A rate controlled partial equilibrium method was developed to tackle these challenges. The conclusion drawn from these studies is that CO emission from both biodiesel and diesel driven engines extend beyond fuel chemistry and that experimental data for a wide range of biodiesel sources and engine types are needed to test the validity of the various models being proposed.

7.2.2   Materials and Methods

7.2.2.1   Test Sample Preparation

Seeds of moringa and jatropha were collected and oil extraction was achieved via two methods, soaking and soxhlet. Three solvents were employed to determine optimal yield. The solvents were petroleum being either normal hexane (n-hexane) and distilled gasoline (which was used as a wild card). For every 150 g of pulverized, oven dried sample, 400 ml of solvent was used for soaking and 600 ml for soxhlet extraction. The waste oil (yellow grease) biodiesel was processed from used grand cereal oil originally extracted from soybeans. A series of physicochemical properties of the oil where determined. They include: density, viscosity, pour and cloud point, iodine and value, refractive index, flash point, free fatty acid (FFA) value, saponification and peroxide. Value details of the oil and resulting biodiesel properties are given in Table 7.1.

Table 7. 1: Sample properties

Table 1   Sample properties

a. Experimentally determine physio-chemical properties of extracted oil			
Sno.	Properties	Moringa oil	Jatropha oil
1	Viscosity (cS) at 30°C	53.9	41.45
2	Density (Kg/m³)	912.0	890.62
3	Iodine value	64.84	108.40
4	Refractive index	1.458	1.455
5	Flash point (°C)	215	195
6	Free fatty acid (%)	9.96	2.48
7	Saponification value (mgKOH/gm)	185.15	196.44
8	Peroxide value (mEg/kg)	1.84	3.21
9	Pour point (°C)	8	5
10	Cloud point (°C)	12	7

b. Fuel properties of biodiesel			
Properties	Moringa biodiesel	Jatropha biodiesel	Waste oil biodiesel	ASTM D6751-2 (Singh and Padhi, 2009)
Density (Kg/m³) at 30°C	892.9	880.52	897.4	875–900
Viscosity(mm²/s) at 30°C	4.65	4.56	4.27	1.9–6
Heating value (KJ/Kg)	40.05	39.45	39.4	(Diesel – 45.84)

7.2.2.2   Test Engine Setup

The test rig consisted of a single cylinder, four stroke, and air cooled TD111 Tecquipment direct injection diesel engine, a hydraulic dynamometer (TD111) accessorized with various engine measuring devices. The system schematic set up is shown in Figure 7.1 and equipment details in Table 7.4. A hydraulic dynamometer TD 115 also from Tecquipment with water flow 6 m - 12 m head was used to measure the torque which is displayed on the instrument display panel TD114. TD114 also displays the engine speed, exhaust temperature, air flow and the fuel flow pipette which measures the fuel flow rate. Measurement input signals are received from the test bed via tachometer connector, thermocouple terminal, torque transducers and manometer tapping from the air bag. The engine speed is measured electronically by a pulse counting system. An optical head mounted on the dynamometer chassis contain an infrared transmitter and receiver. A rotating disc with radial slot is situated between the optical sources and the sensor. As the engine and slotted disc rotates the beam is interrupted. Engine torque is measured by the TD115 hydraulic dynamometer and transmitted to a torque meter located on the TD114 instrument unit. A linear calibration of the torque meter is checked intermittently to confirm accuracy of the data set via an eight step process on the equipment manual (Techquipment, 2003). The exhaust gas temperature is measured with a chrome/alumina thermocouple located in a 1/8"BSP union brazed into the exhaust lock of the engine. Color coded leads from the thermocouple are connected to terminals underneath the TD114 instrumentation unit.

Figure 1   Test rig set-up (see online version for colours)
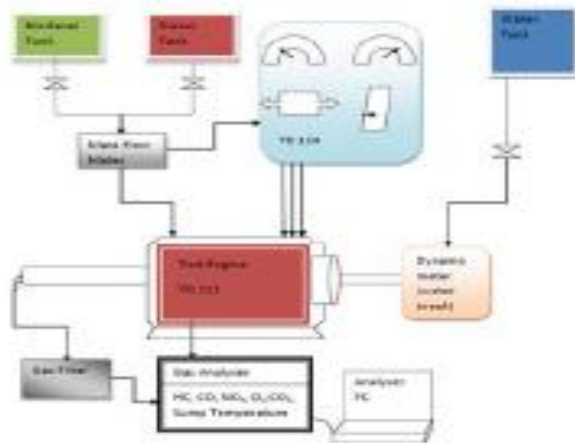
Table 2   Technical specifications of test rig equipment

Device	Description	Detail
Engine	Model	TQ:TD 111
	Maximum power (Kw)	3.5
	Type	Naturally aspirated, four strokes
	Rated speed(rpm)	3900
	Number of cylinder	1
	Compression ratio	17.5:1
	Combustion	Direct injection

Figure 7. 1: System schematics

Table 7. 2: Technical specifications

Table 2   Technical specifications of test rig equipment (continued)

Device	Description	Detail
Hydraulic dynamometer	Model	TQ:TD115
	Type	Hydraulic
	Water pressure	6–12 m head of water (60 KPa)
	Range	0–14 Nm
	Water flow rate	4 lt/min
Exhaust gas analyser	Model	SV-5Q
HC	Range	1–10,000; 10^{-6} (ppm) vol.
	Resolution	1 ppm
CO	Range	1–1,000; 10^{-2} (%) vol.
	Resolution	0.01%
CO_2	Range	0–20; 10^{-2} (%) vol.
	Resolution	0.01% vol.
O_2	Range	0–25; 10^{-2} (%) vol.
	Resolution	0.01% vol.
NO_x	Range	0–50,000; 10^{-6} (ppm) vol.
	Resolution	1 ppm

7.2.2.3   Test Procedure

The test engine is a 3.5 kw rated, direct injection (DI), single cylinder diesel engine. Selected test speeds were 1800 rpm, 2500 rpm and 3600 rpm. Each test cycle at selected torque consisted of running the engine for 1 minute at idle speed and 9 minutes at selected load in

accordance with test cycle G3 of ISO 8178-4 (European Commission, 1999). The engine rated power was taken as 100% load. The test cycle were repeated for 20%, 40%, 60% and 80% load. This test cycle procedure was followed for petroleum diesel, jatropha, moringa and waste oil biodiesel. The SV-5Q exhaust gas analyzer, in accordance with ND112 (Non-Dispersive infra-Red) method utilized via micro computer analysis was used to measure the thickness of HC, CO and CO_2 in the exhaust gas and to inspect the density of NO_X and O_2 via electrochemical sensors. The excess air coefficient, λ, was also computed automatically by the analyzer. The sampling probe was installed in the exhaust line where gas could be drawn through a filter into the analyzer. Thermometer tube extended from the back of the filter to the sample gas vent of the analyzer. Leak checks to ensure there was no leakage were conducted subsequently; auto-zeroing procedures were initiated to prepare the analyzer for actual measurement. HC and NO_X are measured in ppm while CO, CO_2 and O_2 are measured in percentages. The filter packing was replaced at the end of every test cycle and the weight difference between used and unused packing noted to compute average PM emissions per test cycle. A weighting device with 1 micrograms resolution was used to weigh the filter pack. Given the standard measure stipulated by ISO 8178-4, it was necessary to convert the emission measured in percentages (%) and parts per million (ppm) measurement into g/kWh using the air and fuel flow method (Cornell, 2015). Details of the correlations are given:

$$W_{NOx} = \left(G_{air} + G_{fuel}\right) \times \frac{M_{NO_2}}{M_{exh}} \times WNO_x \times K_H \times \frac{1}{10^6} \tag{10}$$

$$W_{HC} = \left(G_{air} + G_{fuel}\right) \times \frac{M_{HCexh}}{M_{exh}} \times WHC \times \frac{1}{10^6} \tag{11}$$

$$W_{CO} = \left(G_{air} + G_{fuel}\right) \times \frac{M_{CO}}{M_{exh}} \times WCO \times \frac{1}{10^6} \tag{12}$$

Where

$W_{NOx}, W_{HCexh}, W_{CO}$: *mass flow-rates of NO_x, HC and CO in exhaust (g/hr)*

G_{air}: *Intake of air mass flow-rate in dry basis (g/hr)*

G_{fuel}: *Fuel mass flow-rate (g/hr)*

M_{exh}: *Molecular weight of total exhaust given by*

$$M_{exh} = \frac{M_{HCexh} \times WHC}{10^6} + \frac{28.01 \times WCO}{10^2} + \frac{44.1 \times WCO_2}{10^2} + \frac{46.01 \times WNO_x}{10^6}$$
$$+ \frac{2.016 \times WH_2}{10^2} + 18.01(1 - K) + \frac{28.01}{10^2} \tag{13}$$

$$M_{HCexh} = 12.01 + 1.008a \tag{14}$$

A	*Hydrocarbon/carbon atomic ratio of the fuel*
WHC	*HC volume concentration in exhaust ppm, wet*
WCO	*CO percent concentration in exhaust, wet*
DCO	*CO percentage concentration in exhaust, dry.*
WCO$_2$	*CO$_2$ percent concentration in the exhaust, dry.*
WNO$_x$	*NO$_x$ volume concentration in exhaust in ppm, wet.*
WH$_2$	*H$_2$ percent concentration in exhaust, wet.*
K	*Correction factor to be used when converting dry measurement to a wet basis*

$$\therefore Wet\ concentration = dry\ concentration \times K \tag{15}$$

$$K = \frac{1}{1 + 0.005\,(DCO + DCO_2)a - 0.01 \times DH_2} \tag{16}$$

$$DH_2 = \frac{0.5a \times DCO \times (DCO + DCO_2)}{DCO + 3DCO_2} \tag{17}$$

W_{CO}	mass rate of CO in exhaust (g/hr)
M_{CO}	Molecular weight of CO (28.01)
WNO	x mass rate of NO$_x$ in exhaust (g/hr)
M_{NO2}	Molecules weight of NO$_2$ (46.01)
K_H	Factor for correcting the effects of humidity in NO$_2$ formation for four stroke gasoline engines and it is given by:

$$K_H = \frac{1}{1 - 0.0329 \times (H - 10.71)} \tag{18}$$

H - Specific humidity of intake air in grams of moisture per kilogram of dry air.

For individual gas component, the reported emission in g/kWh is computed in brake specific terms (BSY$_{wm}$) as:

$$BSY_{wm} = \frac{\sum(W_i + f_i)}{\sum(P_i + f_i)} \tag{19}$$

Y_{wm}	Weighted mass emission level (HC, CO NO$_x$ etc) for a test (g/kWh)
W_i	Average mass flow rate of emission from the test engine during mode i (g/hr)
f_i	Weighting factors for each mode according to test cycle recommendation
P_i	Average power measured during mode i (kw) calculated according to test cycle.

7.2.2.4   Test Environment

The test location was on latitude 10° 18' 57" N and longitude 09º 50' 39" E at an elevation of 2,021 ft (616 m). The prevailing ambient temperature at the time of the test ranged between 30 °C - 33° C and the relative humidity between 71 - 75%. Recorded atmospheric pressure was 92 kPa, air density 1.208 kg/m3 and absolute humidity, 0.022 kg/m^3 from these data, the specific humidity as well as k_H were computed using an Excel spreadsheet.

7.3   Results and Discussion

7.3.1   Engine Performance

At the test speed of 1800 rpm, 2500 rpm and 3500 rpm corresponding to 45%, 65% and 90% rated speed respectively, the biodiesels experienced varying degrees of torque losses in comparison to the petroleum diesel. The losses were observed to increase with decreasing speed. On average, the loss ranged between 6% - 9%. This loss of power when biodiesel substituted petroleum diesel is consistent with results obtained in previous studies (Utlu and Kocak, 2008; Ozgunay et al., 2007). The brake thermal efficiency (BTE) verses load relationship for the sample is shown in Figure 7.2. The difference between petroleum diesel BTE and the biodiesel BTE ranges between 2% - 5% at peak load with instances of some biodiesels (JA100) performing better than diesel at idle load by a margin of 4%.

The BTE for MO100 gave consistently lower values in comparison to other samples for the entire load spectrum. BTE as a measure of how efficient the heat release rate and conversion takes place in the engine, depends on the heating value, transport properties, combustion efficiency and ignition properties of the fuel samples. Petroleum diesel has a higher heating value than biodiesels, its density and viscosity is lower, hence it has a better transport property. Biodiesels on the other hand, because of the oxygenated nature of their molecules and higher cetane values, have better combustion efficiency and ignition properties. Amongst the biodiesel samples, JA100 and WO100 have higher proportions of saturated fatty acid methyl esters (FAMEs), as a result, their cetane values and ignition properties are higher than those of MO100. At idle speed, cetane value, ignition properties and combustion efficiencies play key roles in BTE value. These factors are responsible for the performance of JA100 and WO100 at idle speed. As the engine picks up speed and increases its load, a more steady combustion phase is reached where the advantage of higher heating value and transport properties begin to

reflect on the BTE data for petroleum diesel. The high proportion of unsaturated FAMEs in MO100 makes it less reactive, leading to a consistently low BTE. These observations are consistent with earlier findings (Lin et al., 2009; Ghobadian et al., 2009; Qi et al., 2009).
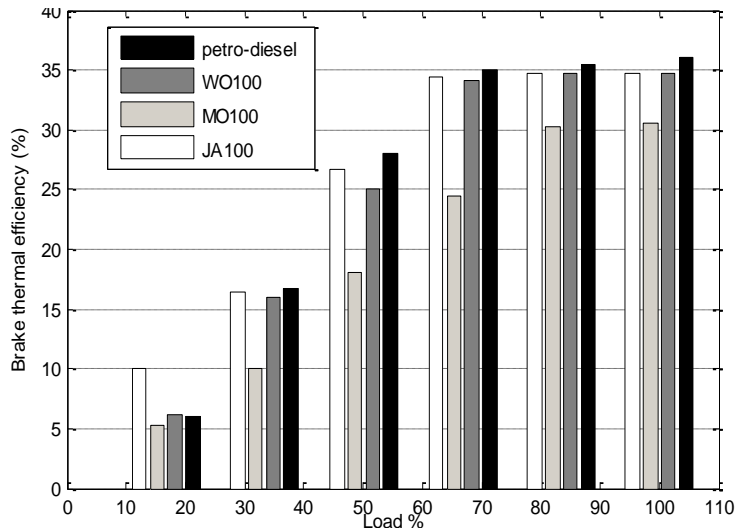
Figure 7. 2: BTE vs load

The brake specific fuel consumption (BSFC) data shows a decreasing fuel consumption as engine load increases (see Figure 7.3). The degree of reduction was between 81% - 72% with WO100 having the largest reduction and petroleum diesel the least. The average BSFC across the load spectrum for WO100, petroleum diesel, MO100 and JA100 were 300 g/kWh, 250 g/kWh, 182 g/kWh and 180 g/kWh respectively. Low average BSFC and fluctuation have significantly positive impact on the running and maintenance cost of engines. Where BTE differences are marginal, lower BSFC are always preferred. From these results, it is clear that the engine scale and JA100 ignition properties had the combined effect of high BTE at low BSFC. It is generally expected that given the lower heating value for biodiesel, BSFC for biodiesel should be higher than that of petroleum diesel. This has been widely reported by some authors (Ozsezen et al.. 2009; Karabektas, 2009; Choi and Oh, 2006). More specifically, Armas et al. (2010) observed that BSFC of B100 biodiesel which had LHV 12.5% lower than diesel increased approximately 12% on a 2.5 L DI and TU, common rail diesel engine operated at 2400 rpm and 64 Nm. Lin et al. (2009) observed a similar trend for a water cooled, four strokes DI engine. A point to note is that most of these engines are large units either TU with multiple cylinders and higher unit efficiencies. But it is also not uncommon to find situations where BSFC for biodiesel is lower than that of diesel (Ozgunay et al., 2007; Reyes and

Sepulveda, 2006; Ulusoy et al., 2004; Song and Zhang, 2008). Some authors reported no significant difference (Dorado et al., 2003; Sahoo et al., 2007). This shows that beyond fuel chemistry, the engine type, technology and operating conditions plays some role in the determination of performance where difference in fuel composition is marginal. Exhaust gas temperature (EGT) plot against the load is shown in Figure 7.4. The EGT increases with increasing load. Petroleum diesel showed a slightly higher EGT output in all the loading profile regimes. This is clearly attributed to it having higher heating value in comparative terms. The difference between it and MO100 being slightly less than those of WO100 and JA100 apparently because only MO100 exceeded petroleum diesel in BSFC trend. This is an indication that the mechanism of heat release rate in a well primed engine operating at optimal load condition greatly depends on heat content and fuel flow rate.
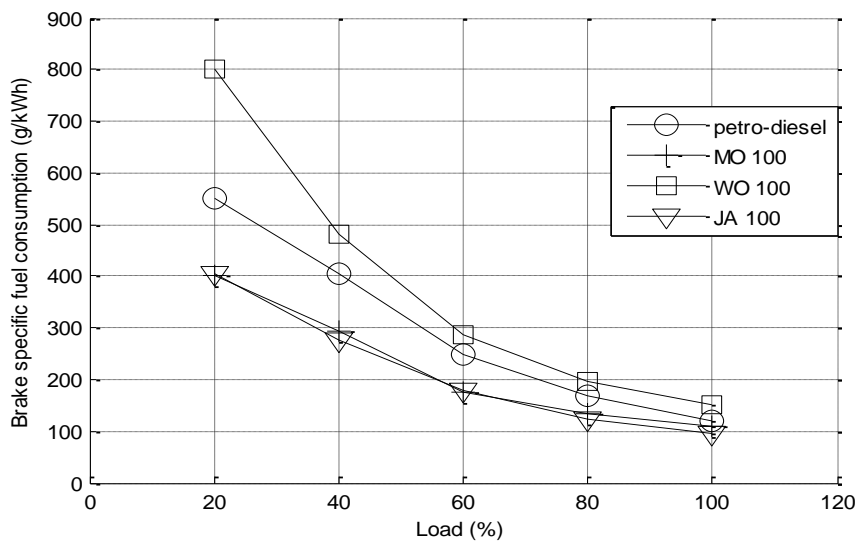
Figure 7. 3: BSFC vs load
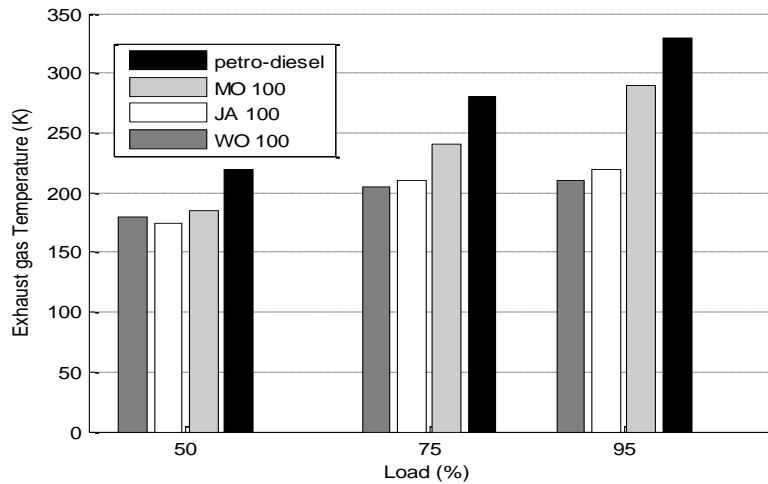
Figure 7. 4: EGT profile

7.3.2   Oxide of Nitrogen (NO$_x$) Emission

Figure 7.5 shows the emission trend (in ppm) of NO$_x$ against load for the biodiesels and petroleum diesel. The result is mixed as there were no marked difference between the biodiesels and petroleum diesel. But a plot of BSNO$_x$ against load showed a NO$_x$ emission trend for petroleum diesel exceeding those of the biodiesels in Figure 6.6. This trend was observed with a high margin at idle to low load but the margin reduced progressively as the loading profile approaches its peak value. The underlying fact gleaned from previous work and information observed in this work point is the fact that biodiesel NO$_x$ emission pattern is precisely governed by the process described by the Zeldvich mechanism. Figure 6.7 makes this fact clear; it shows data of maximum exhaust gas temperature, air/fuel ratio in the NO$_X$ emission in ppm for the biodiesels and petroleum diesel. A strong correlation is observed between EGT and air/fuel ratio leading to high NO$_X$ emissions. It also showed that high oxygen concentration is important for this process.
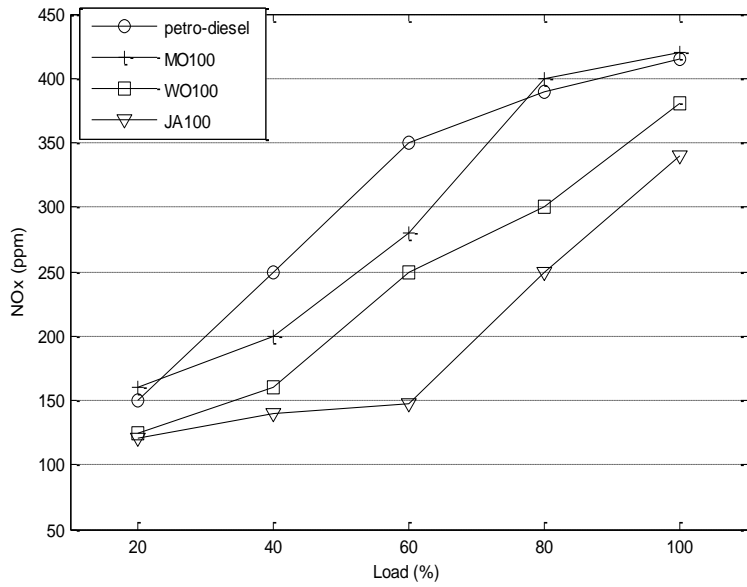
Figure 7. 5 : NOX (ppm) emission vs load
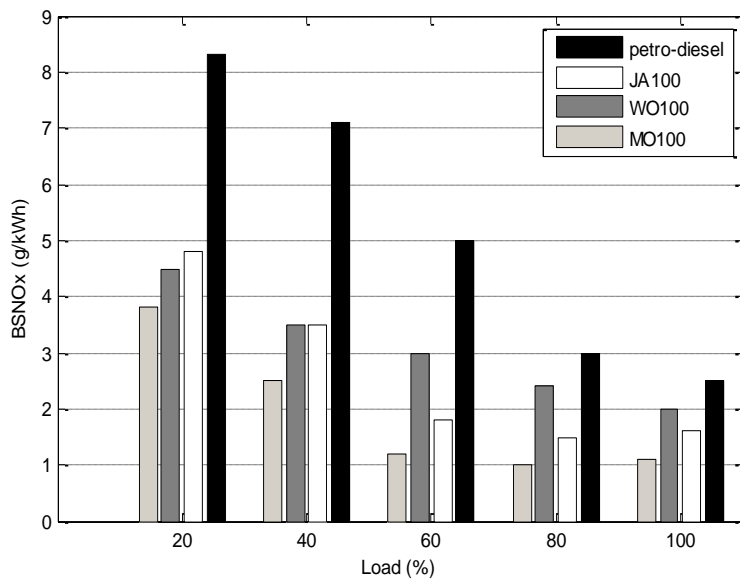
Figure 7. 6: Brake specific NOX vs load
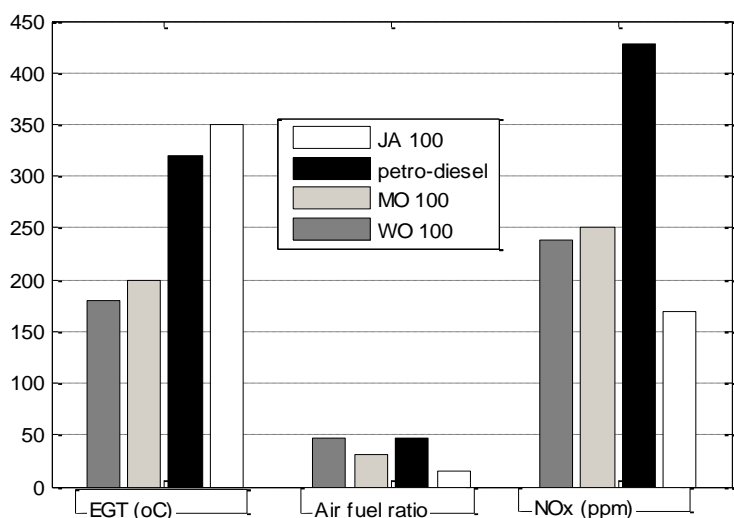
Figure 7. 7: NOX trend against air/fuel ratio and EGT

High temperature is the main trigger for the process. The reason for this is fairly obvious, the first reaction in the Zeldovich mechanism requires high activation energy to break the triple bond of N_2 gas for the mechanism to commence, inferring that even in the presence of large oxygen molecules, if there is not sufficient energy (high combustion temperature which correlates to high EGT), high NO_X emission will not manifest even for biodiesel, as seen in this work. In Figure 7.7, JA100's highest exhaust gas temperature at 350°C was not sufficient to trigger the highest NO_X because its excess air was the least at 12.5%. Petroleum diesel on the other hand satisfied the necessary condition of high temperature (325°C) as well as the sufficient condition of high excess air (49%). This fact has been established in a validated numerical work to compute NO_x emission using the Zeldovich mechanism (Liviu-Constantin and Daniela-Elena). The study concluded, amongst other things, that nitric oxide formation is determine by only five chemical species (O, H, OH, N and O_2) and not exclusively by the primary fuel chemistry, that the formation process of NO_X starts by the thermal decomposition of the stable triple bond of N_2 at a considerably high temperature and as a result, a partial equilibrium of the first two reactions can be assumed. Based on these assumptions, their work produced a much stronger correlation with experimental data than those predicted by wave 5 code produced by Ricardo. It is worth mentioning that owing to the water tolerant nature of the biodiesel used in this study which allow for a water content of between 2% - 4%, the combustion temperature was tamed below (for the most part) the NO_X formation threshold of 1650 K, making it possible to achieve lower BSNO$_X$. All the biodiesel fuel samples were able to meet both the EPA and EU BSNO$_X$ emission caps of 9.3 g/kWh and 9.2 g/kWh respectively at all loading condition (EPA, 2004; European Commission, 2003).

7.3.3 Carbon Monoxide (CO) Emission

Carbon (II) oxide emissions in percentages across the load profile are shown in Figure 7.8. CO emissions in JA100 were too small to be observed. The plot showed a slightly tilted bathtub curve for all the fuel samples where idle load (corresponding to low temperature) gave higher CO emission with petroleum diesel recording a 0.035% CO emission (5.7% and 28.5% higher than MO100 and WO100 samples respectively). This emission reduced to 0.02% at 80% load (with a slightly lower marginal difference between it and the rest of the samples) and recorded a small increase at peak load. A different picture emerges when the emission is computed in brake specific format as shown in Figure 7.9. BSCO plotted against load revealed a rapid decline from a high of 120 g/kWh at idle load to 7 g/kWh at peak load for petroleum diesel. The trends in MO100 and WO100 showed similar decline, but with lower values than petroleum diesel. At all loading conditions, CO emission for petroleum diesel exceeded those of the biodiesel samples. It is normal to see a reduction in CO emission when biodiesel replaces petroleum diesel as fuel in a diesel engine (Aydin, 2010; Hazar, 2009; Ozsezen et al., 2009).
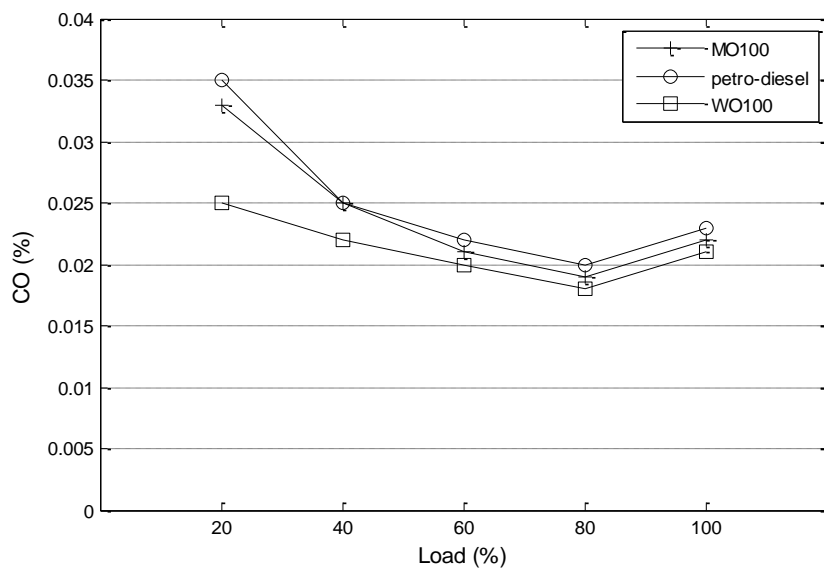
Figure 7. 8: CO emission vs load
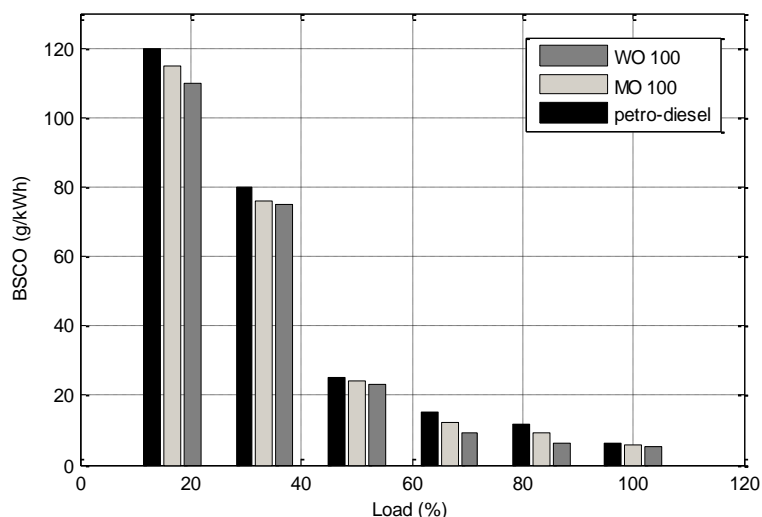
Figure 7. 9: BSCO vs load

CO emission when measured in specific terms, gives high value at low to medium load conditions. From the data obtained, the samples failed the EPA and EC emission caps as shown (European Commission, 2003, EPA, 2004). Biodiesel emits less CO at medium to elevated engine operating conditions primarily because of its oxygenated nature, higher cetane value and the resulting higher combustion efficiency of the fuel. Existing literature supports this conclusions (Ramadhas et al., 2005; Tsolakisa et al., 2007; Nabi et al., 2009). A more significant observation made in this work is the effect of temperature on CO emission for biodiesel on the one hand and diesel on the other hand. Figure 6.10 shows that at low temperature CO emission of biodiesel exceeds those of petroleum diesel but as the temperature increases, the reverse is the case. CO emission increases with increasing temperature for petroleum diesel and is reduced for biodiesel. For biodiesel, this trend is as a result of viscosity of the fuel. At low temperature, high viscosity impedes fuel spray droplet formation, atomization, air/fuel mixing, delays evaporation and ignition, thus, leading to incomplete combustion. But as the temperature increases, these processes improve and a more complete combustion scenario ensues leading to a reduction in CO emission.
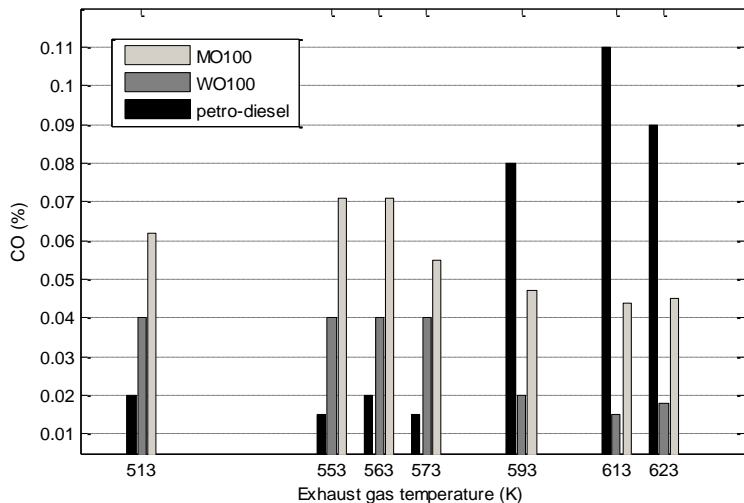
Figure 7. 10: CO emission vs EGT

In petroleum diesel, CO emission is observed to increase with increasing temperature because beyond peak temperature, post flame, the concentration of CO determined by equilibrium is different from those of the rate controlled CO concentration. The frozen CO concentration caused by gas dissociation does not recombine fast enough to bring the level to equilibrium state (Keck, 1970). Hence, the higher the temperature, the higher the frozen CO concentration. This process is tamed in biodiesel because the equilibrium concentration of CO in biodiesel combustion, post flame, is lower than that of petroleum diesel combustion owing to the oxygenated nature of the former.

7.3.4   Relation Between Other Emissions and Exhaust Gas Temperature

Unburnt hydrocarbons (UHC) and particulate matter (PM) constitute some of the emissions from diesel engines that poses danger to the environment. In this study, UHC for all the biodiesel test samples were lower than those of normal diesel at all loading conditions. The only exception was MO100 between the load ranges of 20% - 40% where an UHC emission of 0.04 g/kWh - 0.03 g/kWh, exceeded those of petroleum diesel by about 25%. These low loads coincide with low combustion temperature. This confirms the fact that incomplete combustion always produces CO, UHC and PM simultaneously in biodiesels. MO100's low reactivity because of its higher proportion of unsaturated FAME results in incomplete combustion. However, generally, the results showed a reduction of UHC for the biodiesel samples of between 50% - 80% when compared with petroleum diesel. The peak values (which coincide with low temperature) for the biodiesel were between 0.015 g/kWh -0.025 g/kWh, but for

petroleum diesel was 0.03 g/kWh. The lowest point for the biodiesel was between 0.005 g/kWh - 0.01 g/kWh, coinciding with high temperature. But for petroleum diesel a combination of high temperature and richer fuel/air mix led only to a marginal drop in UHC to a low of 0.02g/kWh. Hence for biodiesel, UHC decreases with increasing temperature but for normal diesel, it was observed that increasing temperature coincides with increasing fuel/air ratio (rich mix which increases the tendency for incomplete combustion because of thermal as well as charge stratification). Therefore, UHC emission reduction is only marginal. This is consistent with findings from other studies (Murillo et al., 2007).

7.4   Conclusion

The performance, NO_X and CO emission for 100% biodiesel derived from moringa, jatropha and waste restaurant oil were evaluated in comparison to those of petroleum diesel. The following conclusions are drawn:

[1]   Where high ambient temperature exists, flow properties of biodiesel (especially biodiesels with higher proportion of saturated FAME like JA100) produce higher combustion efficiency at low combustion temperature and results in a BTE that is slightly better than that of petroleum diesel at idle load and a close value at peak load.

[2]   Petroleum diesel's advantage of low BSFC at high to peak load as result of its higher heating value and better transport properties was well matched with biodiesel's better combustion efficiency, higher cetane value, and good reactivity (because of biodiesel's oxygenated nature) resulting in lower average BSFC across load spectrum for the biodiesels. This is an important advantage for biodiesel in a multi-scale load condition such as vehicle transportation provided the application is in a warm ambient condition.

[3]   Oxides of nitrogen (NO_X) emission are primarily temperature dependant regardless of fuel type. The susceptibility of biodiesel to emit high NO_X at high temperature (owing to their oxygenated nature) can be curtailed through low temperature combustion by utilizing the water tolerant nature of biodiesel, as seen in this study, to keep combustion temperature under control.

[4]   High CO emission in biodiesel at idle load is associated with low temperature. At low temperature, the flow properties of the biodiesel deteriorate. CO emission strongly correlates with UHC and PM emissions. It was also a good indicator of

combustion efficiency. It could therefore be concluded that mitigation strategies for CO emissions could potentially fix several challenges associated with biodiesel. For petroleum diesel, high CO emission at high to peak load condition is associated with thermal as well as charge stratification. Therefore, engine retrofitting holds the key to its remediation.

[5] The use of distilled gasoline as a solvent for biodiesel oil extraction holds significant potential and should be further explored.

References

AL-WIDYAN, M. I., TASHTOUSIR, G. & ABU-QUDAIS, M. 2002. Utilization of ethyl ester of waste vegetable oils as fuel in diesel engines. *Fuel process Technology,* 79: 91-103.

ARMAS, O., YEHLIU, K. & BOEHMAN, A. L. 2010. Effect of alternative fuels on exhaust emissions during diesel engine operation with matched combustion phasing. *Fuel,* 89: 438-456.

ASHRAFUR RAHMAN, S. M., MASJUKI, H. H., KALAM, M. A., ABEDIN, M. J., SANJID, A. & IMTENAN, S. 2014. Effect of idling on fuel consumption and emissions of a diesel engine fueled by Jatropha biodiesel blends. *Journal of Cleaner Production,* 69: 1-8.

AYDIN H, B. H. 2010. Performance and emission analysis of cottonseed oil methyl ester in a diesel engine. *Renewable Energy,* 35: 588-592.

BANAPURMATH, N. R., TEWARI, P. G. & HOSMATH, R. S. 2009. Effect of biodiesel derived from Honge oil and its blends with diesel when directly injected at different injection pressures and injection timings in single-cylinder water-cooled compression ignition engine. *Procedings of the Institution of Mechanical Engineers, Part A: Journal of Power and Energy,* 223: 31-40.

BRAKORA, J. L. & REITZ, R. D. 2010. Investigation of NOx predictions from biodiesel-fueled HCCI engine simulations using a reduced kinetic mechanism. *SAE paper no.,* 01-0577.

ARRARETTO, C., MACOR, A., MIRANDOLA, A., STOPPATO, A. & TONON, S. 2004. Biodiesel as alternative fuel: experimental analysis and energetic evaluations. *Energy,* 29: 2195-2211.

CHOI, S. H. & OH, Y. 2006. The emission effects by the use of biodiesel fuel. *Intertional Journal of Modern Physics B,* 20**,** 4481-4486.

COHEN, B. 2006. Urbanization in developing countries: current trends, future projections, and key challenges for sustainability, committee on population. Washington DC: National Research Council, Committee on Population,

CORNELL 2015. http://www.Law.cornell.edu./cfr/text/40.91 10 March, 2015.

DORADO, M. P., BALLESTEROS, E., ARNAL, J. M., GOMEZ, J. & LOPEZ, F. J. 2003. Exhaust emissions form a diesel engine fueled with transesterified waste olive oil. *Fuel,* 82, 1311-135.

EPA, U. S. 2004. Emission standards for non-road diesel engines [Online]. Available: https://www.dieselnet.com/standards/us/nonroad.php,

EUROPEAN COMMISSION. 1999. Emission testing of engines to be installed in non – road mobile machinery, environment nuclear safety, civil protection.

EUROPEAN COMMISSION. 2003. Directive 2003/44/ of the European Parliament and of the council of 16th June 2003 amending directive 94/25/EC on the approximation of the laws, regulations and administration provisions of the member stated relating to recreational craft. *Official Journal L214*: 18-35.

GHOBADIAN, B., RAHIMI, H., NIKBAKHT, A. M., NAJAFI, G. & YUSAF, T. F. 2009. Diesel engine performance and exhaust emission analysis using waste cooking biodiesel fuel with an artificial neural network. *Renewable Energy,* 34: 976-982.

HAZAR, H. 2009. Effects of biodiesel on low heat loss diesel engine. *Renewable Energy,* 34: 533-537.

HEYWOOD, J. B. 1976. *Internal combustion engine fundamentals*. New York: McGraw-Hill.

JOHNSON, T. 2008. Diesel engine emissions and their control: an overview. *Platinum Metals Review,* 52(1): 23-37.

KALE, S. V. Performance characteristics of DI-CI engine using pongomia biodiesel-diesel blend as fuel. *International Journal of Advance Engineering Research and Studies.*

KARABEKTAS, M. 2009. The effects of turbocharger on the performance and exhaust emission of a diesel engine fuelled with biodiesel. *Renewable Energy,* 34: 989-993.

KECK, J. C. 1970. Mechanism of air pollutant formation in internal combustion engine. *M.I.T.* Available: http://james-keck-memorial-collection.unibs.it/JCKeck-papers/Keck-AcadSciTorino-1970.pdf

KRAHL, J., MUNACK, A., SCHRODER, O., STEIN, H. & BUNGER, J. 2003. Influence of biodiesel and different designed diesel fuels on the exhaust gas emissions and health effects. *SAE paper 2003,* 01-3199.

LAPUERTA, M., HERREROS, J. M., LYONS, L. L., GARCIA-CONTRERAS, R. & BRICE, Y. 2008. Effect of the alcohol type used in the production of waste cooking oil biodiesel on diesel performance and emissions. *Fuel,* 87: 3161-3169.

LIN, B. F., HUANG, J. H. & HUANG, D. Y. 2009. Experimental study of the effects of vegetable oil methyl ester on DI diesel engine performance characteristics and pollutant emissions. *Fuel,* 88, 1779-1785.

LIVIU-CONSTANTIN, S. & DANIELA-ELENA, M. Simplified mechanism used to estimate the NO_X emission of diesel engine. *Proceedings of the 2nd International Conference on Manufacturing Engineering, Quality and Production Systems,* 978-960-474-220-2.

MCILROY, A. 2006. Basic research needs for clean and efficient combustion of 21st century transportation fuels. Report of the Basic Energy Science Workshop on Clean and Efficient Combustion of 21st Century Transportation Fuels, Office of Science, U.S. Department of Energy.

MUBILA, M. 2012. Briefing notes for AfDB long Term strategy. *African Development Bank Group,* 2-3.

MURILLO, S., MIGUEZ, J. L., PORTEIRO, J., GRANADA, E. & MORAN, J. C. 2007. Performance and exhaust emissions in the use of biodiesel in outboard diesel engines. *Fuel,* 86: 1765-1771.

NABI, M. N., NAJMUL HOQUE, S. M. & AKHTER, M. S. 2009. Karanja (Pongamia Pinnata) biodiesel production in Bangladesh, characterization of karanja biodiesel and its effect on diesel emissions. *Fuel Process Technology,* 90: 1080-1086.

OZGUNAY, H., C¸ OLAK, S., ZENGIN, G., SARI, O., SARIKAHYA, H. & YUCEER, L. 2007. Performance and emission study of biodiesel from leather industry pre-fleshings. *Waste Management,* 27: 1897-1901.

OZSEZEN, A. N., CANAKCI, M., TURKCAN, A. & SAYIN, C. 2009. Performance and combustion characteristics of a DI diesel engine fuelled with waste palm oil and canola oil methyl esters. *Fuel,* 88: 629-636.

QI, D. H., GENG, L. M., CHEN, H., BIAN, Y. Z. H. & REN, X. C. H. 2009. Combustion and performance evaluation of a diesel engine fuelled with biodiesl produced from soybean crude oil. *Renewable Energy,* 34: 2106-2113.

RAHEMAN H, P. A. 2004. Diesel engine emissions and performance from blends of karanja methyl ester and diesel. *Biomass and Bioenergy,* 27: 393-397.

RAMADHAS, A. S., MURALEEDHARAN, C. & JAYARAJ, S. 2005. Performance and emission evaluation of a diesel engine fueled with methyl esters of rubber seed oil. *Renewable Energy,* 30: 1789-1800.

REYES, J. F. & SEPULVEDA, M. A. 2006. PM-10 emissions and power of a diesel engine fueled with crude and refined biodiesel from salmon oil. *Fuel,* 85: 1714-1719.

SAHOO, P. K., DAS, L. M., BABU, M. K. G. & NAIK, S. N. 2007. Biodiesel development from high acid value polanga seed oil and performance evaluation in a CI engine. *Fuel,* 86: 448-454.

SEITZMAN, J. K. 2012. Chemical kinetics: NO_X mechanism. College of Engineering, School of Aerospace Engineering, Georgia Tech. Powerpoint presentation [Online]. Available: http://seitzman.gatech.edu/classes/ae6766/kineticsNOx.pdf.

SHI, X., PANG, X., MU, Y., HE, H., SHUAI, S., WANG, J., CEN, H. & LI, R. 2006. Emission reduction potential of using ethanol-biodiesel fuel blend on a heavy-duty diesel engine. *Atmospheric Environment,* 40: 2567-2574.

SIGAR, C. P., SONI, S. I., MATHUR, J. & SHARMA, D. 2009. Performance and emission characteristics of vegetable oil as diesel fuel extender. *Energy Source Part A,* 31: 139-48.

SINGH, R. K. & PADHI, S. K. 2009. Characterization of Jatropha oil for the preparation of biodiesel.*Natural Product Radiance,* 8(2): 127-132.

SONG, J. T. & ZHANG, C. H. 2008. An experimental study on the performance and exhaust emissions of a diesel engine fuelled with soybean oil methyl ester. *Proceedings of the Institute of Mechanical Engineers D-J Aut* 222: 2487-2496.

TECHQUIPMENT 2003. TD110 – TD115 small engine test bed and instrumentation. *TQ Education and Training Ltd.*

TSOLAKISA, A., MEGARITIS, A., WYSZYNSKI, M. L. & THEINNOI, K. 2007. Engine performance and emissions of a diesel engine operating on diesel-RME (rapeseed methyl ester) blends with EGR (exhaust gas recirculation). *Energy,* 32: 2072-2080.

ULUSOY, Y., TEKIN, Y., C, E., M. & KAPAOSMANOˇGLU, F. 2004. The engine tests of biodiesel from used frying oil. *Energy Source Part A,* 26: 927-932.

UTLU, Z. & KOCAK, M. S. 2008. The effect of biodiesel fuel obtained from waste frying oil on direct injection diesel engine performance and exhaust emissions. *Renewable Energy* 33: 1936-1941.

WU, F., WANG, J., CHEN, W. & SHUAI, S. 2009. A study on emission performance of a diesel engine fueled with five typical methyl ester biodiesels. *Atmospere & Environment,* 43: 1481-1485.

XUE, J., GRIFT, T. E. & HASSEN, A. C. 2011. Effect of biodiesel on engine performance and emissions. *Renewable and Sustainable Energy Review,* 15: 1098-1116.

CHAPTER 8

SUMMARY AND CONCLUSION

8.1 Introduction

This work has provided additional insight on the technical issues surrounding the extraction, production and utilization of biodiesel derived from moringa, jatropha and waste restaurant oil and how addressing the identified challenges could play to the strength of sub-Sahara Africa in it searches for universally accessible, cost effective and renewable energy sources. The findings have revealed opportunities in new approaches to methods of extraction, the need for quality assurance guarantees using ISO certification tools that are predictable with high repeatability, the opportunities and challenges associated with performance and emission behaviour of the samples in a CI engine. The likely remediation strategies and the opportunities that exists when effective remediation are implemented both on the short and long term have been presented. The summary and conclusions appear below.

8.2 Summary

On the extraction, properties and property prediction tools, the findings revealed that the samples have biodiesel properties that are similar to other biodiesels and conventional diesel. They also met the ASTM standards for biodiesel use in CI engines. The findings also revealed that using prediction tools for property determination not only saves cost, time and reduces errors associated with experiments but also the prediction tools can be used as a benchmark for ensuring quality assurance of biodiesel production sources if the properties are computed inter-alia and codified using ISO certification. What this finding contributes to the study of biodiesel is that when the ASTM standard is used alongside an ISO certified property prediction tool, commercial production of biodiesel will become more standardized and the process leading to the production of biodiesel from any source will become quality focused.

Study of the samples' performance and emission in a CI engine when compared with conventional diesel and the emission regulation of the US EPA and EU, the findings revealed that there exists no significant difference between the samples and diesel as the results were generally mixed. It was also revealed that with regard to emission regulations, the evaluated samples and diesel face similar challenges with regard to meeting US EPA and EU emission regulations on exhaust gas emission. It was also established that while some remediation

strategies could assist in curbing some emissions for both the samples and diesel, other emission curbing strategies may need to be more fuel, gas or engine specific to make any difference. The contribution of this findings to the knowledge base on biodiesel is that some remediation in the short term may only require simple engine retrofitting or slight changes in fuel mix. In the longer term, fuel chemistry can be altered through bioengineering and genetic modification of oil sources and the development of a generic novel engine to combust these new fuels in an efficient and less harmful way.

In evaluating the sources of NOx and CO emission from the samples, the finding reveals that while fuel chemistry contribute to these emissions, the most significant cause is engine condition during combustion. Therefore, regardless of fuel source, optimal engine settings are the most effective means to control NOx and CO emission not only in the biodiesel sources evaluated but also for conventional diesel fuel. The significance of this finding to biodiesel utilization is that the gas with the most challenging emission, NOx, can be controlled through changes in engine setting or the development of novel combustion strategies.

Finally, from the reviews of biodiesel and the proposal for new combustion strategies, it is safe to submit that it is possible to numerically determine the right FAME composition for any given engine type and to precisely validate any prediction made in such computation. Algae bioengineering and novel engine development emerged clearly as the future of biodiesel research from this work. This is because the potential for higher oil yield, flexible genetic modification, greater engine performance and zero NOx and CO emission can all be achieved through research focussed in these two areas.

8.3   Recommendations for future work

This study, to some extent, has established that biodiesel cold flow properties (transport properties) limitation and, the mismatch between biodiesel and the compression ignition strategy constitutes some of the technical barriers to the wider commercialization drive for this fuel type. But the property limitations have been proven to arise on account of defective production process that is unable to rid the pure fuel of free glycerol. In addition, the fuel combustion strategy mismatch is a technical issue that can be resolve via targeted computational fluid dynamic (CFD) studies supported with the right set of engine diagnostic tool for validation purpose. The aimed being to propose novel combustion strategy with generic capability that takes into account the eclectic nature of the FAME chemistry. Such a proposal,

when executed with biodiesel derived from samples used in this study, has the capacity to open up new opportunities for growth in the energy/service sector of the economy on the short to medium term while on the long term, enhancing the evolution of a knowledge based economy built around successful franchise and intellectual property ownership which will aggressively fan out across sub-Saharan Africa and beyond.

On the fuel side, the method involve using computational technique to develop a property prediction scheme base on group contribution (of contributing organic chemistry family), double bond and carbon chain length (which can be couple to a CFD solver) to be used as a benchmark for standardisation of biodiesel production from any source. Experimental tools for the determination of FAME composition and physio-chemical properties could be used to provide feed and validation data respectively. Outcomes from this segment will guide new method of biodiesel production that guarantees the convergence of theoretical data with experimental physio-chemical results.

On the engine side, homogenously charged compression ignition (HCCI) strategies with a few contrive changes holds significant potential to mitigate the observed challenges and is proposed for future work. Modula kinetic and premixed/direct injection (DI) strategy in HCCI environment could be explored. Using a higher proportion of formulated hybrid unsaturated fatty acid methyl ester (FAME) for the premix port injection as bulk charge to delay ignition, a higher proportion of saturated FAME is proposed for use in small quantity direct injection (DI) around top dead centre (TDC) to trigger ignition. Low temperature combustion (LTC) could be achieved by exhaust gas recirculation (EGR) via negative valve overlap (NVO). At the computational side, the Reynolds average Navier – Stokes (RANS) turbulent model could be employed to compute the physics of the flow events and MDBio (methyl decanoate bio-chemical kinetic model that sufficiently describe chemical event of saturated and unsaturated FAME could be employed to compute the chemical events for a wide range of formulated hybrid of FAME mixture to determine the mix with the most optimal results for engine performance and emission. Near zero oxides of nitrogen (NO_X) and soot is envisioned since the model will be structured so that the 1650k mark will not be breached. Furthermore, high homogeneity and the oxygenated nature of the mix will provide a designed ceiling for unburnt hydrocarbon (UHC) and carbon monoxides (CO) emission as the typical combustion efficiency is expected to be sufficiently high enough to limit incomplete combustion. The outcome from

these computational as well as experimental studies will form part of the guide to new strategies for short-term engine retrofit and fuel production process.

To achieve this research objective, the purchase of a fully license CFD software (with full access to all the range of chemical kinetic mechanism needed to construct fuel surrogate that closely replicate the reaction pathway of the FAME mix being tested) and optical engine diagnostic test rig fully accessorized with planar laser induced incandescence capability in both the special and temporal domain is recommended. A fully license/supported purchase of ANSYS forte (with a compatible CAD geometry file, piston and valve lift profile text file of the optical engine diagnostic test rig installed) is therefore recommended.

8.4   Conclusion

The conclusions drawn from this work are stated below.

1. Biodiesel that meet ASTM standards can be produced from moringa, jatropha and waste restaurant oil sourced from the wild in the case of the first two and in any regular restaurant, in the of the last sample.
2. Extraction of oil can be achieved via non-traditional solvents such as distilled gasoline with competitive yields at a significantly reduced cost.
3. Property prediction tools can be used as a safeguard for guaranteeing commercial production of high quality biodiesel from any sample source.
4. The performance and emission data of the fuels sampled are quite competitive with conventional diesel. Challenges identified can be tackled through novel combustion strategies.
5. More work is needed on engines to enable the samples tested and diesels to meet EPA and EU regulations on emissions in all loading conditions.
6. Oil sources that are good for food are not necessarily good for the engine and vice versa as moringa oil has shown here. High levels of poly unsaturation FAME components in moringa reduces its reactivity and energy releasing ability while increasing its capacity to produce comparatively higher levels of unburnt hydrocarbons and particulate matter. Poly unsaturated oil are desirable properties in edible oil. Most waste restaurant oil comes with high levels of saturated FAME components because of polymerization and pyrolysis as seen for the samples used in this study. This is good for the engine despite being discarded as unfit for human consumption. The implications of this finding is that

a symbiotic approach to edible/fuel oil production and utilization may put an end to the food verses fuel debate.

7. For any given biodiesel sample, heat release rate and combustion efficiency in the CI engine depends on the FAME composition. Hence the fuel ignition properties are determined by the FAME composition. This is an indication that there exists a right mix of FAME composition in biodiesel that could produce optimal performance at acceptable emissions in CI engines. Obtaining this right mix can be achieved via mixing of different biodiesel sources, bio-engineering oil sample sources, or, chemically processing any particular oil sample.

LIST OF APPENDIXES

APPENDIX I: Data logging template for engine

speed (rev/min)										
Torque (Nm)										
Brake Power (kw)										
Fuel: Time for 8ml(s)										
Fuel mass flowrate(Kg/hr)										
Specific fuel comsumption (g/KWh)										
Air: mmH_2O										
Air:Kg/hr										
Corrected Air: Kg/hr										
Air/Fuel ratio										
Exhaust Temperature (^{o}C)										
Oil Sump Temperature ($_o$C)										
Volumetric efficiency (%)										
Brake Thermal efficiency (%)										
% Heat lost to exhaust										
Corresponding gas emission										
Carbon-monoxide, CO (%)										
Carbon-dioxide, CO_2 (%)										
Unburnt Hydrocarbon, HC (ppm)										
Oxides of Nitrogen, Nox (ppm)										
Oxygen, O_2 (%)										
λ										

APPENDIX II: Code to compute biodiesel property.

```cpp
//Biodiesel Parameters Computation

#include <iostream>
#include <cmath>
#include <string>

using namespace std;
int Biodiesel_Type;
std::string Biodiesel;
float NC, N_DB, Zi;
float C_weight = 12.011, H_weight = 1.008, O_weight = 15.999;
float Mi, Di, Pi, Ni, OctN, Tf, Pp, CFPP;
float Ufame;

int main()
{
    system("CLS"); // Clears the screen
    cout <<"Biodiesel Parameters Calculator\n\n";
    cout << "Select the corresponding Biodiesel\n";
    cout << "1 - Myristic       2 - Palmitic          3 -
Palmitoleic\n";
    cout << "4 - Stearic        5 - Oleic        6 - Linoleic\n";
    cout << "7 - Linolenic         8 - Araclidic        9 -
Ficosenic\n";
    cout << "10 - Behemic       11 - Erucic           12 -
Tetracosenic\n";

    cin >> Biodiesel_Type;

    switch (Biodiesel_Type)
    {
        case 1:
            NC = 14;
            N_DB = 0;
            Zi = 0; // Zi = 0; Zi = 0.9;
            Biodiesel = "Myristic";
        break;

        case 2:
            NC = 16;
            N_DB = 0;
            Zi = 6.5; //Zi = 15.3; Zi = 20.4;
            Biodiesel = "Palmitic";
        break;

        case 3:
```

```
            NC = 16;
            N_DB = 1;
            Zi = 2.0; //Zi = 1.1; Zi = 4.6;
            Biodiesel = "Palmitoleic";
    break;
    case 4:
            NC = 18;
            N_DB = 0;
            Zi = 6.0; //Zi = 6.4; Zi = 4.8;
            Biodiesel = "Stearic";
    break;
    case 5:
            NC = 18;
            N_DB = 1;
            Zi = 72.2; //Zi = 40.1; Zi = 52.9;
            Biodiesel = "Oleic";
    break;
    case 6:
            NC = 18;
            N_DB = 2;
            Zi = 1.0; //Zi = 36.9; Zi = 13.5;
            Biodiesel = "Linoleic";
    break;
    case 7:
            NC = 18;
            N_DB = 3;
            Zi = 0; //Zi = 0.2; Zi = 0.8;
            Biodiesel = "Linolenic";
    break;
    case 8:
            NC = 20;
            N_DB = 0;
            Zi = 4.0; //Zi = 0; Zi = 0.12;
            Biodiesel = "Araclidic";
    break;
    case 9:
            NC = 20;
            N_DB = 1;
            Zi = 2.0; //Zi = 0; Zi = 0.84;
            Biodiesel = "Ficosenic";
    break;
    case 10:
            NC = 22;
            N_DB = 0;
            Zi = 0; //Zi = 0; Zi = 0.03;
            Biodiesel = "Behemic";
    break;
    case 11:
            NC = 22;
```

```
                    N_DB = 1;
                    Zi = 0; //Zi = 0; Zi = 0.07;
                    Biodiesel = "Erucic";
              break;
              case 12:
                    NC = 24;
                    N_DB = 0;
                    Zi = 0; //Zi = 0; Zi = 0.04;
                    Biodiesel = "Tetracosenic";
              break;
        }

    //*********** Calculating Mi (Molecular
Weight)***************
        if (N_DB == 0)
        {
             Mi = (n+1)*C_weight +(2*n+2)*H_weight+2*O_weight;
        }

        if (N_DB == 1)
        {
             Mi = (n+1)*C_weight +(2*n+1)*H_weight+2*O_weight;
        }
        if (N_DB == 2)
        {
             Mi = (n+1)*C_weight +(2*n)*H_weight+2*O_weight;
        }
        if (N_DB == 3)
        {
             Mi = (n+1)*C_weight +(2*n-1)*H_weight+2*O_weight;
        }

    //*********** Calculating Pi (Density)***************
        Pi = 0.8463 + (4.9/Mi) + 0.0118*N_DB;

    //*********** Calculating Di (High Heating
Value)***************
        Di = 49.9 - (1794/Mi) - 0.2*N_DB;

    //*********** Calculating Ni (Kinematic
Viscosity)***************
        Ni = 0.235*NC - 0.468*N_DB;


    //*********** Calculating OctN (Octane
Number)***************
        OctN = 3.930*NC - 15.936*N_DB;
```

```cpp
        //*********** Calculating Tf (Flash Point)***************
        Tf = 23.362*NC - 4.854*N_DB;

        //*********** Calculating Pp (Pour Point)***************
        Pp = 18.880*NC - 1.00*(Ufame);

        //*********** Calculating CFPP (Cold Flow Plugging
Point)***************
        CFPP = 18.019*NC - 0.804*(Ufame);

        cout << "\n Biodiesel Type = " << Biodiesel << "\n";
        cout << "Density = " << Pi << "\n";
        cout << "Kinematic Viscosity = " << Ni << "\n";
        cout << "Flash Point = " << Tf << "\n";
        cout << "Pour Point = " << Pp << "\n";
        cout << "Octane Number = " << OctN << "\n";
        cout << "Cold Flow Plugging Point = " << CFPP << "\n";


        system("pause");
        return 0;
}
```

FAME	Nc	Ndb	Mc	Mh	Mo	Mi
Myristic (C14:0)	15	0	12.011	1.008	15.999	256.43
Palmitic (C16:0)	17	0	12.011	1.008	15.999	284.484
Palmitoleic (C16:1)	19	1	12.011	1.008	15.999	311.53
Stearic (18:0)	19	0	12.011	1.008	15.999	312.538
Oleic (C18:1)	19	1	12.011	1.008	15.999	311.53
Linoleic (C18:2)	19	2	12.011	1.008	15.999	310.522
Linolenic (C18:3)	19	3	12.011	1.008	15.999	309.514
Araclidic (C20:0)	21	0	12.011	1.008	15.999	340.592
Eicosenic (C20:1)	21	1	12.011	1.008	15.999	339.584
Behenic (C22:0)	23	0	12.011	1.008	15.999	368.646
Erucic (C22:1)	23	1	12.011	1.008	15.999	367.638
Tetracosanic (C24:0)	25	0	12.011	1.008	15.999	396.7

Moringa fraction, Z_i	Jatropher fraction, Z_i	Waste res Z_i	FAME density(MO)
0	0	0.009	0.865408529
0.065	0.153	0.204	0.863524167
0.04	0.011	0.046	0.873828822
0.06	0.064	0.048	0.861978094
0.72	0.401	0.529	0.873828822
0.01	0.369	0.135	0.88567988
0	0.002	0.008	0.897531271
0.04	0	0.0012	0.860686715
0.02	0	0.0084	0.87252942
0	0	0.0003	0.859591884
0	0	0.0007	0.871428328
0	0	0.0004	0.858651903

density fraction(MO)	FAME density(JA)	density fraction(JA)	FAME density (WO)
0	0.865408529	0	0.865408529
0.056129071	0.863524167	0.132119198	0.863524167
0.034953153	0.873828822	0.009612117	0.873828822
0.051718686	0.861978094	0.055166598	0.861978094
0.629156752	0.873828822	0.350405358	0.873828822
0.008856799	0.88567988	0.326815876	0.88567988
0	0.897531271	0.001795063	0.897531271
0.034427469	0.860686715	0	0.860686715
0.017450588	0.87252942	0	0.87252942
0	0.859591884	0	0.859591884
0	0.871428328	0	0.871428328
0	0.858651903	0	0.858651903
0.832692517		0.875914209	

density fraction(WO)	FAME heating Val(MO)	Heat Val Fraction(MO)	FAME heating val(JA)
0.007788677	42.1939387	0	42.1939387
0.17615893	42.8838457	2.78744997	42.8838457
0.040196126	43.23132507	1.729253003	43.23132507
0.041374948	43.449898	2.60699388	43.449898
0.462255447	43.23132507	31.12655405	43.23132507
0.119566784	43.01263157	0.430126316	43.01263157
0.00718025	42.79381631	0	42.79381631
0.001032824	43.92270071	1.756908028	43.92270071
0.007329247	43.70706559	0.874141312	43.70706559
0.000257878	44.32354275	0	44.32354275
0.00061	44.11019976	0	44.11019976
0.000343461	44.66769095	0	44.66769095
0.864094572		41.31142656	

Heat val Fraction(JA)	FAME heating val(WO)	heat val fraction(WO)	Kinematic viscosity(MO)
0	42.4039387	0.381635448	3.525
6.561228392	43.0938457	8.791144523	3.995
0.475544576	43.44132507	1.998300953	3.997
2.780793472	43.659898	2.095675104	4.465
17.33576135	43.44132507	22.98046096	3.997
15.87166105	43.22263157	5.835055262	3.529
0.085587633	43.00381631	0.34403053	3.061
0	44.13270071	0.052959241	4.935
0	43.91706559	0.368903351	4.467
0	44.53354275	0.013360063	5.405
0	44.32019976	0.03102414	4.937
0	44.87769095	0.017951076	5.875
43.11057648		42.91050065	

Kinematic Viscosity Frac(MO)	Kinematic Viscosity (JA)	Kinematic Viscosity Frac(JA)
0	3.525	0
0.259675	3.995	0.611235
0.15988	3.997	0.043967
0.2679	4.465	0.28576
2.87784	3.997	1.602797
0.03529	3.529	1.302201
0	3.061	0.006122
0.1974	4.935	0
0.08934	4.467	0
0	5.405	0
0	4.937	0
0	5.875	0
3.887325		3.852082

Kinematic Viscosity (WO)	Kinematic Viscosity Frac(WO)	CN(MO)	CN fraction(MO)	CN(JA)
3.525	0.031725	58.95	0	58.95
3.995	0.81498	66.81	4.34265	66.81
3.997	0.183862	58.734	2.34936	58.734
4.465	0.21432	74.67	4.4802	74.67
3.997	2.114413	58.734	42.28848	58.734
3.529	0.476415	42.798	0.42798	42.798
3.061	0.024488	26.862	0	26.862
4.935	0.005922	82.53	3.3012	82.53
4.467	0.0375228	66.594	1.33188	66.594
5.405	0.0016215	90.39	0	90.39
4.937	0.0034559	74.454	0	74.454
5.875	0.00235	98.25	0	98.25
	3.9110752		58.52175	

CN fraction(JA)	CN(WO)	CN fraction(WO)	Flash piont(MO)	Fp fraction(MO)	Flash piont(JA)
0	58.95	0.53055	350.43	0	350.43
10.22193	66.81	13.62924	397.154	25.81501	397.154
0.646074	58.734	2.701764	439.024	17.56096	439.024
4.77888	74.67	3.58416	443.878	26.63268	443.878
23.552334	58.734	31.070286	439.024	316.09728	439.024
15.792462	42.798	5.77773	434.17	4.3417	434.17
0.053724	26.862	0.214896	429.316	0	429.316
0	82.53	0.099036	490.602	19.62408	490.602
0	66.594	0.5593896	485.748	9.71496	485.748
0	90.39	0.027117	537.326	0	537.326
0	74.454	0.0521178	532.472	0	532.472
0	98.25	0.0393	584.05	0	584.05
55.045404		58.2855864		419.78667	
				146.78667	

Fp fraction(JA)	Flash piont(WO)	Fp fraction(WO)	Pour point(MO)	Pp fraction(MO)	Pour piont (JA)
0	350.43	3.15387	206.2	0	205.1
60.764562	397.154	81.019416	243.96	15.8574	242.86
4.829264	439.024	20.195104	281.72	11.2688	280.62
28.408192	443.878	21.306144	281.72	16.9032	280.62
176.048624	439.024	232.243696	281.72	202.8384	280.62
160.20873	434.17	58.61295	281.72	2.8172	280.62
0.858632	429.316	3.434528	281.72	0	280.62
0	490.602	0.5887224	319.48	12.7792	318.38
0	485.748	4.0802832	319.48	6.3896	318.38
0	537.326	0.1611978	357.24	0	356.14
0	532.472	0.3727304	357.24	0	356.14
0	584.05	0.23362	395	0	393.9
431.118004		425.4022618		268.8538	
158.118004		152.4022618		-4.1462	

Pp fraction (JA)	Pour point (WO)	Pp fraction(WO)	CFPP(MO)	CFPP fraction(MO)	CFPP(JA)
0	211.19	1.90071	208.377	0	207.4926
37.15758	248.95	50.7858	244.415	15.886975	243.5306
3.08682	286.71	13.18866	280.453	11.21812	279.5686
17.95968	286.71	13.76208	280.453	16.82718	279.5686
112.52862	286.71	151.66959	280.453	201.92616	279.5686
103.54878	286.71	38.70585	280.453	2.80453	279.5686
0.56124	286.71	2.29368	280.453	0	279.5686
0	324.47	0.389364	316.491	12.65964	315.6066
0	324.47	2.725548	316.491	6.32982	315.6066
0	362.23	0.108669	352.529	0	351.6446
0	362.23	0.253561	352.529	0	351.6446
0	399.99	0.159996	388.567	0	387.6826
274.84272		275.943508		267.652425	
1.84272		2.943508		-5.347575	

CFPP fraction(JA)	CFPP(WO)	CFPP fraction(WO)
0	212.3166	1.9108494
37.2601818	248.3546	50.6643384
3.0752546	284.3926	13.0820596
17.8923904	284.3926	13.6508448
112.1070086	284.3926	150.4436854
103.1608134	284.3926	38.393001
0.5591372	284.3926	2.2751408
0	320.4306	0.38451672
0	320.4306	2.69161704
0	356.4686	0.10694058
0	356.4686	0.24952802
0	392.5066	0.15700264
274.054786		274.0095244
1.054786		1.0095244

Paper 5: A PROPOSAL TO PERFORM COMPUTATIONAL AND EXPERIMENTAL EVALUATION OF BIODIESEL IN HCCI USING A COMBINED MODULA KINETIC AND PREMIXED/DI STRATEGY

E. I. Onuh[*] and Freddie Inambao.

Mechanical Discipline, School of Engineering, University of Kwazulu-Natal, Durban, South Africa.

[*]*Corresponding email:212561710@stu.ukzn.ac.za*

inambaof@ukzn.ac.za

Abstract

Biodiesel as a renewable alternative to diesel with the capacity to reduce emission and broaden energy access is constrained by some performance and emission concerns. A comparatively marginal drop in thermal efficiency due to lower heating value, susceptibility to emitting of higher oxides of Nitrogen (NO_X) at high temperature in addition, to a higher carbon-monoxide (CO) and unburnt hydrocarbon (UHC) emission at low temperature constitutes some of the challenges. Homogenously charged compression ignition (HCCI) holds significant potential to mitigate these challenges. Modula kinetic and premixed/DI strategy in HCCI environment is hereby proposed. Using a higher proportion of unsaturated fatty acid methyl esters (FAME) for the premix port injection as bulk charge to delay ignition, a higher proportion of saturated FAME is proposed for use in small quantity direct injection (DI) around top dead centre (TDC) to trigger ignition. Low temperature combustion (LTC) is achieved by exhaust gas recirculation (EGR) via negative valve opening (NVO). On the computational side, the Reynolds average Navier-stoke turbulence model should be used to compute the physics of the flow events and MDBio in KIVA-3V will compute the chemistry. The computational model proposed is the 3D CFD with multi-zone detail chemistry (20 zone at the least). It is anticipated that high indicated mean effective pressure (IMEP) will be achieve because of high heat release rate (HHRR) of the unsaturated FAME and high spontaneity of combustion. Near zero NO_X and soot is envisioned since the 1650 k mark will not be breached. Also, high homogeneity and the oxygenated nature of the mix will provide a designed ceiling for UHC and CO emission.

Keywords

Thermal efficiency, Emission, Homogenously charged compression ignition (HCCI), Modula kinetic, premixed/DI, Fatty acid methyl ester (FAME), Low temperature combustion (LTC), Biodiesel Surrogates.

Nomenclatures/Symbols

4D   :   Fully Resolved Spatial and Temporal Dimension

ATDC :   After Top Dead Centre

BTDC :   Before Top Dead Centre

CAI   :   Control Auto Ignition

CFD   :   Computational Fluid Dynamics

CI   :   Compression Ignition

CN   :   Cetane Number

DNS   :   Direct Numerical Simulation

EGR   :   Exhaust Gas Recirculation

EVO   :   Exhaust Valve Opening

HCCI   :   Homogenous Charge Compression Ignition

HRR   :   Heat Release Rate

HTHR :   High Temperature Heat Release

HTR   :   High temperature reaction

ID   :   Ignition Delay

IMEP   :   Indicated Mean Effective Pressure

ISFC   :   Indicated Specific Fuel Consumption

IVC   :   Inlet Valve Closing

KMC   :   Kinetic Monte Carlo

LIF   :   laser Induced Fluorescence

LII   :   Laser Induced Incandescence

LLNL :   Lawrence Livermore National Laboratory

LTC	:	Low Temperature Combustion
LTK	:	Low Temperature Kinetics
LTR	:	Low temperature reaction
MB	:	Methyl Butanoate
MK	:	Modulated Kinetics
NVO	:	Negative Valve overlap
ϕ	:	Fuel /Air Ratio
ON	:	Octane Number
PLTF	:	Planner Laser Induced Fluorescence
PM	:	Particulate matter
RGF	:	Residual Gas Fraction
ROHR	:	Rate of Heat Release
TDC	:	Top Dead Centre
VVT	:	Variable Valve Timing

5.1   Introduction

In the global energy scene, the challenge of increasing demand for, and increasing depletion rate of fossil fuel and the negative environmental impact of unregulated use of conventional energy sources makes advocacy for renewable energy source (RES) a global imperative. In terms of demand, based on British Petroleum estimates, global energy consumption is estimated to be 9.7 Gtoe with a significant proportion consumed in North America [1]. This region's demand is projected to grow at 1.5% from 2002 to 2030. The Asia pacific will grow at 3.9% within the same period and global energy demand is expected to peak at 16487 Mtoe by the year 2030 [1]. The observed trend in demand growth shows that developing and underdeveloped regions have higher scope for demand growth than developed regions such as North America and Europe. This is an indication that demand strain will only get more challenging. On the supply side, finite fossil (petroleum, natural gas and coal) account for 80% of global energy sources. Nuclear energy as at 2009 accounts for about 13% leaving renewable energy sources to account for the rest [2]. Petroleum derived energy source has a chequered history; 63% of global oil reserves occur in the Middle East and given its finite nature, peak

production of oil is projected to occur between 2015 - 2030 [1]. The highly localized nature of oil discoveries come with significant geopolitical risk and this has often precipitated into conflict, price fluctuation and supply uncertainty. The existential threat posed by any potential accident ensuing from the use of nuclear energy has heightened public resistance to its proliferation. After Chernobyl, and Fukushima, a phasing-out policy has been adopted in Japan and Germany [3]. This is an indication that in the energy sector, supply from fossil and nuclear sources are constrained. Added to this are the issues of environmental sustainability. Griffin Shay [4] and many others have stated that increased use of petroleum fuel will intensify global warming caused by carbon dioxide (CO_2) emissions not to mention the other countless health risk posed by the unregulated emissions of oxides of Nitrogen (NO_X), soot, carbon monoxide (CO), unburnt hydrocarbons (UHC) and aldehydes [5]. Against this background, renewable energy sources (RES) have been identified as the only energy sources that meet sustainability criteria. It is evident that a significant percentage of energy is consumed in the transportation sector and since internal combustion engines are a key component of this sector, a renewable energy source option availability will play a vital role in the drive for sustainability.

5.2 Biodiesel and Novel Combustion Strategies

Biodiesel is composed of fatty acid methyl esters (FAMEs) produced from vegetable oil or animal fat through a trans esterification process. This is achieved using alcohol in the presence of an alkaline catalyst. Besides being carbon neutral, the use of biodiesel in internal combustion engines has been reported to result in the reduction of carbon monoxide (CO), unburnt hydrocarbons (UHC), particulate matter (PM) and soot precursors [6]. It's primary challenge has been a marginal drop in engine power [7, 8], increases in oxides of nitrogen (NOx) emission at high combustion temperature [9, 10] and poor reactivity leading to higher emission of CO and UHC at start-up or low load conditions due to poor flow properties at low temperature. These advantages and challenges have triggered intense research effort aimed at finding combustion strategies that could harness the potentials of biodiesel and mitigate the challenges obstructing its wider application. Alrikson and Denbratt [11] in their computation of the equivalent ratio-temperature (∅–T) map for soot and NO concentration using the SENKIN code observed that NO_X and soot emission could be completely eliminated regardless of equivalent ratio if the combustion temperatures are kept below 1650 k. The term, 'low temperature combustion' (LTC) is the process by which combustion temperature is kept below the NO_X and soot production threshold. This is often achieved via exhaust gas recirculation (EGR) to reduce oxygen concentration [12]. In another study a temperature floor has also been

determined to be 1400 k [13]. Below this temperature, it has been observed that the oxidation rate of CO to CO_2 becomes too low leading to unacceptable levels of CO and UHC emission. In the 1990s, a strategy with the best potential to reduce NO_X and soot emission came to light and began to receive wide research attention. Homogenous charge compression ignition (HCCI) sometime called control auto-ignition (CAI) is a combustion strategy that relies heavily on the chemical kinetic of the fuel for the start of ignition. It is characterized by the induction of premixed charge, ignition in the combustion chamber, as a result of elevated temperature and pressure, during the compression stroke near the TDC. Because the charge is premixed, equivalent ratio is calibrated near stoichiometric air, and given that combustion is spontaneous with multiple flame fronts, a higher thermal efficiency was observed in comparison to compression ignition (CI) engine. All HCCI studies have consistently reported significant reductions in NO_X and soot emission as a result of the low temperature regime [12]. However, HCCI also faces some challenges including: combustion phasing, UHC and CO (mostly in diesel fuel runs) emission and problems with cold start. The motivation here is that given biodiesel's oxygenated nature, warm EGR achieved via negative valve opening (NVO) could deliver sufficient heat into the cylinder to improve charge homogeneity and a higher combustion efficiency which could eliminate the UHC and CO emissions. Given the array of parameters that need to be observed and controlled, the most cost effective way to conduct the study will be through numerical means, using very specific experimental data for result validation.

5.3 Numerical Study and Validation Tools

Given the size of parameters, properties and systems features that need to be controlled, monitored and evaluated in combustion studies, direct physical experimentation is often unhelpful. The most efficient means, in terms of cost and research time, to conduct combustion studies is through numerical methods. This is often accompanied with well-targeted experiments to obtain data for validation purposes. The approach requires a careful selection of study parameters that closely approximate the physical reality being investigated. Combustion is a multi-phase, multi-state and thermally intense process with significant levels of thermal and charge stratification. As a result of these, surrogate chemical kinetic mechanisms that closely represent the chemical properties and processes of the charge to compute the chemistry are selected. The physics of flow processes and thermal exchanges in the HCCI also guides the selection of the model that will compute the flow and thermal behavior of the charge.

The study involves a proportionally high unsaturated FAME at the premixed sage of HCCI as the main fuel injection stream with a smaller DI near TDC of a proportionally high saturated FAME to serve only as an ignition trigger as proposed in the MK [14, 15] strategy. The fuel injection strategy at the premix stages is through port injection hence the detailed MDBio surrogate chemical kinetic mechanism of LLNL [16] which has been successfully reduced to 77 species and 209 reactions by Brakora et al. [17].KIVA-3V (which is now available as an open source code) is here proposed to compute the chemistry. The quazi-dimensional, multi-zone reduced chemical kinetic code built into the 3D-CFD code (KIVA) proposed by Aceves et al. [18-20] will be used to compute the physical flow process along with MDBio to solve the ID spray phenomena and SOI. The species concentration and emission trend, it is hoped, will adequately resolve the special and temporal domain. Data obtained from previous HCCI or CI combustion strategies with close proximity in test features to the proposed strategy could be used as effective engine diagnostic tools to validate the numerical results. Or where funding permits, a suitable optical engine diagnostic test rig with fully fitted PLIF test kit [21] could be used to obtain specific data for validation purposes.

## 5.4   Background of CFD Method and Engine Diagnostics

A computational approach to research in internal combustion engine (ICE) and engine development has had a long and successful history. Progressive application of models with increasingly higher fidelity alongside state of the art engine diagnostic tools has resulted in the full resolution of most important processes in fuel combustion in ICE, making it possible to predict engine performance and emissions with increasing level of accuracy. Further, this approach enables the proposal of novel combustion strategies that improve performance and mitigate or eliminate undesirable emissions. The convergence of biodiesel potential with CFD capability is bringing closer the possibility of a perfectly 'green ICE', a scenario where a carbon neutral fuel source produces zero UHC, CO, NO_X and PM with a high cycle efficiency in an internal combustion engine. Computational studies in ICE often involve the use of chemical kinetic mechanisms, appropriate flow models with multi-scale (spatial and temporal resolution) and multi-phase capability, coupled with the use of specific experimental data obtained with appropriate engine diagnostic tools for validation of any given combustion strategy.

5.4.1   Chemical Reaction Pathways and Surrogates

Onishi [22] and Noguchi [23] suggested that, unlike SI combustion which is spark assisted and relies strongly on flame propagation, and CI which relies on air/fuel mixing, HCCI relies

exclusively on chemical kinetics for SOI hence chemical reaction pathways and LTK play crucial roles in its processes. And since it is not practicable to adopt the chemical composition of actual biodiesel in numerical studies to compute the chemistry owing to its complexity, simple and well characterized chemical kinetics are used as surrogates to mimic the behaviour of the actual fuel [24]. Biodiesel surrogates are grouped into small (short carbon chain, < 5) or large (long carbon chain, > 5) [25]. Small surrogates have been used more extensively because of their inherent advantages which include; short CPU runtime, availability of a wide range of in-cylinder engine validation data, and flexibility of use. However, it also faces significant challenges which include; reduced accuracy, lack of low temperature reactivity, unclear NTC region, differences in auto-ignition characteristics from actual biodiesel, amongst other things. Large surrogate mechanisms fully addresses these challenges but with their own new set of difficulties which include; an unwieldy and complex structure, heavy dependence on smaller sub-mechanisms, longer CPU runtime and limited in-cylinder engine validation data [25].
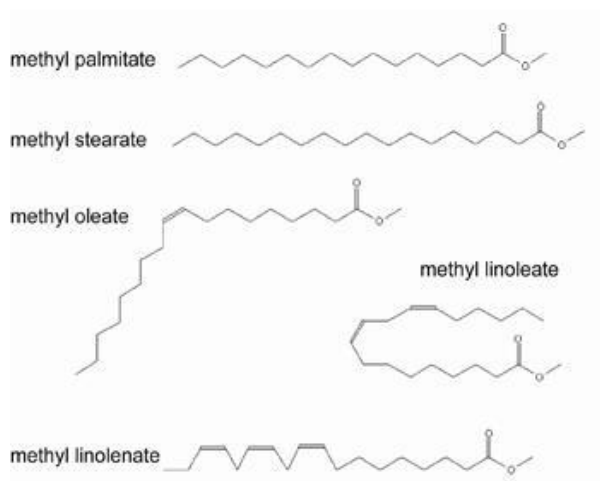
Table 2: Common biodiesel structure

i. Small surrogates include;

(1) Methyl butanoate (MB < $C_5 H_{10} O_2$), developed by Brakora et al. [26], Golovitchev and Yang [27], Fisher et al. [28] and has been coupled to KIVA-3, CHEMKIN.

(2) Methyl (E) − 2 butenoate (MB2D, $D_5 H_8 O_2$), developed by Gail et al. [29] to mimic unsaturated FAMEs which MB failed to properly do. It has complies with CHEMKIN.

(3) MBBio developed by Mohamed Ismail et al. [30]. It is generic in nature and could be tailored further for any specific application. It complies with open FOAM.

ii. Large surrogates include:

(1) Methyl Decanoate (MD, C_{11}, H_2 O_2) developed by Glaude et al. [31] through the use of EXGAS. It complies with CHEMKIN. The unsaturated versions, methyl-5-decanoate (MD5D, C_{11} C_2 O_2) and methyl-9-decanoate (MD9D, C_{11} C_{20} O_2) have also been developed.

(2) MD Bio developed in LLNL [32] and reduced by Luo et al. [33]. It complies with CONVERGE, CHEMKIN AND KIVA-3V.

(3) Methyl stearate (C_{19} H_{38} O_2) developed by Herbinet et al. [34] through the use of EXGAS. The same prodedures were used to develop methyl palmitate (C_{17} H_{34} O_2) by Hakka et al. [35].

(4) Westbrook et al. [36] developed methyl oleate, stearate, palmitate, linoleate and linolenate.

5.4.2   CFD Flow Model

Numerical techniques developed for flow studies range from highly refined to coarse grained depending on the level of fidelity required for a given investigation [basic research need]. Among the fine grains, Quantum Mechanics (QM) occupies prime position followed by Molecular Dynamic (MD) and Kinetic Monte Carlo (KMC) with spatial and temporal domains ranging from 10^{-12} m x 10^{-12} s (Pico scale) to 10^{-9} m x 10^{-9} s (Nano scale). These computations can capture processes ranging from intra-atomic processes for a small number of atoms to intermolecular activities. The effort required to compute at this level in terms of computing resources and CPU runtime is quite rigorous but the benefit of the additional information obtained thereby does not necessarily make any substantial difference in prediction capability, particularly for CFD application in biodiesel studies.

Direct numerical simulation (DNS), large eddy simulation (LES) and Reynolds averaged Navier-Stokes (RANS) are the band most often mentioned in CFD studies. Their spatial and temporal domains range from Nano scale (10^{-9} m x 10^{-9} s), through micro scale (10^{-6} m x 10^{-6} s) to milli scale (10^{-3} m x 10^{-3} s). RANS has the coarsest grain size in combustion studies, but LES is gaining an increasing foothold with power and data storage capacity [37]. There are primarily five categories of application in biodiesel computation, as summarized below.

5.4.2.1 Zero Dimension, Single Zone with Detailed Chemistry

This is the simplest model, applying the first law of thermodynamics in engine simulation. Often, heat exchanged between charges and mass-blow-by are neglected. Both the thermodynamic and transport properties are considered homogenous. This model often over estimates results because thermal and charge stratification constitute significant processes altering realities in ICE. The model gives good results in estimating ID and NO_X formation because both events are linked to the highest temperature which is close to the mean gas temperature. Brakora and Reitz [38] used this model to estimate NO_X formation from biodiesels.

5.4.2.2 Quazi Dimensional, Multi Zone with Detailed reaction

The over simplification of combustion processes in the single zone model was addressed by the proposal for a multi-zone model which divides the combustion chamber into several regions or zones with each having uniform thermodynamic and transport properties. Different initial parameters are used for reach zone. Normally, crevices and boundary layers (low temperature zones) are included to obtain good resolution of UHC and CO for HCCI processes. They are described as quazi-dimensional because the dimensions are phenomenologically determined to represent crevices, core adiabatic zones and boundary layers. Fiveland and Assanis [39] developed and used this model to predict performance and emissions under turbocharge conditions. Figure 7.2 details the scheme.
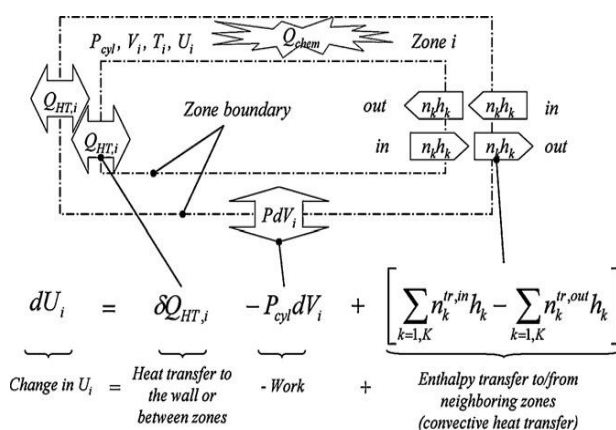

$$dU_i \quad = \quad \delta Q_{HT,i} \quad -P_{cyl}dV_i \quad + \quad \left[\sum_{k=1,K} n_k^{tr,in} h_k - \sum_{k=1,K} n_k^{tr,out} h_k \right]$$

Change in U_i = Heat transfer to the wall or between zones — Work + Enthalpy transfer to/from neighboring zones (convective heat transfer)

Table 3: Quazi-dimensional, multi-zone model [41]

5.4.2.3 1D Full Engine Cycle with Detailed Chemistry

Zero and quazi-dimensional computation only captures engine processes at the start of intake valve closure (IVC) and the end of exhaust valve opening (EVO). This implies that parameters

have to be specified at IVC creating substantial scope for computational error. This is because average mixture temperature, equivalent ratio and residual gas fraction (RGF) are difficult to determine. To overcome these challenges 0D and quazi-dimensional models are combined with engine cycle simulation codes which compute the parameters and IVC. These 0D codes predict engine parameters from air intake to exhaust pipe making it possible to model the gas exchange processes. Ogink [40] produced the BOOST-SENKIN, single zone model which predicts auto ignition timing and heat release rate for a HCCI gasoline engine using this approach. Milovanovic et al. [41] studies the variable valve timing (VVT) impact on gas exchange processes in HCCI using the same approach.

5.4.2.4 3D CFD, Multi-zone with Detailed Chemistry

Despite the improvement recorded with 1D full engine cycles with detailed chemistry, some challenges still persisted. These included poorly specified charge and thermal stratification and RGF at IVC. Aceves et al. [18-20] proposed that in order to overcome these challenges and achieve finer resolution than the CFD model could provide while at the same time avoiding computational stiffness and reducing computation chemistry can be computed in 3D CFD, thereby adopting a segregated sequenced multi-zone model. This procedure used 3D CFD code (KIVA) for the flow computation and a quazi-dimensional multi-zone detailed chemical kinetic code to compute the chemistry. The KIVA code is a transient, 3D, multiphase, multi-component scheme that analyses chemical reacting flows with sprays. This code is under development at the Los Alamos National Laboratory [42] and is open sourced. The approach requires that the fluid mechanic code is first executed to evaluate temperature distribution within the cylinder without combustion between the zones. This information is then used in the chemical kinetic code. Hence, every zone in the multi-zone chemical kinetic code is ascribed differential initial temperatures and parameters obtained from the CFD code. These steps fully account for the thermal gradient. It initially used 10 zones but was latter increased to 40 for higher resolution. Babajimoponlos et al. [43] and Flower et al. [44] used this model with good results. The only drawback encountered is its over-estimation of CO. This is the model that is being proposed for this work.

5.4.2.5 3D CFD with Detailed Chemistry

Multi-dimensional computational fluid dynamics with detailed chemistry possess the best potential to predict more accurately engine activities when the complete geometry of the combustion chamber is fully resolved and detailed kinetic chemistry is employed to evaluate

chemical events. The computational resources for such procedures are significant and depend on CFD mesh resolutions and the size of the chemical kinetic mechanism. Agarwal and Assanis [45] performed a simulation of natural gas ignition consisting of detailed chemical kinetic mechanism of 22 species and 104 reactions using the multi-dimensional CFD reacting flow code KIVA-3V. The purpose was to explore auto-ignition of natural gas injected into a quiescent chamber in CI like conditions. The complete kinetic was executed up to the ignition point.
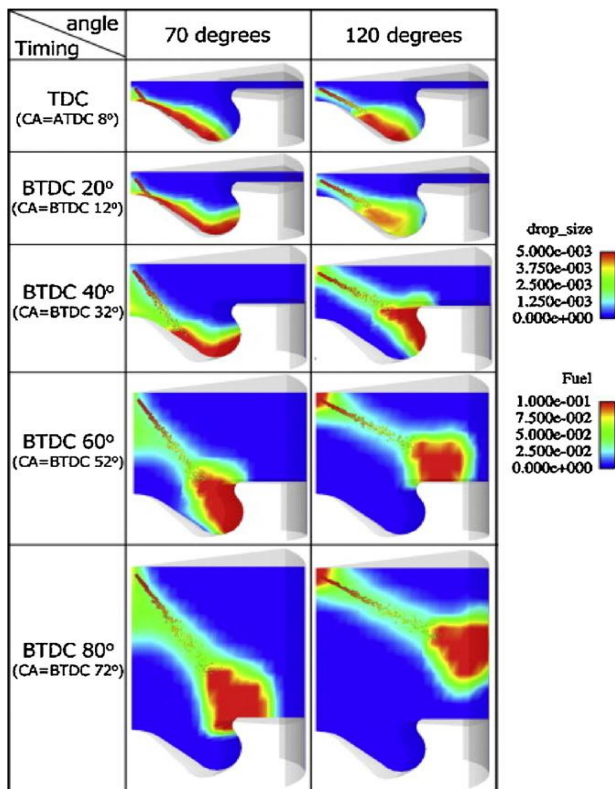
Table 4: Modelled effect of injection angle and time on spray and evaporation [46]

5.4.3 HCCI Strategies

Homogenous charge compression ignition (HCCI) has the potential to significantly reduce NO_X (because it is an LTC concept) and soot emission in the exhaust, its unthrottled operation leading to higher indicated thermal efficiency and operation at near stoichiometric places it in a good position to address some of the drawbacks associated with the use of biodiesel in CI engines. The challenges of engine control, load scaling and UHC/CO emission are currently being addressed through various research strategies. UHC and CO emission, particularly, occur as a result of bulk quenching at low loads, wall quenching and crevice flow at high load. But those are being resolved using a plethora of strategies that includes warm/hot EGR at steady state operation to improve reactivity. These strategies are clearly useful for FAME combustion in ICE. The fear of oxygen starvation resulting from tight EGR regime is mitigated by the oxygenated nature of FAME. This, clearly, is the focus of this proposal.

HCCI strategies are broadly categorized into: early direct injection, late injection and premixed/DI injection. Early direct injection includes premixed lean diesel combustion (PREDIC) developed by Takeda et al. [47], UNIBUS developed by Yanagihara et al. [48], MULINBUMP developed by Su et al. [49] and small angle injection strategy developed by Kim and Lee [46]. Late injection strategies include modulated kinetic (MK) developed by Nissan Motor company and described by Kawashima et al. [14] and the second generation MK recommended by Kawamoto et al. [50]. The other HCCI strategies are the premixed/DI HCCI and the LTC HCCI strategy. Given the focus of this paper, the strategies that will be described are the modulated kinetic and the premixed/DI strategies.

5.4.3.1 Modulated Kinetics (MK)

The modulated kinetic (MK) combustion system was developed by Nissan Motor Company as a late injection HCCI strategy. Kawashima et al. [14] and Kimura et al. [51] provided details of this strategy. To achieve the diluted homogenous mixture needed for HCCI, a long ignition delay and rapid mixing was required. The ignition delay was achieved by retarding injection timing from 1° BTDC to 3° ATDC and using a higher EGR to lower oxygen concentration to 15% - 16%. Rapid mixing was accomplished by using high swirl with toroidal combustion bowl geometry. The operating range for the first generation MK was limited to 1/3 peak torque and ½ speed. This strategy effectively reduced NO_X to about 50 ppm with increases in PM for gasoline combustion. Combustion phasing was achieved by injection timing.

The second generation MK expanded the operating range through various modifications [15]. Higher injection pressure (through a high pressure common-rail fuel system) was executed to reduce fuel injection time at all speeds. The ignition delay was increased by reducing the compression ratio and adding EGR cooling to reduce intake temperature. To reduce fuel spray wall impingement, piston bowl was increased from 47 mm to 56 mm. This significantly reduced UHC emission during cold start. It was observed that the second generation MK strategy could be used for the entire range of engine operation, and also met the target of about ½ load and ¾ speed. NO_X emission was reduced by 98% compared to conventional EGR and PM emission was similar to conventional CI engine. The most strategic advantage of MK is that it does not require additional hardware and its operation with existing hardware did not negatively impact the engine's specific power output. However, the injection timing retardation reduced engine cycle efficiency and gave rise to higher UHC emission [12].

5.4.3.2 Premixed/DI HCCI

This strategy incorporates port injection as the primary fuel supply source to create a homogenous charge and the DI fuel injection is used at the secondary stage to change the concentration and spatial position of the rich regions with the sole purpose of triggering ignition and as means of HCCI combustion control.

Odaka et al. [52] proposed a homogenous charge compression ignition diesel combustion (HCDC) which used the premixed/direct-injection HCCI system. In this system, most of the fuel was injected into the intake manifold to form a homogenous premixture in the cylinder and a small amount of fuel was directly injected into the homogenous premixed in the cylinder. This strategy reduced both NO_X and smoke emission better than the conventional CI engine. It was also observed that smoke is reduced uniformly as the premixed fuel ratio increased.

Midlam-Mohler et al. [53, 54] also built a premixed/direct-injected HCCI system. A low pressure atomizer system was employed to achieve port/manifold fuel injection and a high pressure injection system was employed for the direct injection of fuel into the combustion chamber. In low load mode, the main torque comes from the premixed lean homogenous fuel and the DI fuel only serves to initiate ignition at high loads. The maximum homogenous charge is employed and DI fuel proportion is increased to fuel load. Atomization to droplet size of less than 1 am mean diameter allows fast evaporation during the compression stroke, making the heating of intake unnecessary. Results obtained showed that by varying intake conditions, IMEP of up to 4.7 bar can be achieved at a speed range of between 1600 rpm - 3200 rpm. In

addition, the strategy achieved very low NO$_X$ of less than 4 ppm and smoke emission of 0.02FSN.

The most interesting strategy in the premixed/DI HCCI was proposed by Inagaki et al. [55]. In this strategy, gasoline (high octane, low cetane number) was used at the intake port for the homogenous premixed and diesel fuel (low octane high cetane number) was injected at DI to initiate ignition at timing BTDC. It was observed that ignition phasing of the combustion can be controlled via the changing of fuel ratio for the two stages to the extent that combustion proceeds mildly. The operating load range where NO$_X$ and smoke emission were 10 ppm and 0.1 FSN respectively were extended to an IMEP of 12 bar where an intake air boost system was employed.

5.4.4   Biodiesel Properties Solver

The thermo-physical properties of FAME to be used in CFD computation required great accuracy of prediction to achieve high fidelity and given their large number and the cost associated with experimental determination, the best option is to compute their value using well validated correlations [1]. The properties could either be transport or thermodynamic. It is well known that both transport (viscosity, density, bulk modulus, surface tension) and thermodynamic (heat capacities, conductivities, vapour pressure, latent heat of vaporization etc.) properties have a strong coupling to FAME structure. For example, densities increase with increases in carbon chains and are higher with highly unsaturated esters [56], kinematic viscosity increases with increased carbon chain length and decrease as unsaturation increases [57] etc.

Given that thermo physical properties are key determining factors in the outcome of combustion processes and which subsequently determine engine pre-combustion strategy, engine performance and emissions, it is important to obtain great accuracy in determining their values in an efficient and cost effective manner. Two hand books are useful in the estimation of FAME properties when developing a code to compute biodiesel properties. These are the work of Reid et al. [58, 59] and Poling et al. [60] which provide useful references for the comprehensive compilation of groups' contribution and experimentally determine correlations. Software has been developed for use in the estimation of hydrocarbon thermo-physical properties. Packages include Knovel critical tables [61], DIPPR [62] and BDProp [63, 64]. Mixing rules [65, 66] are also considered because they are important considerations when computing FAME properties.

5.4.5   Engine Diagnostic and Experimental Validations

Model fidelity is often validated with a plethora of engine diagnostic tools and well-designed experiments. Since 1979 when optical diagnostics was discovered, it has continued to play an important role in in-cylinder process observations [12]. This tool has been refined to such a degree that comprehensive information on flow pattern, species and temperature distribution with high spatial and temporal resolution can now be obtained, very importantly, their non-intrusive, in-situ capability enables process observation without distortion [21]. Consequently, their use has been wide spread. Richter et al. [67] used planar laser induced fluorescence (PLIF) in HCCI to evaluate distribution of fuel and OH radicals in the combustion chamber. Glassman [68] used chemicluminiscence at low temperature to observe fuel oxidation and heat release for diesel in a study to test the efficacy of chemiluminiscence and spectral analysis in in-cylinder observation.

PLIF was also used to study NO emission from an engine by Dec and Canacin [69]. Laser induced incandescence (LII) was used by Singh et al. [70] and Huestis et al. [71] to study soot propagation and destruction processes by applying a two-colour optical pyrometer in LTC. Musculus [72] used LII in the study of soot luminosity and soot laser induced incandescence.

A significant data base of engine test result exist, which can be used to perform validation studies of model results but, where specific data set are needed for a narrow band of engine test protocol, building a test rig with sufficient diagnostic tools does not pose any serious challenge.

5.5   Method/Test Protocol and Expected Outcome

Broadly stated, the proposed strategy is a partial merger of the premixed/DI and Modula Kinetic to improve cycle efficiency, increase IMEP, eliminate NO_X and soot emission, reduce UHC and CO emission. The fuel is a multi-blend FAME of saturated and unsaturated mix. At the premixed injection stage, less reactive and low cetane unsaturated FAME will constitute the bulk of the fuel to be introduced via port injection. The purpose being to delay ignition to enable the formation of a diffused homogenous charge. This will also be helped by the EGR via NVO so that ignition delay will be retarded from 7^oBTDC to approaching $1^o - 0^o$ BTDC. A small quantity of high proportion saturated FAME blend will be injected via DI around $2^o - 1^o$ BTDC to change charge mix, creating rich zone that will trigger ignition and form the spark kernel at just about the time that the rest of the charge is about to ignite. The spontaneous global combustion that will ensue will be rapid and deep given the milder thermal and charge stratification. Peak temperature will be calibrated not to exceed 1650^ok via the EGR means to

177

achieve zero NO$_X$ and soot formation. It is envisioned that with good bowl geometry selection, swirl level and the partially warm EGR, a controlled thermal stratification will create a temperature floor of 1400 k and prevent build- up of UHC and CO from wall quenching and crevices region. Cycle efficiency will improve since charge mix is near stoichiometric and ignition is calibrated to occur BTDC.

The following are proposed for the work.

1.   **Model type**: 3D CFD, multi-zone with detailed chemistry.

2.   **Surrogate**: methyl Decanoate bio (MDBio) built into KIVA-3V with proportional alteration for the premix and DI stage.

3.   **Property solver**: A developed property solver code coupled to the model to compute on demand properties for the chemistry and physics of the process.

4.   **Validation**: Existing validation code for ID NOx map will be used to validate the ID and NOx formation data. The resulting scaler quantities will be used to compute the IMEP and ISFC.

5.   **Test Rig**: A suitable diagnostic test rig with PLIF capability will be used to fully resolve and validate the CO and UHC history. PM formation, if any, will also be determined through the same method.

6.   **Post processing and Optimization**: Subsequent to validation, a broad range of parameter grids will be simulated to optimize output and make useful prediction.

5.6   Conclusion

Given the tools currently available for biodiesel combustion studies, it is now technically possible to determine the best combustion strategy that can increase engine performance, eliminate emission and, more importantly, determine the right mix of FAME that can achieve that. The latter is a very important fact. Biodiesel is simply a mixture of varying components of FAME. If through numerical studies, we are able to determine the mixture with the best outcome in a given engine strategy, it becomes possible in the short term to mix that proportion for use from existing biodiesel and, in the long term, genetically engineer a plant algae source that could produce an exact oil copy. This clearly is the future of renewable energy research;

walking backward from the answer to the problems that prevents us from obtaining the answers we desire is the key to unlocking the potentials inherent in biodiesel fuel sources.

References

1.   Pandey, R.K., A. Rehman, and R.M. Sarviya, *Impact of alternative fuel properties on fuel spray behavior and atomization* Renewable and Sustainable Energy Reviews, **2012. 16**: pp. 1762-1778.

2.   Energy Statistics, E., *http://epp.eurostat.ec.europa.eu/portal/page/*. portal/energy/data/database [accessed on 31.10.11]. 2011.

3.   Komninos, N.P. and C.D. Rakopoulos, *Modeling HCCI combustion of biofuels: A review.* Renewable and Sustainable Energy Reviews 2012. **16:** pp. 1588-1610.

4.   Griffin Shay, E., *Diesel fuel from vegetable oils: status and opportunities.* Biomass and Bioenergy 1993. **4**: pp. 227-442.

5.   U.N.D. Programme, , *World energy assessment.* Energy and the Challenge of Sustainability, New York: United Nations, 2000.

6.   Ng, J.-H., H.K. Ng, and S. Gan, *Characterisation of engine-out responses from a light-duty diesel engine fuelled with palm methyl ester (PME).* Applied Energy 2012, **90**: pp. 58-67.

7.   Murrilo, S., J.L. Mıguez, J. Porteiro, E. Granada, J.C. Moran., *Performance and emission study in the use of biodiesel in outboard diesel engines.* Fuel, 2007. **86**: pp. 1765-1771.

8.   Zheng, X.L., T.F. Lu, and C.K. Law, *Experimental counterflow ignition temperatures and reaction mechanisms of 1,3-butadiene. Proceedings of the Combustion Institute*, 2007. **31**: pp. 367-375.

9.   Lapuerta, M., O. Armas, and J. Rodriguez-Fernandez, *Effect of biodiesel fuels on diesel engine emissions.* Effect of biodiesel fuels on diesel, 2008. **34**: p. 198-223.

10.   Fontaras, G., .G, Karavalakis, M.Kousoulidou, T. H. Tzamkiozis, L. Ntziachristos, E. Bakeas, S. Stournas, Z. Samaras, *Effects of biodiesel on passenger car fuel consumption, regulated and nonregulated pollutant emissions over legislated and real-world driving cycles.* Fuel, 2009. **88**: pp. 1608-1617.

11.   Alriksson, M. and I. Denbratt, *Low temperature combustion in a heavy duty diesel engine using high levels of EGR.* SAE paper 2006-01-0075, 2006.

12.   Yao, M., Z. Zheng, and H. Liu, *Progress and recent trends in homogeneous charge compression ignition (HCCI) engines.* Progress in Energy and Combustion Science, 2009. **35**: pp. 398-437.

13.   Potter, M., R. Durrett, and G. Motors, *Design for compression ignition high-efficiency clean combustion engines.* 12th Annual diesel engine emissions reduction (DEER) conference, 2006.

14.   Kawashima, J.I., H. Ogawa, and Y. Tsuru, *Research on a variable swirl intake port for 4-valve high-speed DI Diesel engines.* SAE paper 1998 982680, 1998.

15. Kimura, S., A. Osamu, O. Hiroshi, M. Shigeo, and E. Yoshiteru , *New combustion concept for ultra-clean and high-efficiency small DI diesel engines.* SAE paper 1999-01-3681, 1999.

16. Kong, S.C., et al., *Modeling and experiments of HCCI engine combustion using detailed chemical kinetics with multidimensional CFD.* SAE paper 2001-01-1026, 2001.

17. Brakora, J.L., Y. Ra, and R.D. Reitz, *Combustion model for biodieselfueled engine simulations using realistic chemistry and physical properties.* SAE paper 2011-01-0831, 2011.

18. Aceves, S.M., D.L. Flowers, F. Espinosa-Loza, J. Martinez-Frias, J.E. Dec, M. Sjöberg, R.W. Dibble, R.P. Hessel., *Spatial analysis of emissions sources for HCCI combustion at low loads using a multi-zone model.* SAE paper 2004-01-1910, 2004.

19. Aceves, S.M., J. Martinez-Frias, D. Flowers, F. Espinosa-Loza, R. Dibble, M. Christensen, B. Johansson, R. Hessel.. *Cylinder-geometry effect on HCCI combustion by multi-zone analysis.* SAE paper 2002-01-2869, 2002.

20. Aceves, S.M., D. L. Flowers, C. K. Westbrook, J. R. Smith, W. Pitz, R. Dibble, M. Christensen and B. Johansson., *A multi-zone model for prediction of HCCI combustion and emissions. .* SAE paper 2000-01-0327, 2000.

21. Ma, X, C. Jiang, H. Li, G. Tian, H. M. Xu, and M.L. Wyszynski., *Optical diagnostics of flow and combustion,* 2015. Available: www.birmingham.ac.uk, date accessed: 10/09/2015

22. Onishi, S., et al., *Active thermo-atmosphere combustion (ATAC) - a new combustion process for internal combustion engines.* SAE paper 1979 790501, 1979.

23. Noguchi, M., T. Tanaka, and Y. Takeuchi, *A study on gasoline engine combustion by observation of intermediate reactive products during combustion.* SAE paper 1979 790840, 1979.

24. Dagaut, P., S. Gail, and M. Sahasrabudhe, *Rapeseed oil methyl ester oxidation over extended ranges of pressure, temperature, and equivalence ratio: Experimental and modeling kinetic study.* Proceediings of the Combustion Institute, 2007. **31**: pp. 2955-2961.

25. Cheng, X., et al.., *Advances in computational fluid dynamics (CFD) modeling of in-cylinder biodiesel combustion.* Energy Fuels, 2013. **27**: pp. 4489-4506.

26. Brakora, J.L., Y. Ra, and R.D. Reitz, *Development and validation of a reduced reaction mechanism for biodiesel-fueled engine simulations.* SAE Tech. Pap. Ser. 2008. No. 2008-01-1378.

27. Golovitchev, V.I. and J. Yang, *Construction of combustion models for rapeseed methyl ester bio-diesel fuel for internal combustion engine applications.* Biotechnology Advances, 2009. **27**(5) pp. 641-655.

28. Fisher, E.M., et al., *Detailed chemical kinetic mechanisms for combustion of oxygenated fuels.* Proceediings of the Combustion Institute, 2000. **28**: pp. 1579-1586.

29. Gail, S., et al.., *Experimental and chemical kinetic modelling study of small methyl esters oxidation: Methyl(E)-2-butenoate and methyl butanoate.* Combustion and Flame, 2008. **155**: pp. 635-650.

30. Mohamed Ismail, H., et al., *Development of reduced combustion kinetics of a generic biodiesel fuel surrogate for CFD spray combustion modelling of a light-duty diesel engine.* Fuel, 2012. DOI: 10.1016/j.fuel.10.015.

31. Glaude, P.A., et al., *Modeling the oxidation of methyl esters: Validation for methyl hexanoate, methyl heptanoate and methyl decanoate in a jetstirred reactor.* Combustion and Flame, 2010. **157**: pp. 2035-2050.

32. Lawrence Livermore Laboratory. Available: *https://www-pls.llnl.gov/?url=science_and_technology-chemistry-combustion-biodiesel.* Accessed July 26, 2012.

33. Luo, Z., et al., *A reduced mechanism for high-temperature oxidation of biodiesel surrogates.* Energy Fuels, 2010. **24** (12): pp. 6283-6293.

34. Herbinet, O., W.J. Pitz, and C.K. Westbrook, *Detailed chemical kinetic mechanism for the oxidation of biodiesel fuels blend surrogate.* Combustion and Flame, 2010. **157**: pp. 893-908.

35. Hakka, M.H., et al., *Experimental study of the oxidation of large surrogates for diesel and biodiesel fuels.* Combustion and Flame, 2009. **156**: pp. 2129-2144.

36. Westbrook, C.K., et al., *Detailed chemical kinetic reaction mechanisms for soy and rapeseed biodiesel fuels.* Combustion and Flame, 2011. **158**: pp. 742-755.

37. McIlroy, A.,, *Basic research needs for clean and efficient combustion of 21st century transportation fuels.* Report of the basic energy sciences workshop on clean and efficient combustion of 21st century transportation fuels. Office of Science, U.S. Department of Energy, 2006.

38. Brakora, J.L. and R.D. Reitz, *Investigation of NOx predictions from biodiesel-fueled HCCI engine simulations using a reduced kinetic mechanism.* SAE paper 2010-01-0577, 2010.

39. Fiveland, S.B. and D.N. Assanis, *A four-stroke homogeneous charge compression ignition engine simulation for combustion and performance studies.* SAE paper 2000-01-0332, 2000.

40. Ogink, R. and V. Golovitchev, *Gasoline HCCI modeling: an engine cycle simulation code with a multi-zone combustion model.* SAE paper 2002-01-1745, 2002.

41. Milovanovic, N., et al., *Influence of the variable valve timing strategy on the control of a homogeneous charge compression (HCCI) engine.* SAE paper 2004-01-1899, 2004.

42. http://www.lanl.gov/orgs/t/t3/codes/kiva.shtml. Date accessed: 14/12/2014

43. Babajimopoulos, A., D.N. Assanis, and S.B. Fiveland, *An approach for modeling the effects of gas exchange processes on HCCI combustion and its application in evaluating variable valve timing control strategies.* SAE paper 2002-01-2829, 2002.

44. Flowers, D.L., et al., *Prediction of carbon monoxide and hydrocarbon emissions in isooctane HCCI engine combustion using multi-zone simulations.* Proceedings of the Combustion Institite, 2002. **29**(1): pp. 687-694.

45. Agarwal, A. and D.N. Assanis, *Modeling the effect of natural gas composition on ignition delay under compression ignition conditions.* SAE paper 1997 971711, 1997.

46. Kim, M.Y. and C.S. Lee, *Effect of a narrow fuel spray angle and a dual injection configuration on the improvement of exhaust emissions in a HCCI diesel engine,* Fuel, 2007. **86**(17-18): pp. 2871-2880.

47. Takeda, Y., N. Keiichi, and N. Keiichi, *Emission characteristics of premixed lean diesel combustion with extremely early staged fuel injection.* SAE paper 1996 961163, 1996.

48. Yanagihara, H., *Ignition timing controlat Toyota ''UNIBUS'' combustion system.* In: Proceedings of the IFP international congress, 2001: pp. 35-42.

49. Su, W.H., T.J. Lin, and Y.Q. Pei, *A compound technology for HCCI combustion in a DI diesel engine based on the multi-pulse injection and the BUMP combustion chamber,* SAE paper 2003-01-0741, 2003.

50. Kawamoto, K., et al., *Combination of combustion concept and fuel property for ultra-clean DI diesel,* SAE paper 2004-01-1868, 2004.

51. Kimura, S., et al., *Ultra-clean combustion technology combining a low-temperature and premixed combustion concept for Meeting Future Emission Standards.* SAE paper 2000-01-0200, 2000.

52. Odaka, M., et al., *Search for optimizing method of homogeneous charge diesel combustion.* SAE paper 1999-01-0184, 1999.

53. Midlam-Mohler, S., Y. Guezennec, and G. Rizzoni, *Mixed-mode diesel HCCI with external mixture formation: preliminary results.* 9th Diesel engine emissions reduction (DDER) workshop, 2003.

54. Midlam-Mohler, S., *Diesel HCCI with external mixture preparation.* 10th Diesel engine emissions reduction (DEER) workshop, 2004.

55. Inagaki, K. and T. Fuyuto, *Combustion system with premixture-controlled compression ignition.* R&D Rev Toyota CRDL 2006. **41**(3): pp. 35-46.

56. Yamane, K., A. Ueta, and Y. Shimamoto, *Influence of physical and chemical properties of biodiesel fuels on injection, combustion and exhaust emission characteristics in a direct injection compression ignition engine.* International Journal of Engine Research, 2001. **2**(No.4): pp. 1-13.

57. Knothe, G. and K.R. Steidley, *Kinematic viscosity of biodiesel fuel components and related compound. influence of compound structure and comparison to petrol diesel fuel components.* Fuel, 2005. **84**: pp. 1059-1065.

58.   Reid, R.C., J.M. Prausnitz, and T.K. Sherwood, *The properties of gases and liquids.* 3rd ed. New York: McGraw-Hill, 1977.

59.   Reid, R.C., J.M. Prausnitz, and T.K. Sherwood, *The properties of gases and liquids.* 4th ed. New York: McGraw-Hill, 1987.

60.   Poling, B.E., J.M. Prausnitz, and J.P. O'Connel, *The properties of gases and liquids.* 5th ed. New York: McGraw-Hill, 2001.

61.   http://knovel.com/web/, *Knovel critical tables,* 2nd ed. Accessed July 26, 2012.

62.   http://knovel.com/, *Design institute for physical property data.* Aaccessed July 26, 2012.

63.   Stringer, V., et al., *Modeling biodiesel spray breakup with well-defined fuel properties,* . Chicago, IL: ILASS-Americas, May 15-18, 2007.

64.   Yuan, W., A.C. Hansen, and Q. Zhang, *Predicting the physical properties of biodiesel for combustion modeling.* Transactions of the ASABE American Society of Agricultural and Biological Engineers 2003. **46**(6): pp. 1487-1493.

65.   Lee, B.I. and M.G. Kesler, *A generalized thermodynamic correlation based on three-parameter corresponding states.* AIChE Journal, 1975. **21**: pp. 510-527.

66.   Kay, W.B., *Density of hydrocarbon gases and vapors.* Industrial and EngineeringChemistry, 1936. **28**: pp. 1014-1019.

67.   Richter, M., et al., *The influence of charge inhomogeneity on the HCCI combustion process.* SAE paper 2000-01-2868, 2000.

68.   Glassman, I., *Combustion.* 3rd ed. New York: Academic Press, 1996.

69.   Dec, J.E. and R.E. Canaan, *PLIF imaging of NO formation in a DI diesel engine.* SAE paper 980147.

70.   Singh, S., R.D. Reitz, and P.B. Musculus Mark, *2-Color thermometry experiments and high-speed imaging of multi-mode diesel engine combustion.* SAE paper 2005-01-3842, 2005.

71.   Huestis, E., P.A. Erichkson, and P.B. Musculus Mark, *In cylinder and exhaust soot in low-temperature combustion using a wide-range of EGR in a heavy-duty diesel engine.* SAE paper 2007-01-4017, 2007.

72.   Musculus Mark, P.B., *Multiple simultaneous optical diagnostic imaging of early-injection low-temperature combustion in a heavy-duty diesel engine.* SAE paper 2006-01-0079, 2006.

Engine Theory and Correlation.

The compression ignition (CI) engine is a hybrid of the internal combustion engine developed in 1892 by the German engineer Rudolf Diesel (1858 – 1913). In that patent, Diesel outline a concept of initiating combustion by injecting liquid fuel into air heated solely by compression thus facilitating a significant increase in efficiency compared to other competing combustion strategies during that period.

In the CI engine, air is drawn into the cylinder through either naturally aspirated (atmospheric air induction), turbocharged (exhaust driven turbine-compressor combination) or, supercharged (compression by a mechanically driven pump) means. The liquid fuel is injected into the cylinder just before the combustion process is required to start. Load scaling is achieved by varying the amount of fuel injected per cycle.

For a four-stroke naturally aspirated CI engine, the operation is represented in figure 1. The compression ratio typically ranges from 12-24 depending on the air induction means. The inducted air is at near atmospheric pressure during the intake stroke and is compressed to about 4 MPa and temperature of about 800 k during the compression stroke. Fuel is injected at 20° before top centre (BTC). Liquid fuel jet atomization and air entrainment occurs in engine subsequent to which evaporation, vapour mixing with air and spontaneous ignition (auto-ignition) combustion starts.


Plate 1: CI Test rig showing emission measuring device
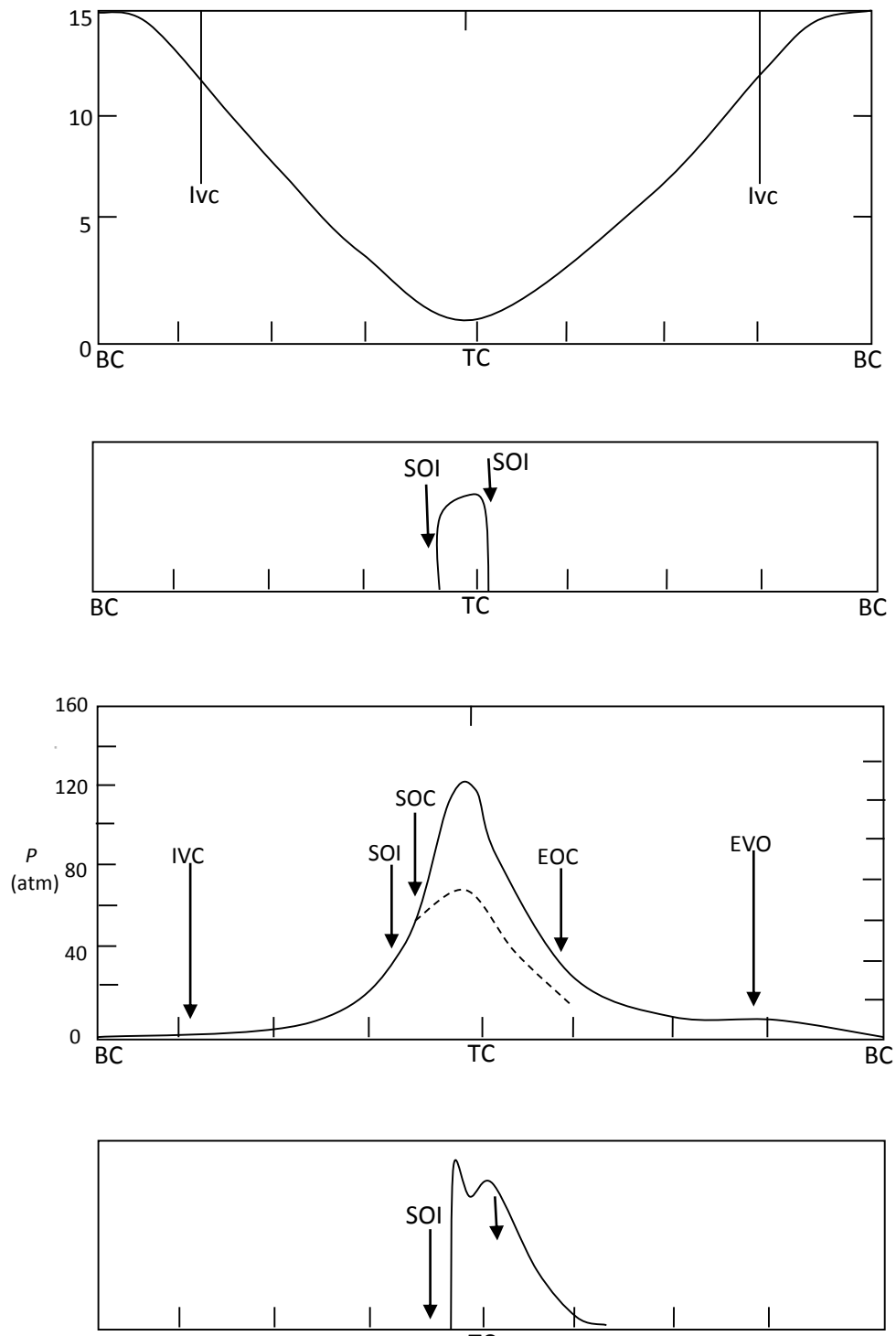
Figure 1: Sequence of events during compression, combustion, and expansion processes of a naturally aspirated compression-ignition four-stroke engine operating cycle. Cylinder volume/clearance volume *V/V_e*, rate of fuel injection m_fi, cylinder pressure p (solid line, firing cycle; dashed line, motored cycle), and rate of fuel burning (or fuel chemical energy release rate) m_fb are plotted against crank

Naturally aspirated CI engine operating cycle

The air temperature and pressure are above the fuel ignition point. Therefore, after a short delay, spontaneous ignition (auto-ignition) of parts of the non-uniform fuel air mixture initiates the combustion process, and the cylinder pressure (solid line in Figure 2c) rises above the non-firing engine level. The flame spreads rapidly through that portion of the injected fuel which has already mixed without sufficient air to burn. As the expansion process proceeds, mixing between fuel, air and burning gases continues, accompanied by further combustion. At full load, the mass of fuel injected is about 5% of the mass of air in the cylinder. Increasing levels of black smoke in the exhaust limit the amount of fuel that can be burned efficiently. The exhaust process is similar to that of the four stroke SI engine. The cycle is repeated at the end of the exhaust stroke.

In the two-stroke CI engine cycle, compression, fuel injection, combustion and expansion processes are similar to the equivalent four-stroke cycle processes; it is the intake and exhaust pressure which are different. The sequence of events in a loop-scavenged two-stroke engine is illustrated in Figure 2. In loop-scavenged engine both exhaust and inlet ports are at the same end of the cylinder and are uncovered as the piston approaches Bottom Centre (BC) Figure 2a. After the exhaust port opens, the cylinder pressure falls rapidly in a blow down process (Figure 1b). The inlet ports then open, and once the cylinder pressure P falls below the inlet pressure P_i, air flows into the cylinder. The burned gases, displaced by this fresh air, continue to flow out of the exhaust port (along with some of the fresh air). Once the ports are closed as the piston starts the compression stroke, compression, fuel-injection, fuel-air mixing, combustion and expansion processes proceed as in the four-stroke CI engine cycle.
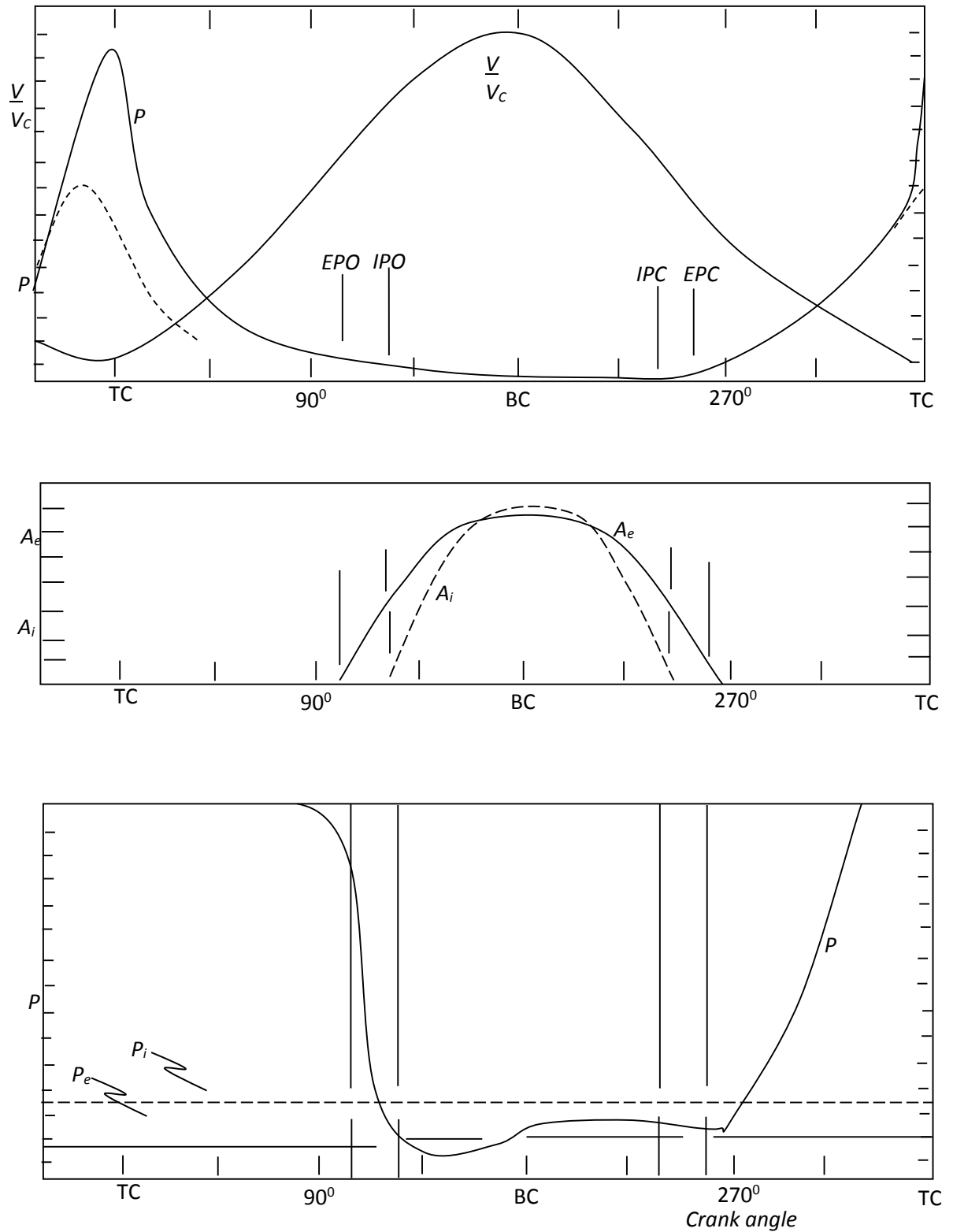
Figure 2 (a-c): Sequence of events during expansion, gas exchange, and compression processes in a loop-scavenged two-stroke cycle compression-ignition engine. Cylinder volume/clearance volume V/Ve, cylinder pressure p, exhaust port open area Ae, and intake port open area plotted against crank angle.

Engine Characteristics

i.   Compression ratio, r_c

$$r_c = \frac{maximum\ cylinder\ volume}{minimum\ cylinder\ volume}$$ 1

$$r_c = \frac{V_d + V_c}{V_c}$$

Where V_d is the displaced volume, and V_c is the clearance volume.

Ratio of cylinder bore to piston stroke, R_{bs}

$$R_{bs} = \frac{B}{L}$$ 2

ii.   Ratio of connecting rod length of crank radius, R
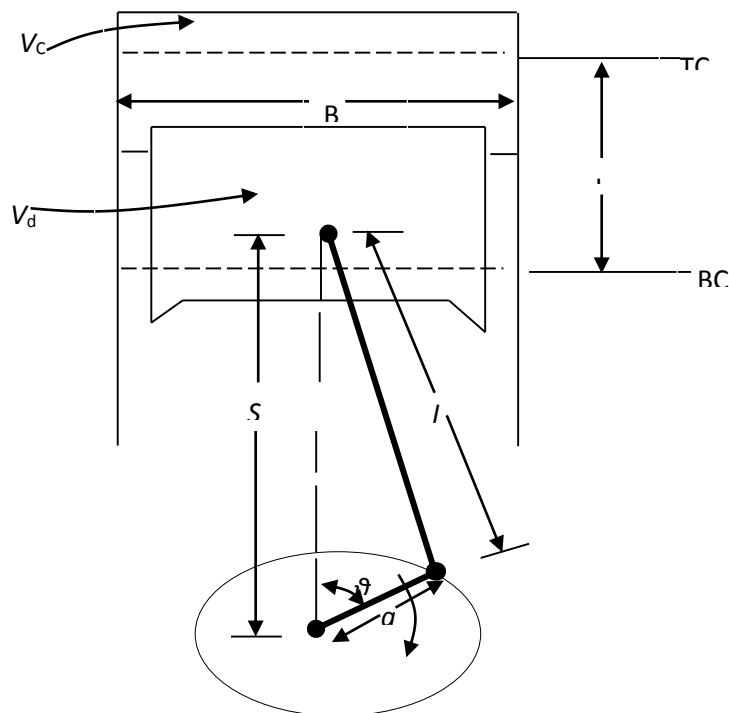
$$R = \frac{L}{a}$$ 3

Stroke, L and crank radius, a are related by

$$L = 2a$$ 4

iii. The cylinder volume, V at any crank position θ is

$$V = V_c + \frac{\pi B^2}{4}(L + a - s)$$ 5

Figure 3: Geometry of cylinder, piston, connecting rod, and crankshaft where B = bore, L = Stroke, I = connecting road length, a = crank radius, θ = crank angle

Where S is the distance between the crank axis and the piston pin (Figure 3)

S is given by

$$S = a \cos \theta + (L^2 - a^2 \sin^2\theta)^{1/2}$$ 6

θ is crank angle

Rearranging

$$\frac{V}{V_c} = 1 + \frac{1}{2}(r_c - 1)(R + 1 - \cos \theta - (R^2 - Sin^2\theta)^{1/2} \quad)$$ 7

Combustion chamber surface Area, A at any crank position θ is given by

$$A = A_{ch} + A_p + \pi B(l + a - s)$$ 8

Where A_{ch} cylinder head is surface area

Also mean piston speed $\bar{S}_p$
$$\bar{S}_p = 2LN$$ 9

Where N is crank shaft speed but instantaneous speed, S_p is

$$S_p = \frac{ds}{dt}$$ 10

S_p Is zero at both TC ($\theta = 0^0$) and BC ($\theta = 180^0$) and is a maximum at 90^0. Hence

$$\frac{S_p}{\bar{S}_p} = \frac{\pi}{2} \sin \theta \left[1 - \frac{\cos \theta}{(R^2 - \sin^2\theta)^{1/2}} \right]$$ 11

190

Gas flow drag and inertia forces limit the maximum instantaneous speed to a range of 8 m/s – 15m/s.

Brake Torque and Power

A dynamometer is usually employed to measure engine torque and is normally shafted to the engine on the test bed. Using the weights, springs or pneumatic means, engine Torque T is determined by

$$T = Fb \qquad\qquad 12$$

F is the indicated weight and b is the perpendicular distance between the load cell and rotor axis. Power P is

$$P = 2\pi NT \qquad\qquad 13$$

Where N is the angular speed in revolutions per minute.

Indicated Work per Cycle

Power per cycle P_i

$$P_i = \frac{W_{ci}N}{n_R} \qquad\qquad 15$$

Where n_R is the number of crank revolutions for each power stroke per cylinder. For four-stroke it equals 2; for two-stroke, 1.

Specific Fuel Consumption

Fuel consumption is measured as mass flow rate, $\dot{m}_f$ during engine test. A more specific measure is the specific fuel consumption and is given by Sfc

$$Sfc = \frac{\dot{m}_f}{P} \qquad\qquad 16$$

Where P is power output. The lower the value of specific fuel consumption, the more desirable because it is an indication of how efficient the engine is utilizing the fuel energy.

Fuel conversion efficiency η_f is another means by which engine performance can be looked at, and is given by

$$\eta_f = \frac{P}{\dot{m}_f Q_{HV}}$$
17

Where Q_{HV} is the heating value of the fuel, therefore

$$\eta_f = \frac{1}{Sfc * Q_{HV}}$$
18

Air/Fuel Ratio and Fuel/Air Ratio

Typically, on an engine test rig, provisions are made to measure air mass flow rate $\dot{m}_a$ and the fuel mass flow rate $\dot{m}_f$. These ratios are used to describe engine operating conditions.

$$A/_F = \frac{\dot{m}_a}{\dot{m}_f}$$
19

$$F/_A = \frac{\dot{m}_f}{\dot{m}_a}$$
20

Volumetric Efficiency

The air intake system consisting of the filter, intake manifold, intake port, intake valve etc. restricts the amount of air which an engine of a given displacement can induct. The effectiveness of engine induction processes can be described by the volumetric efficiency, η_v. This parameter is only used for the four-stroke cycle engine. It is defined as the volume flow rate of air into the intake system divided by the rate at which volume is displaced by the piston.

$$\eta_v = \frac{2\dot{m}_a}{\rho_{a,i} V_d}$$
21

Where $\rho_{a,i}$ is the inlet air density and alternative expression is given as

$$\eta_v = \frac{m_a}{\rho_{a,i} V_d}$$
22

Where m_a is the mass of air inducted into the cylinder per cycle.

## Engine Specific Weight and Specific Volume

The weight and bulk volume of any given engine over the rated power gives an important indication of how material and space has been used in the engine design to optimize power outputted.

$$specific\ weight = \frac{engine\ weight}{rated\ power} \qquad\qquad 23$$

$$specific\ volume = \frac{engine\ volume}{rated\ power} \qquad\qquad 24$$

Stoichiometry

Combustion stoichiometry defines the chemically correct or theoretical proportions of fuel and air where there is just enough oxygen for conversion of all the fuel into completely oxidized products. The stoichiometry air/fuel or fuel/air ratios depend on the fuel compression. That is, if sufficient oxygen is available a hydrocarbon fuel can be completely oxidized. The carbon in the fuel is then converted to carbon dioxide (CO_2) and the hydrogen to water (H_2O). For a biodiesel fuel, for example, this is given as shown.

$$C_xH_yO_z + Y_{cc}(O_2 + 3.773N_2) \rightarrow xCO_2 + \left(\frac{y}{2}\right)H_2O + y_{cc}O_2 + 3.773y_{cc}N_2$$

$$3.44$$
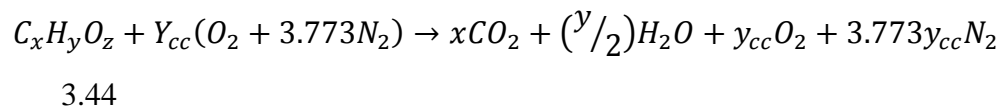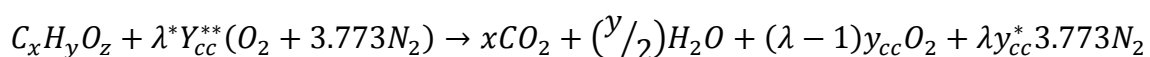
Where   X   -   No. of moles of carbon

               Y   -   No. of moles of hydrogen

               Z   -   No. of moles of oxygen

Stoichiometric AFR (air fuel ratio), y_{cc}

$$y_{cc} = x + \left(\frac{y}{4}\right) - \left(\frac{z}{2}\right) \qquad\qquad 25$$

Assuming excess air factor, λ the equation is modified to give [7]

$$C_xH_yO_z + \lambda^*Y_{cc}^{**}(O_2 + 3.773N_2) \rightarrow xCO_2 + \left(\frac{y}{2}\right)H_2O + (\lambda - 1)y_{cc}O_2 + \lambda y_{cc}^*3.773N_2$$

Note: The equivalent ratio is the ratio of the actual fuel/air ratio over the stoichiometric fuel to air ratio.

That is:

$$\emptyset = \frac{(F/A)_{actual}}{(F/A)_{stoichiometric}} \qquad\qquad 26$$

The inverse of $\emptyset$ is the relative air/fuel ratio, λ

$$\lambda = \emptyset^{-1} \qquad\qquad 27$$

For lean fuel mixture; $\emptyset < 1, \lambda > 1$
For stoichiometric mixture; $\emptyset = \lambda = 1$
For fuel-rich mixture; $\emptyset > 1, \lambda < 1$

Heating Value

Where the exact composition of a particular fuel is not known, it is difficult to compute the enthalpy of the reactant from the enthalpies of formation of the reactant species. The alternative means will be to measure the heating value of the fuel directly. The heating value Q_{HV} or calorific value of fuel is the magnitude of the heat of reaction at constant pressure or at constant volume at a standard temperature (normally 25°C) for complete combustion of a unit mass of fuel. Heating value

$$Q_{HV_p} = -(\Delta H)_{PT_o} \qquad\qquad 28$$
$$Q_{HV_V} = -(\Delta U)_{V,T_o} \qquad\qquad 29$$

The term higher heating value Q_{HHV} (or gross heating value) is used when the H_2O formed is all condensed to the liquid phase, while lower heating value Q_{LHV} (or net heating value) is used when the H_2O formed is all in the vapour phase. The two are related by

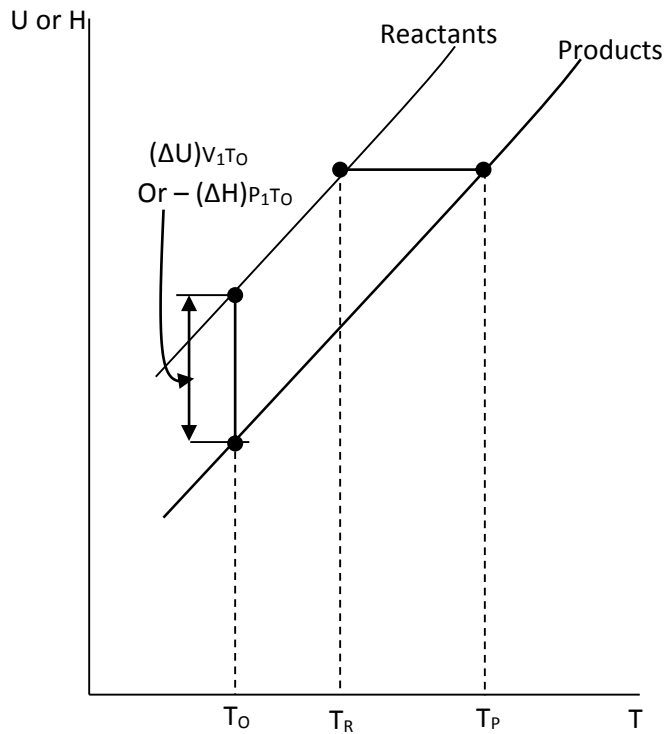$$Q_{HHV_P} = Q_{LHV_P} + \left(\frac{M_{H_2O}}{M_f}\right) h_{fgH_2O} \qquad\qquad 30$$

Where (M_{H2O}/M_f) is the ratio of mass of H_2O produced to mass of fuel burned. Heating values are determined experimentally using a bomb calorimeter.

Adiabatic Combustion Process

To analyse constant volume and constant pressure process, for an adiabatic constant – volume process

$$U_p - U_R = 0 \qquad\qquad 31$$

Figure 4: Adiabatic constant-volume combustion process on U- T diagram or adiabatic constant pressure combustion process on H-T diagram

Normally standard reference temperature is known, T_0. In Figure 5 if values of reactant are known, the final state of the product can be determined (as to shown in the figure).

The final temperature of the products in an adiabatic process is called the adiabatic flame temperature.

Combustion Efficiency, η_c

$$\eta_c = \frac{H_R(T_A) - H_P(T_A)}{m_f Q_{HV}} \qquad\qquad 32$$

Where T_A – ambient temperature and H_R, H_p and Q_{HV} are as defined earlier and m and m_f can be replaced by $\dot{m}$ and $\dot{m}_f$ also

$$[H_R(T_A) - H_P(T_A)] = m\left(\sum_{i,reactant} n_i \Delta \bar{h}_f^o - \sum_{i,product} n_i \Delta \bar{h}_{f,i}^o\right) \qquad 33$$

Maximum Work from CI Engine

Considering an open system with surrounding as the atmosphere. The reactant (fuel + air) flows into the system, and the product (exhaust gasses) flows out, given a mass of fluid m. The first law is

$$\Delta Q - \Delta W_u = \Delta H \qquad 34$$

Where ΔW_u the useful work is transferred (non PdV work) and $\Delta H = H_P - H_R$ since heat transfer ΔQ occurs only with the atmosphere at temperature T_A, the second law gives

$$\frac{\Delta Q}{T} \leq \Delta S \qquad 35$$

Combining 1st and 2nd law, gives

$$\Delta W_u \leq -(\Delta H - T_A \Delta S) = -B \qquad 36$$

Where B is the steady flow availability function, H - T_AS.

Normally $P_R = P_A$ and $T_R = T_A$. Maximum work is obtained when $P_P = P_A$ and $T_P = T_A$.

Given this condition

$$\Delta W_{umax} \leq -\left[(H - TS)_{P_{TAPA}} - (H - TS)_{R_{TAPA}}\right] = -(\Delta G)_{T_A P_A} \qquad 37$$

G_A is Gibbs free energy, H = TS, and $(\Delta G)_{T_A P_A}$ will be maximum where combustion is complete. Hence available conversion efficiency, η_a

$$\eta_a = \frac{\Delta W}{\Delta W_{umax}} = -\frac{\Delta W}{(\Delta G)_{T_A P_A}} \qquad 38$$

But Gibbs is not easily measured, hence, fuel conversion efficiency, η_f can be used

$$\eta_f = \frac{W_c}{m_f Q_{HV}} \qquad\qquad 39$$

Again, in practice, not all fuel energy is released in the engine cylinder due to incomplete combustion. In order to account for these inefficiencies, thermal conversion efficiency can be used, that is, η_t

$$\eta_t = \frac{W_C}{H_R(T_A) - H_P(T_A)} = -\frac{W_c}{(\Delta H)_{T_A}} \qquad\qquad 40$$

$$\eta_t = \frac{W_C}{\eta_C m_f Q_{HV}} \qquad\qquad 41$$

The relationship between the efficiencies is given by

$$\eta_f = \eta_c \eta_t \qquad\qquad 42$$

Figure 5: Model of engine processes

Process	Assumption
Compression (1 − 2)	1. Adiabatic and reversible (1 isentropic)
Combustion (2 − 3)	1. Adiabatic
	2. Combustion occurs at
	(a) Constant volume (b) Constant pressure (c) Part at constant volume and part at constant pressure
	3. Combustion is complete
Expansion (3 − 4)	1. Adiabatic and reversible
Exhaust (4 − 5 − 6) And intake (6 − 7 − 1)	1. Adiabatic
	2. Value event occurs at top and bottom-centre
	3. No. change in cylinder volume as pressure difference across value drop to zero
	4. Inlet and exhaust pressure constant.
	5. Velocity effects is negligible.